

---

---

# Technical Bases for Estimating Fission Product Behavior During LWR Accidents

---

---

## U.S. Nuclear Regulatory Commission

Office of Nuclear Regulatory Research  
Office of Nuclear Reactor Regulation  
Battelle Columbus Laboratories  
Oak Ridge National Laboratory  
Sandia National Laboratories



Available from

GPO Sales Program  
Division of Technical Information and Document Control  
U.S. Nuclear Regulatory Commission  
Washington, DC 20555

Printed copy price: \$8.00

and

National Technical Information Service  
Springfield, VA 22161

---

---

# Technical Bases for Estimating Fission Product Behavior During LWR Accidents

---

---

Manuscript Completed: March 1981  
Date Published: June 1981

**Office of Nuclear Regulatory Research  
Office of Nuclear Reactor Regulation  
U.S. Nuclear Regulatory Commission  
Washington, D.C. 20555**

**Battelle Columbus Laboratories  
Columbus, OH 43201**

**Oak Ridge National Laboratory  
Oak Ridge, TN 37830**

**Sandia National Laboratories  
Albuquerque, NM 87185**





## ABSTRACT

The objective of this report is to provide the Nuclear Regulatory Commission and the public with a description of the best technical information currently available for estimating the release of radioactive material during postulated severe accidents in commercial light water reactor nuclear power plants. This report focuses on a spectrum of postulated accidents ranging from minor fuel damage to severe core damage and core meltdown. Particular emphasis is placed on the accident behavior of radioactive iodine since: (1) radioiodine is predicted to be a major contributor to public exposure, (2) current regulatory accident analysis procedures focus on iodine, and (3) several technical questions have recently been raised about the magnitude of iodine release. The generation, transport, and attenuation of aerosols were also investigated in some detail to assess their effect on fission product release estimates and to determine the performance of engineered safety features under accident conditions exceeding their design bases.

This report addresses several major questions which have been raised concerning past methods for estimating the release of fission products to the environment during severe accidents in commercial light water reactor plants. Concisely, these issues are:

- (1) Is cesium iodide, rather than elemental iodine as has been assumed in the past, the predominant radioiodine form released during severe accidents?
- (2) Since cesium iodide is less volatile than elemental iodine and is much more soluble in water, is the airborne release of iodine to the environment during postulated reactor accidents currently being overestimated?
- (3) Have the expected consequences of the most severe postulated accidents been overpredicted in past analyses (e.g., the Reactor Safety Study) by several orders of magnitude because natural fission product removal mechanisms (such as chemical reactions, aerosol settling, and the effects of moisture) were not properly accounted for?
- (4) Will the engineered safety features designed for iodine control be effective and optimal for the actual iodine behavior rather than the behavior currently assumed and how will these engineered safety features perform under postulated severe core damage and core meltdown accident conditions?

After surveying the available data base, and performing calculations with the most advanced computer models that exist, the results of this study support the following conclusions with respect to the above questions:

- (1) The current data base suggests that cesium iodide will be the expected predominant iodine chemical form under most postulated light water reactor accident conditions. The current evidence regarding the chemical form of iodine released from fuel at high temperature (>1400°C) is inconclusive. However, thermodynamic calculations

predict that formation of CsI should occur in the gaseous reducing atmosphere in the reactor coolant system following release from fuel even if iodine is not released from the fuel as CsI. The formation of some more volatile iodine species (e.g. elemental iodine and organic iodines), however, cannot be precluded under certain accident conditions.

- (2) The assumed form of iodine (either cesium iodide or elemental iodine) was not predicted to have a major influence on the estimated magnitude of iodine attenuation in the containment for severe accident sequences with early containment failure in which there is little time for natural fission product retention mechanisms to be effective. However, the assumed chemical form of iodine can influence the predicted attenuation within the reactor coolant system, where, in general, the attenuation factor will be greater for cesium iodide than for elemental iodine (i.e. less iodine will escape into the containment).
- (3) A number of accident sequences were examined in this report including several core melt sequences which had been found to be the most important contributors to risk in the Reactor Safety Study (RSS). Reevaluation of fission product release from the fuel indicates the RSS may have underpredicted the release of certain important radionuclide species during these core melt events. Mechanistic analyses of fission product transport in the containment atmosphere were in reasonable agreement with the empirically based analyses in the RSS. Predictions of the retention of radioactive material within the reactor coolant system (which was not accounted for in the RSS for most accident sequences) range from very little to substantial retention for specific accident sequences involving a water bounded reactor coolant system (e.g. TMI). In addition, for certain transient initiated core melt sequences where steam flow rates through the reactor coolant system are low and aerosol generation is high, attenuation of fission products within the reactor coolant system could be substantial as a result of agglomeration and fallout of aerosols. Consequently, for certain accident sequences considered in the RSS the release of radionuclides to the environment may have been significantly overpredicted. However, for other accident sequences (such as large or medium size pipe break accidents) the estimated releases in this report are in approximate agreement with the RSS estimates.
- (4) Certain engineered safety features (e.g., containment sprays, BWR pressure suppression pools, PWR ice condenser beds) will perform effectively in removing fission products regardless of their chemical form (i.e., vapor or particulate) and under most severe accident conditions (e.g., aerosol loads) for a wide range of potential accident sequences. Other engineered safety features (e.g., containment recirculating filter systems, BWR main steam line leakage control systems, BWR standby gas treatment systems and secondary containments) are less effective in mitigating fission product release under severe accident conditions for a variety of reasons,

although these systems would be effective for limited fuel damage accidents where containment integrity is maintained.

This study indicates that the magnitude of the release of fission products and structural material aerosols from-the-fuel under severe core damage and core melt accidents can be reasonably approximated using the results from existing experiments and models, although there are very large uncertainties in the release rates for specific radionuclide species. Knowledge of the chemical forms of the released radionuclides is however quite limited.

The transport behavior of fission products within the reactor coolant system is subject to large uncertainties resulting from limitations in the ability to predict severe accident phenomena, thermal hydraulic conditions, and fission product physical and chemical forms.

In contrast, the ability to predict the behavior of fission products within the containment structure after release from the primary system is comparatively good for large volume PWR containments. Less well known is the fission product behavior within pressure suppression containments such as in boiling water reactors and in pressurized water reactor ice condenser plants where the potential attenuation of fission products within the pressure suppression pool and ice beds is subject to large uncertainties. One of the largest uncertainties associated with predicting the amount of radionuclides released to the environment during the most severe accidents (i.e., core melt accidents with containment failure) result from limitations in the ability to predict the timing, mode, and location of containment failure.

The extent to which fission product release to the environment may have been overestimated (or underestimated) in previous studies is difficult to quantify since the range of uncertainty associated with these predictions is very large as a result of the identified limitations in the data base and the early state of development and verification of the predictive methodology. Gaps and limitations in the available data base are identified in the report as a guide to future research.

The analyses in this report concentrate on those postulated severe accidents involving core melt, containment failure and failure of plant engineered safety feature. These accidents, although of very low probability, are predicted to dominate the risk to public safety because of the high consequences associated with these events. The reader should not infer from this treatment that the report authors expect severe consequences for all accidents. Indeed, the analyses in this report indicate for those (higher probability) accidents sequences which do not involve containment failure or loss of containment engineered safety features the anticipated releases of radioactive material to the environment would result in relatively minor public hazard. (The TMI-2 accident is a vivid illustration of this type of accident).

The information presented in this report will be used to guide and focus future NRC research programs and to develop a revised set of radiological source terms for realistic assessment of accident consequences. Information presented in this report has been used in support of a companion NRC staff report, "Regulatory Impacts of Nuclear Reactor Accident Source Term Assumptions," NUREG-0771.

## ACKNOWLEDGMENTS

A large number of individuals have contributed to the development of this report. These individuals are listed below.

M. Silberberg - Report Coordinator - NRC

Chapter 1.0 R. R. Sherry, Chapter Lead, NRC  
M. A. Cunningham, NRC  
C. N. Kelber, NRC  
M. Silberberg, NRC

Chapter 2.0 R. S. Denning, Chapter Lead, Battelle Columbus Laboratories, (BCL)

Chapter 3.0 R. S. Denning, Chapter Lead, BCL

Chapter 4.0 R. P. Wichner, Chapter Lead, Oak Ridge National Laboratory, (ORNL)  
T. S. Kress, ORNL  
R. A. Lorenz, ORNL

Chapter 5.0 R. M. Elrick, Chapter Co-Leader, Sandia National Laboratory  
(Section 5.1 and 5.2)  
J. T. Bell, Chapter Co-Leader, ORNL (Section 5.3)  
R. A. Sallach, Sandia  
L. M. Toth, ORNL  
D. O. Campbell, ORNL  
A. P. Malinauskas, ORNL

Chapter 6.0 J. A. Gieseke, Chapter Lead, BCL  
M. R. Kuhlman, BCL

Chapter 7.0 J. A. Gieseke, Chapter Lead, BCL  
R. S. Denning, BCL  
K. W. Lee, BCL  
H. Jordan, BCL  
T. C. Davis, BCL  
T. C. Kress, ORNL

Chapter 8.0 W. F. Pasedag, Chapter Lead, NRC  
A. K. Postma (NRC Consultant)  
R. Adams, ORNL

F. Mynatt organized and directed the ORNL participation in this study.

J. Rest and S. Gehl of Argonne National Laboratory and D. Oseteck and R. Hobbins of EG&G Idaho contributed material for Chapter 4.0.

A. Evans and R. Bellemey of Savannah River Laboratory contributed background information for the analyses in Chapter 5.0.

We wish to acknowledge our appreciation to Dr. W. Schoeck of the Kernforschungszentrums, Karlsruhe, Federal Republic of Germany for the computer code (NAUA) analysis he provided for this study.

Technical Bases for Estimating Fission Product  
Behavior During LWR Accidents

Table of Contents

	<u>Page</u>
Abstract.....	i
Acknowledgments.....	iv
Table of Contents.....	v
List of Figures.....	vii
List of Tables.....	x
1. INTRODUCTION, SUMMARY AND CONCLUSIONS.....	1.1
1.1 Introduction.....	1.1
1.2 Summary.....	1.9
1.3 Conclusions.....	1.13
1.4 Data Base Limitations.....	1.19
References - Chapter 1.....	1.23
2. FISSION PRODUCT FORMATION.....	2.1
2.1 Atomic Nucleus and the Fission Process.....	2.1
2.2 Barriers to the Release of Fission Products.....	2.2
2.3 Health Hazards from Exposure to Fission Products.....	2.5
References - Chapter 2.....	2.10
3. ACCIDENT SEQUENCE CHARACTERISTICS.....	3.1
3.1 Design Features of Nuclear Power Plants.....	3.1
3.2 Accident Classifications.....	3.13
3.3 General Description of Accident Sequences.....	3.15
References - Chapter 3.....	3.22
4. FISSION PRODUCT RELEASE FROM FUEL.....	4.1
4.1 Fission Product Behavior in Fuel.....	4.1
4.2 Fission Product Release From Fuel Data.....	4.11
4.3 Estimated Total Releases during Postulated Accident Sequences.....	4.21
4.4 Effect of Zircaloy-UO <sub>2</sub> Interaction on Fission Product Release from Fuel.....	4.26
References - Chapter 4.....	4.30
5. CHEMISTRY OF CESIUM AND IODINE.....	5.1
5.1 Introduction.....	5.1
5.2 Fission Product Chemistry in the Vapor State.....	5.1
5.3 Aqueous Iodine Chemistry.....	5.13
References - Chapter 5.....	5.28

Table of Contents (continued)

	<u>Page</u>
6. FISSION PRODUCT TRANSPORT in PRIMARY SYSTEM to CONTAINMENT.....	6.1
6.1 The TRAP-MELT Code.....	6.1
6.2 Uncertainties Associated with TRAP-MELT Predictions.....	6.2
6.3 TRAP-MELT Accident Analysis.....	6.5
6.4 Effects of Iodine Species Distribution.....	6.19
6.5 Primary System Retention of Other Fission Products.....	6.19
References - Chapter 6.....	6.21
7. FISSION PRODUCT TRANSPORT THROUGH the CONTAINMENT.....	7.1
7.1 Transport and Deposition Rate Processes.....	7.1
7.2 Computer Models.....	7.3
7.3 Experimental Evaluation of Transport in Containment.....	7.6
7.4 Fission Product Behavior in Severe Core Damage Sequences....	7.12
7.5 Uncertainties and Parametric Studies.....	7.27
7.6 Radionuclide Transport Through the Containment Barrier.....	7.35
7.7 Radionuclide Transport Outside Containment.....	7.39
7.8 Effect of Radionuclide Source on Release from Containment...	7.40
References - Chapter 7.....	7.41
8. ENGINEERED SAFETY FEATURE EFFECTIVENESS.....	8.1
8.1 Engineered Safety Features and Their Design Basis.....	8.1
8.2 Loadings Imposed by Representative Accidents.....	8.3
8.3 Comparison of Accident Loads with Capabilities of Selected Engineered Safety Feature Systems.....	8.8
8.4 Summary and Conclusions Regarding the Performance of Engineered Safety Feature Systems.....	8.13
References - Chapter 8.....	8.15
 Appendices	
A. General Description of Core Meltdown Accident Sequences.....	A-1
B. Aerosol Release Calculations.....	B-1
C. Chemistry of Cesium and Iodine.....	C-1
D. Transport Calculations for the Reactor Coolant System.....	D-1
E. Deposition Models for Containment Transport Analysis.....	E-1
F. Response to Comments on Draft Report.....	F-1

## List of Figures

<u>Figure</u>		<u>Page</u>
2.1	A Fuel Rod.....	2.3
2.2	A Fuel Assembly.....	2.4
3.1	PWR Reactor Coolant System.....	3.2
3.2	PWR Nuclear Steam Supply System.....	3.4
3.3	Large, High Pressure Containment.....	3.6
3.4	Ice Condenser Design.....	3.7
3.5	BWR Nuclear Steam Supply System.....	3.8
3.6	BWR Mark I Containment Design.....	3.10
3.7	BWR Mark II Containment Design.....	3.11
3.8	BWR Mark III Containment Design.....	3.12
4.1	Release Rate Constants from Fuel - Noble Gases and Volatiles.....	4.19
4.2	Release Rate Constants from Fuel - Low Volatiles.....	4.20
4.3	Fission Product Release Rate Constants from Fuel - Smoothed Curves.....	4.22
4.4	The U-O-Zr Ternary Phase Diagram at 1500°C.....	4.28
4.5	The UO <sub>2</sub> - ZrO <sub>2</sub> Binary Phase Diagram.....	4.29
5.1	Relative Abundance of Iodine Species in the Iodine- Hydrogen-Oxygen System for the Conditions Given.....	5.6
5.2	The Fraction of Total Iodine That Exists as I <sub>2</sub> .....	5.19
5.3	The Fraction of Total Iodine That Exists as I <sub>2</sub> .....	5.20
5.4	Partition Coefficients for Aqueous Iodine Systems at Equilibrium.....	5.24
5.5	Partition Coefficients for Aqueous Iodine Systems before Iodate Formation Begins.....	5.25
6.1	Flow Diagram of Relationships Among Risk Assessment Codes...	6.3

<u>Figure</u>		<u>Page</u>
6.2	Influence of Steam Flow Rate on Iodine Escape from Primary System in a Terminated LOCA in a PWR.....	6.7
6.3	Aerosol Mass Concentration Reduction Predicted by 'QUICK' Code for Initial Mass Concentrations and Residence Times....	6.13
7.1	Estimated Accident and Experimental Conditions for Iodine Vapor Transport.....	7.9
7.2	Comparison of Estimated Accident and Experimental Conditions Influencing Aerosol Behavior.....	7.10
7.3	Comparison of Predicted and Experimental Airborne UO <sub>2</sub> Particle Concentrations for NSPP Experiment 204.....	7.11
7.4	Large Pipe Break with Delayed ECC Injection.....	7.15
7.5	Airborne Concentrations for Case with Sprays Operational....	7.20
7.6	Airborne Concentration for Case without Safeguards Operational.....	7.21
7.7	Effect of Containment Failure on Mass Leaked from Containment.....	7.23
7.8	Airborne Concentration for Case without Sprays but with Recirculation Filters.....	7.24
7.9	Effect of Particle Source on Mass Leaked from Containment...	7.28
7.10	Airborne Aerosol Concentrations Predicted for TMLB <sup>1</sup> with 1000 kg Aerosol Source.....	7.31
7.11	Airborne Aerosol Concentrations Predicted for TMLB <sup>1</sup> with 2000 kg Aerosol Source.....	7.32
7.12	Comparison Among HAARM-3, CORRAL-2, NAUA-4, and QUICK for Total Airborne Particulate.....	7.33
7.13	Effects of Source Aerosol on Airborne Concentration, HAARM-3 Code Calculations.....	7.34
7.14	Distribution of Particulate Mass After 3 Hours as Calculated by HAARM-3 for TMLB <sup>1</sup> .....	7.37
7.15	Distribution of Particulate Mass after 50 hours as Calculated by HAARM-3 for TMLB <sup>1</sup> .....	7.38
A.1	Low Pressure Recirculation System Schematic Diagram.....	A.9
B.1	MARCH Results for AB Sequence.....	B.5

<u>Figure</u>		<u>Page</u>
B.2	MARCH Results for S <sub>2</sub> C Sequence.....	B.6
B.3	Aerosol Source Term for AB Sequence.....	B.8
B.4	Aerosol Source Term for S <sub>2</sub> C Sequence.....	B.9
B.5	Aerosol Generated by Melt/Concrete Interaction in Sequence AB.....	B.13
C.1	Relative Abundance of Iodine Species in the Cesium-Iodine-Hydrogen-Oxygen System for the Conditions Given.....	C.6
C.2	Relative Abundance of Iodine Species in the Cesium-Iodine-Hydrogen-Oxygen System for the Conditions Given.....	C.7
C.3	Relative Abundance of Iodine Species in the Cesium-Iodine-Hydrogen-Oxygen System for the Conditions Given.....	C.8
C.4	Relative Abundance of Iodine Species in the Cesium-Iodine-Hydrogen-Oxygen System for the Conditions Given.....	C.9
D.1	Flow Paths, Fluid Velocities, and System Temperatures for a Sequence Involving Little or No Fuel Damage in a PWR.....	D.3
D.2	Influence of System Temperatures on Elemental Iodine Deposition on Primary System Internals in a Sequence Involving Minor or No Fuel Damage.....	D.4
D.3	Flow Paths, Control Volume Parameters, and System Temperatures for TMLB' in a PWR.....	D.5
D.4	Flow Paths, Control Volume Parameters, and System Temperatures for the Base Case AD (Cold Leg) in a PWR.....	D.12
D.5	Flow Paths, Control Volume Parameters, and System Temperatures for the AD (Cold Leg) in a PWR, with Altered Thermal Hydraulic Conditions.....	D.16
D.6	Flow Paths, Control Volume Parameters, and System Temperatures for the AD (Hot Leg) in a PWR.....	D.18
D.7	Flow Paths, Control Volume Parameters, and System Temperatures for the TC in a BWR.....	D.22
D.8	Flow Paths, Control Volume Parameters, and System Temperatures for the AE (Wet) in a BWR.....	D.24
E.1	HAARM-3 Calculation Results for Aerosol Concentration and Leaked Aerosol Mass.....	E.11
F.1	Major Comments.....	F.2-F.3

## List of Tables

<u>Table</u>		<u>Page</u>
1.1	Radionuclide Contribution to Risk.....	1.6
2.1	Important Radioactive Nuclides.....	2.9
3.1	ANS Classification of Sequences.....	3.14
4.1	Iodine, Xenon, and Cesium Fission Product Isotopes Showing Yields and Half-lives.....	4.2
4.2	Characteristics of Some Key Materials.....	4.6
4.3	Summary of Iodine Release Species in Lorenz's Experiments...	4.12
4.4	Summary of Aerosol Release Estimates.....	4.25
4.5	Comparison of Fraction Release Estimates.....	4.25
5.1	Vapor Forms of Fission Products.....	5.3
5.2	Equilibrium Concentration and Partition Coefficients of Aqueous Iodine Species.....	5.17
5.3	Equilibrium Concentration and Partition Coefficients of Aqueous Iodine Species.....	5.18
5.4	Hypothetical Concentrations of HOI.....	5.21
6.1	Summary of TRAP Predictions of Iodine Distribution Among the Four States at the End of the Accidents Considered.....	6.12
7.1	Comparison of Containment Codes.....	7.7
7.2	Source Terms for Full Core Meltdown.....	7.16
7.3	Summary of Predicted Releases in Accidents Involving Severe Core Damage.....	7.17
7.4	Computer Calculation Results for Hypothetical Accident Conditions.....	7.29
7.5	Uncertainty Spread for Predicted Release Fractions.....	7.30
7.6	Distribution of Aerosol Particulates for TMLB' as Calculated by HAARM-3.....	7.36
8.1	Containment Parameters Used to Evaluate ESFs in PWRs Using a Large High Pressure Containment.....	8.4

<u>Table</u>	<u>Page</u>	
8.2	Containment Parameter Used to Evaluate ESFs in PWR Ice Condensers and BWR Pressure Suppression Containments.....	8.6
A.1	Key to PWR Accident Sequence Symbols.....	A.2
A.2	Key to BWR Accident Sequence Symbols.....	A.3
B.1	Approximations of the Fraction Release Coefficient $K = Ae^{BT}$	B.2
B.2	Fraction of Core Within 200°F Temperature Interval as Function of Time for Sequence AB, Temperature, °F ± 100.....	B.3
B.3	Fraction of Core Within 200°F Temperature Interval as Function of Time for S <sub>2</sub> C, Temperature, °F ± 100.....	B.4
B.4	Aerosol Concentration (g/m <sup>3</sup> ) [A] = exp (-19000/T (24V + 3.3) 1000.....	B.11
B.5	Results of Melt/Concrete Interaction Calculations.....	B.12
C.1	Temperature at Which Partial Pressure Equals Vapor Pressure.	C.3
C.2	Postulated Conditions for CsOH Reaction with Stainless Steel	C.4
C.3	Selected Thermodynamic Data for Major Vapor Species.....	C.5
C.4	Reaction Rate Constants (hr <sup>-1</sup> ) for Methyl Iodide Reacting with Water, K <sub>7</sub> , and Hydroxide, K <sub>8</sub> , at 25 and 100°C.....	C.19
D.1	Input Thermal Hydraulic Conditions Used in TRAP for TMLB' Base Case Calculations.....	D.6
D.2	TRAP Predictions of the Distribution of Fission Product Iodine Among the Various States During Accident Sequence TMLB'-1 (Base Case).....	D.7
D.3	TRAP Predictions of the Distribution of Fission Product Iodine Among the Various States During Accident Sequence TMLB'-2 (Large Size Particle Source).....	D.8
D.4	TRAP Predictions of the Distribution of Fission Product Iodine Among the Various States During Accident Sequence TMLB'-3 (Weak Particulate Source).....	D.9
D.5	Input Thermal Hydraulic Conditions Used in TRAP for TMLB' With Altered Thermal-Hydraulics.....	D.10
D.6	TRAP Predictions of the Distribution of Fission Product Iodine Among the Various States During Accident Sequence TMLB'-4 (Altered Thermal Hydraulic Conditions).....	D.11

<u>Table</u>		<u>Page</u>
D.7	TRAP Predictions of the Distribution of Fission Product Iodine Among the Various States During Accident Sequence AD-1 (Base Case).....	D.13
D.8	TRAP Predictions of the Distribution of Fission Product Iodine Among the Various States During Accident Sequence AD-2 (Large Size Particle Source).....	D.14
D.9	TRAP Predictions of the Distribution of Fission Product Iodine Among the Various States During the Accident Sequence AD-3 (Weak Particulate Source).....	D.15
D.10	TRAP Predictions of the Distribution of Fission Product Iodine Among the Various States During Accident Sequence AD-4 (Altered Thermal Hydraulic Condition).....	D.17
D.11	TRAP Predictions of the Distribution of Fission Product Iodine Among the Various States During Accident Sequence AD (Hot Leg).....	D.19
D.12	TRAP Predictions of the Distribution of Fission Product Iodine Among the Various States During First 472 s of Accident Sequence S <sub>2</sub> D Initiated by a Break in the Surge Line.....	D.20
D.13	TRAP Predictions of the Distribution of Fission Product Iodine Among the Various States During Accident Sequence AB Initiated by a Break in the Surge Line.....	D.21
D.14	TRAP Predictions of the Distribution of Fission Product Iodine Among the Various States During Accident Sequence TC.....	D.23
D.15	TRAP Predictions of the Distribution of Fission Product Iodine Among the Various States During Accident Sequence AE (Wet).....	D.25
E.1	Scrubbing Factors as Function of Rise Time and Bubble Size..	E.13
E.2	Particle Scrubbing Factors as Function of Particle Size.....	E.14
E.3	Accident Events as a Function of Time as Used for Calculation.....	E.16-E.18
E.4	Dimensions of Various Reactors Used for Calculation.....	E.19
E.5	Input Information on Spraying.....	E.20

## TECHNICAL BASES FOR ESTIMATING FISSION PRODUCT BEHAVIOR DURING LWR ACCIDENTS

### 1. INTRODUCTION, SUMMARY AND CONCLUSIONS

This chapter presents a summary of the work carried out in this study, its findings and conclusions, and identifies the important gaps in the data base used for estimating fission product behavior during light water reactor (LWR) accidents. The historical perspective and background leading up to this report are also provided along with a brief discussion on the scope of the study.

#### 1.1 Introduction

Since the inception of commercial nuclear power plant operation, individuals involved with nuclear safety have been concerned with the possible magnitude of the public consequences of severe accidents in commercial light water reactor plants. Over the past 25 years a continually developing understanding of reactor accident phenomena and the mechanisms affecting the release of radionuclides during reactor accidents has allowed more detailed and realistic estimates to be made of the hazards from operation of commercial nuclear power plants.

The objective of this report is to provide the Nuclear Regulatory Commission and the public with a description of the best technical information currently available for estimating the release of radioactive material during postulated reactor accidents, and to identify where gaps exist in our knowledge. This report focuses on those low probability-high consequence accidents involving severe damage to the reactor core and core meltdown that dominate the risk to the public. Furthermore, in this report particular emphasis is placed on the accident behavior of radioactive iodine since: (1) radioiodine is predicted to be a major contributor to public exposure, (2) current regulatory accident analysis procedures focus on iodine, and (3) several technical issues have been raised recently about the magnitude of iodine release. The generation, transport, and attenuation of aerosols were also investigated in some detail to assess their effect on fission product release estimates and to determine the performance of engineered safety features under accident conditions exceeding their design bases.

The Nuclear Regulatory Commission is currently involved in deliberations directed at determining the need for fundamental changes to regulatory policies which have guided nuclear plant design and siting over the past 25 years. In particular, the Commission has initiated rulemaking actions for determining requirements for reactor sites and emergency plans, for determining which aspects of very severe accidents should be considered when licensing a plant, and for determining what types of engineered safety features should be required in commercial plants. The magnitude of the potential hazard to the public from the accidental release of radioactive material has a direct impact on the need for, and benefits of, certain features being considered in the above rule-

making actions. This report is intended to provide information which can be used as a basis for decisions in these areas. The information presented in this report has been used in support of a companion NRC staff report "Regulatory Impacts of Nuclear Reactor Accident Source Term Assumptions."<sup>1.1</sup> The Regulatory Impacts Report assesses the impact on regulatory requirements of potential source term modifications arising from changes to assumptions about the chemical forms of fission products and the amount of attenuation of fission products within the plant during severe accidents.

### 1.1.1 Historical Perspective

In March 1957, a report (WASH-740)<sup>1.2</sup> was issued which attempted to provide realistic upper bounds of the potential public hazards resulting from certain severe hypothetical accidents. Since a definitive understanding of all the physical processes associated with accident phenomena was lacking at that time, pessimistic values were used for many factors influencing the magnitude of the estimated accident consequences. Two particular limitations were the inability at that time to estimate the probabilities of various severe accident sequences resulting in multiple failures of the barriers to fission product release and to quantitatively describe the physical mechanisms governing the release and transport of radionuclides from the core to the environment during severe accidents.

In late 1958, the Atomic Energy Commission staff began efforts to develop criteria to guide the selection and evaluation of reactor sites. These efforts culminated in April 1962, with the issuance of 10 CFR Part 100.<sup>1.3</sup> Under Part 100, the quantitative analysis of one postulated accident is required as a key test of facility/site suitability. This accident is a "major accident, hypothesized for purposes of site analysis or postulated from consideration of possible accidental events, that would result in potential accidental hazards not exceeded by those from any accident considered credible". The maximum credible accident at the time of the writing of Part 100, was considered to be a core melt with the containment barrier functional but pressurized to that value resulting from a large pipe rupture. Part 100 does not provide specific criteria or guidelines regarding the various assumptions to be made on the magnitude of the fission product release from the fuel, fission product transport within the facility, or removal of fission products by natural or engineered safety features. However, Part 100 did refer to a procedural method and sample calculation (TID-14844)<sup>1.4</sup> that could be used to satisfy the requirements of Part 100.

In TID-14844 a set of acceptable assumptions for estimating the consequences of the maximum credible accident for the purpose of judging the suitability of the proposed reactor site was presented. The major assumptions contained in TID-14844 regarding the fission product source term were that 100 percent of the core noble gas inventory, 50% of the halogens and 1% of the solid fission products would be released into the reactor containment. In addition, TID-14844 provided assumptions for containment leakage and the atmospheric transport of the fission products. However, as stated in TID-14844, it was recognized that the procedures and results specified in TID-14844 were "approximations, sometimes

relatively poor ones, to the results which would be obtained if the effects of the fullplay of all the variables and influencing factors could be recognized and fixed with certainty--an impossibility in the present state of the art".

The choice of the maximum credible accident to be a contained core melt accident appears to have been influenced by a number of factors. Most notably were the probability estimates developed from "the best judgement of the most knowledgeable experts" which were presented in WASH-740. In that report the likelihood of accidents which would release significant amounts of fission products outside the reactor vessel but not outside the containment building was estimated to range between one chance in 1,000 to one in 10,000 per reactor year. Estimates for the likelihood of accidents which would release major amounts of fission products outside containment ranged from 1 chance in 100,000 to one chance in 1 billion per reactor year.

At the time 10 CFR 100 and TID 14844 were developed the maximum size of reactors in operation was small (~500 Mwt) and it was generally believed that a reactor containment building would remain intact even in the event of a core melt accident. As reactor designs grew larger over the years the need for engineered safety features to cool the core and prevent core heatup and melting in the event of a loss of coolant accident (LOCA) became apparent since the ability of the containment to remain intact during core melt accidents could not be assured. As a result, in the late 1960s Emergency Core Cooling (ECC) systems were required for all new plants and the successfully terminated LOCA accident became the design basis for many containment systems. However, even with the incorporation of ECC systems into plants, the maximum credible accident assumptions for fission product release which were based on core melting still were applied for the Part 100 site suitability dose calculations. The fission product release assumptions for the maximum credible accident given in TID-14844 (and later in Regulatory Guides 1.3 and 1.4) are for a hypothetical accident which is more severe than a successfully terminated LOCA accident.

Since the inception of Part 100, it has been the policy of the Commission to allow for the compensation of unfavorable site characteristics by the incorporation of appropriate and adequate compensating engineered safety features. Features which have been incorporated into plants to reduce the radiological consequences of accidents include improved containments, containment spray systems, and internal filter systems. The design basis fission product release source term for determining the adequacy of these systems became the assumptions and procedures originally delineated in TID-14844.

In October 1975, the Reactor Safety Study<sup>1.5</sup> (WASH 1400) was issued. The objective of the Reactor Safety Study was to provide realistic estimates of the public risks from potential accidents in commercial nuclear power plants. In order to quantitatively assess the risks from nuclear power plant accidents, analytical methods for determining both the probabilities and consequences of accidents were developed. Event trees, and fault trees were used to define important accident sequences and to quantify the reliability of engineered systems.

## 1.4

Detailed investigations were performed to realistically predict the release of fission products to the environment (and the public consequences) for various accident sequences. The major areas which were investigated included fission product release from the reactor fuel under various accident conditions, and fission product behavior within the reactor containment building. Calculations were performed for a number of accident sequences and the results of these calculations were used to define a series of release categories into which all of the identified accident sequences could be distributed. A major conclusion of the Reactor Safety Study was that the low probability-high consequence accidents involving core meltdown, containment failure, and failure of the plant engineered safety features dominated the risk to the public.

### 1.1.2 Recent Developments

Development of the "Technical Basis Report" was prompted by several recent events. On August 14, 1980, a letter<sup>1.6</sup> was sent to NRC Chairman Ahearn from three scientists at Oak Ridge National Laboratory (ORNL) and Los Alamos Scientific Laboratory (LASL). In this letter these scientists questioned the validity of the currently accepted methods for estimating the release of radioiodine under certain accident conditions and indicated that they believed that the "risk to the general public presented by iodine is lower than estimated, perhaps by orders of magnitude for these accidents". (The accident specifically referred to in this letter was an accident "in which substantial amounts of water are present" and "reasonable containment integrity is maintained".)

In their letter these scientists proposed that under accident conditions in LWR reactors the expected chemical form (CsI) of the iodine released from the fuel would be much less volatile than the molecular iodine form which is currently assumed. Since CsI is much less volatile than molecular iodine and is also very soluble in water, they believe that much less iodine would escape during LWR accidents. They cite the experience at TMI-2 and from past accidents and destructive tests in experimental reactors to support their proposals. Regarding the accident at the Windscale reactor<sup>1.7</sup> in which relatively large quantities of radioiodine was released they note that the presence of oxidizing conditions during the accident (as evidenced by uranium and graphite combustion) and the absence of water resulted in molecular iodine formation and, consequently, the large releases. These conditions would not be typical of an accident in a LWR. These scientists also recommend that the engineered safety features designed for iodine control be reexamined to assure effectiveness and optimization for actual iodine behavior rather than the behavior currently assumed.

A second letter<sup>1.8</sup> was sent to Commissioner Hendrie on September 2, 1980, from Chauncey Starr, Vice Chairman of the Electric Power Research Institute (EPRI). In this letter, and the attached papers, arguments are presented to show that "the theoretical source term traditionally used in nuclear risk evaluations is one to two orders of magnitude greater than the realistic magnitude which might actually result from the ultimate accidents". In the

first paper enclosed with this letter, Levenson and Rahn state that natural processes including "chemical reactions, aerosol settling, effects of moisture, etc." prevent a public catastrophe from occurring independent of the operation of engineered safeguards. They further state that the current methods for estimating the consequences of severe accidents do not adequately account for these intrinsic natural removal processes that will act to limit the release of radioactive materials from a plant.

Principally as a result of these two letters a Commission meeting was held on November 18, 1980, with the authors of these two letters, the NRC staff, and other interested persons to discuss the behavior of iodine and to determine the adequacy of current methods for estimating the release of fission products during reactor accidents.

Following the Commission meeting, Chairman Ahearne met with the NRC staff to review the perceived gaps and uncertainties in our state of knowledge. He then directed the staff to develop plans to resolve the issues, the first step being the preparation of this report and a companion document describing potential regulatory impacts.

On December 21, 1980, the Nuclear Safety Oversight Committee (NSOC) sent a letter<sup>1.9</sup> to President Carter noting recent questions regarding iodine release which should be answered by analyses and experimentation on an expedited basis. This report is responsive to the NSOC recommendation.

### 1.1.3 Iodine Risk Perspective

Although much of the discussion leading to this report, as well as the report itself, emphasize radioiodine accident behavior, it is important to emphasize that iodine is not the sole radionuclide of importance in nuclear accident analyses. An assessment of the relative importance of iodine has been obtained from sensitivity studies which are discussed in the companion "Regulatory Impact Report." These studies analyzed the consequences of the risk dominant accidents in the Reactor Safety Study, (i.e., those which resulted in core meltdown and large atmospheric releases of radioactive material). The results of these analyses indicated that a relatively few fission product species are responsible for most of the consequences of these severe accidents - most notably iodine, cesium, tellurium, and ruthenium. Table 1.1 summarizes the results of this study. Radioactive iodine contributes roughly one-half of the dose resulting in early fatalities and illnesses, but only about five percent of the dose resulting in latent cancers. Cesium isotopes have a very strong influence on calculated property damage, but a less strong (but still important) influence on health effects. An important conclusion of this work was that because of the contribution of a number of radionuclides, reductions in severe accident consequence predictions can only be realized by the systematic reduction in the predicted atmospheric releases of all of the significant radionuclide species.

TABLE 1.1 RADIONUCLIDE CONTRIBUTION TO RISK

	Iodine	Other Radionuclides
Early Fatalities	50%	50%
Early Injuries	30%	70%
Cancers (Man-Rem)	<10%	>90%
Property Damage	<<10%	>>90%

#### 1.1.4 Scope

As stated previously, the objective of this report is to provide a description of the best available technical bases for estimating the release of fission products during postulated severe LWR accidents, and to identify where gaps exist in our knowledge. The scope of this study includes (1) evaluations of the data base related to the physical and chemical behavior of fission products, and (2) analyses of the important physical and chemical processes using state-of-the-art methods, in order to determine the magnitude of fission product attenuation at various points along the pathway from release from the fuel to its potential release from containment. This analysis was performed for a spectrum of accidents with a wide range of environmental conditions, degrees of core damage, and failed engineered safety features.

Schedule constraints imposed on the study required the following limitations on the scope of this study:

- (1) Systematic analysis of fission product transport from the fuel to the environment, for each accident sequence, was not performed during this study. Because of the short period of time available to complete the study it was not possible to calculate fission product release rates from fuel, then calculate fission product behavior in the reactor coolant system, and then containment fission product behavior. Since each of these tasks were required to proceed in parallel, the reactor coolant system and containment analysis was performed parametrically.
- (2) Consequently, a revised set of recommended quantitative source terms for the release of fission products from the plant is not provided. Further, the detailed analyses needed to quantify the uncertainties and sources of the uncertainties in the calculations in this report were not performed. These analyses will be performed in follow-on studies to this report.

- (3) In some cases only a cursory examination of the transport behavior of potentially important fission product species (e.g. Te, Ru, Sr) other than cesium and iodine has been made. In particular, the chemistry of these other fission products under accident conditions was not examined in detail.
- (4) Only a limited number of severe accident sequences could be evaluated. Although these cases were chosen to cover a broad range of potential accident conditions including thermal hydraulics conditions, leak pathways, chemical conditions, and types of engineered safety features in operation, the full range of possible conditions appropriate to all LWR plant designs for all accident conditions may not be adequately covered.
- (5) A number of physical processes which may have the potential to significantly affect fission product behavior were not evaluated in depth either because of a lack of a physical understanding of the processes involved or lack of applicable data. Examples of these include the effects of hydrogen combustion within containment on the physicochemical form of the airborne fission products and aerosols and the potential for fission product attenuation in the leak path through the containment structure.
- (6) Except for the use of a TMI-2 type accident within the spectrum of accident sequences evaluated in this study, fission product behavior during previous reactor accidents and destructive tests were not analyzed in this report. An evaluation of these accidents was not attempted because of the paucity of detailed information on these accidents resulting from insufficient instrumentation, uncertainties in the physical and chemical conditions, and absences of detailed fission product mass balances; all of which are required for detailed modeling and analysis. Detailed analyses of such experience may be of limited value for the aforementioned reasons, and because of the dissimilarities in reactor design and accident conditions for these accidents, and postulated accidents in commercial LWR nuclear plants. However, because of the wide interest in this subject the NRC will conduct analyses of fission product behavior during past reactor accidents as follow-on work to this report. The companion "Regulatory Impact Report" did briefly review previous accidents, for insights into fission product behavior.
- (7) Fission product release and transport behavior during accident sequences where steam explosions are postulated to occur (which either fail or do not fail containment) were not addressed in this study. Recent experimental and analytical studies indicate that containment failure caused by steam explosions are significantly less probable than indicated in the Reactor Safety Study. However, this work also indicates that steam explosion events which do not fail containment appear quite likely. The effect of steam explosions, which do not fail containment, on the release and transport

behavior of fission products may be significant and will be addressed in ongoing studies.

Although it was not possible to rigorously examine the effect of these limitations on the results of this study, we believe that the overall results obtained would not have been dramatically altered if these limitations were not present.

#### 1.1.5 Report Structure

The report is structured such that succeeding chapters describe distinct physical processes which affect the potential release of fission products from the containment. Detailed technical discussions, supporting calculations, and responses to the major comments on the report are contained in appendices located at the end of the report.

A summary of the report, the major conclusions, and the more important data limitations are presented in Chapter 1.

In Chapter 2 a brief description of the fission process and the generation of radioactive fission products in the core is presented. A description of the physical barriers to the release of radionuclides from the plant is presented. The health hazards resulting from exposure to radionuclides are also discussed.

Chapter 3 presents a description of a number of specific accident sequences which are typical of postulated severe core damage and core meltdown accidents in LWRs and which were used in subsequent chapters to estimate fission product behavior.

Chapter 4 describes the release of fission products and non-radioactive aerosols to the reactor coolant system following a loss of coolant accident and core heatup. Release of fission products and aerosols during the interaction of molten fuel with concrete in the lower cavity following reactor vessel failure is also discussed.

Chapter 5 presents a discussion of fission product chemistry under accident conditions. This chapter is divided into two parts: the chemistry of fission products in aqueous reactor coolant solutions and the chemistry of fission products in mixtures of high temperature steam, air and hydrogen gas.

Chapter 6 describes the transport behavior of fission products and aerosols within the reactor coolant system following release from the fuel. The effect of the assumed physicochemical form of the released radionuclides is evaluated parametrically.

Chapter 7 describes the processes which could affect fission product transport within the reactor containment building. The effects of both natural and engineered safety feature fission product removal mechanisms are evaluated. Particular emphasis is placed on evaluating the effect of aerosol agglomeration and settling.

In Chapter 8 the effect of different iodine physicochemical forms on the performance of engineered safety features is addressed. In addition the performance of ESF system under the severe environmental conditions associated with severe core damage and core melt accidents is evaluated.

## 1.2 Summary

### 1.2.1 Fission Product Formation (Chapter 2)

This chapter provides background information on: how radioactive material is generated within a nuclear reactor; what barriers to its escape into the environment are included in a plant's design; and what types of radioactive material are judged to represent the most serious health hazards.

### 1.2.2 Accident Sequence Characteristics (Chapter 3)

In the chapter on accident sequence characteristics, the general concepts of pressurized and boiling water reactors are discussed and specific systems within these plants which can be important to safety under accident conditions are described.

A variety of accident sequences are possible that have a wide range of consequences depending upon the extent of core damage, conditions in the reactor coolant system and the operability of containment safety features. In order to provide a basis for evaluating fission product behavior a number of specific accident sequences were selected for analysis. These accidents have been chosen to provide an envelope of environmental conditions for the detailed fission product behavior analyses described in later chapters. These postulated accident sequences range from controlled loss-of-coolant accidents through "TMI-like" accidents to the extreme cases which involve core melt, containment failure, and failure of the plant engineered safety features.

### 1.2.3 Fission Product Release From Fuel (Chapter 4)

In the chapter on fission product release from the fuel (1) the evidence regarding the chemical form of iodine in the fuel is examined, (2) fission product release-from-fuel experiments are reviewed, and release data from three experimental programs are compared in terms of a release rate coefficient, (3) employing these evaluated data, total releases of fission products and aerosols from the core are estimated for two accident sequences, and (4) the qualitative effect of high temperature  $UO_2$ -Zircaloy cladding reactions on fission product release is postulated.

Fission product behavior within the fuel matrix and the mechanisms responsible for the movement of individual atoms through the  $UO_2$  fuel matrix are discussed. The chemical form of cesium and iodine that escape from the fuel matrix to the fuel-cladding gap region appear to be determined by a complex set of reactions which occur between the  $UO_2$  and the cesium and between Cs and I. Previous thermodynamic calculations of  $UO_2$ -Cs-I systems are discussed. In addition, observations regarding the state of cesium and iodine

in fuel pellets is reviewed. This review included: (1) measured concentration profiles and the observed solid phases in discharged fuel, (2) thermomigration experiments performed using fresh  $UO_2$  and simulated fission products, and (3) fission product release experiments.

Five principal mechanisms which control the rate of release of fission products from LWR fuel under accident conditions are discussed. They are: (1) burst release, (2) diffusional release of the pellet-to-cladding "gap" inventory, (3) grain boundary release, (4) diffusion from the  $UO_2$  grains, and (5) release from molten material.

Release rates for important fission product and structural material aerosols as a function of temperature were developed based on the results from three sets of experiment data. Release rates from fuel for the noble gases, Cs, I, Te, Ag, Sb, Ba, Sr, Zr, and Ru are expressed in terms of a release rate coefficient,  $k$ , defined as the fractional release of current inventory per minute. These release rates were in turn used to generate estimates for the release of fission products and aerosols for the in-vessel heatup and melting phase of two core melt accident sequences. These estimates are then compared to the "melt" release fraction estimates presented in the Reactor Safety Study. Aerosol release rates during the interaction of the molten core with the concrete in the lower reactor cavity were estimated using a correlation which was based on observations made during one small scale (20 kg) melt-concrete interaction test, and two larger scale (200 kg) tests.

The effect of the formation of low melting point  $UO_2$  phases on fission product release resulting from interactions with the Zircaloy cladding is addressed.

#### 1.2.4 Chemistry of Cesium and Iodine (Chapter 5)

The discussion in the chapter on fission product chemistry focuses on species of cesium and iodine that could be formed in a steam or water environment in the reactor coolant system or containment. In water, the soluble fission products are ionized. In the high temperature vapor state the fission products are present as atoms or molecules and when reacted with other vapors they form atomic or molecular species. Because the chemical nature of the ionized fission products in water is quite different than the chemical nature of molecular or atomic species in the vapor state, the two chemistries are discussed in separate sections in this chapter.

The vapor phase behavior of fission products depends critically on the particular molecular forms that exist. In the chapter on fission product chemistry the predominant fission product vapor species which might exist and the conditions which affect the stability of these species were examined parametrically.

Chemical equilibrium thermodynamic calculations were performed on four high temperature vapor systems to determine system compositions resulting from the reactions of fission products with steam, hydrogen, oxygen and other

fission products. The four systems considered were: (a) iodine in the presence of steam and hydrogen or oxygen (I-H-O), (b) cesium in the presence of steam and hydrogen or oxygen (Cs-H-O), (c) tellurium in the presence of steam and hydrogen or oxygen (Te-H-O), and (d) cesium and iodine in the presence of steam and hydrogen or oxygen (Cs-H-I-O). For each of these systems the fission product chemistry was calculated over the following range of conditions:

Temperature - from 600°C to 2300°C

Pressure - 1 bar (about 14.7 psi) and 150 bar.

Fission Product (FP) concentrations in the steam.  
[FP to water ratio, FP (moles)/H<sub>2</sub>O (moles),]

FP/H<sub>2</sub>O -  $2 \times 10^{-7}$  to  $2 \times 10^{-1}$

Oxidizing, inert and reducing atmospheres.

The vapor phase equilibrium concentration of fission product species can be changed if either condensation on surfaces or chemical reactions with surfaces occur. These effects are discussed, as are the possible effects of radiolysis on fission product vapor phase chemistry.

The section on aqueous iodine chemistry includes discussions of: (1) reduction-oxidation reactions of iodine species, (2) hydrolysis and disproportionation reactions, (3) organic iodide formation and reactions, (4) radiation effects on aqueous iodine species and (5) liquid-gas phase partitioning.

The mechanisms of the formation of organic iodine (CH<sub>3</sub>I) and the reactions of CH<sub>3</sub>I with aqueous solutions are reviewed. The effect of radiolysis on iodine aqueous chemistry is discussed. Also discussed are chemical reactions which influence the partitioning of iodine between the aqueous phase and the surrounding vapor phase. Equilibrium aqueous systems where the I<sub>2</sub>-H<sub>2</sub>O reactions produce HOI, I<sup>-</sup> and IO<sub>3</sub><sup>-</sup> are considered. Total iodine partition coefficients for solutions at 25 and 100°C with total iodine concentrations from 10<sup>-9</sup> to 10<sup>-4</sup> M and pH values of 5 to 10 have been calculated.

#### 1.2.5 Fission Product Transport in Primary System to Containment (Chapter 6)

The pathway for transport of fission products and other materials from the fuel to the containment building consists of various portions of the primary system prior to melthrough of the reactor pressure vessel. As they move along this pathway, fission products may be deposited to an extent dependent on the accident sequence and the resulting conditions along the flow path. In order to assess the importance of this deposition and to evaluate the effects of fission product chemical and physical form, transport calculations have been made for various assumed accident sequences and various assumed source terms.

The calculations of radionuclide transport in the primary system employed the TRAP-MELT code. Transport through and retention within LWR primary systems are treated in terms of an appropriate number of control volumes for which the physical conditions are specified by thermal hydraulic codes for the accident sequences of interest. In each of the control volumes radionuclide species can exist in either particulate or gaseous form. These species are assumed to be well mixed within each volume and to transport with the hydrodynamic flow between control volumes. Mass transfer coefficients describe the rates of transport of each species between the physical forms and to surfaces within the volumes. Calculations of aerosol coagulation within the reactor coolant system were performed using the QUICK code.

#### 1.2.6 Fission Product Transport Through the Containment (Chapter 7)

Fission products will enter the containment on release from the primary coolant circuit and will be transported and deposited within the containment before being released to the environment through leak paths or a failed containment. Since these processes are influenced by the assumed accident sequence, a variety of sequences have been used as bases for calculations of radionuclide transport to demonstrate major effects of containment conditions and to evaluate the effects of radionuclide source characteristics.

Radionuclides introduced into the containment building are subject to various natural and engineered removal processes. The important natural processes are: radionuclide phase change, vapor sorption, transport due to convective flow, diffusion of vapors and particles to the containment walls, and the sedimentation, thermophoresis, diffusiophoresis, and agglomeration of aerosol particles. The engineered safety systems that are designed to, or act to, reduce the concentration level in the containment building include for example, aqueous sprays, recirculating or once-through filters, pressure suppression pools and ice condensers. To the extent that physical models of the mechanisms are included in available computer codes or are available individually, calculations based on these mechanisms are used to illustrate and estimate transport and deposition in the containment. The computer codes employed in these analyses included CORRAL-2, HAARM-3, QUICK, and NAUA.

The available experimental data used both to develop and to verify the various containment transport and deposition codes are summarized for iodine, and dry aerosol behavior. The range of data are compared with ranges for postulated PWR and BWR accidents, for aerosol mass concentration and vessel size. Comparisons of aerosol behavior code predictions with experimental results for several regimes of mass concentrations are presented.

#### 1.2.7 Engineered Safety Feature Effectiveness (Chapter 8)

Eight representative engineered safety feature (ESF) systems were studied in order to determine their performance when under various accident conditions. These systems are:

- (1) Containment Leakage Requirements

- (2) Containment Sprays
- (3) Containment Recirculating Filter Systems
- (4) Auxiliary Building Filter Systems
- (5) Main Steam Line Isolation Valve (MSIV)  
Leakage Control Systems (BWR)
- (6) Pressure Suppression Pools (BWR)
- (7) Standby Gas Treatment Systems (BWR)
- (8) Pressure Suppression By Ice (PWR)

A range of classes of postulated accidents (identified in Chapter 3) were considered.

Existing ESF systems were designed using iodine and noble gas source terms defined in NRC Regulatory Guides. A key objective of this study was to evaluate how these systems would perform with a realistically-chosen source term. While it was recognized that severe accidents would impose loads which are well beyond the design basis for these systems, such accidents were considered to help identify those ESFs which provide appreciable benefits for a spectrum of severe accidents.

### 1.3 Conclusions

The major conclusions from the principal chapters in the report are summarized in the following sections.

#### 1.3.1 Fission Product Release From Fuel (Chapter 4)

Several different approaches were used in an attempt to ascertain the chemical form of iodine in the fuel pellet. Observed cesium and iodine radial concentration profiles in discharged fuel were inconclusive. Results from out-of-pile thermomigration experiments using fission product simulants were contradictory; one concluding that cesium iodide did form while another concluding that it did not. Similarly, observations of release rates of iodine and cesium relative to the noble gases, which could conceivably provide an indication of the nature of the released iodine species, also lead to unclear results.

The experiments of Lorenz et al., fortunately did include a rather crude iodine species identifier. In several of these tests, when helium was used as the carrier gas, more than 90% of the released iodine was apparently cesium iodide. However, in tests using steam, the percent of the released iodine identified as cesium iodide ranged from 4 to 90% with the balance as the molecular species and as particulates. Several reasons for low cesium iodide release fractions in some of the steam runs are discussed (e.g., reactions with the test apparatus, reactions with trace oxygen contaminants in the steam), but are not conclusive.

Results of equilibrium thermodynamic calculations for the chemical form of Cs and I in the fuel-cladding gap (for temperatures up to about 950°C) indicate that the predominant form of iodine would be CsI, and the other major form of cesium would be a compound of cesium, uranium, and oxygen (cesium uranate).

In general, the fission product release-from-fuel experiments show significantly different results for fission product release from elevated temperature fuel, mainly due to differing experimental materials, techniques, and gaseous environments. Early tests, which provided most of the data base for the Reactor Safety Study (RSS) estimates, were conducted in helium and air on low-irradiated, nonclad  $UO_2$ . Later studies indicated that release rates in steam could be significantly higher than similar tests conducted in air, that some fission products (mainly iodine) appear to be retained at lower temperatures by the presence of zircaloy cladding, and that low and trace-irradiated fuel exhibits lower release rates than fully irradiated fuel. These plus other experimental differences contribute to a wide scatter in release rate data.

Fission product release rate estimates were developed and applied to two postulated accident sequences -- one a large pipe break event with simultaneous electrical failure which results in rapid core heat-up, and the second a small pipe break with delayed meltdown -- to determine core-wide fission product releases. For the first case (rapid heat-up), it is estimated that release of noble gases, cesium and iodine from the fuel is virtually complete in 18 minutes while complete removal occurs in 60 minutes for the slower heat-up case.

The new release estimates for the large pipe break accident were compared with the "melt" release fraction estimates made in the RSS. Although in general agreement for cesium and iodine, this study estimated significantly higher in-vessel releases for Te, Sb, Ba and Sr than did the RSS.

The uncertainty of the predicted release rates is estimated at plus or minus one order of magnitude. However, this uncertainty pertains to the rate of release from the fuel; there is less uncertainty regarding the total amounts released.

Total aerosol releases were calculated for both cases. For the large pipe break the total amount of aerosol released up to the time of reactor core support plate failure was calculated to be 770 kg. The total aerosol release for the small pipe break was 1450 kg at the time of core support plate failure. This analysis also indicates that the cesium and iodine will be essentially completely released prior to the bulk of the remainder of the aerosols indicating that the fission products and structural materials will be initially nonhomogeneously distributed in the aerosol source.

For both cases, the amount of aerosol material generated by core/concrete interaction was estimated. The highest calculated aerosol release from melt/concrete interactions was ~510 kg and occurred for the large pipe break event. Most of these aerosols are from non-radioactive structural materials and are released during the first one-half hour following contact of the molten core with the concrete.

### 1.3.2 Chemistry of Cesium and Iodine (Chapter 5)

The equilibrium thermodynamic calculations for the cesium-iodine-hydrogen-oxygen gas system indicate that three iodine containing species are dominant

(I, CsI and HI). Monatomic (elemental) iodine dominates only in oxidizing atmospheres. In reducing atmospheres and at lower temperatures CsI dominates. As temperature is increased, CsI begins to dissociate with the iodine transforming to I and/or HI. Under most LWR accident conditions CsI (or HI) would be the expected chemical form of iodine in the vapor phase in the primary system, although the formation of some elemental iodine cannot be precluded for certain accident conditions.

The major cesium containing species are CsOH, CsI and Cs (monatomic cesium vapor). In oxidizing environments the CsOH molecule is stable at all temperatures and pressures examined. However in the reducing conditions expected in the core during reactor accidents Cs vapor can become an important species at higher temperatures. The abundance of Cs is greatly enhanced when large excesses of hydrogen are present.

Chemical equilibrium calculations for the tellurium-hydrogen-oxygen system showed that, in reducing atmospheres, the major vapor species are  $\text{Te}_2$  and Te, while in oxidizing atmospheres the major species are  $\text{TeO}_2$  (or  $\text{TeO}(\text{OH})_2$ ) and TeO. The relative abundances are sensitive to system parameters. Possible compounds of tellurium with other fission products ( $\text{Cs}_2\text{Te}$ ,  $\text{TeI}_4$ , and  $\text{TeI}_2$ ) do not appear to be stable in the gas phase.

Several percent of the total iodine available after the accident will be produced by the radioactive decay of tellurium to iodine. If this iodine is born in the containment or in the primary system during times when little Cs is available, the formation of elemental iodine is possible.

The relative abundance of CsOH, CsI, and other fission product species in the gas phase may be limited by physical condensation on aerosols and other surfaces. Chemical reaction of fission products with stainless steel surfaces in the reactor primary system could also reduce their vapor phase concentrations. These processes, if extreme, could change the vapor phase equilibrium conditions.

Radiolysis appears to have a negligible effect on gas phase fission product chemistry at the temperatures expected within the reactor coolant system during severe LWR accidents.

Iodine in aqueous solutions at equilibrium under LWR accident conditions will exist as the stable ionic iodide and iodate species, I<sup>-</sup> and  $\text{IO}_3^-$ . A source of molecular iodine,  $\text{I}_2$ , dissolved in LWR accident water will hydrolyze and form iodide and iodate, and hence can be contained by the water. A source of iodide dissolved in that water can be partially oxidized by dissolved oxygen and that iodine would be further oxidized to the stable iodate state. Concentrations of hypoiodous acid, HOI, will be negligible in equilibrated solutions. Partition coefficients for aqueous iodine at equilibrium with no organic iodide will be at least 10, and are not especially sensitive to temperature. These calculated partition coefficients have assumed an initial iodine source of molecular iodine dissolved in water and reacted with water to produce equilibrium concentrations of the various iodine species.

Estimates of the nonequilibrium iodine partition coefficient can be made by assuming only partial hydrolysis reactions yielding a nonequilibrium partition coefficient ranging from a minimum of approximately 100 to the equilibrium partition coefficient value of  $10^5$ . Conclusions about nonequilibrium aqueous solutions of iodine are subject to large uncertainties, because they lack a complete experimental basis. However, in solutions where the only iodine species is iodide, the partition coefficient will be much larger.

The experimental data base for the formation of organic iodine under accident conditions has been reevaluated. The best estimate for fractional conversion, to methyl iodide, of the total elemental iodine released to the containment atmosphere is judged to be 0.03%. Direct conversion of iodine, in the form of CsI, to methyl iodide is not expected.

### 1.3.3 Fission Product Transport Through the Primary System (Chapter 6)

TRAP-MELT analyses of radionuclide retention in LWR primary systems were obtained for postulated accident sequences which represent a wide range in core damage, radionuclide source rate, and thermal-hydraulic conditions. The first, and most obvious, conclusion to be drawn from the analyses is that if the iodine is released from the core region and transported in its elemental form, there will be no significant attenuation in the primary system for any of the sequences in which the pathway to containment is dry. If the flow path contacts water, however, the removal of elemental iodine from the gas phase is expected to be quite substantial, the extent of removal being mainly dependent on the efficiency of contact.

The second apparent conclusion is that the predicted retention of CsI in the primary system is very high for sequences not involving a full core melt. This is due to the relatively low system surface temperatures and the availability of water for dissolution of the CsI in these sequences. For sequences leading to a complete core melt, however, the predicted retention is highly variable, ranging from almost none to greater than 50% under certain conditions. The dependence of CsI retention on particulate source characteristics (primary particle size, concentrations, and input rate) and thermal hydraulic conditions is very pronounced and retention estimates are subject to the numerous uncertainties associated with these parameters.

The retention of particles in the primary system is variable for the sequences involving a core melt, and is determined by the thermal hydraulic conditions pertinent to the accident. For those sequences characterized by very low steam flow rates, such as TMLB<sup>1</sup> and TC, only a small fraction of the total aerosol mass evolved from the core is expected to be released from the primary system. For the accidents with higher steam flow rates, such as the AD sequences, only 20 percent or less of the aerosol mass generated is expected to be retained in the primary system. And for an accident in which the fuel rods rupture but the ECC system prevents the core from starting to melt, retention of the released fuel fragments in the primary system would be nearly 100 percent due to the expected large size of this material.

The results of the chemical thermodynamic analyses performed for this report indicate that CsI becomes the dominant species at higher fission product

concentrations, lower temperatures, and in more reducing atmospheres. The implications of those results, in light of anticipated primary system conditions during a melt are that (1) nearly all of the fission product iodine should be in the form of CsI in the vicinity of the core due to the high concentrations of fission products and the highly reducing atmosphere and (2) as the gas leaves the core region and is diluted and becomes less reducing, the temperature is lowered such that the majority of the iodine would remain in the form of CsI.

#### 1.3.4 Fission Product Transport Through the Containment (Chapter 7)

In general the results of the analyses of fission product containment transport indicated that the behavior of elemental and particulate iodine would not be dramatically different even though the controlling mechanisms are different for each form. For most sequences, less retention of particulate than vapor forms was predicted. Within the uncertainties of the methods, however, the difference cannot be considered significant. It should also be recognized that the containment analyses did not account for attenuation or significant agglomeration and growth of the particle source within the reactor coolant system before entering the containment.

The effect of steam condensation on aerosol removal processes in the containment was treated to a limited extent using the NAUA-4 code. These calculations showed a reduction in leaked mass resulting from steam condensation of up to 20% for the cases studied.

For the most severe accident sequences analyzed for both PWR and BWR designs, the attenuation factors for radioactive iodine in the containment building were on the order of a factor of two (i.e., approximately 50% of the material released to the containment escaped from it) for iodine in either vapor or particulate form. These accident sequences involved above-ground failure of the containment and impairment of the containment safety features (sprays, pools, or ice beds) as well as core meltdown. The uncertainties in the validity of these results appear to be more a function of uncertainties in the assumptions made about containment failure mode, location and time and subsequent system behavior, than in the effectiveness of the fission product retention mechanisms.

For the severe core damage accident (~50% core melt) assuming delayed ECCS operation, no loss of containment integrity, and containment engineered safety features operable the predicted containment attenuation factor was greater than 100,000 for all fission product species considered in the analysis.

In some instances relevant data could not be found to evaluate the comparative behavior of the two iodine forms. This was true of the potential for iodine retention in suppression pools and ice beds.

The source term for release of radionuclides and other materials indicates that the composition of the released material varies with time. Most notable is the early time release of iodine and cesium relative to much of the less

volatile materials. This means that for particulate releases, the composition of airborne materials, the deposited material, and the leaked mass may each have different compositions and these compositions may vary with time.

### 1.3.5 Engineered Safety Feature Effectiveness (Chapter 8)

The analysis conducted in the chapter on the performance of engineered safety features supports the following conclusions regarding the performance of ESF systems.

#### Containment Leakage Requirements

Limitations on containment leakage have significance mainly for sequences in which containment integrity is maintained. For most core melt sequences, some type of breach in containment is encountered, and the release of radioactive material is not greatly affected by pre-accident leak requirements.

#### Containment Sprays

Containment sprays would perform their pressure suppression function for most accident sequences. Scrubbing of particulate iodine would be less rapid than for elemental iodine in sequences involving limited core damage (where the mean particle size would be relatively small), but for severe accidents (with relatively larger particles), spray washout of aerosols would be comparable to what has been predicted for elemental iodine.

#### Containment Recirculating Filter Systems

Containment recirculating filter systems would perform effectively only for accident sequences wherein aerosol loadings are minimal. Under most severe accident conditions, the attendant high aerosol concentrations in the containment atmosphere would plug the filters, rendering the system inoperative within a few minutes.

#### Auxiliary Building Filter Systems

Filter trains of current design would effectively trap the modest quantity of fission products transported to the auxiliary building via leakage from fluid systems outside containment. For event V, where the blowdown occurs in the auxiliary building the filter system would not significantly mitigate the release of radioactive materials as a result of failure of auxiliary building walls and ventilation system duct work.

#### MSIV Leakage Control System (BWR)

This BWR system would control the leakage of radioactive materials for the design basis accident conditions and under degraded core conditions for accidents where electric power was available. This system would offer little benefit for accidents where the dominant leakage paths to the environment bypass the main steam line.

### Pressure Suppression Pools (BWR)

Pressure suppression pools would perform the steam condensation function for many severe accident sequences. The amount of decontamination in pressure suppression pools is a function of the fraction of noncondensable gases in the bubble, bubble size, and pool depth. Under most conditions, the decontamination of iodine passing through the pool should be substantial. The scrubbing effectiveness for aerosols would depend upon the size of the particles with larger particles being removed more effectively. The particle size itself would depend upon conditions affecting agglomeration and condensation in the reactor system or drywell.

### Dual Containment and Standby Gas Treatment System

The SGTS would effectively trap contaminants which leaked from the primary containment provided that reasonable primary containment integrity is maintained. The system would be ineffective for most severe accidents because of damage to the secondary containment or reactor building, and leak paths which bypass the SGTS.

### Pressure Suppression by Ice (PWR)

Pressure suppression by ice beds would be effective for a number of accident sequences including many severe accident sequences. The ice condenser system with ice containing sodium hydroxide has been demonstrated to be effective for elemental iodine removal. Its effectiveness for scrubbing of aerosols is difficult to quantify without further study. Based on analyses of analogous heat and mass transfer phenomena, larger particles are expected to be removed more effectively than smaller particle aerosols.

## 1.4 Data Base Limitations

A number of limitations in the available data base were identified during the study. These limitations are presented in this report as a guide for future research efforts. The relative importance of each identified data need has not been assessed. In order to determine the relative importance of uncertainties in individual parameters an evaluation of the potential range of uncertainties is required and systematic propagation of these uncertainties through the analysis to determine their effect on the predicted release of fission products from the plant. Because of the short time available for this study this was not possible. Verification of iodine chemical behavior and more precise quantification of the potential attenuation of fission products during postulated accidents by natural processes are not possible at the present time, because of limitations, gaps, and uncertainties in the currently available models and data base.

### 1.4.1 Fission Product Formation (Chapter 2)

Calculations of fission product inventories in the fuel made with the ORIGEN code have typically been within approximately 30% of the values

measured in inventories of actual irradiated fuel rods. This uncertainty in predicting the fission product inventory is relatively small when compared with the uncertainties associated with the conditions affecting the release and transport of radionuclides.

#### 1.4.2 Accident Sequence Characteristics (Chapter 3)

A large source of uncertainty in the prediction of fission product release is associated with limitations of available thermal-hydraulic models in predicting the distribution of fluid and surface temperatures within the reactor coolant system and containment under core melt accident conditions. These uncertainties coupled with uncertainties in our understanding of many of the physical processes associated with core melt events place limits on the accuracy of estimates of fission product release to the environment independent of uncertainties in our understanding of fission product transport behavior.

#### 1.4.3 Fission Product Release From Fuel (Chapter 4)

Unambiguous identification of the chemical form of iodine (and other fission products) at the time of release from fuel at elevated temperatures is required. Because of the complex chemical reactions that are possible these measurements should be done with actual clad irradiated fuel in a prototypic steam/hydrogen environment.

Additional information is required on the release rates of fission products and structural material aerosols from irradiated fuel above about 1200°C. Again these tests should be conducted with real irradiated fuel and in the expected environment. Larger scale experiments to determine fission product, and structural material, aerosol generation rates from molten pools of UO<sub>2</sub>, Zircaloy and structural materials in prototypic atmospheres are needed.

The effects of the formation of low melting point UO<sub>2</sub>-Zircaloy phases on fission product release should be determined.

In order to develop a detailed understanding of the mechanisms of iodine, cesium, tellurium and other relatively volatile, fission product species release, mechanistic models (such as the GRASS-SST code which models noble gas release from elevated temperature fuel) should be extended to these species.

Additional work is required to refine the predictions of aerosol release from molten fuel during interaction with concrete in the reactor cavity. The current correlation in use is based on only three tests and does not provide details of the aerosol composition. In particular, the amount of release of refractory radionuclide species (e.g. PuO<sub>2</sub>) is not well characterized.

#### 1.4.4 Chemistry of Cesium and Iodine (Chapter 5)

High temperature thermochemical data are needed for many fission product species. Additional information is also required on reactions of fission products with reactor materials, with other fission products and with

constituents of the vapor (steam, hydrogen, oxygen) at high temperature. Both equilibrium and chemical reaction kinetic information are needed.

Information is needed on aqueous iodine chemistry, especially at elevated temperatures (100°C - 300°C). The kinetics of known reactions and the stability of suspected intermediate species (especially HOI) require additional research. Attention should be given to the mechanisms and rates of organic iodide formation at low concentration levels since these iodides may be the primary gas phase iodine species for many accident sequences. An incomplete understanding exists of the effects of radiation on fission product chemistry.

#### 1.4.5 Fission Product Transport in Primary System to Containment (Chapter 6)

The currently available code (i.e. TRAP-MELT) for primary system fission product behavior does not include models for fission product chemical reactions and chemical species transformation. This effect could be important and the need for such models should be determined.

In addition, the TRAP-MELT code does not currently contain models for fission product-gas phase/liquid phase partitioning, or liquid phase fission product transport within the primary system, both of which are known to be important for some severe accident sequences (e.g. TMI).

The TRAP-MELT code has been developed based on theoretical principles and small scale experiments and has never been subjected to integral experimental validation. Such experimentation in a well characterized facility would be useful for assessing the uncertainties in TRAP-MELT transport predictions separately from the uncertainties typically introduced with the input data from thermal-hydraulics codes and source term models.

The TRAP-MELT code currently is unable to model the growth of aerosols by coagulation. This mechanism has been shown to be important for some accident sequences and this capability should be added to the code. Insufficient information exists to develop models for the formation (e.g., self nucleation) of primary aerosol particles.

In a number of PWR accident sequences the leak path from the primary system to containment involves release through the pressurizer relief (or safety) valves and into the pressurizer quench tank. Because of uncertainties in the physical arrangement and water levels in the quench tank no credit was taken in the analysis for attenuation in the quench tank. This attenuation could be potentially significant and should be investigated.

#### 1.4.6 Fission Product Transport Through Containment (Chapter 7)

Additional information is needed on the processes and mechanisms governing fission product vapor and aerosol removal in BWR suppression pools and in the ice beds in PWR ice condenser plants. In particular, additional experimental data on the removal of particulates in mixtures of steam and noncondensable gases passing through suppression pools and ice beds is required.

More must be known about the possible modes, locations, and timing of containment failure since uncertainties in these phenomena are major contributors

to uncertainties in the amount of fission product attenuation which will occur in the containment building. Better information in this area is required before it can be determined if fission product attenuation along the leak path through a failed containment is important.

Information is needed on the effect of a hydrogen deflagration in containment on the physical and chemical form of fission product vapors and aerosols suspended in the containment atmosphere and deposited on containment surfaces.

The effect of steam condensation on aerosol particles is a potentially important mechanism influencing aerosol fallout. The German NAUA code has been used to evaluate the importance of this phenomenon. However, limitations on the ability of available thermal-hydraulic models to predict the detailed thermal conditions in the containment atmosphere which control the condensation process limit the accuracy of the NAUA code. More work in this area is needed.

Coupled models are needed for containment fission product behavior which include both the natural removal mechanisms and the effects of engineered safety features (e.g. containment sprays) for both aerosols and vapors. In addition more detailed models of aerosol washout by containment sprays are needed.

Separate effects experiments and tests in large vessels are needed for the development and validation of models which can predict multi-species (fission product and structural material) aerosol behavior in a condensing steam environment.

## REFERENCES TO CHAPTER 1

- 1.1 W. F. Pasedag, et al., "Regulatory Impacts of Nuclear Reactor Accident Source Term Assumptions," NUREG-0771, to be published July 1981.
- 1.2 "Theoretical possibilities and Consequences of Major Accidents in Large Nuclear Power Plants," WASH-740, March 1957.
- 1.3 Title 10, Code of Federal Regulations, Part 100 - Reactor Site Criteria.
- 1.4 J. J. DiNunno, et al., "Calculation of Distance Factors for Power and Test Reactors Sites, TID-14844, March 23, 1962.
- 1.5 "Reactor Safety Study - An Assessment of Accident Risks in U.S. Commercial Nuclear Power Plants," WASH-1400 (NUREG-75/014), October 1975.
- 1.6 Letter from W. R. Stratton, A. P. Malinauskas, and D. O. Campbell to NRC Chairman J. Ahearne dated August 14, 1980.
- 1.7 "The Technology of Nuclear Reactor Safety," Volume 1, Reactor Physics and Control, M.I.T. Press, 1964.
- 1.8 Letter from Chauncey Starr to NRC Commissioner J. Hendrie dated September 2, 1980, with enclosed papers:
  - M. Levenson and P. Rahn, "Realistic Estimates of the Consequences of Nuclear Accidents," draft paper for presentation at the ANS meeting in Washington, D.C. November 17-21.
  - H. Morewitz, "Fission Product Releases from Degraded Core Accidents," Draft ANS paper.
  - Z. T. Mendosa, G. A. Stevens, and R. L. Ritzmann, "Radiation Release from the SL-1 Accident" Draft ANS paper.
- 1.9 Letter from Nuclear Safety Oversight Committee to President Jimmy Carter dated December 21, 1980.

---

\*These papers have been recently published in Nuclear Technology, Volume 53, May 1981.



## 2. FISSION PRODUCT FORMATION

In order to understand the significance of fission products in reactor accidents, it is necessary to describe how they originate and why they are hazardous to human health. We will begin with brief descriptions of the atomic nucleus and the fission process.

### 2.1 The Atomic Nucleus and the Fission Process

The atomic nucleus is composed of neutrons (neutrally charged atomic particles) and protons (similar to neutrons but with positive electric charge) bound together by nuclear forces. In a neutrally charged atom there are the same number of orbiting electrons as protons bound in the nucleus and the charges of each cancel each other. All of the nuclei of an element have the same number of protons. For example, the nucleus of an iodine atom has 53 protons. Different varieties of an element, called isotopes, can have different numbers of neutrons. An iodine nucleus could have as few as 62 neutrons or as many as 87 neutrons. The isotopes are identified by adding the number of protons and neutrons together. Thus, the isotope of iodine with 78 neutrons is called iodine-131 ( $53+78=131$ ). Although different isotopes of an element are virtually indistinguishable chemically, their nuclear properties can differ substantially.

The energy in a nuclear power plant comes from the splitting or fissioning of atomic nuclei. Fission occurs when a fissionable nucleus captures a free neutron. This capture upsets the force balance between the neutrons and protons in the nucleus and the nucleus splits into two nuclei. These nuclei are called fission products. Only a few isotopes of the elements that exist in high abundance on the earth (the 92 "natural" elements) are fissionable. In the reactors in common use today, fission primarily occurs in uranium-235, one of the isotopes of uranium.

A fission event begins with a neutron colliding with the nucleus of a uranium-235 atom and results in the release of: energy, two or three neutrons, and at least two fission products. The energy is used in the form of heat to produce electricity. The released neutrons also perform an essential function. On the average, one of the neutrons must go on to produce another fission in order to sustain the chain reaction. The fission products, on the other hand, are the remnants of the reaction and are the source of the potential hazard from accidents in nuclear power plants. The problem with fission products is that some are radioactive (they are unstable). If a nuclide does not have the right balance of neutrons and protons in the nucleus, it will be unstable and emit radiation. Iodine, for example, has one stable isotope, iodine-127. The other 25 isotopes of iodine are radioactive. The average length of time a radioactive nuclide will remain before decaying

into another nuclide is characterized by its half-life. At the end of one-half life, half of the initial quantity of the nuclide will remain. Through the emission of radiation, the nucleus decays from one nuclide to another nuclide until a stable configuration is reached. As long as the fission products remain in the fuel, the radiation which is emitted during decay is absorbed in the fuel, coolant and reactor structures. If, on the other hand, the radioactive fission products are released to the environment as the result of an accident, they can be transported by air or water to man and the emitted radiation can produce a health hazard.

There are many radioactive nuclides produced in a nuclear reactor. Some are the direct products of fission, others are the result of transmutation in which one nuclide is converted through interaction with a neutron into another nuclide, and still others are radioactive "daughters" which are moving by radioactive decay through a sequence of nuclide states until the chain is ended with a stable nuclide. Computer codes are available which can be used to predict the inventory of nuclides in a nuclear reactor as they increase during powered operation and die away following shutdown. The ORIGEN2<sup>(2.1)</sup> code is commonly used for this type of calculation. It is capable of analyzing each of the basic processes: fission, transmutation, and decay. Cross sections, which are averaged over ranges of neutron energy, are used in predicting the reaction rates for fission and transmutation. Standard descriptions of radioactive decay chains and accepted values of nuclear constants, such as half-life and fission yield, have been incorporated into the code. Because of code limitations, ORIGEN2 cannot predict the spatial distribution of nuclides within the reactor. It can, however, be used to estimate either the average inventory in the reactor or the inventory in a particular region of the reaction if the power generation in that region is specified as a function of time. Predictions made with the ORIGEN2 code have been compared with measurements of the inventories of actual fuel rods. The agreement has typically been within approximately 30% of the measured value.<sup>(2.2)</sup> This accuracy in predicting the inventory of fission products in the fuel is quite acceptable for reactor safety analysis. In comparison, the uncertainties associated with the conditions affecting the release and transport of fission products are quite large.

## 2.2 Barriers to the Release of Fission Products

In the current generation of reactors, the uranium is in the form of uranium dioxide. Uranium dioxide is a ceramic material, similar to fire brick, which melts at high temperature. The uranium dioxide is formed into cylindrical pellets, less than 1/2 inch in diameter and 1/2 inch in length. As illustrated in Figure 2.1, the pellets are then stacked into long thin metallic tubes, called cladding. The total fuelled length is typically twelve feet. The uranium dioxide with cladding is called a fuel rod. The pins are bundled together to form a fuel element as shown in Figure 2.2.

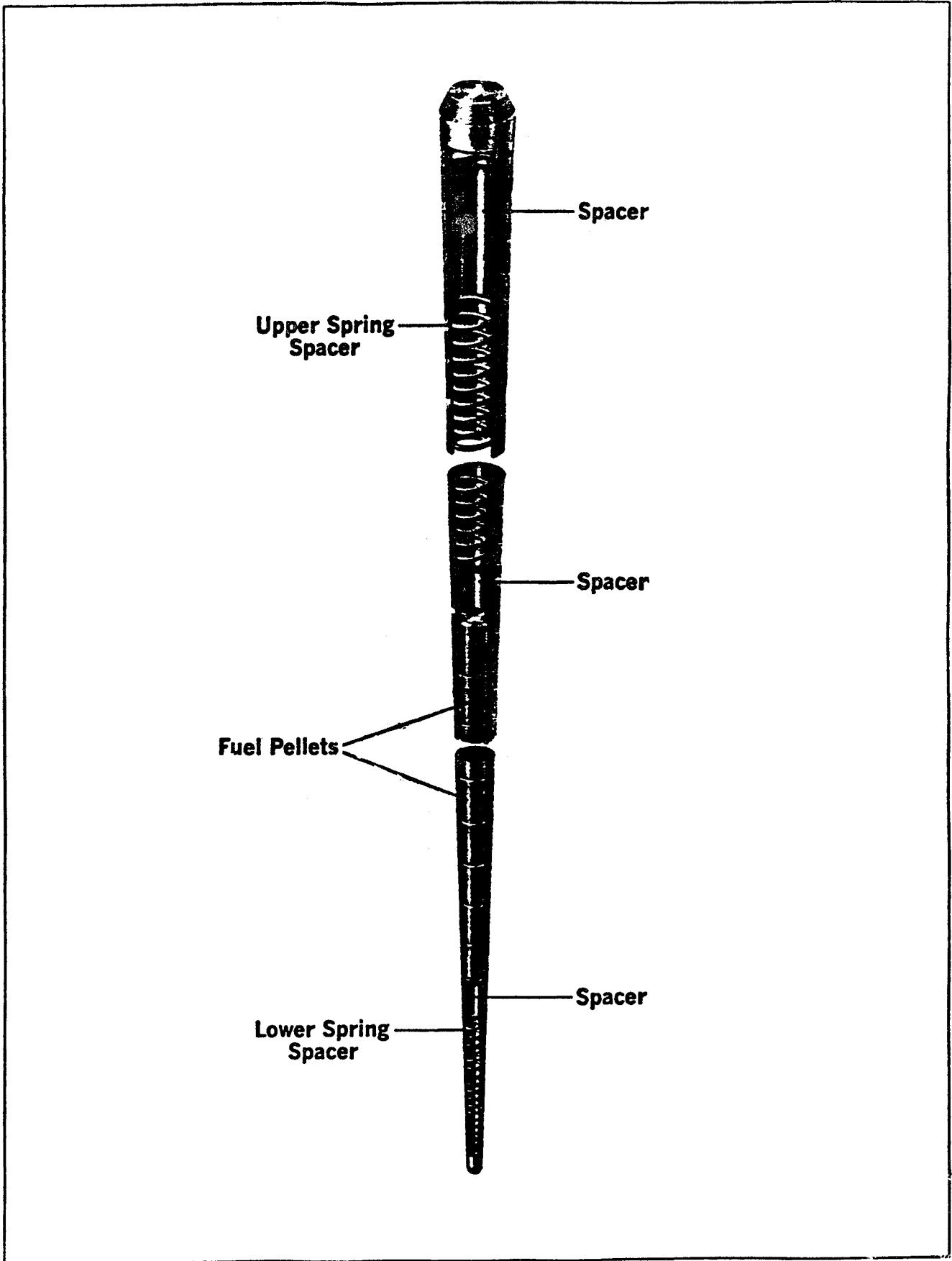


FIGURE 2.1 A FUEL ROD

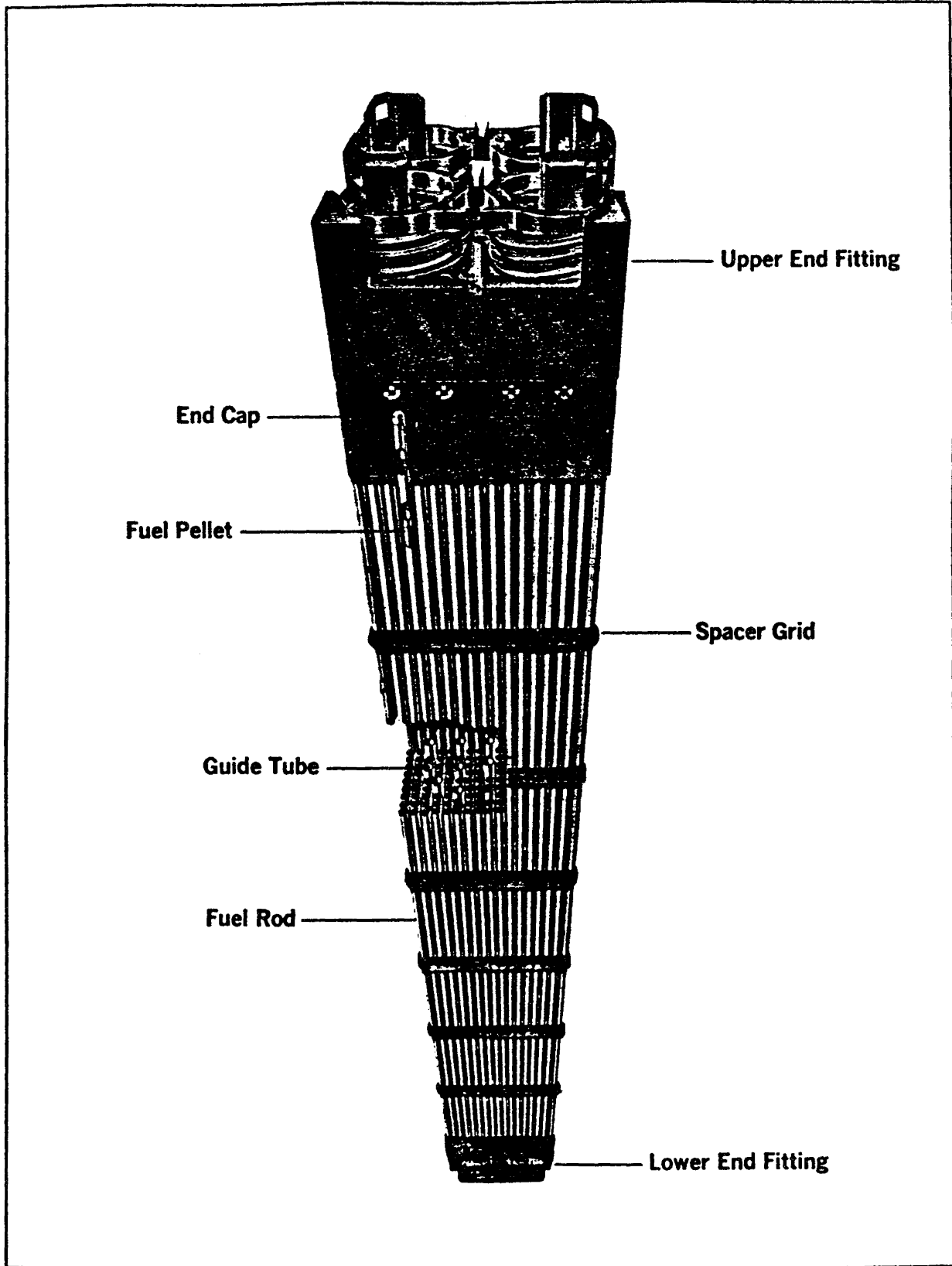


FIGURE 2.2 A FUEL ASSEMBLY

The fuel elements are stacked within the reactor vessel to make a right circular cylinder approximately twelve feet in diameter and twelve feet high.

While the reactor is operating, the fission products are produced within the uranium dioxide fuel. Most of the fission products will remain within the matrix of the uranium dioxide until the fuel is removed from the reactor for disposal. Some of the fission products, typically a few percent or less, will migrate to the gap between the fuel and the metallic cladding. If leaks form in the cladding during operation (reactors are typically permitted to operate with up to 1 percent of the fuel rods with cladding leakage) the fission products in the gap can be released to the coolant water in the reactor. A cleanup system strips the radioactive material from the coolant system and stores it for disposal or until the magnitude of the radioactive material has decayed to a low enough level that it can be released. This is the principal source of the very low levels of radioactive materials released to the environment during normal operation.

Major accumulations of fission products found within the plant are: the fuel within the reactor vessel, spent fuel in the storage pool, the coolant water, and the radioactive waste holdup tanks. In performing safety analyses for the plant, consideration must therefore be given to accident sequences which could fail the various barriers that prevent this material from being released to the environment. Of these potential sources of release, the largest by far is the fuel within the reactor vessel. For this reason, this source has been provided the greatest protection. In order for significant quantities of fission products to be released from the fuel to the environment, four barriers must be breached:

- (1) the fuel matrix,
- (2) the fuel cladding,
- (3) the reactor vessel and primary system piping,
- (4) the containment building.

If any of these barriers were to remain intact in the accident, the consequences to the public would be minor. Accidents in which melting of the fuel can occur are of particular concern in reactor safety because the potential can exist in these accidents for the progressive failure of all four barriers.

### 2.3 Health Hazards from Exposure to Fission Products

In the decay of radioactive nuclides, three types of radiation are of concern to human health: alpha particles, beta particles, and gamma rays. The names were given to these ionizing forms of radiation in the early days of nuclear physics when they were discovered to mysteriously

## 2.6

expose photographic film but the true nature of the radiation was unknown. Alpha particles have been subsequently determined to be highly energetic, charged nuclei of helium atoms (2 protons and 2 neutrons). Beta particles are energetic electrons. Gamma rays are electromagnetic radiation, essentially the same as x-rays but of higher energy.

Because alpha particles and beta particles are charged, they have a very short range in human tissue. Alpha and beta emitters are therefore a lesser hazard as an external source than if taken into the body through inhalation or ingestion. Gamma radiation is a much more penetrating form of radiation. As a result, it can be a significant hazard from an external source such as radioactive material in a passing cloud as well as from an internal source.

Two types of hazards exist from exposure to radiation which can be differentiated by the level of exposure and the time period of the effect. For very high exposure to radiation over a short term, the subject can experience the symptoms of radiation sickness ranging from nausea to death within a few weeks. The levels of exposure required to produce these effects are quite high. Methods of analysis used in risk studies<sup>(2.3)</sup> have indicated that these exposure levels would be expected to occur only for the most severe accident conditions and within a few miles of the plant. In addition, radiation is known to be a carcinogenic (cancer causing) agent. Even at a low level of exposure, below that required to produce recognizable health effects, a member of the exposed population may have an increased likelihood of incurring cancer. An increase in the frequency of cancers in the exposed groups would not be realized until 10 to 40 years after the accident. An increase in genetic defects can also result from radiation exposure which could be carried forward into future generations. These delayed effects would be indistinguishable in character from cancers and genetic defects in the population resulting from other natural and man-made causes. Depending upon the magnitude of the exposure, however, an increase in the number of these effects could be detectable in a large population of exposed individuals.

Table 2.1 identifies a number of nuclides that represent the greatest hazard to humans in a reactor accident according to the results of accident analyses.<sup>(2.3)</sup> The table shows the half-lives of the important nuclides and a typical value for the activity of each in an operating reactor. The activity, in units of curies, is a measure of the number of nuclei in the reactor that are undergoing radioactive decay per unit of time. The manner in which the radioactive nuclides can affect human health varies with the half-life, the quantity of material released, the type of emitted radiation, the mechanisms of transport to humans, and the chemical reactions within the human body. Whether or not a particular nuclide will be an important contributor in a given accident will depend upon the conditions of the accident and the manner of exposure of an individual. In the following paragraphs, the behavior of some of the more important radioactive nuclides is described.

Iodine Isotopes. The radioactive isotopes of iodine emit both energetic gamma rays and beta particles. Iodine-131, -132, -133, and -135 are potential major contributors to the dose received by an individual from the passing cloud of radioactive material in a severe accident. They also are predicted to contribute to the external dose to the body in the first day following the accident due to radioactive materials deposited on the ground. As a result, the iodine isotopes could have a major influence on the likelihood of radiation sickness or early death. Ingested iodine is concentrated in the thyroid gland and would result in much higher localized doses to this organ than to the rest of the body. Under these conditions, iodine-131 with the longest half-life is the most important isotope. Exposure of the thyroid can result in the growth of nodules, either benign or malignant. Approximately half of the nodules would be malignant requiring surgical removal. The mortality rate for malignant nodules is approximately 5 percent.

Noble Gases. The radioactive noble gases are particularly difficult to contain in an accident because they are both chemically inactive and a gas at room temperature. They will not deposit naturally or in general be filtered effectively along the release pathway to the environment. On the other hand, they will not react with or be retained in the human body. The health concern therefore relates only to the exposure received during passage of the radioactive cloud. The short-lived nuclides, krypton-88, xenon-133, and xenon-135, can be significant contributors to the predicted early exposure received by an individual and influence the likelihood of radiation sickness and early fatality. In accidents where the engineered safety features are effective in retaining the chemically reactive fission products, the noble gases will be the principal form of radionuclides released. This was the case for the Three Mile Island accident. Although the initial activity of krypton-85 is not as high as for the other noble gases, because of its long half-life, it will with time become the principal form of noble gas activity. This was the nuclide that remained in the TMI containment building and had to be vented prior to the beginning of recovery operations within the building.

Cesium Isotopes. The cesium isotopes will be discussed separately, partly because of the possible relationship of cesium to iodine as it affects the chemical form of iodine but also because they are potentially major contributors to delayed cancer fatalities in reactor accidents. Approximately ten times as many cesium atoms as iodine atoms are produced in a reactor. There are therefore more than enough cesium atoms potentially available to combine with all of the iodine if the conditions in an accident favor the formation of cesium iodide.

The cesium isotopes are beta and gamma emitters. The shorter lived isotope, cesium-134, can be a significant contributor to the predicted early exposure as the result of inhalation. Both cesium-134 and -137 are potential contributors to predicted delayed health effects due to long-term exposure from ground contamination or as the result of inhalation.

Other Fission Products. A number of other fission products are also important in terms of human health impact in an accident. Tellurium-132 and barium-140 could be contributors to early doses and early effects. The other fission products identified in Table 2.1 would primarily contribute to the long term dose and delayed effects. Strontium-90 is a particular hazard to bone doses and associated malignancies such as leukemia. Ruthenium-106 is potentially a major hazard to the lung.

Actinide Nuclides. Because of their somewhat unique behavior, some mention should be made of the actinide or transuranic nuclides. These nuclides are not truly fission products. They result from nuclear reactions in which a neutron is captured by a heavy nucleus such as uranium. Instead of causing fission, a capture reaction leads to the buildup of heavier nuclides and the creation of "man-made" elements. The most familiar examples are several isotopes of plutonium and curium. The transuranic nuclides frequently are alpha particle emitters with very low energy gamma rays. They typically are not external dose hazards and because they usually have low solubility are not concentrated in food supplies. The principal hazard arises from resuspension of deposited radioactive material and subsequent inhalation. Because of their long half-lives, these nuclides could have a major influence on the predicted long term exposure to the population in the time period of 10 to 50 years if released to the environment in a severe accident.

Table 2.1. Important radioactive Nuclides

	Half Life (days)	Radioactive Inventory* (curies x 10 <sup>-8</sup> )
Iodine Isotopes		
Iodine 131	8.05	0.87
Iodine 132	0.0958	1.3
Iodine 133	0.875	1.8
Iodine 135	0.280	1.7
Noble Gases		
Krypton 85	3,950	0.0066
Krypton 85M	0.183	0.32
Krypton 87	0.0528	0.57
Krypton 88	0.117	0.77
Xenon 133	5.28	1.8
Xenon 135	0.384	0.38
Cesium Isotopes		
Cesium 134	750	0.13
Cesium 137	11,000	0.065
Other Fission Products		
Strontium 90	11,030	0.048
Ruthenium 106	366	0.29
Tellurium 132	3.25	1.3
Barium 140	12.8	1.7
Cerium 144	284	0.92
Actinide Isotopes		
Plutonium 238	32,500	0.0012
Plutonium 239	8.9 x 10 <sup>6</sup>	0.00026
Plutonium 240	2.4 x 10 <sup>6</sup>	0.00029
Plutonium 241	5,350	0.052
Curium 242	163	0.014
Curium 244	6,630	0.00084

\* The inventories of fission products in this table and discussed later in this report are for a 3412 MW reactor operated for three years as predicted by the ORIGEN code.

## REFERENCES FOR CHAPTER 2

- 2.1 Croff, A. G., "ORIGEN2--A Revised and Updated Version of the Oak Ridge Isotope Generation and Depletion Code", ORNL-5621 (July, 1980).
- 2.2 Goode, J. H., Stacy, R. G., and Vaughen, U.C.A., "Comparison Studies of Head-End Reprocessing Using Three LWR Fuels", ORNL/TM-7103 (June, 1980).
- 2.3 "Reactor Safety Study, An Assessment of Accident Risks in U.S. Commercial Nuclear Power Plants", WASH-1400, Appendix VI (October, 1975). Available free upon written request to the Division of Technical Information and Document Control, U.S. Nuclear Regulatory Commission, Washington, DC 20555.

### 3. ACCIDENT SEQUENCE CHARACTERISTICS

The purpose of this chapter is to describe the behavior of potential accident sequences in nuclear power plants that could result in the release of radioactive materials to the environment. Since the likelihood and character of accident sequences is strongly influenced by plant design, Section 3.1 describes the principal design features of the plants currently operating in the United States. Particular emphasis is given to the engineered safety features which provide for the confinement of radioactive material. Section 3.2 discusses the classification of reactor accidents into groups which would be expected to have similar behavior or consequences. In Chapters 6 and 7, a number of specific accident sequences are analyzed which are intended to be representative of broader classes of accidents. In Section 3.3, brief descriptions are provided for these accident sequences.

#### 3.1 Design Features of Nuclear Power Plants

The discussions in this report are limited to two types of light-water cooled reactors that are currently being operated in the United States for commercial nuclear power generation: pressurized water reactor (PWR) and the boiling water reactors (BWR). Each type of plant will be described separately.

##### 3.1.1 Pressurized Water Reactors

In the United States, pressurized water reactors are designed by three companies, Westinghouse, Combustion Engineering, and Babcock & Wilcox. While each design has its own characteristics, the three designs are sufficiently similar with respect to their effect on the transport and removal of radioactive material to be described generically.

Reactor Coolant System. The reactor coolant system of a PWR is illustrated in Figure 3.1. The principal components of the system are the reactor vessel, the reactor coolant pumps, the steam generators, the pressurizer, and the interconnecting piping. Water in the reactor coolant system is maintained at high pressure by the operation of heaters in the pressurizer. The reactor coolant pumps force the water through the system. Water flows into the reactor vessel and up through the reactor core. The heat produced by fission in the fuel is transferred to the water. The hot water then flows to the steam generators. The steam generator is essentially a pot of water with tubes running through it. The reactor coolant water inside the tubes transfers heat to the water in the steam generator. This water, which is at lower pressure, boils and steam which is produced flows to a turbine-generator to produce

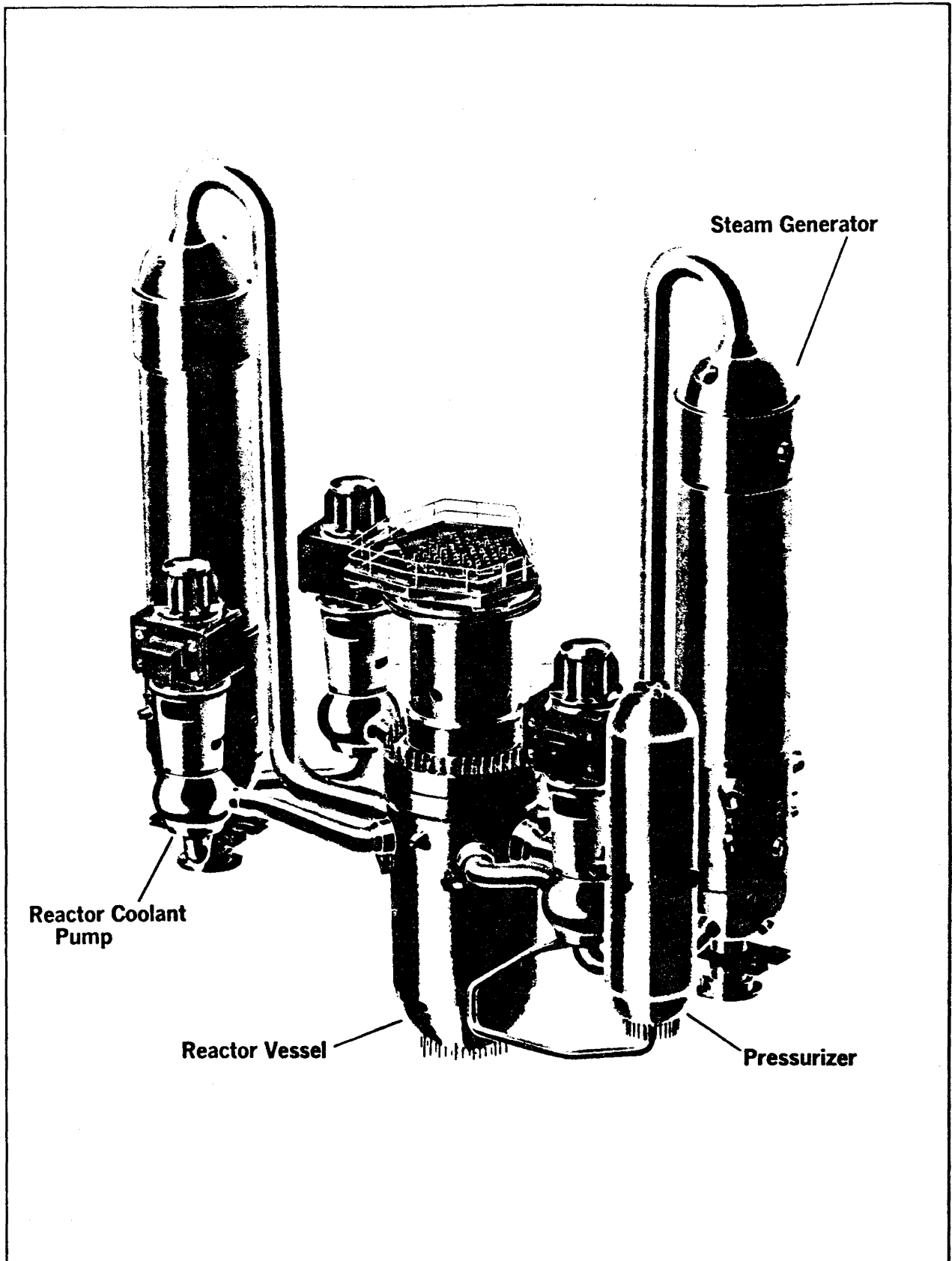


FIGURE 3.1 PWR REACTOR COOLANT SYSTEM

electricity as illustrated in Figure 3.2. After being cooled and condensed, the secondary water is pumped back into the steam generator. As described in Section 2.2, the boundary of the reactor coolant system provides the third barrier to the release of fission products.

In order to perform specific functions, a number of additional systems are connected to the reactor coolant system. Four of the most important systems are: the reactor shutdown system, the letdown and purification system, the decay heat removal system, and the emergency core cooling system.

**Reactor Shutdown System.** The chain reaction in the core is controlled by neutron absorbing rods that can be withdrawn or inserted from above the core. In the event of an accident, these rods can be rapidly inserted to shut off the chain reaction. The fission products in the core, however, will continue to release large amounts of heat even after the chain reaction is terminated.

**Letdown and Purification System.** During operation, some reactor coolant is continually diverted through a letdown system to remove fission and activation products and to adjust the chemistry of the coolant as necessary.

**Decay Heat Removal System.** In the operating mode, heat is removed from the reactor by means of the steam generators. However, when the plant is in the shutdown mode, for example for refueling, a decay heat removal system is needed to remove the heat released by the radioactive decay of fission products.

**Emergency Core Cooling System.** If the reactor core were to become uncovered, the fuel could heat up, the cladding could rupture, and radioactive materials could be released to the reactor coolant system. The purpose of the emergency core cooling system is to rapidly replace water to the reactor coolant system in the event of coolant loss in an accident. In a PWR, electrically powered pumps provide for the injection of emergency cooling water. In addition, pressurized tanks of water automatically dump coolant water into the vessel in the event the pressure drops below a preset level.

**Reactor Containment Building.** As mentioned in Chapter 2, the final barrier to the release of fission products is the building that houses the reactor coolant system. This building must be designed to withstand the loads imposed by the accidental depressurization of the reactor coolant system as well as to retain fission products released within the building. Two major design variations are currently in use.

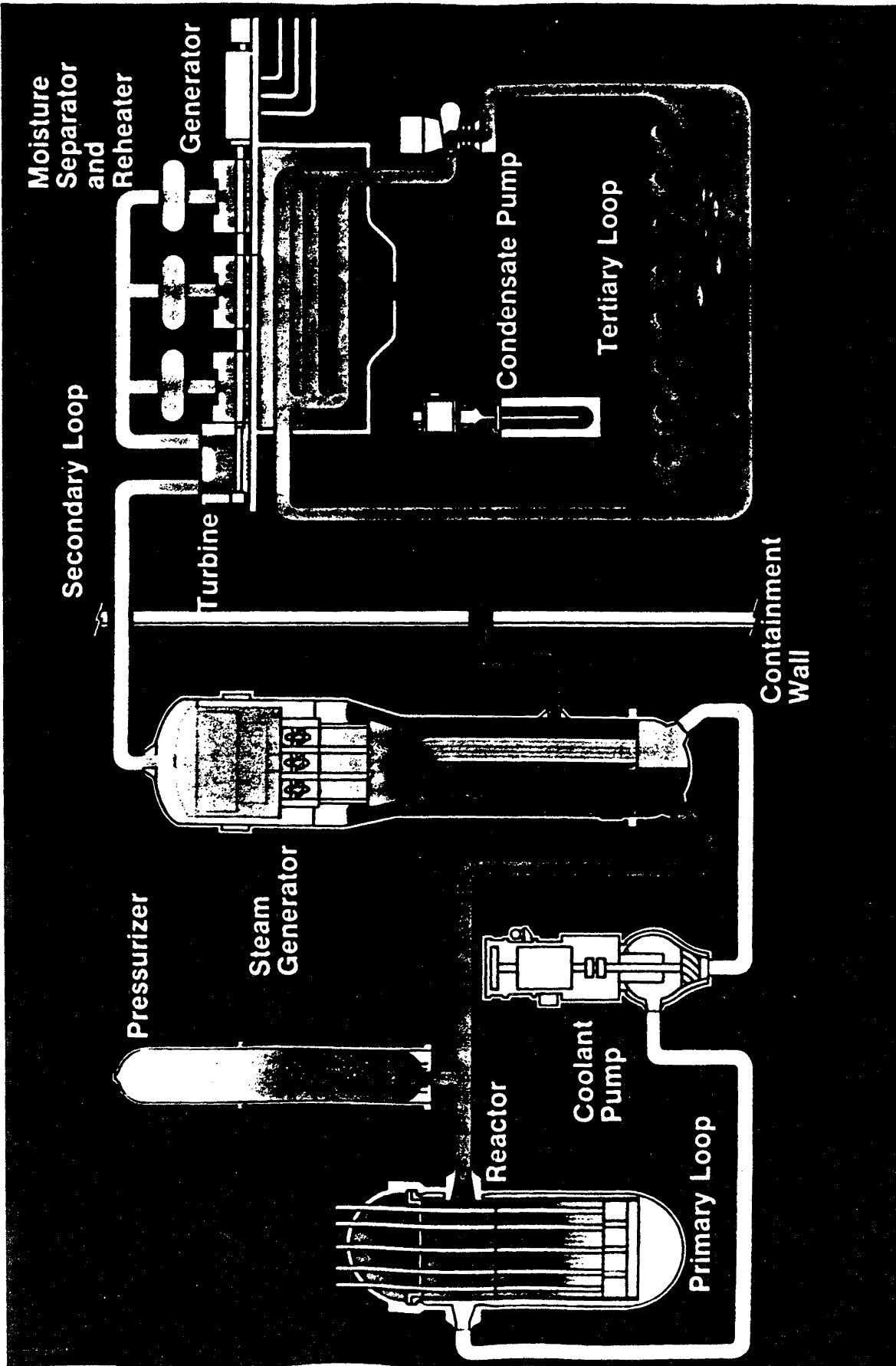


FIGURE 3.2 PWR NUCLEAR STEAM SUPPLY SYSTEM

**Large, High-Pressure Design.** Through the combination of large volume and high design pressure capability, this type of containment building is able to withstand the pressure increase resulting from depressurization of the reactor coolant system. A typical design is illustrated in Figure 3.3. These designs are also equipped with water spray systems to condense steam within the containment building atmosphere. In addition to reducing the pressure in the containment building in an accident, these systems would remove fission products from the containment atmosphere. Chemical additives are mixed with the spray water to make it more effective in removing elemental iodine.

There are a number of variations in the design of large, high pressure containments. One type has internal filters for cleaning recirculating air before it passes through the containment air coolers. All containment designs have an automatic system to close non-essential vents, lines, and other penetrations through the building walls to minimize the leakage of radioactive materials in the event of an accident.

**Ice-Condenser Design.** The ice-condenser containment design employs a fundamentally different approach to the control of steam release in the accidental depressurization of the reactor coolant system. In this design, the released steam is directed to large beds of ice in which the steam is cooled and condensed. In this way the volume and pressure-rating of the building can be significantly reduced. In Figure 3.4, an ice-condenser design is illustrated. A spray system is provided in the upper compartment to condense steam that bypasses the ice beds. Both the spray system and the ice beds would be expected to have some degree of effectiveness in scrubbing fission products from the containment atmosphere. A fan system circulates air from the upper compartment back to the lower compartment and through the ice following an accident.

### 3.1.2 Boiling Water Reactors

In the United States, boiling water reactors (BWRs) are now manufactured only by the General Electric Company. Although there are a number of generations of the design of this reactor type, it is sufficient for this report to discuss the various reactor coolant system designs as one, while providing some individual discussion of the three associated containment designs.

**Reactor Coolant System.** The purpose of the reactor coolant system in a BWR is fundamentally the same as that for a PWR--to provide water flow through the core region, allowing the water to heat, and to transfer this heat in the form of steam to a turbine-generator so that the electricity can be produced. The difference in a BWR, as illustrated in Figure 3.5,

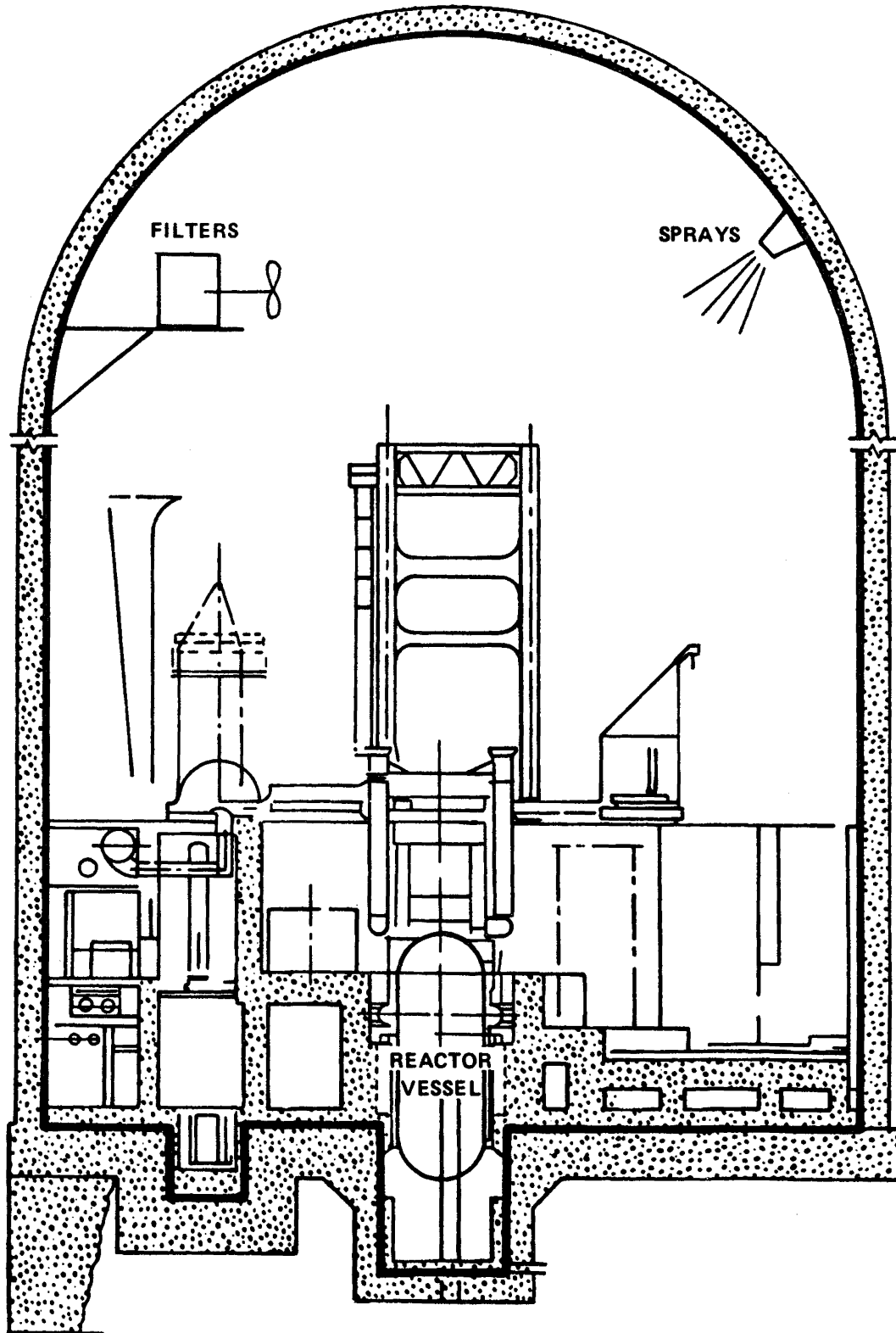


FIGURE 3.3. LARGE, HIGH PRESSURE CONTAINMENT

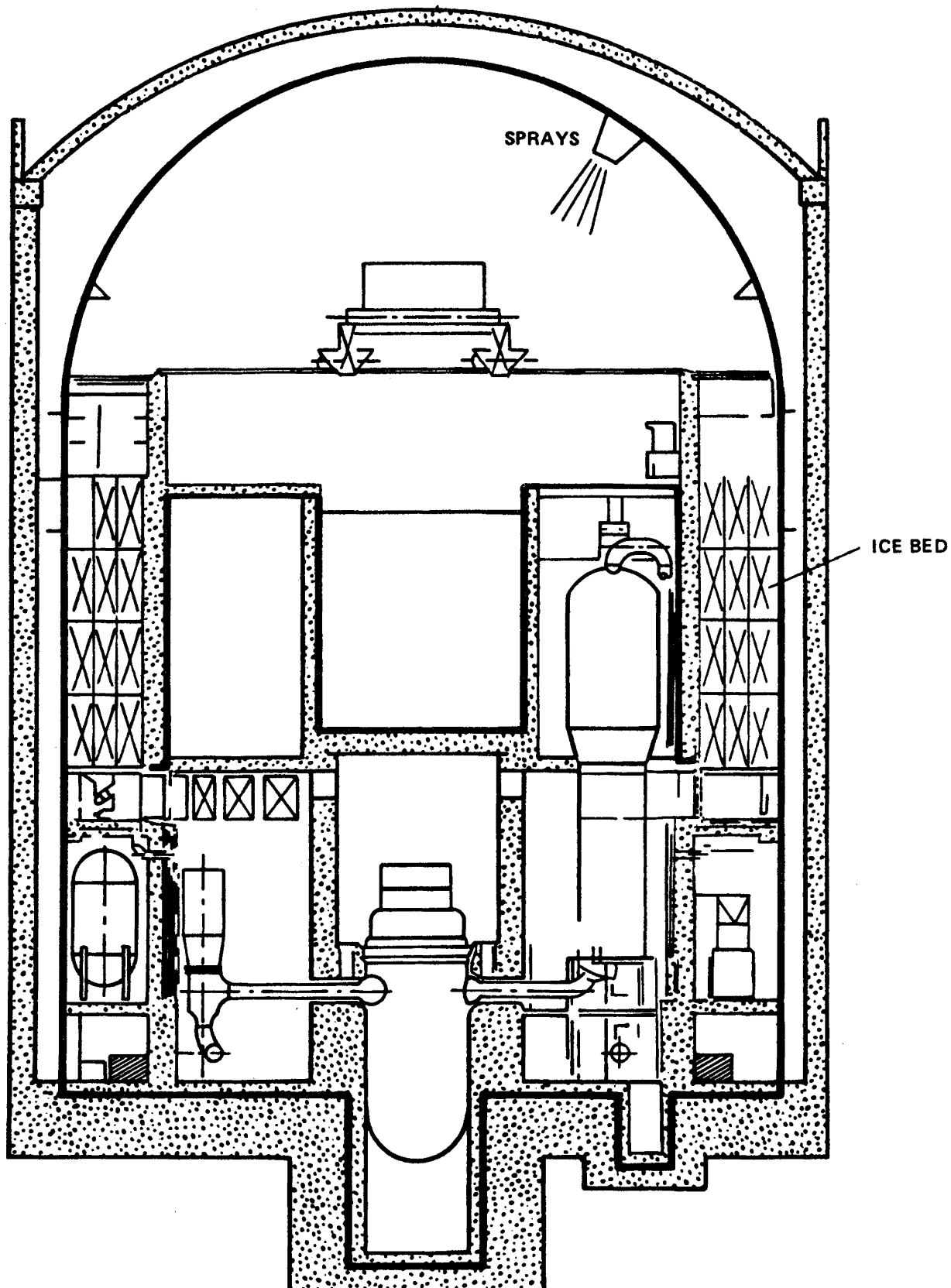


FIGURE 3.4. ICE CONDENSER DESIGN

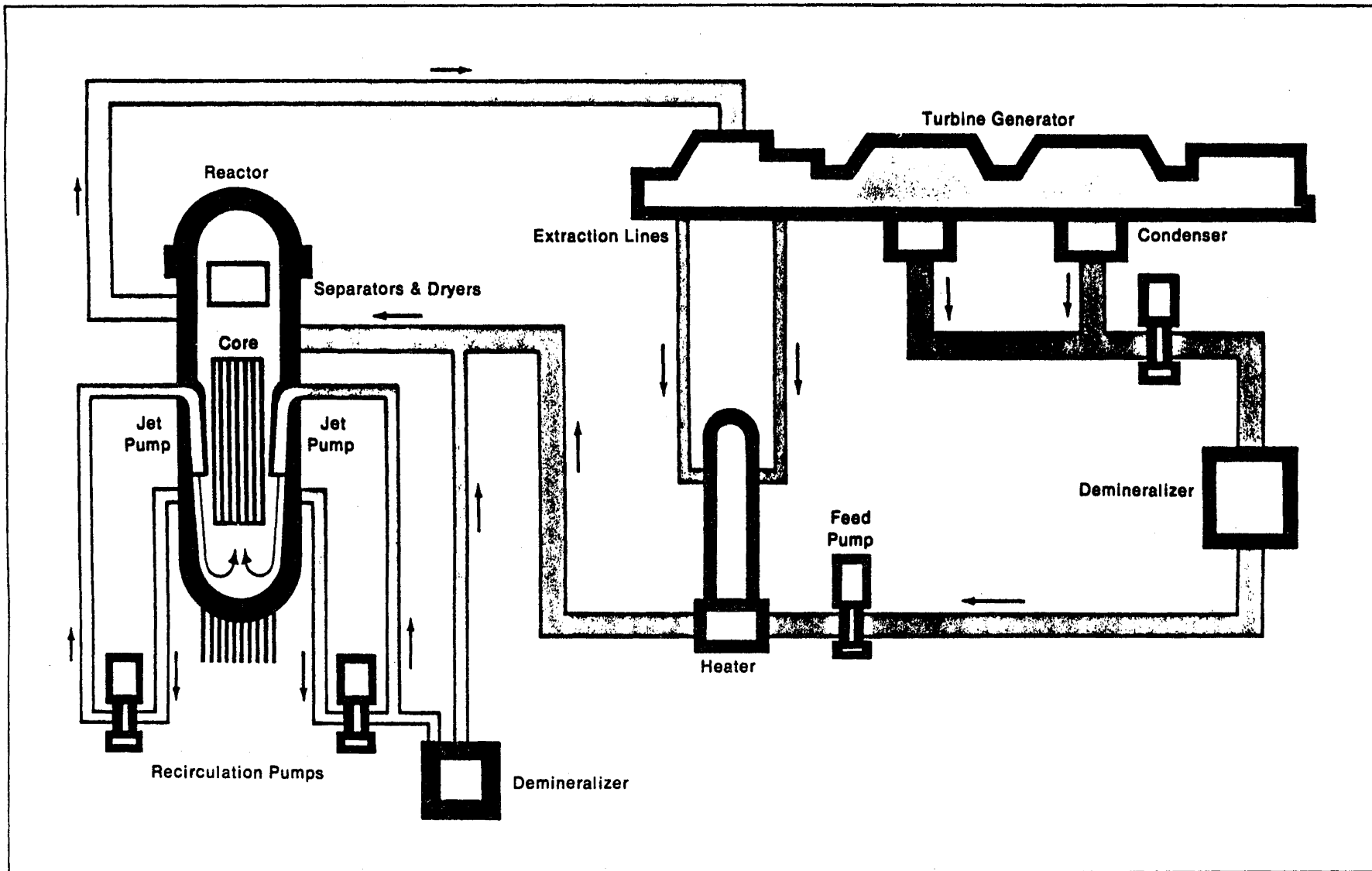


FIGURE 3.5 BWR NUCLEAR STEAM SUPPLY SYSTEM

is that this is all done in one coolant loop rather than the two loops in a PWR. That is, in a BWR, the water flowing through the core is allowed to boil and flow directly to the turbine-generator. Two external recirculation loops are used to pump water into the reactor core. In the event of an accident, isolation valves in the steam line to the turbine would be closed. As for the PWR, the boundary of the reactor coolant system provides the third barrier to the release of fission products.

A number of systems are related to the operation of the reactor coolant system that can affect the course of an accident.

**Reactor Shutdown System.** In the BWR, the control elements are blades which fit between the fuel elements. These are manipulated from the bottom of the core. They can be rapidly inserted in the event of an accident.

**Reactor Core Isolation Cooling System.** This system provides emergency coolant water to the reactor vessel with steam turbine driven pumps. It is capable of maintaining coolant inventory in anticipated transient events or some small pipe break accident.

**Standby Core Cooling System.** The standby core cooling system provides emergency coolant to the reactor vessel in the event of a loss of coolant accident. Spray systems are used to cool the fuel from above while the core is also being reflooded from below.

**Residual Heat Removal System.** In the shutdown mode, the residual heat removal system removes decay heat from the reactor coolant system. It also prevents the suppression pool (see below) from overheating in an accident.

**Reactor Containment Building.** Three types of BWR containment designs exist. Each design involves the use of a large water pool to provide pressure suppression in an accident. The Mark I design, shown in Figure 3.6, has a separate toroidal pool (wetwell) that is connected to the main part of the containment (drywell) by large vent pipes. This concept has a volume that is by comparison quite small and a high design pressure. The Mark II design, shown in Figure 3.7, is called the "over-under" design because the drywell is located directly above the wetwell. The layout of the Mark III design in Figure 3.8 is more like the ice-condenser plant. The wetwell is in an annular region at the periphery of the containment. The vapor space of the wetwell actually forms the upper containment compartment. In this concept, the volume is somewhat greater than for the other two BWR containment designs and the design pressure is substantially lower.

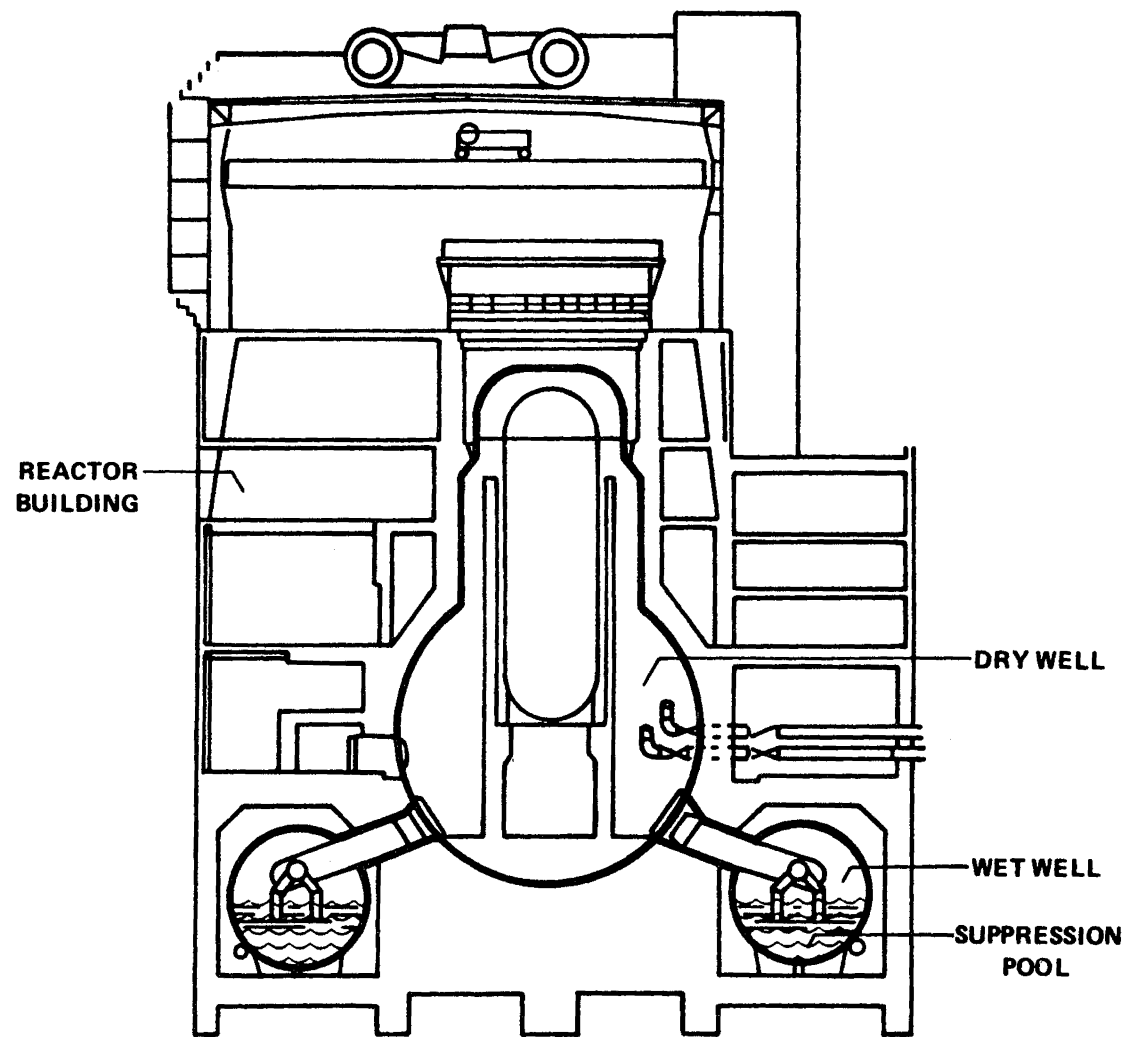


**FIGURE 3.6. BWR MARK I CONTAINMENT DESIGN**

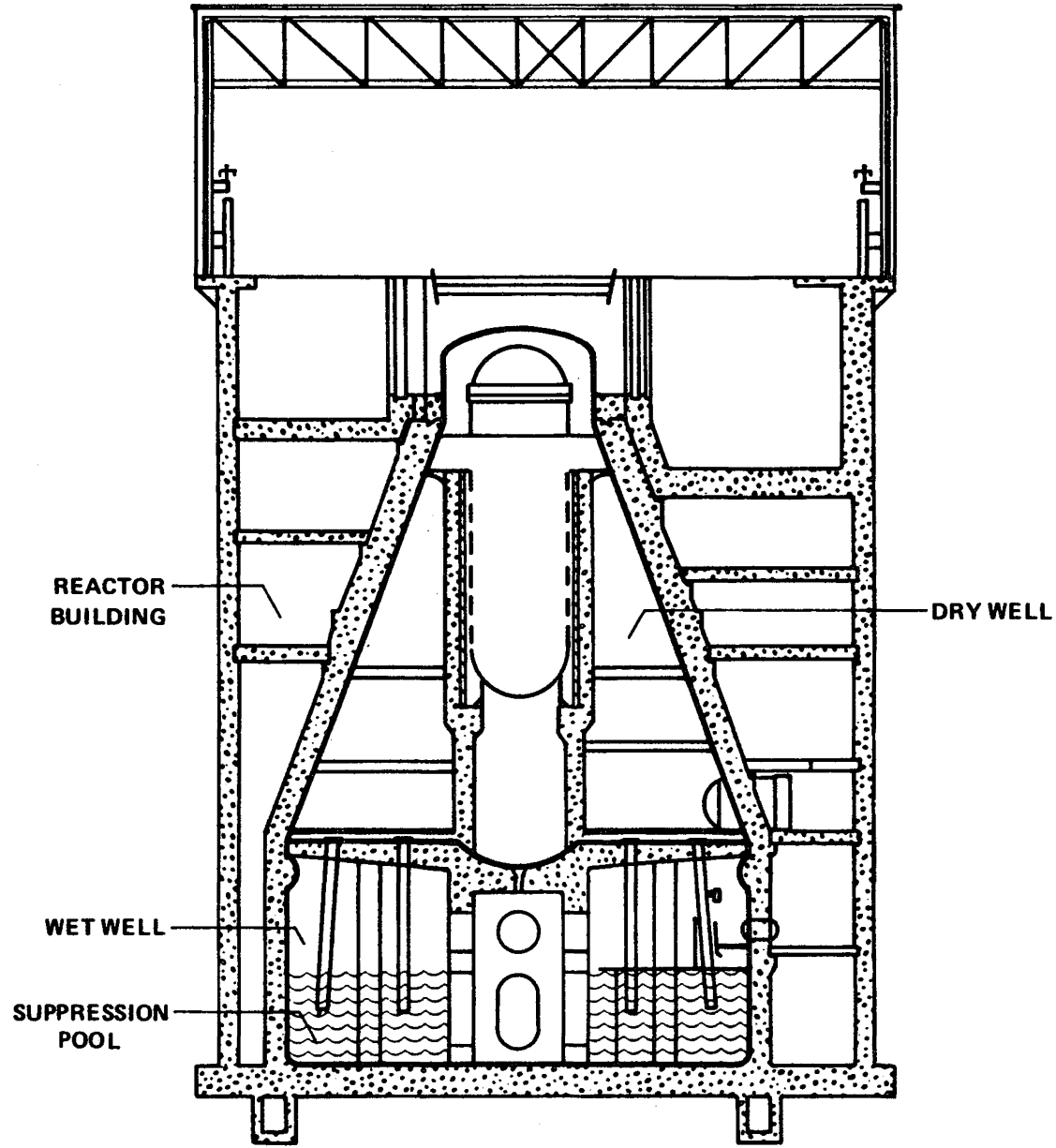


FIGURE 3.7. BWR MARK II CONTAINMENT DESIGN

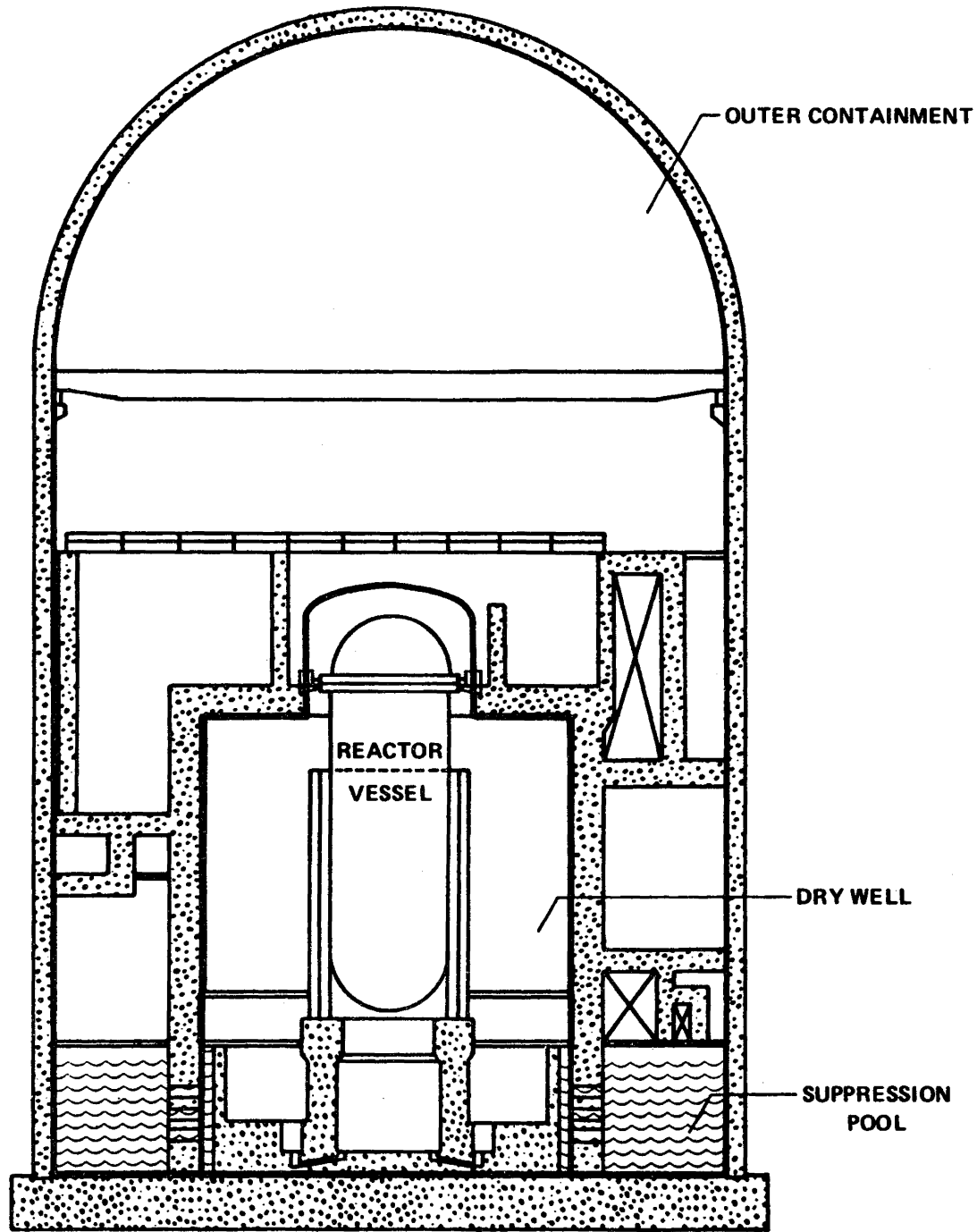


FIGURE 3.8. BWR MARK III CONTAINMENT DESIGN

In addition to condensing steam in an accident, the BWR suppression pools would remove fission products from the flow of gases passing from the drywell to the vapor space of the wetwell. Sprays systems are also included in these designs but would not necessarily be activated in an accident.

### 3.2 Accident Classification

A variety of accident sequences are considered in the safety analysis of a nuclear power plant including: a fuel handling accident in the spent fuel storage pool, rupture of a waste gas storage tank, ejection of a control rod from the core, seizure of a coolant pump, and rupture of a reactor coolant pipe. In this report, we will limit our consideration to accidents which can potentially affect the integrity of the fuel in the core. This is not because these other accidents are unimportant but because the potential consequences of accidents that affect the fuel can be much greater.

Different methods have been used to categorize accident sequences. An approach developed by the American Nuclear Society groups sequences according to the likelihood of the event and the resulting condition of the plant. The four categories are described in Table 3.1. Accidents in each of these categories are analyzed in safety analysis reports. The most limiting of these accidents are referred to as design basis accidents because they establish criteria for the design of the plant and the performance of the engineered safety features. At some level of probability, combinations of system faults can lead to accidents that are more severe than accidents that fall within the design basis envelope. These accidents are not usually analyzed in safety analysis reports. They are considered in risk studies and are currently being evaluated in the assessments of the environmental impacts of accidents.

Using the conservative analysis methods required for safety analysis reports, the isotopes of iodine, in particular iodine-131, are found to dominate the consequences for many of the Condition II, III, and IV accidents. In 1977, Brookhaven National Laboratory undertook a program to estimate the risk to the public from accidents that fall within the design basis envelope.<sup>(3.1)</sup> Based on the state of technology at that time, an attempt was made to estimate the consequences of these accidents realistically. The results indicated that only a small amount of iodine would be released from the fuel and that most of this would be retained in water in the system. For most accident sequences, releases of noble gases were found to represent the principal health hazard to the public.

The maximum extent of damage to the fuel that could be realistically expected in Condition I to IV accidents would involve cladding rupture of some rods. In the event of multiple system failures, however, more extensive damage could occur, up to and including fuel melting. Because they have not been included in licensing analyses, there has been

TABLE 3.1  
ANS Classification of Sequences

Condition	Description	Examples
I	Normal Operation and Operational Transients	Power operation, plant heatup and cooldown, response to minor load changes
II	Faults of Moderate Frequency	Loss of external electrical load, turbine trip, loss of normal feedwater flow
III	Infrequent Faults	Complete loss of reactor coolant flow, minor steam piping failure, small pipe breaks
IV	Limiting Faults	Large pipe breaks, reactivity accidents, steam generator tube rupture

much less research into the physical processes of severe core damage accidents than for the design basis accidents. The Reactor Safety Study, performed from 1972 to 1975, was the first systematic attempt to describe core meltdown sequences and to estimate their consequences realistically.<sup>(3.2)</sup> Most of the effort in the Study was directed toward core meltdown sequences because of their importance to the risk to the public. Using methods based upon the existing state of technology, the consequences of core meltdown sequences were calculated to be much larger than those of the Condition I to IV events. Because the predicted consequences were so much more severe, core meltdown sequences were found to dominate the risk despite their low probability of occurrence.

In order to provide a framework for evaluating the state of technology for predicting fission product behavior in accidents, analyses will be performed in the succeeding chapters of this report for a number of accident sequences. These sequences will be considered under two major headings: accidents involving minor or no fuel damage, and severe core damage accidents. Severe core damage accidents are further divided into degraded core sequences and meltdown sequences.

### 3.3 General Description of Accident Sequences

The accident sequences that are described in this section provide the context in which the phenomena of fission product release, chemical form, transport in the reactor coolant system, and transport in the containment building are analyzed in subsequent chapters of this report. A number of criteria were used in the selection of sequences for analysis. It was desired that the sequences span a broad range of core damage, reactor coolant system conditions, and containment conditions. Since one of the objectives of the report is to examine the realism of the accident consequence predictions in previous risk studies, a number of the most important accident sequences for the two WASH-1400 plants were selected for analysis. In addition, it was desired to examine the behavior of fission product transport in other types of containment designs. Sequences for analysis in these designs were selected in a manner such that the effectiveness of the engineered safety features in retaining fission products could be explored.

A number of qualifying statements should be made regarding the sequences analyzed. A disproportionate emphasis in the selection of accident sequences has been placed on severe core damage sequences involving not only complete melting of the fuel but also the impairment of containment safety features. The likelihood of these sequences is very small and it should not be inferred by the reader that these consequences are typical of reactor accidents or even of core meltdown accidents. The emphasis is placed on the analysis of these accidents because their predicted consequences using the types of methods in WASH-1400 are by comparison so

large that they have dominated previous risk studies. They are also the principal focus of public concern. Accidents in which the containment does not fail, in which containment failure is substantially delayed, or in which safety systems (e.g., sprays, pools, ice beds, or filters) are effective in retaining a large fraction of the fission products do not pose an immediate threat to the lives of the public.

The accident sequences that have been analyzed are just a small sample of those possible for a given plant design. Many important accident sequences have not been analyzed. Furthermore, because of limitations in the codes that are available, it was not possible to do a consistent systematic analysis for the sequences that were analyzed to account for interactions between the release from the fuel, transport in the primary system and transport in the containment building. Each of these stages of release and transport is treated separately (see Chapters 4, 6, and 7). The results of the analyses can therefore be used to examine fission product retention mechanisms in each stage but they cannot be used directly to obtain revised estimates for the release of fission products to the environment for specific accident sequences. The systematic analysis of accident sequences (in particular the reanalysis of WASH-1400 accident sequences) is being given high priority in the on-going research programs.

#### 3.3.1 Sequences Involving Minor or No Fuel Damage

Because the anticipated consequences of these accident sequences are expected to be quite small, limited consideration is given to their analysis in this report. If one of the large reactor coolant pipes were to rupture, the fuel would be expected to become exposed before the emergency core cooling system could refill the vessel and recover the core. As a result, the temperature of some fuel rods would rise to a level at which the cladding would rupture and release some fraction of the inventory of fission products in the interconnected voids in the fuel rod, most notably the gap between the fuel and the cladding. An accident of this type is analyzed in Chapter 6 to evaluate the potential for retention of these fission products within the reactor coolant system.

#### 3.3.2 Severe Core Damage Sequences

Severe core damage sequences would not necessarily involve complete core meltdown. The Three Mile Island accident is an obvious example of a sequence that exceeded some design bases but which did not result in core meltdown. Although the consequences of severe core damage sequences could vary greatly, the conditions leading to core damage would always be similar. Either the rate of heat generation in the fuel must rise to a level that is too great to be removed by the coolant or the coolant must

be lost from the reactor system so that the fuel is no longer cooled. The latter situation is the more likely type of accident leading to core damage. Because the fission products in the fuel are radioactive, they continue to generate heat even after the chain reaction has been terminated. The emergency core cooling systems described in Section 3.1 are provided in reactors to assure that if water were lost from the reactor coolant system, a reliable supply would be available to refill the system, cover the fuel, and remove the heat produced by the fission products.

A characteristic accident sequence leading to core damage would be one in which a combination of failure results both in water loss from the system and in the failure of the emergency core cooling system to function properly. In such an event, water loss would gradually result in uncovering of the core with subsequent heatup and damage to the fuel rods. If there were delayed or partial performance of the emergency core cooling system, core damage might be arrested as in the Three Mile Island accident. If the cooling water were not supplied in time, core meltdown would result.

Degraded Core Sequences. In this report, two types of accident sequences are analyzed. These are considered to be representative of accidents in which severe damage to the fuel would occur but in which full core meltdown would be averted. The first sequence is a TMI-like accident in which fission products are released into a water-filled environment. The purpose of analyzing this accident is not to attempt to reproduce the conditions in the Three Mile Island accident and in some respects the sequence evaluated differs from the actual accident. Rather, the purpose is to examine the behavior of an accident which has some interesting features which are believed to be characteristic of a broader class of accidents.

The second sequence analyzed is a loss-of-coolant accident with delayed performance of the emergency core cooling system. This accident is quite similar to a core meltdown sequence described later in this section, except that melting of the fuel is assumed to be arrested by operation of the emergency core cooling system with the core approximately half melted. (See sequence AD, page 3.19.) During the time period of fission product release in this accident the pathway through the reactor coolant system to the containment would be expected to be dry.

Both of the degraded core sequences examined were for a PWR. Analogous sequences are also possible in a BWR. When considering partial performance of engineered safety features, as required for degraded core sequences, the spectrum of possible outcomes is very broad ranging from consequences typical of accidents within the design basis envelope to consequences similar to full core meltdown accidents.

Core Meltdown Sequences. A number of core meltdown sequences are analyzed in this report. In general, these sequences will provide the greatest challenge to the engineered safety features in the plant. They involve both large releases of radionuclides and aerosols from the fuel and structures as well as severe physical events, such as rapid hydrogen burning and molten fuel-coolant interactions, with the potential to damage or fail the containment building.

In order for the radioactive material released from the fuel in a meltdown accident to be a health hazard to the public, it would have to escape to the environment. The first stage of release from the fuel would occur in the reactor vessel. Before this material could reach the containment atmosphere, several mechanisms could operate on it to retain it on surfaces or in water, if there is water in the flow-path to the containment building. In Chapter 6, the degree of fission product retention that might be expected in the reactor coolant system is explored as a function of the assumed chemical form.

A number of retention mechanisms also act on the radioactive material that reaches the containment atmosphere. In PWR containment designs, spray systems are provided which would assist in removing fission products from the containment atmosphere. Spray systems are also available in BWR designs but would not necessarily be activated in all cases. Even in accident sequences in which the spray systems are assumed to fail, natural mechanisms such as settling of aerosols would remove material from the atmosphere with time. In the pressure suppression designs, the method of steam suppression, water pools, or ice beds, could also be very effective in trapping fission products.

The amount of radioactive material released to the environment in an accident sequence depends not only on the effectiveness of retention mechanisms but also on the mode of release from the containment. If the integrity of the containment building were maintained throughout the accident, there would be a small leakage of radioactive material to the environment but the resulting health consequences would be minor. This would also be true if the molten core were to penetrate the concrete basemat of the plant and release fission products into the underlying soil. If on the other hand, there should be an atmospheric failure of the containment, the amount of release could be much greater.

In Appendix A, a generic description is provided for the conditions which would affect the release, chemical form, and transport of fission products in the reaction vessel and containment building for different types of core meltdown sequences. The intent of this appendix is to illustrate the possible pathways of release from the fuel to the environment, the likely conditions in the pathways and the influence of engineered safety features on the transport and retention of fission products. Many accident sequences are possible which are covered by the generic discussion

in Appendix A. For the purposes of this report, it was necessary to select a few sequences for analysis from this spectrum of possible accidents. These sequences were chosen to examine the performance of a specific safety system or a particular range of accident conditions.

Each of the sequences analyzed is briefly described in this section. The nomenclature for the sequences is adopted from the Reactor Safety Study.<sup>(3.2)</sup> Tables A.1 and A.2 in Appendix A relate the letters used in the accident identifier to the type of event and to the failure of engineered safety systems.

These sequences are all believed to be very low probability events. It should be recognized that there are large uncertainties both in the ability of the methods of reliability analysis to estimate the likelihood of these sequences and in the methods of accident analysis to predict the course of the accident, in particular the mode of containment failure. Assumptions have been made in the description of each accident sequence which can have a significant effect on the pathway of fission product release and the magnitude of the predicted consequences. For example, in some of the BWR sequences, it has been assumed that failure of the containment would occur in the torus region. This assumption was based on structural analyses presented in WASH-1400 which are subject to significant uncertainties. If instead containment failure were to occur in the drywell, the leak pathway and predicted consequences would differ. In reviewing the description for each accident sequence, the reader should recognize the uncertainties that may exist in predicting accident pathways. The pathway described may be only one possibility which is consistent with a given set of assumptions.

PWR Sequences. Large Pipe Break Accident, Failure of ECC System (AD). In the event of a large pipe break, coolant would be rapidly lost from the reactor vessel and the core would become uncovered. If the emergency core cooling system were to fail to deliver water to the reactor coolant system, core heatup and meltdown would follow. The location of the break, in the outlet or inlet piping to the reactor vessel, can have a substantial effects on the conditions encountered by radioactive nuclides as they transport through the reactor coolant system. Engineered safety features unrelated to the cause of failure of the ECC system, such as the containment heat removal system, would be expected to operate and to influence the course of the accident.

Small Pipe Break Accident, Failure of ECC System (S<sub>2</sub>D). A small pipe break accident would result in a slower depressurization of the reactor coolant system and, in the event of failure of the emergency core cooling system, a more delayed uncovering of the core. Containment safety features would be expected to be operational for this type of

accident sequence. However, the containment spray system might not be automatically activated if the containment pressure does not exceed a preset level.

Loss of All AC Power, Loss of Reactor Coolant System Heat Removal (TMLB'). Reactors are designed such that if offsite power is lost and the diesel generators which provide an emergency source of AC power fail to operate, decay heat can continue to be removed from the reactor coolant system through the steam generators fed by steam-turbine driven pumps. With this mode of heat removal failed, however, the ECC pumps which are driven by AC power would not operate and the inventory of reactor coolant water would eventually be boiled away through pressure relief valves. Similarly the AC powered containment safety features, such as the containment heat removal system, would not operate. The likelihood of containment failure by overpressurization in this sequence would be very high and the consequences potentially severe.

Interfacing Systems Loss of Coolant Accident (V). Check valves provide a barrier between the low pressure ECC system and the high pressure piping of the reactor coolant system. In the event that these valves should fail, pressures beyond the design capability of the low pressure system could be imposed on it. The subsequent failure of the system would result not only in loss of reactor coolant, but potentially also in failure of the emergency core cooling system. Since the low pressure piping is located in the auxiliary building, the failure of the reactor coolant system would be external to the containment building and released radioactive material would bypass the containment safety features. In the Reactor Safety Study, this sequence was assessed to be the highest contributor to risk for the specific design analyzed.

Large Pipe Break Accident, Loss of All AC Power (AB). Loss of all AC power would result in failure of the emergency core cooling system and subsequent core meltdown. Similarly the engineered safety features in the containment which are dependent on AC power would not operate and the likelihood of an atmospheric failure of the containment building would be high. The behavior within the reactor coolant system would be essentially the same as for sequence AD. The response within the containment building would be similar to that of TMLB'.

Small Pipe Break Accident, Failure of Containment Spray Injection (S<sub>2</sub>C). In some plant designs, there is a potential common cause failure relationship between failure of the containment spray injection system, in a small pipe break accident, with loss of containment heat removal capability. In this accident sequence, the containment building would overpressurize and fail prior to core meltdown. Fuel melting would be delayed approximately one day after the start of the accident. Fission products would be released into a failed containment building.

Small Break, Failure of the Recirculation Modes of the Emergency Core Cooling System and the Containment Spray System (S<sub>2</sub>HF). This sequence has been analyzed for the ice-condenser plant because a potential common cause failure of the two recirculation systems is possible. If the return lines from the upper deck to the containment sump are left closed or become blocked, water sprayed into the upper compartment would remain there. After the ice was all melted and the sump ran out of water, the recirculation systems would fail. The fuel would become uncovered, heatup, and melt. Neither the ice nor the containment spray system would be available at this point to condense steam or remove radioactive material from the containment atmosphere.

BWR Sequences. Large Pipe Break, Failure of the Standby Core Cooling System (AE). A large break in the piping of the recirculation loop piping would result in loss of reactor coolant and uncovering of the core. If the standby core cooling system were not to operate to refill the reactor coolant system, the fuel would heatup and melt. Radioactive material released from the reactor coolant system to the drywell would be scrubbed as it passes through the suppression pool. The release of hydrogen and non-condensable gases from the molten core-concrete interaction is predicted to eventually fail the containment by overpressurization.

Anticipated Transient, Failure of Reactor Shutdown Systems (TC). If the control rods failed to insert and the backup liquid neutron absorber system failed to operate in a transient event requiring reactor shutdown, the reactor power would level off at a heat generation rate well above decay heat. At the estimated power level, the high pressure coolant injection system would not have adequate capacity to match the boiloff of water from the coolant system. The core would eventually become uncovered, heatup, and possibly melt. The large quantity of heat transferred to the suppression pool would result in boiling in the pool, preventing further steam suppression and reducing the capability for scrubbing radioactive material.

Anticipated Transient, Failure of Decay Heat Removal (TW). If the decay heat removal system failed, the suppression pool would be predicted to heatup, boil, and, after an extended period of time, fail the containment by overpressurization. For the specific design analyzed, during depressurization of the containment, the emergency coolant pumps would be expected to cavitate with potential to stop delivering cooling water to the reactor vessel. Subsequently, the fuel could become uncovered, heatup, and melt. Fission products released from the fuel to the drywell might pass through the boiling suppression pool or bypass the pool depending on the location of containment failure.

Anticipated Transient, Failure of All Makeup Water (TQUV). In this sequence, it is assumed that none of the potential sources of makeup water are available following a transient-initiated shut-down of the reactor. In this event, steam would be released from the reactor coolant system through pressure relief lines to the suppression pool. The fuel would become uncovered, heatup, and melt.

#### REFERENCES TO CHAPTER 3

- 3.1 R. E. Hall, et al., "A Risk Assessment of a Pressurized Water Reactor for Class 3-8 Accidents", NUREG/CR-0603 (October, 1979).\*
- 3.2 "Reactor Safety Study, An Assessment of Accident Risks in U.S. Commercial Nuclear Power Plants", WASH-1400 (October, 1975).\*\*

\*Available for purchase from the NRC/GPO Sales Program, U.S. Nuclear Regulatory Commission, Washington, DC 20555, and/or the National Technical Information Service, Springfield, VA 22161.

\*\*Available free upon written request to the Division of Technical Information and Document Control, U.S. Nuclear Regulatory Commission, Washington, DC 20555.

## 4.1

### 4. FISSION PRODUCT RELEASE FROM FUEL

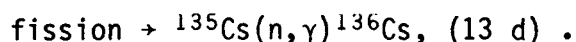
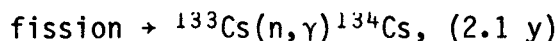
#### 4.1 Fission Product Behavior in Fuel

Understanding of the initial state of iodine and other fission products in the fuel pellet is helpful in tracing its subsequent movement into the primary and secondary system under accident conditions. The fuel pellet forms the initial boundary for fission products, and their chemical form on leaving the pellet governs the initial behavior in an accident environment.

##### 4.1.1 Precursor Effects

Fission products in their radiologically important form are born as elements of slightly lower atomic number and decay to progressively more stable elements by emitting  $\beta$ -particles. Table 4.1 summarizes this situation for the mass numbers 127 through 138 which includes isotopes of the elements tin (Sn), antimony (Sb), tellurium (Te), iodine (I), xenon (Xe), cesium (Cs), and barium (Ba). The second column of Table 4.1 denotes the yield for each mass number, i.e., the number of atoms of that particular mass produced in 100 fissions. The [brackets] denote the element at birth, with  $\beta$ -decay at each mass number producing the elements to the right at a rate depending on the half-life of the specie. From Table 4.1 we note the following:

Relatively stable Cs fission products isotopes (half-lives greater than one day) exceed relatively stable iodines by a factor of 4.7. This ratio is increased by significant amounts of  $^{134}\text{Cs}$  and  $^{136}\text{Cs}$  which build in by neutron absorption via



Therefore, the total amount of cesium significantly exceeds iodine. All important iodine isotopes (except  $^{135}\text{I}$ ) spend significant time from 25 min to 78 h) as tellurium. Therefore, tellurium mobility and chemistry could play a role in the overall picture of iodine release, especially since it is relatively volatile and shows a chemical affinity for cesium ( $\text{Cs}_2\text{Te}$ ). The yield for relatively stable Te species ( $T_{1/2} > 1 \text{ day}$ ) is 2.3 times that for relatively stable I species. (If one counts  $^{133}\text{I}$  with  $T_{1/2} = 21 \text{ h}$ , this ratio falls to 0.63.)

Precursor effects for cesium may be significant only for the formation of  $^{134}\text{Cs}$  which spends 21 h as  $^{133}\text{I}$  and 5.3d as  $^{133}\text{Xe}$  prior to subsequent activation to  $^{134}\text{Cs}$ . Therefore, we should not be surprised to find  $^{134}\text{Cs}$  behaving differently from the other cesium isotopes.

##### 4.1.2 Fission Product Behavior in the Fuel Pellet

The average fission fragment begins its life with a kinetic energy of about 80 MeV, which is roughly  $10^7$  times the energy of a typical chemical bond. Therefore, each fragment causes considerable lattice dislocation before either coming to rest within the  $\text{UO}_2$  crystal (or adjacent

## 4.2

Table 4.1. Iodine, xenon, and cesium fission product isotopes showing yields and half-lives. The bracket denotes elements at birth

Mass No.	Total yield (%)	$\beta$ -decay						
		Sn	Sb	Te	I	Xe	Cs	Ba
127	0.14	[4.4 m]	3.8 d	9.4 h	$\infty$			
128	0.46	[60 m]	10 m	$\infty$				
129	1.0	[7.5 m]	4.3 h	70 m	$\sim\infty$			
130	2.0	[3.7 m]	[6.3 m]	$\infty$				
131	2.93		[23 m]	[25 m]	8.0 d	$\infty$		
132	4.31		[2.8 m]	[78 h]	2.3 h	$\infty$		
133	6.69		[2.7 m]	[55 h]	21 h	5.3 d	$\infty$	
134	7.92			[42 m]	53 m	$\infty$	2.1 y <sup>a</sup>	
135	6.43			[18 s]	[6.6 h]	9.1 h	$\sim\infty$	
136	6.45			[21 s]	[46 s]	$\infty$	13 d <sup>a</sup>	
137	6.18				[25 s]	[3.8 m]	30 y	$\infty$
138	6.71				[62 s]	[14 m]	32 m	$\infty$

<sup>a</sup>By neutron capture.

crystal) or being expelled from the pellet surface. The initial states of fission products are then as individual atoms in interstitial locations in the  $UO_2$  lattice. The precise manner in which these individual atoms move to either microbubbles, metal phase inclusions, or to phases including chemical combination with  $UO_2$  is quite complex and imperfectly understood. Yet this initial phase in the life of a fission product is very important since it represents the major resistance to transport to the pellet exterior.

However, some general characteristics of this early state of fission products in  $UO_2$  are as follows:

Above some critical temperature (between  $1100^\circ$  and  $1400^\circ C$ ) general lattice mobility exists, allowing the individual atoms to move easily to more stable thermodynamic states. For atoms inert to  $UO_2$  (the gases Kr, Xe, and probably I and Te and the noble metals, Ru, Tc, Rh, Pd), this means moving from the interstitial location to either a microbubble or a metallic phase. Other elements (Zr, Nb, and the rare earths) move to locations in the  $UO_2$  lattice to form true solutions. The alkaline earths (Sr, Ba) would migrate to form a separate oxide phase. Cesium would tend to form a separate cesium uranate phase when such is stable ( $T < \sim 1500^\circ C$ ), but its high vapor pressure over cesium uranate would probably remove Cs from high temperature locations by migration with the other gaseous species. If sufficient Cs is available from the Cs/cesium uranate equilibrium, the balance may combine with I to form CsI.

Below the temperature of general mobility in the  $UO_2$  lattice, large atoms inert in  $UO_2$  such as Xe probably migrate as complexes with one U- and two O-vacancy locations. This rather odd behavior is only supposition, but these large atoms are too firmly wedged in interstitial locations to move in a more conventional way.

The manner in which a more active atom, like Cs, moves under these conditions is even more unclear. It is important though to point out that at this phase of life of a fission product, the laws of macro-chemical equilibria may not apply. The Cs and I atoms here migrate as a complex with a set of lattice vacancies. There may or may not be opportunity for significant chemical combinations even when equilibria considerations so dictate.

#### 4.1.3 Predicted Chemical Behavior of Iodine and Cesium in $UO_2$

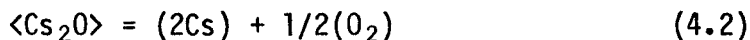
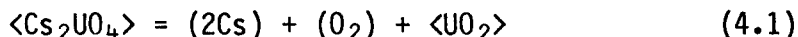
Under normal chemical circumstances, and if the opportunity occurs, iodine prefers to exist predominantly as stable species CsI or some other iodide rather than either atomic I or the molecule  $I_2$ . However, some hedging is necessary here because some features of the environment within a fuel rod differ significantly from conditions forming the basis of usual chemistry or equilibrium chemical thermodynamics. Iodine and cesium atoms are born separately within the  $UO_2$  lattice and initially have quite different chemical tendencies in  $UO_2$ . Iodine, having no chemical affinity for  $UO_2$ , would tend to migrate into the gas

phase along with the noble gases, whereas cesium, with its higher chemical affinity for its surroundings, could behave quite differently. There is no way of predicting whether or not cesium at this stage has an opportunity for combining with iodine, or whether iodine is effectively "swept" from cesium by the migration to the noble gas bubbles.

Assuming an approximately conventional equilibration of Cs, I, O<sub>2</sub>, and UO<sub>2</sub>, two general categories of reactions need to be considered:

(1) dissociation reactions, and (2) vaporization reactions.

Dissociation reactions



Vaporization reactions



The brackets signify the assumed state; < >, { }, and ( ) signify solid, liquid, and gas phases, respectively. The above six reactions are perhaps the most significant ones of the dozens that need to be considered on the determination of equilibrium compositions. In particular, the formation of zirconium compounds, ZrO<sub>2</sub> and ZrI<sub>4</sub> may be significant near the cladding. At any rate, these six reactions are selected here to illustrate the types of interrelationships which may occur between competing reactions.

Reactions (4.1) through (4.6) plus many others form a set of competing reactions, the net result of which is an equilibrium composition of the gas phase plus various amounts of the condensed phases. The manner in which this estimate is performed falls within the realm of chemical thermodynamics. Here we should point out the following interrelationships:

(1) All dissociation and vaporization reactions are coupled, for example, by the following illustration: If conditions favor CsI dissociation [reaction (4.3)] to a degree which would yield an iodine partial pressure greater than the vapor pressure at that temperature [reaction (4.5)], then CsI dissociates and all the iodine transfers to a condensed iodine phase via



Alternatively, if a condensed iodine phase possesses a vapor pressure greater than the dissociation pressure of iodine over CsI under a particular set of conditions, the condensed phase iodine would vaporize and combine with Cs to form CsI by the reverse procedure. A similar discussion would apply as well for Cs dissociation pressures via reactions (4.1) and (4.2) and Cs condensation via reaction (4.6).

(2) If CsI formation by the reverse of reaction (4.3) tends to generate a cesium iodide partial pressure higher than the vapor pressure at that temperature [reaction (4.4)], liquid or solid CsI would form to a degree which equalizes the pressures:

$$P_{\text{CsI}}[\text{reaction (4.3)}] = P_{\text{CsI}}^*[\text{reaction (4.4)}] .$$

(The asterisk denotes vapor pressure above a pure substance.) Conversely, if the association pressure of CsI via reaction (4.3) is less than the vapor pressure of CsI, no condensed phase CsI would form.

(3) Reactions (4.1) and (4.2) illustrate the key role played by the level of the oxygen pressure. Within the  $\text{UO}_2$  lattice, the oxygen pressure is imposed by the degree of hyperstoichiometry, i.e., by the value of  $x$  in  $\text{UO}_{2+x}$ . In fresh LWR fuel, the oxygen excess is such that the chemical potential of oxygen,  $RT \ln P_{\text{O}_2}$ , is normally  $\sim -300$  kJ/mol. Burnup tends to increase the oxygen pressure, but LWR burnup even at discharge does not change it significantly. Under conditions of high heat rating ( $>43$  kW/m), the oxygen pressure is drastically reduced in the vicinity of the clad due to formation of  $\text{ZrO}_2$ .

In addition, progressively higher oxygen pressure tends to favor the formation of cesium uranate (reverse of reaction (4.1)) tending to make cesium unavailable for cesium iodide. Therefore, high oxygen pressure tends to destabilize CsI by



However, chemical thermodynamic estimates predict this to occur at fairly high oxygen pressure ( $\sim -100$  kJ/mol), in the region where  $\text{U}_3\text{O}_8$  is stable, rather than  $\text{UO}_2$ .

Some key properties of the materials in Eqs. 4.1-4.6 are given in Table 4.2. The free energy of formation at 1000 K, given in the first column, is a measure of chemical stability in the presence of their elements, the more negative values indicate greater stability for these conditions. We note also that CsI is a compound of intermediate volatility. If present, it would be predominantly gaseous at central rod temperatures, a liquid at intermediate locations, and a solid near the cladding surface. Cesium oxide ( $\text{Cs}_2\text{O}$  plus other oxides) also fall into this range of intermediate volatility. Cesium uranate  $\{\text{Cs}_2\text{UO}_4\}$  would tend to decompose into (Cs),  $\langle\text{UO}_2\rangle$ , and ( $\text{O}_2$ ) at elevated temperatures ( $> \sim 1500^\circ\text{C}$ ). The cesium uranate phase would be liquid throughout much of the pellet volume and be a separate solid phase near the clad surface.

Methods based on chemical thermodynamics can often be quite helpful in predicting the chemical composition of complex mixtures, but as with all idealized calculations, it is essential to emphasize its inherent limitations. These limitations include the following: (1) kinetic effects frequently determine composition rather than chemical equilibria; (2) conditions within the fuel pellet differ in many respects from that

Table 4.2. Characteristics of some key materials

	Melting point (°C)	Boiling point (°C)
UO <sub>2</sub>	2830	
Cs <sub>2</sub> UO <sub>4</sub>	940	Decomposes
Cs <sub>2</sub> O	490	Decomposes
CsI	626	1280
Cs	30	700
I <sub>2</sub>	114	183

normally encountered, i.e., intense radiation field, large temperature gradients; (3) the solubility of some condensed phases in  $UO_2$  at high temperature is not well known and can cause an uncertain degree of error.

These limitations mean that predictions based on equilibrium chemical thermodynamics, while they are of interest, do not carry the force of direct observation and must be considered as being uncertain. Bearing this in mind, we note that calculations of this type were performed<sup>(4.1)</sup> to determine the chemical forms of I and Cs in  $UO_2$  predicted up to  $\sim 950^\circ C$  in three atmospheric environments: typical in-fuel rod conditions steam, and for a 50-50 steam-air mixture. The value of the oxygen pressure for the normal atmosphere case was assumed to be that imposed by the preponderant  $UO_{2+x}$ . The approach was first to estimate the composition of the cesium species in these environments. Subsequently, a representative amount of I was added to the calculation to determine the composition of I-species. In each case, the addition of Cs to  $UO_2$  or the addition of I to Cs +  $UO_2$ , the addition was assumed to cause negligible perturbation of the preponderant host environment.

Some results of this study<sup>(4.1)</sup> are the following:

- (1) The major form of Cs in  $UO_2$  under normal conditions appears to be the cesium uranate,  $Cs_2UO_4$ , at least up to  $950^\circ C$ . "Normal conditions" means an oxygen potential of between  $-350$  and  $-300$  kJ/mol, corresponding to an oxygen level in  $UO_2$  of from  $UO_{2.0001}$  to  $UO_{2.001}$ . A higher uranate,  $Cs_2U_2O_7$ , may exist at lower temperatures,  $T < \sim 800$  K.
- (2) The major form of a representative quantity of I in the stable  $Cs_2UO_4$  zone is CsI. At somewhat higher oxygen pressures ( $\sim -280$  kJ/mol at 1200 K) or lower temperatures ( $< 800$  K at  $-300$  kJ/mol), a higher uranate form exists ( $Cs_2U_2O_7$ ) over which the cesium pressure is lower, but not to the extent of destabilizing CsI.
- (3) It is thought that oxygen potentials as high as  $\sim -100$  kJ/mol would be required to destabilize CsI by



This would occur in the region where  $UO_3$  is the stable form of uranium oxide, which is highly unlikely in LWR fuel.

- (4) Conditions in a steam environment are predicted to be about the same as for the normal environment case; i.e., the addition of pure steam does not significantly alter the oxygen potential in  $UO_{2+x}$ .
- (5) When a 50-50 steam/air environment is assumed, higher cesium uranates, e.g.,  $Cs_2U_{15}O_{46}$ , are predicted to be the stable form of Cs. These essentially lock up the available Cs, rendering CsI unstable. The stable iodine under these conditions is therefore  $I_2$  or I.

## 4.8

It should be emphasized that these predictions are from an idealized computation based on chemical thermodynamics. There are a number of ways that error can be introduced into these estimates, and they grow more uncertain as temperatures extend above 950°C.

### 4.1.4 Observed Behavior in Fuel

Observations regarding the state of cesium and iodine in fuel pellets fall into three categories: (1) measured concentration profiles and observed solid phases in discharged fuel; (2) thermomigration experiments performed using fresh  $UO_2$  and simulated fission products; and (3) fission product release experiments.

#### Concentration profiles and observed solid phases in discharged fuel

Radial concentration profiles in discharged fuel pellets may be determined using electron microprobe or micro-collimated, gamma spectroscopy. Occasionally, the chemical form of the fission product may be inferred from the nature of the measured profile. For example, Kleykamp (in ref. (4.2)) observed that a cesium concentration peak at the outer radial edge of a pellet extracted from a high heat rated rod (43 kW/m) coincided with concentration peaks of Zr, Sn, and O. For this case then, a chemical association is inferred involving a Cs-Zr-Sn-O compound.

Unfortunately, no similar distinct features in iodine radial profiles have been found from which its chemical state in the fuel may be deduced. Peehs et al. (in ref. (4.2)) measured  $^{137}Cs$  and  $^{129}I$  radial profiles in fuel irradiated at 23, 42, and 56 kW/m. The lowest heat-rated fuel showed essentially no radial redistribution. At the higher heat ratings, radial redistribution in the fuel did occur, and the redistribution of iodine and cesium followed similar trends. However, no conclusions regarding the chemical state of either cesium or iodine can be drawn from observed radial concentration profiles.

Numerous distinct chemical phases may be observed in discharged fuel pellets using metallographic techniques. Determination of the elemental composition of these phases by use of an electron microprobe can lead to an understanding of the chemical nature of fission products in each phase. A summary of phases observed in discharged fuel has been presented by Kleykamp<sup>(4.3)</sup> which represents the state-of-knowledge in this area as of 1972.

Kleykamp observed 22 distinct fission product phases of which three contained cesium. None contained iodine, which probably means that iodine was uniformly distributed throughout the  $UO_2$  and did not segregate in any separate solid phase. The same is true for cesium; the observed cesium-bearing phases were found near the clad and contained cladding material. No distinct cesium-bearing phase was found in the interior of the pellet. However, crystalline deposits containing cesium and iodine have been observed on internal cladding surfaces (Ref. 4.33).

Therefore, we came to an uncertain conclusion regarding direct observations of discharged fuel. Neither published concentration profile measurements nor observed phase compositions have shed light on the chemical form of cesium or iodine in the fuel element.

#### Thermomigration experiments

In these experiments, fission product simulants are added to  $UO_2$  in a manner calculated to approach the environment of a degree of burnup. The  $UO_2$  is then placed in a temperature gradient, and the movement of the fission product simulants followed by gamma spectrometry. The physicochemical state of the fission products is inferred from the extent of its movement. In this way a completely sealed system may be used, thereby preserving the intended oxygen pressure in the fuel pin. A significant disadvantage of this method is that the simulated fission products are applied to the exterior of the  $UO_2$  grain. For refractory fission products, pellet sintering creates some diffusion into the grain, thereby approaching a more realistic initial condition. This is not possible with volatile fission products which would have to be applied to either the  $UO_2$  powder or nonsintered pellet. Therefore, thermomigration experiments exclude a significant chapter in the life and transport of the volatile fission products.

Peehs et al. (in ref. 4.2) conducted several types of thermomigration experiments. In the first I and Cs were uniformly applied to an 11 mm length of  $UO_2$  powder which was placed in an axial temperature gradient between  $\sim 1400^\circ C$  and  $\sim 200^\circ C$ . These tests showed that (1) the Cs and I both migrated to the  $300-320^\circ C$  temperature zone; and (2) a detailed analysis of the measured profiles showed that the I migrated more rapidly than Cs; from which it was concluded that significant amounts of CsI did not form.

The influence of in-grain diffusion of iodine was investigated using trace-irradiated  $UO_2$ . In these tests, the tendency for migration of I was much less, supporting the conclusion that the primary resistance to migration of I exists during its initial state within the  $UO_2$  grain. (In these tests, I remained relatively immobile even at  $\sim 1900^\circ C$ .)

Other tests were conducted to determine the influence of oxygen pressure on Cs and I movement. At near-usual oxygen pressures (corresponding to a formulation of  $UO_{2.02}$ ), the Cs and I both migrated, at first, to the  $1000^\circ C$  location; later, after  $\sim 10$  h, the Cs and I peaks moved down to the  $700^\circ C$  location. A quite different migration pattern occurred at higher oxygen pressures, corresponding to  $UO_{2.1}$ . Under these conditions, the I migrated quickly to  $200^\circ C$  whereas the Cs stabilized at  $1000^\circ C$ . A possible explanation for this behavior is that CsI formed at the lower oxygen pressure and did not form at the higher. At the higher oxygen pressure, cesium uranate formation undoubtedly stabilized the Cs at  $\sim 1000^\circ C$ .

## 4.10

Adamson et al. (in ref. 4.2) studied the movement of Cs, I, Te, and Mo in  $UO_2$  by applying these fission products to one end of ~10-in. length of discharged LWR fuel and placing the length in a temperature gradient ranging from 1400°C to 400°C. The stated conclusions of this study are as follows:

- (1) Cesium migration depends critically on the oxygen pressure, which in the  $UO_{2+x}$  regime, depends on the value of x. Cesium tends to combine with  $UO_2$  to form at least two types of uranates, but at low oxygen pressure, some Cs remains in the metallic state.
- (2) Iodine does not react with  $UO_2$ , but forms CsI when excess Cs is present. CsI is more stable than either Cs-U-O or Cs-Si-O compounds.
- (3) Tellurium migration is complicated in the presence of Cs because both Te and Cs may associate with  $UO_2$ .

Evidence from thermomigration experiments is therefore also somewhat uncertain. In one set of tests (Peehs) CsI apparently did not form in  $UO_2$ . A second test series by the same experimenters using a fuel composition of  $UO_{2.02}$  seemed to indicate CsI formation at least initially. Adamson's tests with low oxygen clearly indicated CsI formation. Subtle differences in technique undoubtedly caused these different results. It is agreed, however, that excess oxygen (in a degree forming  $UO_{2.1}$ ) tends to make iodine appear in the molecular form.

### Fission product release-from-fuel experiments

In principle, at least, the chemical form of volatile fission products, like iodine, may be inferred by observing the rate of evolution from overheated fuels relative to the evolution rate of noble gases. If, for example, the observed release rate of iodine matched closely that of xenon, especially at lower temperatures, (1000°-1400°C), it would speak strongly for iodine being in a highly volatile form in the fuel, i.e., molecular instead of cesium iodide. In fact, in the experiments conducted by Parker<sup>(4.4)</sup> on bare chunks of low-burnup fuel annealed in purified helium, the iodine evolution rate consistently exceeded that of xenon. This bias has been adopted by the ANS 5.4 release rate model in which the recommended diffusion coefficient for iodine is seven times higher than the value for xenon.<sup>4.32</sup>

On the contrary, however, in Lorenz's<sup>(4.5-4.7)</sup> experiments using discharged fuel heated in steam, release of iodine was substantially slower than krypton up to 1400°C. However, we would expect more rapid evolution of noble gases at lower temperatures because surface deposits would be removed in this range, which could not be distinguished experimentally from diffusional release. Therefore, relative release rate data are not useful at this time as an indicator of the nature of the evolved specie.

Lorenz's experiments did, however, contain an approximate means for direct chemical species identification. This was done by observing the

location in the apparatus where the evolved iodine and cesium deposited. Iodine deposit locations above 200°C were presumed to be CsI. The amount of "reactive iodine," which includes I<sub>2</sub>, HI, and CH<sub>3</sub>I, was given by the sum of that found on the charcoal, the filter train (excluding the first filter) plus other cool, nonparticulate deposits. Iodine on particulates was determined principally by the amount on the first filter. (This description is an oversimplification since "reactive iodine" would, to a degree, also deposit on the filter while particulate iodine can deposit in locations besides the filter).

A summary of Lorenz's results is given in Table 4.3, which lists the percent of evolved iodine found as "presumably CsI," "presumably molecular iodine," and as particulates for each test run. We note that for the gap purge tests, which were run in helium (BWR-4 and HBU-12), more than 91% of the released iodine appeared as CsI. The balance of the tests were run in steam and showed smaller percentages of iodine as CsI, ranging from a low of 4% in HBU-8 to 79% in BWR-2. For the steam tests, the molecular iodine ranged from 0.1 up to 88%, and iodine in particulates ranged from 6 to 56%.

Clearly, the fraction of evolved iodine which appeared as CsI was lower in the steam tests than the tests using helium. At least three reasons for this behavior are possible: (1) the iodine evolved as CsI but reacted with steam to form CsOH and HI; (2) the steam contained some air as an impurity which enhanced formation of Cs<sub>2</sub>O, thereby destabilizing CsI; and (3) evolved CsI reacted with quartz to release I<sub>2</sub> in the steam experiments, but had less opportunity to do so in the gap purge tests.

## 4.2 Fission Product Release from Fuel Data

### 4.2.1 Release Rate Mechanisms

Five principal mechanisms control the rate of release of fission products from LWR fuel under accident conditions. They are (1) burst release, (2) diffusional release of the pellet-to-cladding gap inventory, (3) grain boundary release, (4) diffusion from the UO<sub>2</sub> grains, and (5) release from molten material. Each mechanism becomes dominant at a succeeding higher temperature.

The burst release occurs when the overheated fuel rod cladding ruptures. In a LOCA this can be expected to occur in the temperature range 750 to 1100°C depending upon the amount of fission gas and prepressurizing helium in the fuel rod, the primary vessel pressure, and the rate of heatup or time at temperature. When the cladding ruptures, the entire amount of noble fission gases previously accumulated in the plenum and open voids in the fuel rod can be assumed to be released. This amount can range from ~0.25% to ~25% of the total amounts of stable and long half-life fission gas isotopes. Isotopes of gases with half-lives less than 30 days will be present in significantly lower amounts. For instance, the amount of <sup>133</sup>Xe might be a factor of 5 to 9 less in the burst-released plenum gas. (4.8) Approximately 1 to 1.5% of the total

Table 4.3. Summary of iodine release species in Lorenz's(4.5, 4.6, 4.7) experiments

Test No.	Temperature (°C)	Gaseous Environment	Test duration (min)	Amount of I released (µg)	% of each form		
					Presumably CsI	Presumably mainly I <sub>2</sub>	Particulate
BWR-4 <sup>a</sup>	700-1100	helium	300	4800	99.99	0.005	0.02
HBU-12 <sup>a</sup>	700-1200	helium	480	170	91.2	0.27	8.6
HT-1	1300	steam	10	71	70	10	20
HT-2	1445	steam	7	990	90	0.1	9.9
HT-3	1610	steam	3	5400	86	0.2	14
HT-4	1440	steam	0.4	750	78	0.3	22
HBU-1	700	steam	300	0.9	18	72	10
HBU-2	900	steam	120	1.8	14	73	13
HBU-4	500	steam	1200	0.1	40	44	16
HBU-11	1200	steam	27	20	34	8	58
HBU-7 <sup>b</sup>	900	steam	1	11	71	4	25
HBU-8 <sup>b</sup>	900	steam	61	14	4	88	8
HBU-9 <sup>b</sup>	1000	steam	10	17	6	88	6
HBU-10 <sup>b</sup>	1050	steam	11	14	26	53	20
BWR-1 <sup>b</sup>	960	steam	1	490	67	0.4	33
BWR-2 <sup>b</sup>	850	steam	1	1000	79	0.1	21
BWR-3	1200	steam	25	1200	44	0.7	56

<sup>a</sup>Gap purge tests

<sup>b</sup>Burst release tests

fuel rod fission gas inventory is released with or shortly after the burst release in addition to the previously described plenum and void space gas. This amount is believed to be gas atoms shallowly embedded in fuel and cladding surfaces and is released as these surfaces heat up. (4.5)

Cesium and iodine are also released when the fuel rod ruptures, but the quantity carried out with the vented gases is considerably less than for the noble fission gases. The burst release of cesium and iodine depends upon the fuel rod temperature, the total volume of gas vented, and the amount of cesium and iodine initially in the pellet-to-cladding gap space. The LOCA source term model, developed by Lorenz et al.,<sup>4,8</sup> describes the quantitative calculation of their release. Usually only a small fraction of the gap inventory of cesium and iodine is released with the burst.

For a PWR, typical burst releases might be 3% of the stable noble fission gases, including embedded gas release, 0.02% of the total stable cesium, and 0.04% of the total stable iodine. For short half-lived nuclides, the burst releases would be a factor of 3 or more lower than the above. (4.8) For BWRs the releases might be twice the above. Individual high burnup, high heat-rated fuel rods might release ten times the above amounts with the burst.

Following the burst release, the amount of cesium and iodine remaining in the gap space will diffuse out of the rupture opening. This diffusional escape of the gap contents is a slow process and is quantitatively considerably smaller than the burst release unless the fuel rod temperature is raised several hundred degrees above the burst temperature and held for times longer than 10 min. The LOCA source term model<sup>(4.8)</sup> provides a method for calculating diffusional release from the gap space.

Beginning at  $\sim 1350^{\circ}\text{C}$ , fission gases, cesium, and iodine previously accumulated at the grain boundaries are released. Higher temperatures are probably required for low burnup fuel in which the concentration of fission products is lower. The mechanism is driven by the formation, swelling, and coalescence of bubbles of fission gases. At the temperatures involved ( $>1350^{\circ}\text{C}$ ), the bubbles probably include vaporized cesium and iodine species as well as the noble fission gases. The expanded bubbles work to mechanically separate the grains allowing escape of gas and vapor, and also link together to form tunnels, many of which apparently reach open voids. Approximately equal amounts (percentages of total inventory basis) of noble fission gas, cesium, and iodine are released from the grain boundaries. (4.6) For a high burnup fuel rod,  $\sim 20\%$  of the total initial fuel rod inventory of stable isotopes of the above elements would be released. Release from the grain boundaries of lower burnup fuel would probably be less, and temperatures as high as  $1800^{\circ}\text{C}$  might be required.

At completion of the burst release, diffusional escape of the gap inventory, and release of the grain-boundary inventory,  $\sim 60$  to  $90\%$  of the noble fission gases, cesium, and iodine remain in the  $\text{UO}_2$  grains. Differential release from  $\text{UO}_2$  grains follows solid state diffusion mechanics in which the fraction of initial inventory released

increases with the square root of time. Release from the grains is insignificant at cladding burst temperatures (750-1100°C), but the fractional release rate doubles approximately every 100°C so that by 2000°C the fraction of remaining inventory released is about 10%/min for fission gas, cesium, and iodine.

The fifth major release mechanism is escape from molten fuel. The formation of molten material begins with the melting of iron and nickel based alloys (if present), and low melting-point materials in control rods, followed by the melting of Zircaloy and the formation of eutectics. The details of the melting process are complex and imperfectly understood partly because chemical transformations occur simultaneously with the melting process which alter the melting points of key materials. For example, while Zircaloy melts at ~1800°C, oxidation to ZrO<sub>2</sub> occurs at the same time during many accidents, producing a material with a melting point of ~2700°C. Therefore, whether clad melting or clad oxidation occurs more quickly in an accident sequence can profoundly affect the subsequent course of events.

Similarly, both physical and chemical processes occur during fuel pellet melting, some of which are described in Section 4.4. The presence of molten cladding has a prominent effect on the pellet material as it approaches its melting point. At elevated temperatures, zirconium diffuses into the pellet, reducing a part of the UO<sub>2</sub> to form a metallic phase with a much lower melting point. Therefore, fission products whose chemical affinities would cause them to move into the metallic phase would evolve more rapidly during melting than those that are retained in the higher melting UO<sub>2</sub> phase. Thus, the melting process has some structure, and the simple model employed by the Reactor Safety Study, where the amount of fission product released was assumed proportional to the fraction of the core melted, must be seen as a provisional oversimplification. A mechanistic model for fission product release from melting fuel would be based upon (1) the vapor pressure of fission products in their appropriate chemical form and in the appropriate phase (metallic or oxidic), (2) transport effects from the melting surface to bulk of the gas phase, and (3) diffusion to the melt surface.

A mechanistic analysis of noble gas movement in the UO<sub>2</sub> pellet has been incorporated into the GRASS code.<sup>4.31</sup> A series of mechanisms effecting migration are postulated in this code including bubble nucleation and resolution, bubble diffusion, bubble coalescence, channel formation, fuel microcracking, and grain boundary diffusion. Therefore, this code may be used to provide an insight regarding the effect of noble gas concentration on these principally mechanical processes in the fuel. At present, extension of the GRASS code to reactive, volatile fission products is in an early, formulative stage.

#### 4.2.2 Fission Product Release Experiments

Three sets of experiments (Lorenz et al., Parker et al., and Albrecht et al., described below) have been selected to provide the data base for fission product release from LWR fuel rods on an interim basis. Many

other tests, described briefly below, provide fission product behavior information that will require more detailed analysis.

Tests of R. A. Lorenz et al. - commercial fuel rod segments (4.5-4.8)

Fifteen tests were performed with 30.5-cm segments of fuel rods from the H. B. Robinson-2 PWR and the Peach Bottom-2 BWR in steam atmosphere. Holes were drilled in the Zircaloy cladding or the test segments were pressurized and ruptured in the temperature range 850 to 960°C to allow escape of fission products. The test matrix ranged from 20 h at 500°C to 3 min at 1610°C. Released fission products were carried in the flowing steam into a collection system composed of a thermal gradient tube, high efficiency filter papers, and both heated and cold charcoal traps. Two tests were performed with purified helium in which the pellet-to-cladding gap space was purged of the readily releasable fission products while heated incrementally from 700 to 1100 or 1200°C. Heating was by either a tubular electrical resistance furnace or by direct induction heating of the Zircaloy cladding. The fission product species monitored were  $^{85}\text{Kr}$ ,  $^{134}\text{Cs}$ ,  $^{137}\text{C}$ , and  $^{129}\text{I}$ . Occasionally  $^{106}\text{Ru}$  and  $^{125}\text{Sb}$  were detected.

Tests of G. W. Parker et al. - crucible heating of  $\text{UO}_2$  in helium (4.4,4.9)

G. W. Parker et al. investigated the release of fission products from bare  $\text{UO}_2$  in purified helium. Trace-irradiated whole PWR-type pellets and pieces of pellets with 1000 and 4000 MWd/MT burnup reirradiated to trace levels were tested. The trace-irradiated whole pellets were 7 g each, and the chunks of higher irradiated material weighed 0.1 to 0.2 g each with ~10 pieces used in each test. The  $\text{UO}_2$  samples were located in an induction-heated tantalum crucible so that there was no temperature gradient; the time at temperature was usually 5.5 h and the range 980 to 2270°C was investigated. The fission gas isotope  $^{133}\text{Xe}$  was monitored continuously for release; the release of other fission product isotopes was measured only at the end of each test. Parker et al. also measured fission product release from trace-irradiated  $\text{UO}_2$  pellets melted in tungsten crucibles in purified helium. The test parameters included molten times from 0.4 to 10 min, two different helium flow rates, and two different pellet densities.

Tests of H. Albrecht et al. - SASCHA fuel melting tests (4.10,4.11)

In these tests 150 g of Zircaloy-clad fuel pellets and stainless steel are melted in a  $\text{ThO}_2$  crucible in atmospheres of flowing argon, air, or steam. Because of eutectics formed between the various components, the mixture becomes essentially completely molten at about 2300°C. An induction heated tungsten cylinder surrounds the crucible and heats the test sample by conduction and radiation. The usual heatup rate is ~110°C/min.

The  $\text{UO}_2$  pellets are especially fabricated to contain a variety of radioactively traced fission product simulants in concentrations equivalent to a burnup of 44,000 MWd/MT. The cladding and stainless steel may

have been irradiated to provide tracers for typical neutron activation products. Most of the released material forms a dense smoky aerosol. Roughly half of the released material settles (by gravity or diffusion) on the glass container and half reaches the filter papers that are monitored continuously by a multichannel GeLi detector. A higher percentage of the more volatile species (i.e., Cs and I) reach the filter papers whereas much of the less volatile materials (U and Zr) probably deposit on the glassware.

#### Power Burst Facility (PBF) (4.12,4.13)

The PBF is a specialized test reactor designed to test nuclear fuel and components under off-normal operating conditions. The facility is made up of an open pool reactor which is used to drive the nuclear operation of test fuel in a separate in-pile coolant loop. The experiments are mounted in an in-pile tube and cooled by a separate high pressure coolant loop. An experiment consists of one or more LWR-type fuel rods, 0.91 m in length, mounted in coolant flow shrouds inside an instrumented test train. The loop coolant system provides the experiment with water at pressures, temperatures, and flow rates typical of normal operation in a BWR or PWR and any off-normal conditions necessary to simulate a particular accident.

Fuel rods that fail as a result of testing, or rods that may be defective and allow fission products to leak from their interior, produce a fission product source term to the circulating water. A sample of the loop coolant is taken from a tap just upstream of the loop strainer and directed to a shielded detector enclosure. The identity and quantity of radioactive fission products released from test fuel rods can be monitored using on-line gamma spectroscopy techniques to provide an indication of rod failure, the time of the rod failure, and concentration histories of the short-lived fission products within the loop coolant.

#### Other current in-reactor tests - Halden and SILOE

In the Halden reactor, the test assembly IFA-430 contains four 1.28 m long fuel rods loaded with 10% enriched  $UO_2$  pellet fuel. (4.14) Two of the rods are used in fission gas release experiments; each is instrumented with a centerline thermocouple and three axially spaced pressure sensors. These two rods are of typical LWR design with diametral gap sizes representing beginning of life and end of life conditions, respectively. The rods are connected to a gas flow system which permits the fission gases released to the gap to be swept out of the fuel rods to a gamma spectrometer where the isotopic content is quantitatively measured. Only the gaseous isotopes can be measured directly because of the cool sampling lines. The release of  $^{135}I$  can be measured by counting the  $^{135}Xe$  daughter following reactor shutdown. Measurements of  $^{131}I$  and  $^{133}I$  release are also made but with somewhat less accuracy.

In the SILOE reactor in Grenoble, France, (4.15) the emission of fission products from PWR fuel rods containing small defects is being measured in a pressurized water loop. Test parameters include hole location and type, fuel rod linear power, and power cycling effects. A loss-of-coolant accident (LOCA) test series has been initiated.

### Older in-reactor tests

Most of the earlier in-reactor fission product release tests emphasized the measurement of release of long half-life isotopes from pre-irradiated fuel. On-line monitoring capability was limited so that little was learned about the release of short half-life fission products. Several specialized sweep-gas facilities existed for the continuous measurement of fission gas release which did emphasize measurement of short half-life species as do the current in-reactor tests (PBF, Halden, and SILOE).

Parker et al. (4.16) conducted two LOCA fuel rod failure tests in the TREAT reactor with bundles containing six LWR fuel rods 60 cm long prepressurized with helium. Fission heat in the pellets simulated the LOCA decay heat; fission product release from the preirradiated center rod was measured following the Zircaloy cladding expansion and rupture. Parker et al. (4.17, 4.18) also measured fission product release from short low-burnup fuel pins transient-heated to melting under water in the TREAT reactor. More than 20 tests were performed with miniature fuel pins heated by internal fissioning in the Oak Ridge Research Reactor (ORR). (4.19) Test parameters included cladding material (stainless steel or Zircaloy), atmosphere (dry air, moist air, dry helium, moist helium, steam-air, and steam-helium-hydrogen mixtures) burnup (20 to 26,500 MWd/tonne), gas flow rate, and temperature (estimated 2000 to 2900°C).

### Other out-of-reactor tests

Castleman and Tang (4.20) measured fission product release from trace-irradiated uranium (metal) and uranium-molybdenum alloy fuels in air and helium. A quartz thermal gradient tube was used in an attempt to characterize the chemical forms of the released cesium and iodine. D. Davies et al. (4.21) measured the release of fission products from trace-irradiated  $UO_2$  in hydrogen in the temperature range 930 to 2200°C. Many of the  $UO_2$  samples were powders or in other high surface-area forms. The apparatus permitted the periodic measurement of released xenon, cesium, iodine, and tellurium. Hillary and Taylor (4.22) performed tests with stainless-steel clad  $UO_2$  fuel pins with various defects releasing fission products into a  $CO_2/CO$  mixture. Burnup ranged from 10 to 10,000 MWd/tonne. Decay time was usually only about 1 month so that short half-life isotopes could be measured. The emphasis was on comparing xenon, iodine, and cesium releases. Collins et al. (4.23) measured release from low burnup Zircaloy clad  $UO_2$  heated to ~2000°C. Seven tests were performed at 1000°C in steam. The emphasis was on testing systems for trapping iodine, not on fission product release. G. W. Parker et al. (4.24) performed tests in the Containment Mockup Facility (CMF) and the Containment Research Installation (CRI) using either irradiated fuel or simulated fission products. Most tests were conducted in steam-air atmospheres; the emphasis was on fission product behavior in containment vessels. Other fission product release experiments (4.4) included the oxidation of LWR fuels, melting of LWR fuels, and a variety of tests with non-LWR fuels.

### 4.2.3 Best-Estimate Fission Product Release Rates

As discussed in Section 4.2.2, fission product release occurs as a composite of at least five different mechanisms; each of these mechanisms is dependent on many variables. The parameters controlling release include burnup (concentration), fuel density, grain size, and power (temperature) cycling, but the most important are temperature and time.

For simplicity we expressed the data from the first three sets reviewed in Section 4.2.3 (Lorenz et al., Parker et al., and Albrecht et al.) in terms of time and temperature by calculating a fractional release rate coefficient,  $k$ , (fraction of remaining nuclide released per min) defined as

$$k(T) = \frac{df}{dt} \quad (4.7)$$

where  $f$  = fraction of current inventory and  
 $t$  = time (min)  
 $T$  = temperature.

In most experiments the release rate,  $df/dt$  was not monitored continuously, for these the value of  $k$  was estimated from the test end point, the total fractional release and total time:

$$k(T) = \frac{-\ln(1-F)}{t} \quad (4.8)$$

where  $F$  = total fraction released during an isothermal test segment,  
 $t$  = total test time (min) .

For tests in which the temperature was changed incrementally or continuously and the fission product release monitored continuously, we calculated the release rate coefficient in this manner:

$$k(T) = \frac{\Delta f}{\Delta t} \quad (4.9)$$

where  $\Delta f$  = fraction of current inventory released at temperature,  $T$ ,  
 $\Delta t$  = increment of time for which  $\Delta f$  was measured (min) .

The burst release amounts were not included in determining the release rate coefficients.

The results of these release rate coefficients are shown in Figs. 4.1 and 4.2. The large extent of scatter in results is not surprising. In order to obtain the best estimate release for typical reactor fuel rods, the following guidelines were observed.

- (1) The H. B. Robinson results for temperatures  $<1200^{\circ}\text{C}$  were considered to be very low because of the small pellet-to-cladding gap space and the low inventory of fission products in the gap space.
- (2) The H. B. Robinson results at  $1200^{\circ}\text{C}$  were considered to be low because of the low gap inventory. (This test segment and the Peach Bottom-2 test segment used at  $1200^{\circ}\text{C}$  had been ruptured previously so that the pellet-to-cladding gap was opened to a realistic size for a ruptured fuel rod.)

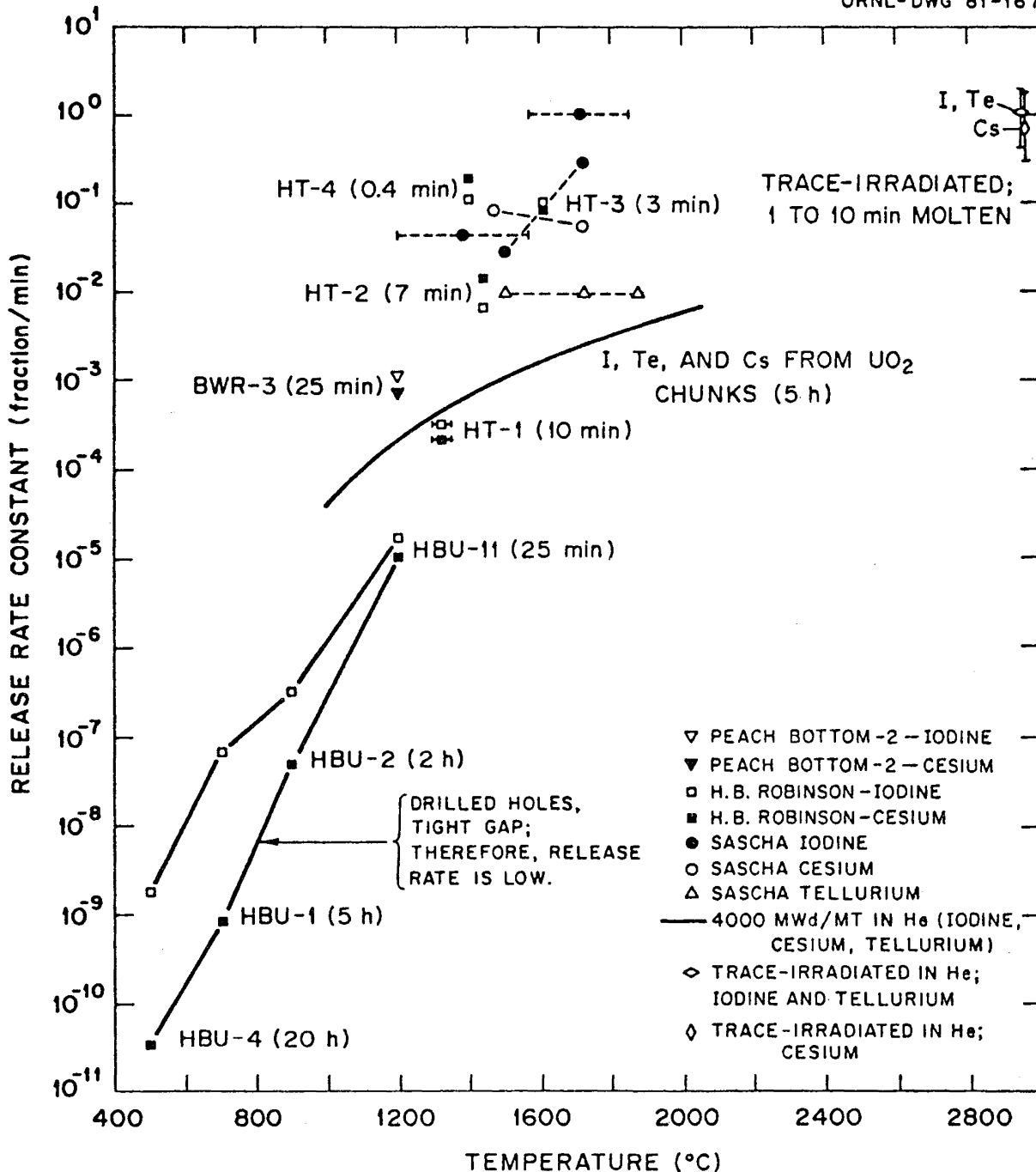


Fig. 4.1. Release rate constants from fuel - noble gases and volatiles.

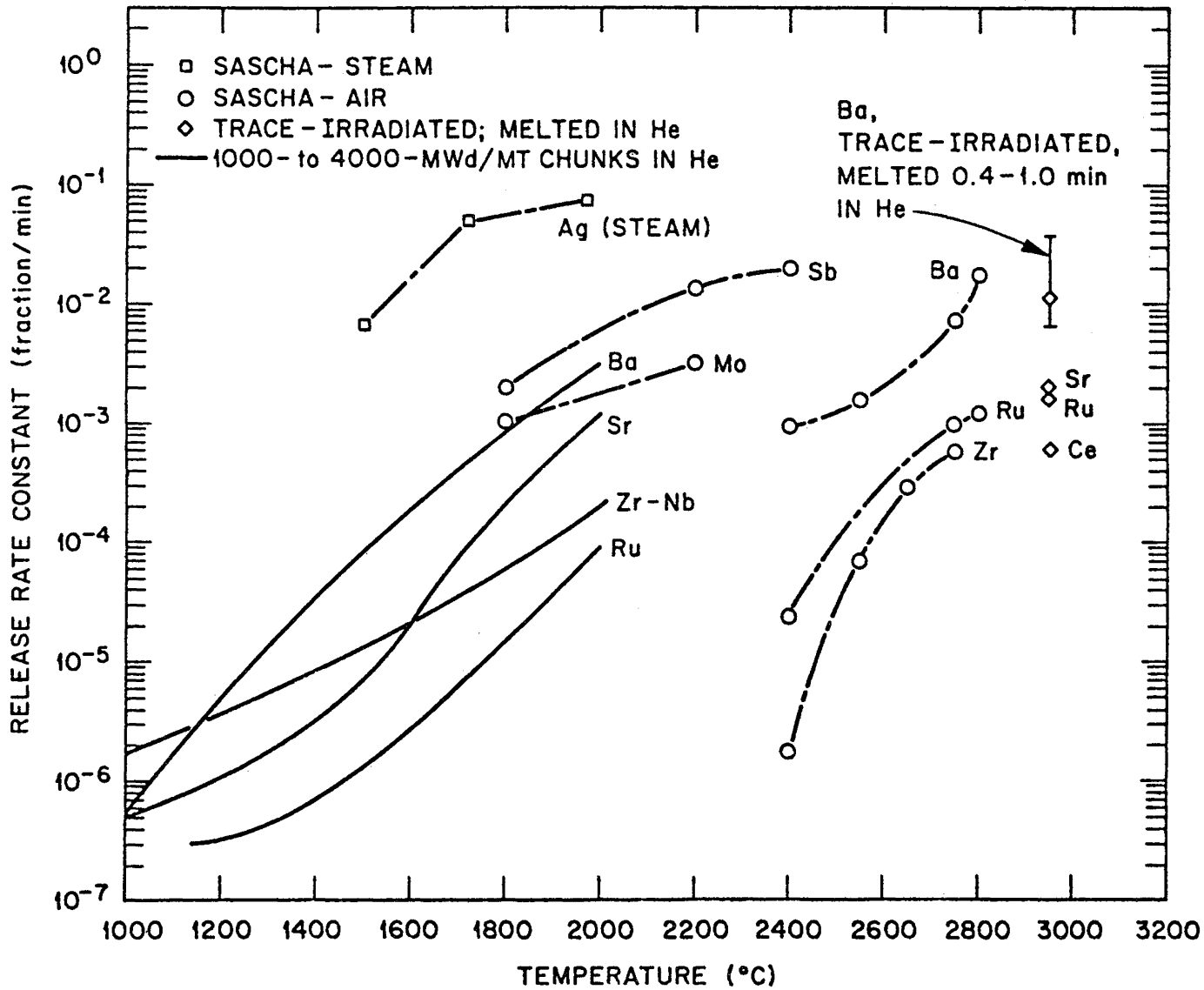


Fig. 4.2. Release rate constants from fuel - low volatiles.

- (3) The Peach Bottom-2 results at 1200°C were high because of the high gap inventory.
- (4) The H. B. Robinson results at 1300-1350°C might be somewhat low because of the low gap inventory.
- (5) The H. B. Robinson results at 1400, 1445, and 1600°C were high because of the short heating times and the one-time rapid release of the grain boundary inventory.
- (6) The SASCHA results for iodine and cesium were high because of the method of incorporating the simulants in the pellets.
- (7) The results of Parker et al. between 1000 and 2200°C were for an overall time period of 330 min and would probably have been higher for shorter heating times. No Zircaloy was present for possible trapping.
- (8) Release results from Parker's melting tests were probably low because of low concentration.
- (9) No special compensation was made for differences in atmosphere.

The best estimate results for release from typical LWR reactor fuel in steam are shown in Fig. 4.3.

As seen in Fig. 4.1, the scatter on the value of the fuel release coefficient for cesium and iodine is about plus or minus one order of magnitude. The smoothed curve through these points in Fig. 4.3 may therefore be taken to be accurate to this degree. (However, we should emphasize that a large uncertainty in the value of the release rate coefficient does not infer that total fission product releases are uncertain to this degree. The uncertainty affects only the rate of release from fuel; i.e., the amounts released up to a specified temperature for a given heatup rate. There exists an insufficient body of data to approximate an accuracy for the low volatiles (Fig. 4.2). In this absence, we assume that roughly the same accuracy exists for the low volatiles, i.e., plus or minus one order of magnitude. It should be emphasized that the factors shown in Fig. 4.3 represent the slower release mechanisms; noble gas burst release of ~3% for PWRs and ~4% for BWRs is not included.

#### 4.3 Estimated Total Release Rates During Postulated Accident Sequences

For making mechanistic transport calculations in primary and secondary containments, estimates are required for the release of all materials from the core as functions of time along with descriptions of the properties (physical and chemical forms) of the released materials. Aerosols can be released to the containment atmosphere during two phases of core-melt accident sequences: (1) as the core materials heat up and melt while still within the primary reactor vessel, and (2) after melt-through while the molten core materials interact with the concrete basemat in the cavity beneath the primary vessel.

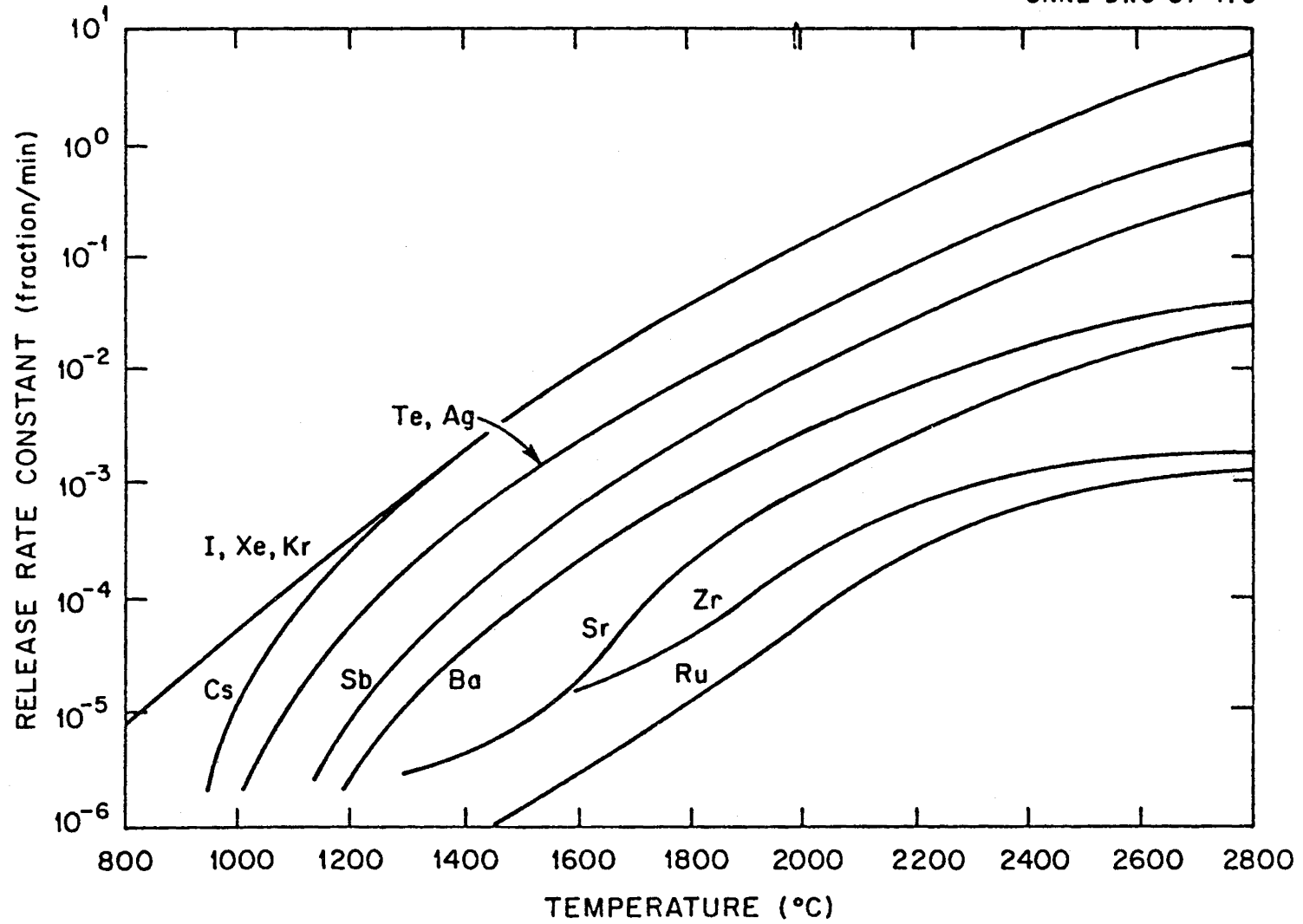


Fig. 4.3. Fission product release rate constants from fuel – smoothed curves.

Components that can be made airborne during the in-primary-vessel phase include fission products, clad, fuel, structure, and control rods. Clad, structure, control rods, and fuel can be expected to exist initially as separate immiscible melt phases. However, as oxidation progresses at higher temperatures, the oxide of clad, structure, and control rods can dissolve in fuel altering the melting temperature and the vaporization rates. The determination of the rate of vaporization of such a mixture involves complex thermal/hydraulic considerations. Similarly, the release of fission products that are more-or-less uniformly distributed within the fuel phase should be a complex time dependent phenomena influenced by chemical state, concentration, transport processes, and geometry. Because of the necessary involvement of these considerations, it is difficult to establish a single model which can successfully predict aerosol release under all situations.

The original formulation in the Reactor Safety Study is still the commonly used method. In this approach, the release rate of a given fission product,  $x$ , from molten fuel is assumed to be a constant,  $RF_x$ .<sup>\*</sup> As noted in Section 4.2.3, we here use a release rate coefficient,  $k_x(T)$ , defined by

$$dM_x/dt = -k_x(T)M_x$$

where  $M_x$  is the mass of material  $x$  in the mixture, and the proportionality coefficient,  $k_x$ , is assumed to be a function of temperature only. This treatment significantly improves that used on the RSS in that fission product releases from the fuel may now be related to core heat-up time. However, the release rate coefficients must be more accurately measured. As discussed in Section 4.2, experiments in the US and Germany were combined to produce Fig. 4.3 which is our present best-estimate of the fractional release rates as functions of temperature.

The fractional release rates for fuel, cladding, and structure would be expected to be determined by their rates of vaporization which would involve complex thermal/hydraulic considerations that are not presently incorporated in risk analysis codes. Consequently, for this report the release coefficients for these elements were adapted from SASCHA air data as approximated below:

Element	Temp (°C)	Release Coeff. (fraction/m)
Fuel	2400	$10^{-6}$
	2700	$10^{-5}$
Clad	2200	$10^{-6}$
	2500	$10^{-5}$
Structure	1800	$10^{-6}$
	2200	$10^{-5}$

Considerable uncertainty exists in the above release coefficients and this is believed to be the least supportable aspect of the release calculation. Since these three elements, using the above uncertain release rate coefficients, make up more than half of the total calculated mass release (see Appendix B), this appears to be an area needing additional work.

<sup>\*</sup>Fraction release.

The application of the above release rate data on a whole core basis is not straightforward because of the complex distributions in time and space of the fuel melt progression and the melt temperatures. With such information, an estimate of the release can be made by dividing the core into finite regions and treating each region independently. This procedure was applied, as shown in detail in Appendix B for two accident sequences as discussed below.

#### 4.3.1 Accident Sequences

Two accident sequences having different heat-up and melt progression rates were chosen to estimate the aerosol source term and to illustrate the application of the fractional release rate technique. The two accident sequences used were the AB and the S<sub>2</sub>C.

The AB sequence is a large pipe break accident with electrical power failure and consequently, no ECC injection. It results in rapid core heat-up and melting. The S<sub>2</sub>C is a small pipe break accident with delayed core meltdown. Consequently, the heat-up of the core is slower, and fuel melting is delayed until after containment failure approximately 30 hours after the pipe break occurs and the reactor is shut down. The results of MARCH calculations to determine the core temperature histories for these two sequences are shown in Tables B.2 and B.3 of Appendix B. For these calculations, MARCH uses 240 control volume regions (10 radial and 24 axial). For making release estimates from a control volume representation of the core, the MARCH results shown in Tables B.2 and B.3 were approximated by establishing rates at which specified regions of the core reached 1000°C and their subsequent rate of heat-up to 2800°C (assumed to be the maximum temperature). For the AB sequence these rates were 10%/min and 250°C/min respectively and 2%/min and 80°C/min for sequence S<sub>2</sub>C, as shown in Figs. B.1 and B.2 of Appendix B.

Approximating the temperature histories in this manner allows one to account directly for the fact that different regions of the core heat-up and melt at different rates and, consequently release materials at different rates and times during the accident progression.

The initial heatup of fuel can be predicted with reasonable accuracy in a core meltdown accident. However, after portions of the fuel and cladding become molten, the subsequent transport of material and its effect on the transient temperature history of the fuel is quite uncertain. Based on evaluation of core slumping behavior, existing models assume that by the time a major fraction of the fuel has melted (e.g., 75%), failure of the core support plate or core barrel could be expected and that the molten fuel would fall into water in the lower plenum of the reactor vessel. During boiloff of this water the core would be resolidified, the fuel would again heat up prior to failure of the reactor vessel. During this phase of the accident an additional release of aerosols would occur but probably of substantially lower magnitude than during the initial heatup phase.

#### 4.3.2 Total Release Rates

The results of the release calculation as discussed in Appendix B for selected materials and fission products are shown as Fig. B.3 for the AB

sequence and as Fig. B.4 for the S<sub>2</sub>C sequence for an arbitrary duration of two hours. The results are presented as fractions of the total core inventories. Using ORIGEN calculations for these inventories (see Appendix B), the total calculated releases are summarized in Table 4.4 for the time of core support plate failure, predicted by the MARCH code, and for an arbitrary accident duration of two hours.

Table 4.4. Summary of aerosol release estimates

Accident sequence	Time of support plate failure <sup>a</sup> (min)	Total mass released at time of grid plate failure (kg)	Total mass released if continued for 2 hours <sup>c</sup> (kg)
AB	20	600	1300 to 2000
S <sub>2</sub> C*	71 <sup>b</sup>	900	1300 to 2000

<sup>a</sup>MARCH predictions.

<sup>b</sup>Times S<sub>2</sub>C are measured from 1857 minutes after the start of the accident which is the time the first core element reaches 1000°C (32 min after start of core heatup).

<sup>c</sup>Each element is allowed to heat at the rate for that sequence until it reaches 2800°C and is then held constant at that value.

Figures B.3 and B.4 illustrate the results of the release rate coefficient technique giving the fractional release of the separate elements as a function of time. In general, the more volatile the element, the earlier and more completely it is released. These calculated releases can be compared to those in the RSS by comparing the release fraction for the AB sequence at 20 minutes (when the core is mostly molten) to the melt release fractions used in the RSS as shown below:

Table 4.5. Comparison of Fraction Release Estimates

This calculations		RSS	
Fission product group	20 min release fraction for AB sequence	Fission product group	Melt release fraction
I, Cs	1.0	I, Br	0.9
Te, Ag, Sb	1.0	Te, Sb, Se	0.15
Ba	0.5		
Sr	0.3	Ba, Sr	0.1
Zr	0.03		
Ru	0.02	Noble metals	0.03
Structure	0.005		
Clad	0.002	Rare earths	0.003
Fuel	0.003		

The calculated releases of Te and Sb are considerably higher by this technique (which reflects actual release rate data) but comparable values are obtained for the other groups. The iodine is calculated to be essentially completely released by both techniques.

### 4.3.3 Release from Fuel Melt/Concrete Interactions

As identified in the Reactor Safety Study, another source of airborne materials that can be introduced into the containment is the vigorous interaction that occurs when molten core materials penetrate the primary vessel and contact the concrete in the basemat of the cavity housing the primary vessel. Currently, core-melt/concrete release experiments and analyses are being conducted at Sandia National Laboratory and results have been reported.<sup>(4.26)</sup> In these tests, Sandia observed that the thermal decomposition of the concrete produces gas which sparges through the melt producing large quantities of aerosols. They developed a preliminary correlation<sup>(4.26)</sup> based on the data from one small scale transient corium/concrete interaction test and two larger scale sustained stainless steel/concrete tests. The application of the correlation requires knowledge of the melt geometry and a thermal analysis of the melt/concrete interaction to determine the heat exchange and the transient temperatures. Such models are presently under development by Karlsruhe (WECHSL code) and Sandia (CORCON code). The WECHSL code was utilized in the Zion/Indian Point Study (Reference 4.26) along with the Sandia correlation to determine release quantities.

For the AB sequence, which had the highest calculated release of ~510 kg, the calculated release as a function of time is shown in Fig. B.5 of Appendix B. The calculation to provide Fig. B.5 is sensitive to the initial melt temperature. For example, if the initial melt temperature in sequence AB were 2500°C instead of the 2377°C used in the calculation, the total release would become ~1600 kg. It is unlikely that the concrete/melt contact temperature will exceed 2500°C. The released materials are mostly nonradioactive aerosols coming from the concrete constituents. The solid materials released were identified to be primarily oxides of silicon, calcium, and aluminum and other inorganic oxides. For aerosol transport calculations, the melt/concrete releases can be considered to be made up of spherical particles, 2  $\mu\text{m}$  in mean aerodynamic diameter, with a geometric standard deviation of 2 for a log-normal distribution.

### 4.4 Effect of Zircaloy-UO<sub>2</sub> Interaction on Fission Product Release

There have been a significant number of studies on the effect of UO<sub>2</sub> on cladding strength, ductility and burst temperature and on the chemical integrity of the cladding exposed to some fission products. However, there seem to be no studies on the related effect - the possible enhanced release of fission products from UO<sub>2</sub> due to its interaction with Zircaloy.

Based on the observed behavior of noble gases in UO<sub>2</sub>, it is certain that UO<sub>2</sub>-Zircaloy interaction causes a significant increase in fission product release from the affected region for at least three reasons:

- (1) Phase change as well as grain boundary motion both tend to liberate species trapped in UO<sub>2</sub>.

- (2) Low melting point phases may form in which atomic mobilities are much higher than in  $UO_2$ . The most likely low melting phase would be a U-rich, metallic material containing Zr(O).
- (3) The melting point of  $UO_2$  is lowered by addition of  $ZrO_2$ . However, the depression is not great ( $\sim 300^\circ C$  maximum) and thus this effect is probably not as significant as the first two.

There is also a potential effect on Cs mobility as Zr is added to  $UO_2$ . For example, Kleykamp (in ref. 4.2) observed that at 43 kW/m heat rating, a layer of  $\alpha$ -Zr(O) or  $ZrO_2$  forms on the pellet, beneath which is  $\sim 5 \mu m$  layer rich in Cs consisting of a Cs-Zr-Sn-O material. It is not clear what this material is, but this illustrates that the effect of Zr is not solely one which alters phases within the U-O-Zr system, but Zr-fission product compound formation is also possible.

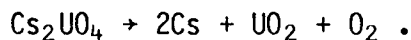
Since there exists no direct information on the effect of Zr/ $UO_2$  interaction on fission product release, the best that can be done at this time is to review the effect of Zr-addition on the  $UO_2$  structure. Following this, one would then have to extrapolate to the potential effect on fission product release.

#### 4.4.1 Phases within the U-O-Zr System

Some key features of  $UO_2/Zr$  interaction are illustrated in the ternary diagram for  $1500^\circ C$  (Fig. 4.4). Here the single phase regimes, U(L),  $UO_2$ ,  $ZrO_2$ ,  $\alpha$ -Zr, and U-Zr, are denoted by the cross-hatched areas. Some notable points are:

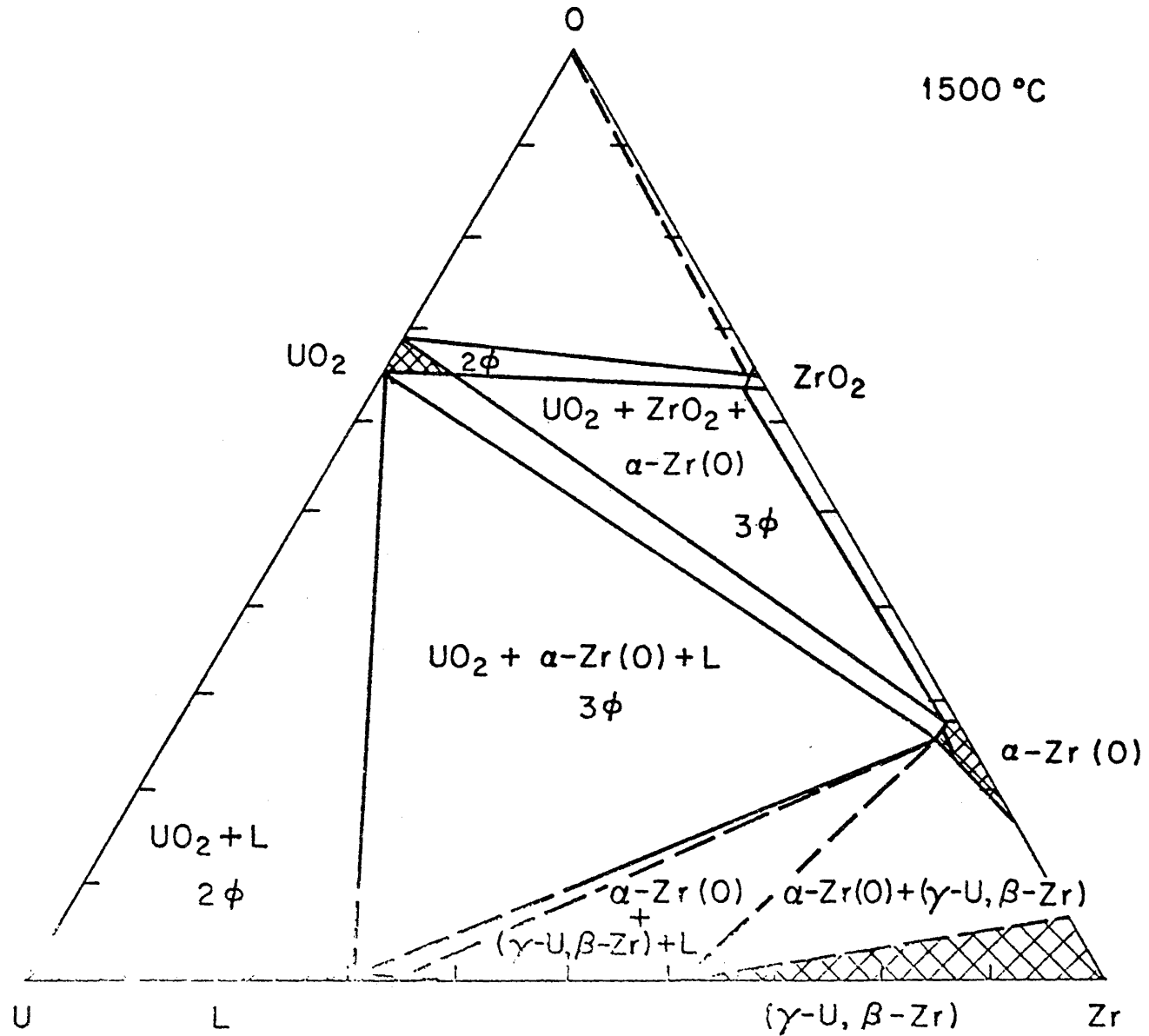
- (1) Metallic Zr and  $UO_2$  do not exist in equilibrium with each other. This is shown by the fact that  $UO_2$  and Zr zones do not exist adjacent to each other. However,  $\alpha$ -Zr(O) can exist in equilibrium with  $UO_2$ .
- (2) A liquid phase already exists at  $1500^\circ C$  consisting of U plus up to  $\sim 30\%$  Zr. Hofmann and Politis<sup>4,29</sup> state that a liquid phase first appears at  $\sim 1300^\circ C$ . Essentially, the liquid phase forms by reducing  $UO_2$  to  $UO_{2-x}$ . Dissolving Zr in the liquid considerably increases the composition range in which this liquid metal phase exists.

Figure 4.5, which shows the  $UO_2-ZrO_2$  binary system, illustrates some further aspects of this system.



Therefore, reduced oxygen pressure would certainly enhance release of Cs, and hence render CsI formation more likely.

For the second effect (addition of  $ZrO_2$  to  $UO_2$ ), we note from Fig. 4.4, that little is expected to occur below  $\sim 1400^\circ C$ . Above  $1400^\circ C$ , the solubility of  $ZrO_2$  in  $UO_2$  rapidly increases. We expect, therefore, enhancement of the release of fission products from  $UO_2$  due to  $ZrO_2$  dissolution to occur at temperatures above  $\sim 1400^\circ C$ .



4.28

Fig. 4.4. The U-O-Zr ternary phase diagram at 1500°C. (From ref. 4.29.)

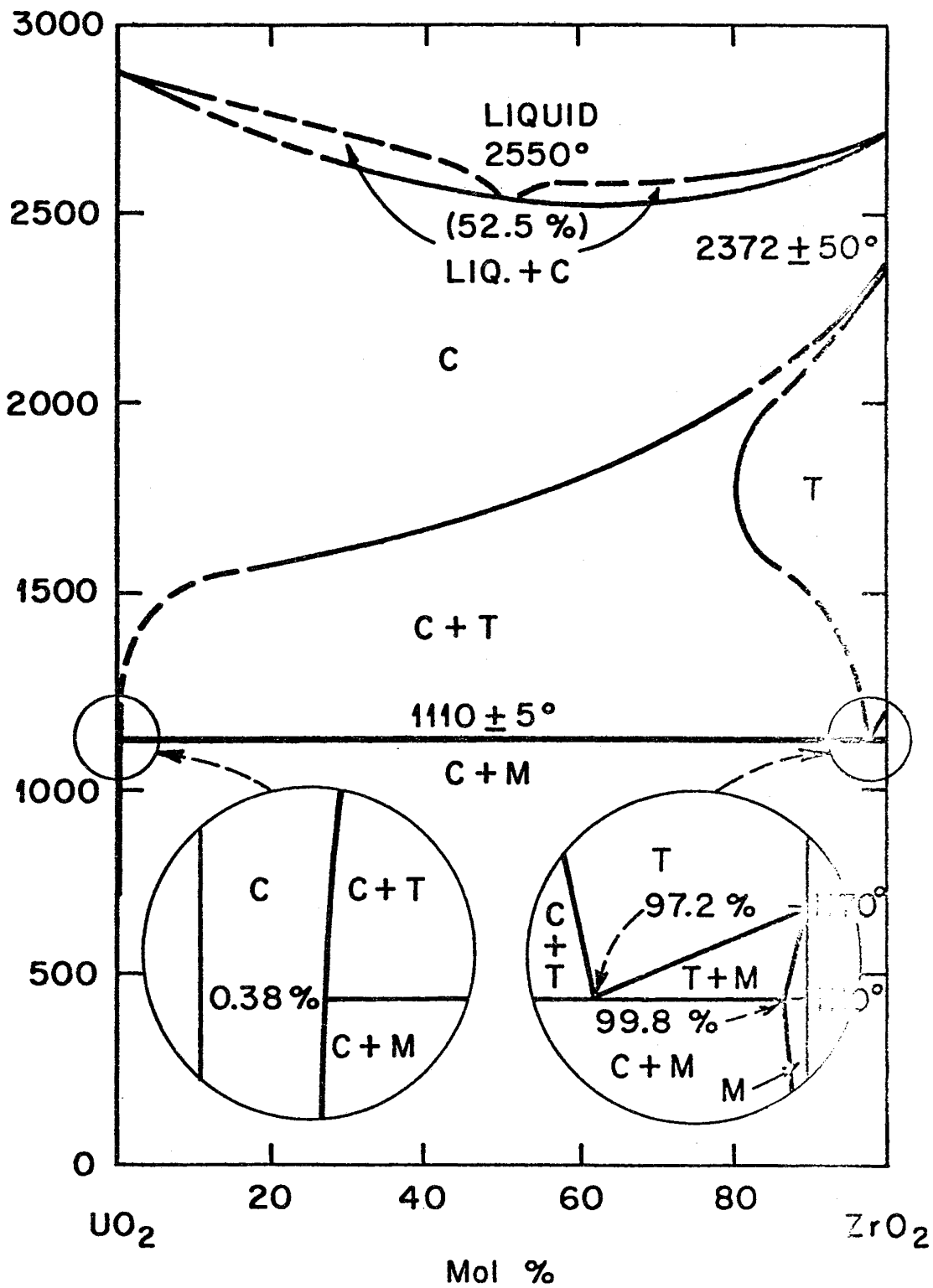


Fig. 4.5. The  $\text{UO}_2$ - $\text{ZrO}_2$  binary phase diagram.  
(From ref. 4.30.)

4.6 References for Chapter 4

- 4.1 T. M. Besmann and T. B. Lindemer, "Chemical Thermodynamics of the System Cs-U-Zr-H-I-O in the LWR Fuel-Clad Gap," *Nucl. Technol.* 40, 297-305 (1978).
- 4.2 International Working Group on Fuel Performance and Technology for Water Reactors, *Proceedings of the Specialists' Meeting on Internal Fuel Rod Chemistry*, Erlangen, Federal Republic of Germany, Jan. 23-25, IAEA, IWGEPT/3.
- 4.3 H. Kleykamp, "Formation of Phases and Distribution of Fission Products in an Oxide Fuel," in *Proceedings of Behaviour and Chemical State of Irradiated Ceramic Fuels*, Vienna, Austria, Aug. 7-11, 1972.
- 4.4 G. W. Parker et al., *Out-of-Pile Studies of Fission-Product Release from Overheated Reactor Fuels at ORNL, 1955-1965*, ORNL-3981 (August 1967).
- 4.5 R. A. Lorenz et al., *Fission Product Release from Highly Irradiated Fuel*, NUREG/CR-0722 (ORNL/NUREG/TM-287) (1980).\*
- 4.6 R. A. Lorenz et al., *Fission Product Release from Highly Irradiated Fuel Heated to 1300-1600°C in Steam*, NUREG/CR-1386 (ORNL/NUREG/TM-346), December 1980.\*
- 4.7 R. A. Lorenz et al., *Fission Product Release from BWR Fuel Under LOCA Conditions*, ORNL/NUREG/TM-388, in preparation.
- 4.8 R. A. Lorenz, J. L. Collins, and A. P. Malinauskas, *Fission Product Source Terms for the LWR Loss-of-Coolant Accident*, NUREG/CR-1288 (ORNL/NUREG/TM-321) (July 1980).
- 4.9 G. W. Parker, W. J. Martin, and G. E. Creek, "Effect of Time and Gas Velocity on Distribution of Fission Products from  $UO_2$  Melted in a Tungsten Crucible in Helium," in *Nuclear Safety Program Semiannual Progress Report for Period Ending June 30, 1963*, ORNL-3483, pp. 19-20 (September 1963).
- 4.10 H. Albrecht, V. Matschoss, and H. Wild, "Release of Fission and Activation Products During Light Water Reactor Core Meltdown," *Nucl. Technol.* 46, 559-565 (mid-December 1979).
- 4.11 H. Albrecht, V. Matschoss, and H. Wild, "Experimental Investigation of Fission and Activation Product Release from LWR Fuel Rods at Temperatures Ranging from 1500-2800°C," *Proceedings of the Specialists' Meeting on the Behaviour of Defected Zirconium Alloy Clad Ceramic Fuel in Water Cooled Reactors*, Chalk River, Canada, September 1979, IWGFPT/6, pp. 141-146.

- 4.12 D. J. Osetek et al., "The Power Burst Facility Fission Product Detection System," *Review Group Conference on Advanced Instrumentation for Reactor Safety Research*, NUREG/CP-0007, October 1979.\*
- 4.13 D. J. Osetek and J. J. King, *Fission Product Release from LWR Fuel Failed During PCM and RIA Transients*, NUREG/CR-1674 EGG-2058, October 1980.\*
- 4.14 A. D. Appelhans, E. Skattum, and D. J. Osetek, "Fission Gas Release in LWR Fuel Measured During Nuclear Operation," *ANS/ENS Topical Meeting on Thermal Reactor Safety, Knoxville, Tenn., April 6-9, 1980*, CONF-800403.
- 4.15 G. Kurka, A. Harrer, and P. Chenebeau, "Fission Product Release from a Pressurized Water Reactor Defective Fuel Rod: Effect of Thermal Cycling," *Nucl. Technol.* 46, 571-581 (1979).
- 4.16 R. A. Lorenz, D. O. Hobson, and G. W. Parker, "Fuel Rod Failure Under Loss-of-Coolant Conditions in TREAT," *Nucl. Technol.* 11, 502-520 (1979).
- 4.17 G. W. Parker, R. A. Lorenz, and J. G. Wilhelm, "Simulated Transient Accidents in TREAT," in *Nuclear Safety Program Annual Progress Report for Period Ending December 31, 1966*, ORNL-4071, pp. 8-20 (March 1967).
- 4.18 G. W. Parker and R. A. Lorenz, "Simulated Transient Accidents in TREAT," in *Nuclear Safety Program Annual Progress Report for Period Ending December 31, 1967*, ORNL-4228, pp. 44-54 (April 1968).
- 4.19 W. E. Browning et al., "Simulated Loss-of-Coolant Accidents in the ORR," pp. 3-29 in *Nuclear Safety Program Semiannual Progress Report for Period Ending June 30, 1965*, ORNL-3843 (September 1965).
- 4.20 A. W. Castleman and I. N. Tang, "Vaporization of Fission Products from Irradiated Fuel," I. *Nucl. Sci. Eng.* 29, 159-164 (1967); II. *J. Inorg. Nucl. Chem.* 32, 1057-1064 (1970).
- 4.21 D. Davies et al., *The Emission of Volatile Fission Products from UO<sub>2</sub>*, AERE-R 4342 (1963).
- 4.22 J. J. Hillary and J. C. Taylor, *The Release of Fission Products from AGR Type Fuel at Around 1000°C*, TRG Report 2317(W).
- 4.23 R. D. Collins, J. J. Hillary, and J. C. Taylor, *Air Cleaning for Reactors with Vented Containment*, TRG Report 1318(W).

- 4.24 G. W. Parker, G. E. Creek, and W. S. Martin, *Fission Product Transport and Behavior in the Stainless Steel Lined Containment Research Installation (CRI)*, ORNL-4502 (February 1971).
- 4.25 *Reactor Safety Study, Appendix VII*, WASH-1400, NUREG 75/014, U.S. Nuclear Regulatory Commission (1975).\*\*
- 4.26 *Report of the Zion/Indian Point Study: Volume 1*, NUREG/CR-1410, SAND80-0617/1, Sandia National Laboratories (1980).\*
- 4.27 M. Reimann and W. G. Murfin, "Calculations for the Decomposition of Concrete Structures by a Molten Pool," *PAHR Information Exchange Meeting*, Ispra, Italy, October 10-12, 1978.
- 4.28 W. B. Murfin, *A Preliminary Model for Core/Concrete Interactions*, SAND77-0370, Sandia National Laboratories, Albuquerque, New Mexico, (1977).
- 4.29 P. Hofmann and C. Politis, "Chemical Interaction between  $UO_2$  and Zry-4 in the Temperature Range between 900 and 1500°C," 4th<sup>2</sup> International Conference on Zirconium in the Nuclear Industry, Stratford-upon-Avon, England, June 26-29, 1978.
- 4.30 E. M. Levin and H. F. McMurdie, *Phase Diagrams for Ceramists 1975 Supplement*, The American Ceramic Society, Columbus, Ohio.
- 4.31 J. Rest, *GRASS-SST: Fission Gas Behavior in  $UO_2$* , NUREG/CR-0202, June 1978.\*\*\*
- 4.32 L. D. Noble, "ANS-5.4 Fission Gas Release Model," in *LWR Fuel Performance*, Conf. 790441-8 ANS Meeting, April 1979, Portland, Oregon.
- 4.33 D. Cubiccotti and J. E. Sanecki, *J. Nuclear Materials*, 78, 96 (1978).

---

\*Available for purchase from the NRC/GPO Sales Program, U.S. Nuclear Regulatory Commission, Washington, DC 20555, and/or the National Technical Information Service, Springfield, VA 22161.

\*\*Available free upon written request to the Division of Technical Information and Document Control, U.S. Nuclear Regulatory Commission, Washington, DC 20555.

\*\*\*Available for purchase from the National Technical Information Service.

## Chapter 5

### Chemistry of Cesium and Iodine

#### 5.1 Introduction

In Chapter 4 evidence was presented that cesium and iodine could be released from the fuel at approximately equal fractional rates or that the iodine may be released as cesium iodide (CsI). For this reason most of the discussion in this chapter focuses on species of cesium and iodine that could be formed in (1) a steam or (2) a water environment. In water the soluble fission products are ionized. In the vapor state the fission products are present as atoms or molecules and when reacted with other vapors they form atomic or molecular species. Because the chemical nature of the ionized fission products in water is quite different than the chemical nature of molecular or atomic species the two chemistries will be discussed in separate sections of this chapter. Fission-product chemistry in the vapor state will be discussed in section 5.2. The discussion of water or aqueous chemistry begins in section 5.3. These sections present summaries of the chemical behavior. Details of the analyses are presented in the chapter appendices.

#### 5.2 Fission Product Chemistry in the Vapor State

Once the cesium and iodine, or for that matter any of the other volatile fission products, have been separated from the fuel and cladding at high temperature in the vapor state they will first mix with steam and the hydrogen produced by reaction of the steam with metals. Interactions will occur among these fission-product vapors and their environment. All of these species, together with their products of reaction, may behave in one or more of the following ways. They may physically condense on structural surfaces or on the surfaces of suspended particles (an aerosol) or they may begin to form their own aerosol. The interaction may not be just a physical condensation; some vapor species may chemically react with nearby surfaces, both structural and aerosol. Each reaction will proceed at its own rate depending on local thermodynamic conditions such as temperature, pressure and the amounts of species involved in the reaction. These reactions may change the environment which in turn may affect the reaction of other species. Those fission product species that are transported to the containment building, either as gases or as condensed on aerosol particles, may react with oxygen if it is present.

The behavior of these fission products depends critically on the particular molecular forms that result from their interactions with the environment. Therefore, the objective of this survey is to identify the predominant vapor chemical species that might exist and to determine those conditions which affect the stability of these species. Once the predominant species are identified, their effect

on fission product transport can be considered. Also the chemical interaction of these species with materials in the primary system must be considered. Species that react strongly with these materials will not be easily transported from the reactor pressure vessel into the containment atmosphere.

The environment created during a reactor accident contains a large number of chemical species and this results in a complex chemistry. Little experimental or analytic literature on the high-temperature vapor-phase chemistry of cesium, iodine and tellurium is available to aid the determination of the predominant species in the atmosphere during a reactor accident. Kinetic data on the rates of reaction of the various species are almost totally absent. The approach used in Reference 5.1 was to determine the thermodynamic equilibrium composition of the gas phase using the published thermodynamic data for the various molecular fission product species. That is, the composition of the atmosphere, once all reactions have gone to completion, was determined. Because reaction rates among species in a high temperature gas (temperatures greater than about 1000°C) are typically rapid, this equilibrium approach is not likely to cause significant errors in the time scales of interest in this temperature regime. As the temperature is lowered, reactions become slower and take longer to reach equilibrium. Also, time for equilibrium to be established varies with the reaction. Although it can't be supported on the basis of existing data, it seems reasonable to exercise caution in applying the equilibrium calculation results at temperatures much less than 600C. This is an area where additional information is needed.

Four simple vapor systems that will be reviewed are believed to contain the important chemical reactions and to illustrate the state-of-the-art for vapor-phase chemistry in steam. The four systems considered were: a) iodine in the presence of steam and hydrogen or oxygen (I-H-O), b) cesium in the presence of steam and hydrogen or oxygen (Cs-H-O), c) tellurium in the presence of steam and hydrogen or oxygen (Te-H-O), and d) cesium and iodine in the presence of steam and hydrogen or oxygen (Cs-I-H-O). Molecular species containing two fission product elements, such as cesium and iodine are thought to be important. However chemical thermodynamic data on only one such species, CsI, are known. There are no data on vapor species containing combinations of tellurium and iodine or cesium and tellurium but reasoning by analogy with somewhat similar species suggests that these molecular species would not be thermodynamically stable in the vapor state.

Some molecular forms that might result from the interaction of cesium, iodine and tellurium with steam and hydrogen or oxygen are listed below in Table 5.1.

TABLE 5.1

## Vapor Forms of Fission Products

<u>Elements Present</u>	<u>Chemical Vapor Species Associated with Elements Present</u>
Cesium (Cs)	CsI, CsOH, (CsOH) <sub>2</sub> , Cs <sub>2</sub> O, CsO, Cs, Cs <sub>2</sub>
Iodine (I)	CsI, I, I <sub>2</sub> , HI
Tellurium (Te)	Te <sub>2</sub> , Te, TeO, TeO <sub>2</sub> , Te <sub>2</sub> O <sub>2</sub> , H <sub>2</sub> Te
Hydrogen (H)	CsOH, (CsOH) <sub>2</sub> , HI, HO, H, H <sub>2</sub> O <sub>2</sub> , HO <sub>2</sub> , H <sub>2</sub> , H <sub>2</sub> Te, H <sub>2</sub> O
Oxygen (O)	CsOH, (CsOH) <sub>2</sub> , CsO <sub>2</sub> , CsO, HO, O, H <sub>2</sub> O <sub>2</sub> , HO <sub>2</sub> , H <sub>2</sub> O, O <sub>2</sub> , TeO, TeO <sub>2</sub> , Te <sub>2</sub> O <sub>2</sub>

This table includes essentially all of the vapor species for the five elements listed for which chemical thermodynamic data are known. However there may be other as yet unknown vapor species of these elements or possible vapor species involving other fission product elements that will be present in an actual reactor accident. What is important in the calculation of chemical composition is the thermodynamic stability of the individual species. To seriously affect the calculations discussed in later sections, any such, as yet unknown, species must be quite stable in these environments.

Chemical thermodynamic data for CsI were obtained from Barin and Knacke (5.2), for the tellurium compounds from Mills (5.3) and the rest of the data from JANAF Tables (5.4). A brief tabulation of thermodynamic data for the major species is given in Appendix C. Published uncertainties in the data are generally less than  $\pm 10\%$ . Vapor species that are marginally stable may have larger uncertainties. Since such vapor species are calculated to be present only in very low concentrations, the effects of their uncertainties on the overall calculated compositions are not significant. Extensive sensitivity studies would be required to determine the effects that the uncertainties of the major species have on the calculated equilibrium composition. Such studies were not done.

A code comparison study was conducted to see if two codes, designed to predict product species and their relative abundances, gave similar results. Six sets of thermodynamic conditions were chosen for the purpose of calculating the stability of cesium and iodine species in steam using two codes -- SOLGASMIX run at ORNL (5.5) and FLUEQU used for the calculations in Reference 5.1 run at Sandia. The thermodynamic conditions covered a broad range of variables that might be encountered in reactor accidents. The amounts of species calculated by the two codes are within 20% of each other at the most sensitive conditions and generally agreed to within several percent. Sensitive conditions are those where there is

a rapid change in the abundance of a species with temperature. Thermodynamic data for CsI obtained from two sources - Reference (5.6) used by ORNL and Reference (5.2) used by Sandia - produced less than a five percent difference in abundances when used in the FLUEQU code for the conditions used for the inter-code comparison. A full comparison has not yet been made.

Again, the objective of the thermodynamic analysis was to identify the predominant species for consideration in fission product transport. As expected, the species depend on the conditions that exist during a reactor accident. Conditions generated by severe reactor accidents are not at all well-known. It was necessary then to determine the product species in the four systems over a range of conditions. These conditions were:

Temperature - from 600C to 2300C

Pressure - 1 bar (about 14.7 psi) and 150 bar.

Fission Product (FP) concentrations in the steam.

FP (moles) to water (moles)\* ratio -  $2 \times 10^{-7}$  to  $2 \times 10^{-1}$

Oxidizing, inert and reducing atmospheres.

Temperatures in the core can rise to about 2300C during a core-melt accident. Normal operating pressures are about 150 bar in the core and about 1 bar in the containment. How the fission-product concentrations above compare with those that might be expected during an accident can be provided by two examples. If all the water in the primary system (as steam) were mixed with all the iodine in the core the concentration would be about  $5 \times 10^{-6}$ , greater than the lower limit of  $2 \times 10^{-7}$ . If one tenth of the water (as steam) in the core were mixed with all of the iodine the concentration would be about  $2 \times 10^{-4}$ . It was recognized that, depending on the details of the release process, considerably higher concentrations may initially be present. Therefore the calculations were extended to an upper limit of  $2 \times 10^{-1}$ . These limits then bound reasonable accident concentrations.

A steam environment with excess oxygen such as in an air filled containment building is a chemically oxidizing atmosphere. A steam environment with excess hydrogen such as in the primary cooling system is a chemically reducing atmosphere. The fission-product chemistry can vary considerably depending on the reducing or oxidizing nature of the atmosphere. These atmospheres could be characterized by a hydrogen to steam ratio and an oxygen to steam ratio, but a convenient shorthand combining these ratios is the ratio of hydrogen to oxygen (H/O in moles/mole). As H/O ranges from greater than 2 through 2 to less than 2, the atmosphere ranges from steam with hydrogen (reducing) to pure steam to steam with oxygen (oxidizing).

\*See Appendix C for comments on this choice for concentration parameter.

Results of the important chemistry in the four systems and under the above conditions are summarized below.

### 5.2.2 Ternary Systems

#### 5.2.2.1 Iodine-Hydrogen-Oxygen (I-H-O) System

Although  $I_2$  is the normal form of iodine vapor at its boiling point (184C), this species dissociates to monatomic iodine (I)



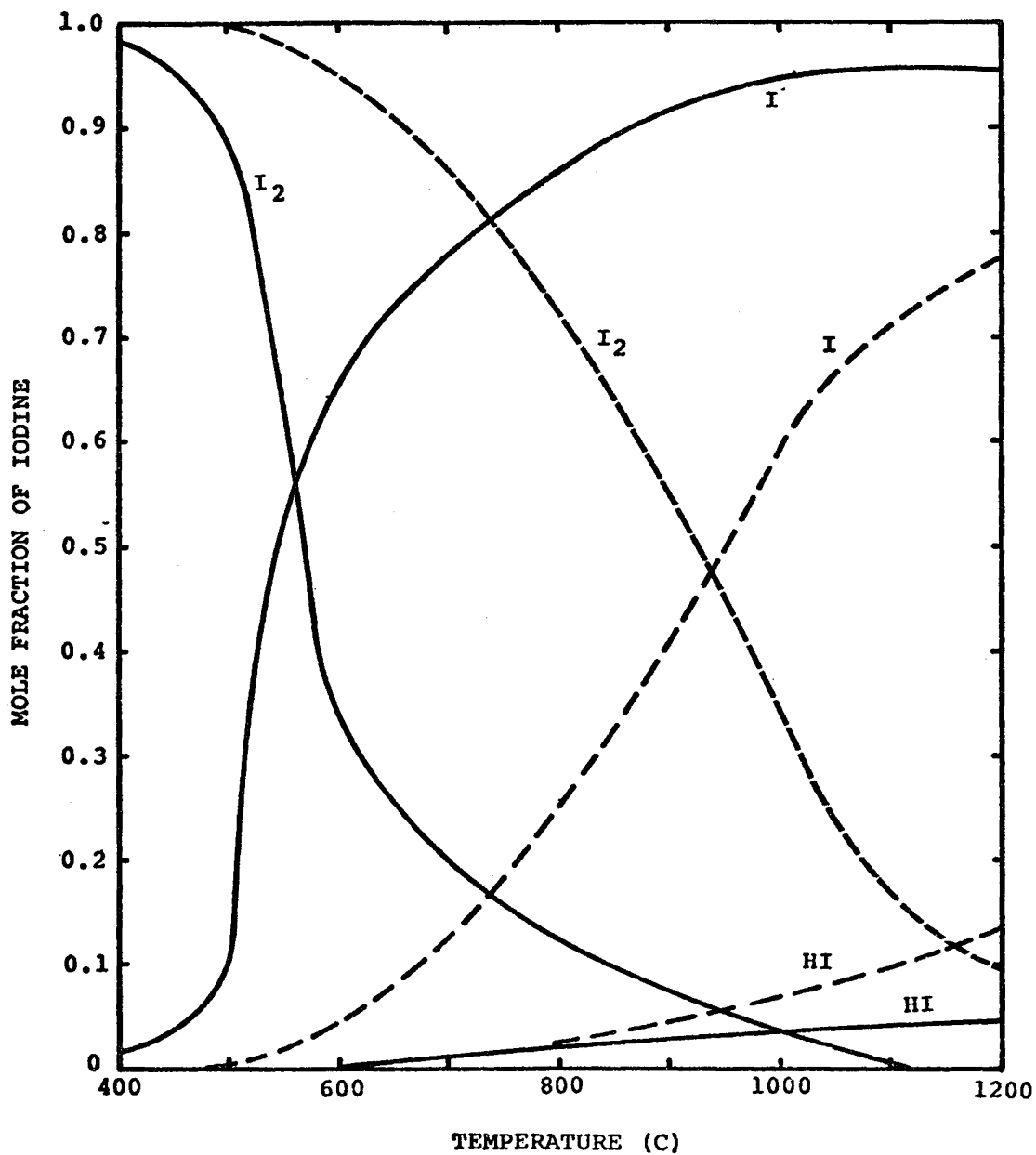
in pure steam ( $H/O = 2$ ) at high temperatures and low concentrations. Even at high concentrations ( $2 \times 10^{-3}$ ) I dominates at temperatures greater than about 600C (Figure 5.1). In high temperature, oxidizing environments ( $H/O$  less than 2), I is the sole species at all but the highest concentrations and pressures where some  $I_2$  persists. In reducing environments ( $H/O$  greater than 2), HI (boiling point - 127C) is the dominant species at lower temperatures. But as the temperature increases, the HI concentration decreases because it also begins to dissociate. Nearly complete dissociation to I has occurred by 1700C. For a given  $I/H_2O$  ratio, increased system pressure (and thus increased partial pressure) promotes the formation of  $I_2$  and HI at the expense of I (Figure 5.1). The formation of iodine containing species other than  $I_2$ , I and HI may occur from the reaction of iodine and steam. The species HOI has been postulated. However there are no thermodynamic data available for HOI nor any other iodine vapor compounds.

As with all vapor species, HI and  $I_2$  will physically adsorb onto surfaces. The amount adsorbed per unit area depends on temperature, vapor pressure, and surface properties. A very simplistic measure of when condensation should begin to be considered is the boiling point at one atmosphere. Removal of iodine species from steam by chemisorption processes or other chemical reactions with aerosols and other surfaces cannot be excluded. For instance, there is a possible reaction of iodine with steels to form  $FeI_2$ . This compound has been investigated within the context of high temperature gas reactors but no reports were found concerning its stability in steam environments.

Several percent of the total iodine continues to be produced after the accident because of the radioactive decay of tellurium to iodine. Therefore the species predicted in this (I-H-O) system may be indicative of the iodine species that are produced at these later times if cesium were absent.

#### 5.2.2.2 Tellurium-Hydrogen-Oxygen (Te-H-O) System

Equilibrium calculations were made based on the vapor species of Table 5.1. These calculations show that the distribution of tellurium among its vapor species is a sensitive function of the



$$\text{I}/\text{H}_2\text{O} = 2 \times 10^{-3}; \text{H}/\text{O} = 2.0;$$

(—) PRESSURE EQUALS 1 BAR.

(---) PRESSURE EQUALS 100 BARS.

Fig. 5.1 Relative abundance of iodine species in the Iodine-Hydrogen-Oxygen System for the conditions given

system parameters. Small amounts of oxygen shift the distribution so that  $\text{TeO}_2$  is a major tellurium containing species. However  $\text{TeO}$  can become important at high temperatures or when the tellurium concentration becomes very low ( $\text{Te}/\text{H}_2\text{O} < 10^{-6}$ ).

Conversely a small amount of hydrogen shifts the distribution so that  $\text{Te}_2$  and  $\text{Te}$  are the predominant forms. High tellurium concentrations and/or low temperatures favor  $\text{Te}_2$  while high temperatures and low tellurium concentrations promote the formation of  $\text{Te}$ .

Condensation of  $\text{TeO}_2$  and  $\text{Te}_2$  may occur. Data are needed for the interaction of  $\text{TeO}_2$  with stainless steel. Compounds resulting from the reaction of tellurium with the components of stainless steel have been investigated. The behavior of these tellurides in steam has not been studied.

The compounds  $\text{Cs}_2\text{Te}$ ,  $\text{TeI}_4$  and  $\text{TeI}_2$  are known only as solids. These compounds apparently vaporize by decomposition to their component elements. If so, these compounds would have no effect on the calculated vapor composition.

The sensitivity of the calculated vapor species distribution to system parameters indicates that a comprehensive evaluation of the accuracy of the tellurium data base is warranted.

[In the review process, the omission of  $\text{TeO}(\text{OH})_2$  as a vapor species was brought out. This vapor species results from the gas phase interaction of  $\text{TeO}_2$  with steam. The published data (5.12) indicate that in largely steam environments much of the  $\text{TeO}_2$  is transformed into  $\text{TeO}(\text{OH})_2$ . This species is thus also present whenever  $\text{TeO}_2$  is calculated to be a major species, i.e. when  $\text{O}_2$  is also present. No independent thermodynamic data for  $\text{TeO}(\text{OH})_2$  is available.]

### 5.2.2.3 Cesium-Hydrogen-Oxygen (Cs-H-O) System

Equilibrium calculations based on the vapor species listed in Table 5.1 indicate that  $\text{CsOH}$  is the dominant cesium-containing species in oxidizing and inert environments ( $\text{H}/\text{O}$  ratio between 1.5 and 2.0) at all temperatures investigated. In reducing environments  $\text{CsOH}$  is the major species at lower temperatures. However as temperature is increased above 1000C there is an increase in the concentration of  $\text{Cs}$  vapor. The concentration of  $\text{Cs}$  vapor is markedly enhanced when there is a large excess of hydrogen present ( $\text{H}/\text{O}$  greater than 3). In the extreme case of very high temperature (greater than 1700C) and a very large excess of hydrogen ( $\text{H}/\text{O} = 30$ ), the calculations indicate that greater than 80% of the cesium is present as  $\text{Cs}$  vapor.

At lower temperatures the  $\text{CsOH}$  vapor concentration may be limited by physical condensation of liquid cesium hydroxide on aerosols and other surfaces. Much more important however may be the removal of  $\text{CsOH}$  from the vapor by its reaction with stainless steel. Possible conditions for this reaction are described in Appendix C.3.

#### 5.2.2.4 Cesium-Iodine-Hydrogen-Oxygen (Cs-I-H-O) System

Equilibrium calculations have identified the major fission product species existing in a predominantly steam environment for the cesium-iodine-hydrogen-oxygen system. The cesium to iodine ratio was 10; the effect of this ratio on system stability is discussed in Appendix C.1.

Three iodine containing species are dominant - I, CsI and HI. Monatomic iodine dominates in oxidizing atmospheres, especially at high temperatures. In reducing atmospheres and at lower temperatures CsI dominates. As temperature is increased CsI begins to dissociate with the iodine transforming to I and/or HI. The relative abundances of these iodine containing species are presented graphically in Appendix C-1.

The major cesium containing species are CsOH, CsI and Cs (monatomic cesium vapor). Again the relative amounts depend on the system parameters. The CsOH molecule is stable at all temperatures and pressures in oxidizing environments (H/O less than 2). However in the reducing conditions expected in the core during reactor accidents Cs vapor can become an important species at higher temperatures. The abundance of Cs is greatly enhanced when large excesses of hydrogen (H/O greater than 10) are present. Reducing environments and lower temperatures also favor the presence of CsI as discussed above.

The effect on the abundance of iodine- and cesium containing species resulting from changes in the system parameters can be summarized as follows:

- an increase in system pressure (thus an increase in partial pressure) increases the relative stability (abundance) of the molecular species CsI, HI and CsOH for a given fission product to water ratio
- an increase in fission product concentration increases the relative stability (abundance) of CsI but has little effect on the stability of CsOH
- an increase in the H/O ratio (that is toward more reducing environments) increases the relative stability of CsI but decreases the stability of CsOH
- a decrease in temperature increases the relative stability (abundance) of both CsI and CsOH

A qualitative description of the effects of changing the system parameters - temperature, pressure, fission product concentration - on the stability (abundance) of CsI can be presented on the basis of a simple physical model. Recall that chemical equilibrium has a dynamic, not static, nature. Molecules are continually dissociating to atoms; in turn atoms are continually combining to form molecules. Equilibrium is attained when the rate of dissociation and recombination

are equal. The probability that a molecule will dissociate is dependent on temperature and becomes greater as temperature is raised. However the probability of recombination is dependent on the probability of a collision between appropriate atoms as well as on temperature. Thus as the fission product atoms Cs and I are brought closer together, which happens with an increase in system pressure or concentration, the formation of the CsI molecule becomes more favored. With CsOH, on the other hand, a cesium atom is always near other oxygen and hydrogen containing species. Its stability is thus little affected by changes in system pressure or cesium concentration. Its stability is affected by system temperature and also by the system H/O ratio. In the latter case the great excess of hydrogen dilutes the oxygen concentration thereby reducing the probability that oxygen atoms are nearby.

#### 5.2.2.5 Other Fission Products

The vapor chemistries of two additional fission products - ruthenium and strontium - are discussed briefly.

##### Ruthenium

Ruthenium is a refractory metal and would vaporize only at the highest temperatures. (Its boiling point is 4150C.) Some ruthenium oxides are moderately volatile; the compound  $\text{RuO}_4$  is very volatile. However these oxides decompose readily when heated in air and would require large overpressures of oxygen in order to be stable at the temperatures considered in this report. Vapor transport of ruthenium oxides appears unlikely. However this does not preclude mechanical transport of ruthenium away from the fuel.

##### Strontium

Strontium metal is moderately volatile (boiling point is 1150C) but reacts readily with water vapor. There are two possible products to this reaction -  $\text{SrO}$  and  $\text{Sr(OH)}_2$ . The oxide,  $\text{SrO}$ , is a refractory material (melting point is 2430C) and thus would not be considered as a vapor species. The hydroxide,  $\text{Sr(OH)}_2$ , melts at 375C and decomposes to the oxide at about 600C. However the JANAF tables do list data for  $\text{Sr(OH)}_2$  vapor. No calculations have been made yet concerning its stability in reactor accident environments.

The iodide compound,  $\text{SrI}_2$ , melts at 402C and may also be a volatile species. Its stability in the presence of water vapor at high temperatures is considered marginal. While no calculations have been performed, the current judgement is that  $\text{SrI}_2$  vapor would not be important if cesium is also present since  $\text{CsI}$  is a more stable species than  $\text{SrI}_2$ .

### 5.2.2.6 Radiolytic Effects

Radiolysis of steam and other molecules has been ignored here. The chemistry resulting from the radiolysis of water vapor has been discussed by Venugopalan and Jones (5.7). One concludes from their discussion that the transient chemical species produced by radiolysis have lifetimes greater than one second only at temperatures less than 300C. Consequently at the temperatures considered here (temperatures greater than 600C) radiolysis would have a negligible effect on the composition of the systems because of the very short lifetimes of radiation-induced species at these higher temperatures.

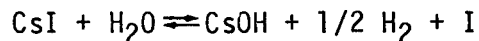
### 5.2.2.7 Physical Condensation and Chemical Reaction on Surfaces: Aerosol and Structural

The absolute amount of any fission-product species in the gas stream can be altered by either of two processes.

One of these processes is the physical condensation of vapor species on surfaces. These surfaces may be either aerosols that are present or structural materials. Condensation will occur whenever a gas is cooled so that the saturation (vapor) pressure of a solid or liquid phase is reached. This process may limit the concentration of CsI, CsOH and other moderately volatile fission product species. In the vapor stream at lower temperatures. CsI and CsOH condensation temperatures for representative FP/H<sub>2</sub>O ratios are presented in Appendix C.2.

The second process that may limit the amount of vapor in the gas stream is chemisorption or chemical reaction of a fission product vapor species with surfaces. For instance the known reaction (5.8) of CsOH with stainless steel at elevated temperatures may limit the CsOH vapor concentration to low levels.

Since there is an equilibrium equation relating the CsI and CsOH vapor concentrations



there is a possibility that, should the CsOH concentration be reduced to very low levels, the concentration of CsI may also be reduced. If so, the iodine previously contained in CsI would be converted to other iodine containing species.

At present there are no experimental data by which to judge whether the above process could occur. One can only make exploratory calculations. These are discussed in Appendix C.3.

It is apparent, however, that strong chemical interactions between individual vapor species and surfaces may alter the proportions of other seemingly unrelated vapor species. For this reason a thorough knowledge of vapor-surface reactions is desirable.

### 5.2.2.8 Conclusions

This survey of high temperature vapor phase chemistry has found a decided lack of thermochemical data necessary to predict and describe the transport of fission product elements in reactor accident environments. Data for the interaction of vapors and surfaces are particularly lacking.

Based primarily on the thermodynamic data tabulated in the JANAF Tables, equilibrium compositions were calculated for the following vapor systems and these predominant vapor species were identified:

#### I-H-O (Iodine-Hydrogen-Oxygen)

Monatomic iodine (I) and hydrogen iodide (HI) are the dominant iodine species. HI occurs whenever excess hydrogen gas is present; its abundance decreases as temperature is increased.

#### Cs-H-O (Cesium-Hydrogen-Oxygen)

Cesium hydroxide (CsOH) is the predominant cesium species for most conditions. Only at high temperatures and large excesses of hydrogen does monatomic cesium (Cs) become an important species.

#### Te-H-O (Tellurium-Hydrogen-Oxygen)

Chemical equilibrium calculations for the tellurium-hydrogen-oxygen system showed that, in reducing atmospheres, the major vapor species are  $\text{Te}_2$  and Te, while in oxidizing atmospheres the major species are  $\text{TeO}_2$  (or  $\text{TeO}(\text{OH})_2$ ) and TeO. The relative abundances are sensitive to system parameters. Possible compounds of tellurium with other fission products ( $\text{Cs}_2\text{Te}$ ,  $\text{TeI}_4$ , and  $\text{TeI}_2$ ) do not appear to be stable in the gas phase.

#### Cs-I-H-O (Cesium-Iodine-Hydrogen-Oxygen)

The stability of CsI makes this compound the predominant iodine species for most conditions. High temperatures, oxidizing environments or low fission product concentrations destabilize the CsI molecule and result in I and HI becoming important. The CsI molecule is more stable than CsOH and is the preferred cesium species. CsOH is formed when there is excess cesium present. Cs vapor can become important at high temperatures and with large excesses of hydrogen.

At low temperatures the concentration of CsOH and CsI in the vapor can be limited by condensation processes. Vapor-solid chemical interactions could also be important processes for removal of vapor

## 5.12

species, but little or no data are available to enable a judgement to be made.

No vapor species containing ruthenium are expected. Strontium hydroxide,  $\text{Sr}(\text{OH})_2$ , is a possible vapor species.

## 5.3 Aqueous Iodine Chemistry

### 5.3.1 Introduction

Molecular iodine,  $I_2$ , in pure form or in solution is very reactive; it reacts with water, organic materials, metal alloys, and even noble metals. An important characteristic of molecular or pure iodine,  $I_2$ , is that it does not stay around; it prefers other states, usually iodide and iodate. Iodine in pure form is a black solid with metallic luster, and in a closed system the solid is in equilibrium with its violet-colored vapor. It is soluble in water and produces a brown solution, whereas it is more soluble in non-polar solvents, such as carbon tetrachloride, and forms purple or violet solutions. Iodine chemistry in these two solutions is completely different; iodine in the purple non-polar solutions is essentially stable, while iodine in water reacts to produce at least four different iodine species, and the relative concentrations of the iodine species will depend on the conditions of the aqueous system: temperature, acidity, etc.

Other common forms of iodine include the chemically reduced or the iodide state and the chemically oxidized or iodate state. Iodide,  $I^-$ , is found in natural brines; there the iodide state is demonstrated to be stable. Oxidized iodine or iodate,  $IO_3^-$ , occurs naturally in salt and rock deposits as sodium iodate,  $NaIO_3$ , and calcium iodate,  $Ca(IO_3)_2$ . This natural occurrence indicates that the iodate form of iodine is also a stable state. Sea water contains about  $50 \mu\text{g}/\ell$  ( $4 \times 10^{-7} \text{ M}$ ) iodine which is primarily iodate; the ratio of iodate to iodide is about four and the concentration of molecular iodine,  $I_2$ , is too low for present analytical determination. It is particularly interesting that elemental iodine,  $I_2$ , is not found in nature, and this fact clearly relates its instability to the stability of iodide, and iodate.

Iodine is the heaviest naturally occurring element in the halogen family. While the general chemical properties of iodine are similar to those for other halogens, bromine and chlorine, the chemistry for iodine species cannot be deduced from general halogen chemistry. Several chemical forms of iodine occur in nature and in industrial systems, and the dominant species will depend primarily on the ambient conditions. One cannot assume that iodine in a particular set of conditions will be equivalent or even similar to that in another system. Iodine behavior will be determined by the chemistry for the particular system, and that chemistry must be defined and considered before iodine behavior is predicted.

### 5.3.2 Chemical Conditions

Aqueous iodine chemistry that is pertinent to an LWR accident will be determined by the conditions of the incident. Perhaps the best defined parameter of the aqueous system in an incident will be the acidity. In pressurized water reactors, PWRs, the coolant is buffered by boric acid with a small amount of lithium hydroxide, while the coolant for boiling water reactors, BWRs, is pure water. Post accident responses generally add boric acid-sodium hydroxide solutions of moderately high pH. An extreme pH range of 5-11 would include both operating and accident conditions.

The temperature of the aqueous systems during and after a reactor accident can vary over a wide range. At the time of iodine release from the fuel, a supercritical,  $>373^{\circ}\text{C}$ , aqueous system can exist, while the post accident temperature of the aqueous system in the reactor containment building can be below normal room temperature.

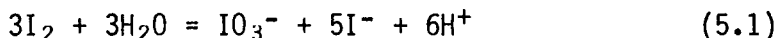
Total iodine concentration in the aqueous system following a reactor accident is limited by the amount of iodine in the fuel core and by the amount of water in the normal coolant system plus the water in the emergency core cooling system. The maximum core inventory of iodine in a light water reactor will be  $15 \pm 0.5$  kg or about 118 moles of iodine atoms. The amount of water in the primary circuit of a PWR is not less than  $10^5$  gallons or about  $4 \times 10^5$  liters. Quantitative dissolution of that iodine into that water gives a maximum concentration of  $3 \times 10^{-4}$  moles per liter, M. (Iodine concentrations will be expressed herein as moles of iodine atoms per liter. The sum of concentrations of iodine species will be  $\sum I = 2[I_2] + [I^-] + [IO_3^-] + [HOI] + [CH_3I]$ .) There are at least two reasons that the aqueous iodine concentration in a reactor incident will be less than the above; first, not all of the iodine will be driven out of the fuel; and second, most accidents activate the emergency core cooling water which can increase the total water volume by substantial factors. Thus, the total iodine concentration would be between  $10^{-6}$  and  $10^{-4}$  M. This could be compared to  $4 \times 10^{-7}$  M of iodate and iodide in sea water. (Since the TMI accident the total iodine concentration in the water in that containment building was  $\sim 10^{-6}$  M.)

### 5.3.3 Specific Chemistry and the Literature

Numerous papers on aqueous iodine chemistry have appeared in the literature in the late 19th and throughout the 20th century, and essentially all experiments have been at ambient conditions with macro concentrations of iodine,  $>10^{-4}$  M. Only a few more recent publications describe experiments with tracer level iodine. This review will summarize (1) redox reactions of iodine species, (2) hydrolysis and disproportionation reactions, (3) organic iodide formation and reactions, (4) radiation effects on aqueous iodine species, and (5) liquid-gas phase partitioning. The first two topics are discussed generally in advanced inorganic chemistry texts such as that by Cotten and Wilkinson;<sup>5.13</sup> these texts in turn frequently refer to the older standard references such as Latimer<sup>5.14</sup> for oxidation potentials. The other topics are reported in topical reports and scientific journals.<sup>5.15-5.51</sup> There are several publications on sea water chemistry<sup>5.52-5.60</sup> that are related to and include some aqueous iodide chemistry. Kinetic studies, rates of reactions and equilibria at high temperature ( $100-300^{\circ}\text{C}$ ) could not be found in the literature. Heterogeneous reactions of aqueous iodine with structural or containment materials are not discussed but are known to consume molecular iodine,  $I_2$ , at appreciable rates. Quantitative information for such reactions is not available and should be established.

### 5.3.4 Redox Potentials for Iodine Species

Correct applications of redox potentials can yield equilibrium constants for aqueous iodine reactions which can be used to calculate concentrations of various species at specified conditions. Molecular iodine,  $I_2$ , equilibrates with water according to the reaction,



and the equilibrium constant at 25°C,  $5.37 \times 10^{-48}$ , was calculated from redox potentials as discussed in Appendix C.5. This calculated constant is compared with and supports that in the next section based on known experimental data. Another calculation given in Appendix C.5 is the equilibrium constant,  $8.9 \times 10^{15}$ , for the oxygen oxidation of iodide to iodate,



That calculation shows that oxygen can oxidize iodide to iodine, but at low acid concentrations, the oxidation of iodine species would continue to iodate. The calculations in Appendix C.5 demonstrate the utilization of redox potentials and reference the best set of tabulated potentials.

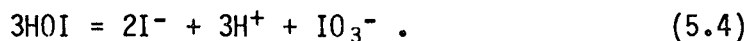
The rate of oxidation of  $\text{I}^-$  by dissolved oxygen is slow as indicated by the stability of iodide solutions. One estimate of that oxidation rate has been based on the  $\text{I}^-/\text{IO}_3^-$  variation near the ocean floor and the rate of mixing of ocean water by eddy diffusion.<sup>5,58</sup> The result is only approximate, but it suggests that half the iodide is oxidized to iodate in about 25 years.

### 5.3.5 Iodine Hydrolysis

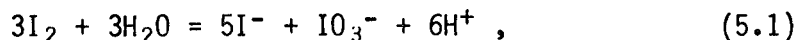
Iodide and iodate salts dissolve in water and produce generally stable solutions that contain essentially all of the iodine in solution. However, some reactions can convert portions of these species to molecular iodine,  $\text{I}_2$ . Then the iodine-water chemistry becomes significant just as if the iodine source were molecular iodine. Molecular iodine,  $\text{I}_2$ , is soluble in water, 0.0013 M at 25°C<sup>5,13</sup> and rapidly reacts with water according to the reaction,



Hypoidous acid, HOI, is not stable because of disproportionation generally described by



The equilibrium constant has not been measured directly.<sup>5,13</sup> Another reaction in aqueous systems unites  $\text{I}_2$  and  $\text{I}^-$  to form  $\text{I}_3^-$ . However, this  $\text{I}_3^-$  species is insignificant for total concentrations of  $10^{-5}$  or less, and will not be included in this discussion. The net reaction for the hydrolysis of iodine is then the sum of reactions (5.3) and (5.4);



and the equilibrium constant is small. The "best" values of equilibrium constants for Reactions (5.3), (5.4), and (5.1) at 25°C are concluded to be respectively,  $4.04 \times 10^{-13}$ ,  $1.06 \times 10^{-10}$ , and  $8.09 \times 10^{-48}$ , because these values are based on all of the known literature, Appendix C.6. The constants for reactions (5.3) and (5.1) at 100°C were estimated to be  $5 \times 10^{-11}$  and  $2.7 \times 10^{-40}$ , respectively, Appendix C.6.

Hypoiodous acid, HOI, is generally accepted to be an intermediate species in the iodine hydrolysis. However, static and equilibrium concentrations are questioned, and the direct observation of HOI has not been verified. Appendix C.6 includes a discussion of information on the HOI species. It appears that careful experimentation can determine the reality and stability of the HOI species.

A cursory evaluation of the small equilibrium constant,  $8.1 \times 10^{-48}$ , for the net hydrolysis reaction (5.1) can give an erroneous implication that the extent of the reaction is low, i.e., the amount of  $I_2$  that reacts is small. However, in a low acid medium such as pH of 6 or greater, the sixth power dependence on the acid concentration dominates the equilibrium. The concentrations of all iodine species can be calculated from the equilibrium constant for a given amount of total iodine in a system at a given acidity; under LWR accident conditions the amount of  $I_2$  in an equilibrated system should be a very low percentage of the total iodine. Table (5.2) gives the concentrations for aqueous solutions at 25°C with total iodine concentrations from  $10^{-9}$  to  $10^{-5}$  M over the pH range 5 to 9. Corresponding data for 100°C conditions are given in Table (5.3). The concentrations of HOI and  $I_2$  at equilibrium with pH greater than 6 are very low. The fraction of total iodine that exists as  $I_2$  in an equilibrated aqueous solution is plotted as a function of total iodine for pH values of 5 to 9 at 25°C (solid lines) and for pH values of 5 to 8 at 100°C (dashed lines) in Fig. (5.2).

There can be periods of time when the aqueous systems in an LWR accident are not at equilibrium. The relative rates of reactions (5.3) and (5.1) will determine the relative amounts of  $I_2$  and HOI. Appendix C.6 discusses the possibility where the HOI concentration could be considerably greater than those given in Table (5.2) for systems at equilibrium. The maximum concentration for HOI in a static system would be that when reaction (5.3) approaches equilibrium but reaction (5.4) has not initiated. Some hypothetical maximum HOI concentrations are given in Table (5.4) for 25 and 100°C based only on reaction (5.3). Concentrations of  $I_2$  that correspond to the maximum HOI concentrations discussed above are plotted against total iodine concentrations in Fig. (5.3). As in Fig. (5.2), the  $I_2$  concentration is a function of the square of the total iodine except at lower pH and lower total iodine.

Iodine hydrolysis could be summarized as follows. Reaction rates for  $I_2$  hydrolysis are not known to an extent that non-equilibrium concentrations of various iodine species can be accurately estimated. The above calculations only establish limits of concentrations, and the realistic values are somewhere in between. Careful experimentation should be done to better determine concentrations of the various iodine species.

ACID	TOTAL I	HOI	I-	I2	IO3-	PC
1.000D-05	1.000D-04	0.142D-06	0.121D-04	0.853D-04	0.240D-05	0.954D+02
1.000D-05	1.000D-05	0.379D-07	0.324D-05	0.608D-05	0.640D-06	0.134D+03
1.000D-05	1.000D-06	0.743D-08	0.634D-06	0.233D-06	0.125D-06	0.344D+03
1.000D-05	1.000D-07	0.933D-09	0.796D-07	0.368D-08	0.157D-07	0.197D+04
1.000D-05	1.000D-08	0.965D-10	0.824D-08	0.394D-10	0.163D-08	0.930D+04
1.000D-05	1.000D-09	0.969D-11	0.827D-09	0.396D-12	0.163D-09	0.156D+05
1.000D-06	1.000D-04	0.748D-07	0.636D-04	0.236D-04	0.127D-04	0.345D+03
1.000D-06	1.000D-05	0.943D-08	0.802D-05	0.374D-06	0.160D-05	0.215D+04
1.000D-06	1.000D-06	0.975D-09	0.829D-06	0.400D-08	0.166D-06	0.181D+05
1.000D-06	1.000D-07	0.979D-10	0.832D-07	0.403D-10	0.166D-07	0.913D+05
1.000D-06	1.000D-08	0.979D-11	0.833D-08	0.404D-12	0.166D-08	0.154D+06
1.000D-06	1.000D-09	0.979D-12	0.833D-09	0.404D-14	0.166D-09	0.165D+06
1.000D-07	1.000D-04	0.976D-08	0.830D-04	0.401D-06	0.166D-04	0.201D+05
1.000D-07	1.000D-05	0.980D-09	0.833D-05	0.404D-08	0.167D-05	0.180D+06
1.000D-07	1.000D-06	0.980D-10	0.833D-06	0.404D-10	0.167D-06	0.911D+06
1.000D-07	1.000D-07	0.980D-11	0.833D-07	0.404D-12	0.167D-07	0.154D+07
1.000D-07	1.000D-08	0.980D-12	0.833D-08	0.404D-14	0.167D-08	0.165D+07
1.000D-07	1.000D-09	0.980D-13	0.833D-09	0.404D-16	0.167D-09	0.166D+07
1.000D-08	1.000D-04	0.980D-09	0.833D-04	0.404D-08	0.167D-04	0.180D+07
1.000D-08	1.000D-05	0.980D-10	0.833D-05	0.404D-10	0.167D-05	0.911D+07
1.000D-08	1.000D-06	0.980D-11	0.833D-06	0.404D-12	0.167D-06	0.154D+08
1.000D-08	1.000D-07	0.980D-12	0.833D-07	0.404D-14	0.167D-07	0.165D+08
1.000D-08	1.000D-08	0.980D-13	0.833D-08	0.404D-16	0.167D-08	0.166D+08
1.000D-08	1.000D-09	0.980D-14	0.833D-09	0.404D-18	0.167D-09	0.166D+08
1.000D-09	1.000D-04	0.980D-10	0.833D-04	0.404D-10	0.167D-04	0.911D+08
1.000D-09	1.000D-05	0.980D-11	0.833D-05	0.404D-12	0.167D-05	0.154D+09
1.000D-09	1.000D-06	0.980D-12	0.833D-06	0.404D-14	0.167D-06	0.165D+09
1.000D-09	1.000D-07	0.980D-13	0.833D-07	0.404D-16	0.167D-07	0.166D+09
1.000D-09	1.000D-08	0.980D-14	0.833D-08	0.404D-18	0.167D-08	0.166D+09
1.000D-09	1.000D-09	0.980D-15	0.833D-09	0.404D-20	0.167D-09	0.166D+09
1.000D-10	1.000D-04	0.980D-11	0.833D-04	0.404D-12	0.167D-04	0.154D+10
1.000D-10	1.000D-05	0.980D-12	0.833D-05	0.404D-14	0.167D-05	0.165D+10
1.000D-10	1.000D-06	0.980D-13	0.833D-06	0.404D-16	0.167D-06	0.166D+10
1.000D-10	1.000D-07	0.980D-14	0.833D-07	0.404D-18	0.167D-07	0.166D+10
1.000D-10	1.000D-08	0.980D-15	0.833D-08	0.404D-20	0.167D-08	0.166D+10
1.000D-10	1.000D-09	0.980D-16	0.833D-09	0.405D-22	0.167D-09	0.166D+10

Table 5.2: Equilibrium concentration and partition coefficients of aqueous iodine species according to the net equilibrium,  $3I_2 + 3H_2O = IO_3^- + 5I^- + 6H^+$ , at 25°C with an equilibrium constant of  $8.1 \times 10^{-48}$ . The net equilibrium is a summation of two reactions,  $I_2 + H_2O = HOI + I^- + H^+$  and  $3HOI = IO_3^- + 2I^- + 3H^+$ , with respective equilibrium constants of  $4.04 \times 10^{-13}$  and  $1.2 \times 10^{-10}$ .

ACID	TOTAL I	HOI	I-	I <sub>2</sub>	IO <sub>3</sub> -	PC
1.000D-05	1.000D-04	0.337D-06	0.747D-04	0.101D-04	0.149D-04	0.907D+02
1.000D-05	1.000D-05	0.371D-07	0.821D-05	0.122D-06	0.163D-05	0.663D+03
1.000D-05	1.000D-06	0.375D-08	0.830D-06	0.124D-08	0.165D-06	0.298D+04
1.000D-05	1.000D-07	0.375D-09	0.831D-07	0.125D-10	0.165D-07	0.465D+04
1.000D-05	1.000D-08	0.375D-10	0.831D-08	0.125D-12	0.165D-08	0.492D+04
1.000D-05	1.000D-09	0.375D-11	0.831D-09	0.125D-14	0.165D-09	0.495D+04
1.000D-06	1.000D-04	0.376D-07	0.832D-04	0.125D-06	0.166D-04	0.645D+04
1.000D-06	1.000D-05	0.377D-08	0.833D-05	0.126D-08	0.167D-05	0.296D+05
1.000D-06	1.000D-06	0.377D-09	0.833D-06	0.126D-10	0.167D-06	0.463D+05
1.000D-06	1.000D-07	0.377D-10	0.833D-07	0.126D-12	0.167D-07	0.490D+05
1.000D-06	1.000D-08	0.377D-11	0.833D-08	0.126D-14	0.167D-08	0.493D+05
1.000D-06	1.000D-09	0.377D-12	0.833D-09	0.126D-16	0.167D-09	0.493D+05
1.000D-07	1.000D-04	0.377D-08	0.833D-04	0.126D-08	0.167D-04	0.296D+06
1.000D-07	1.000D-05	0.377D-09	0.833D-05	0.126D-10	0.167D-05	0.463D+06
1.000D-07	1.000D-06	0.377D-10	0.833D-06	0.126D-12	0.167D-06	0.490D+06
1.000D-07	1.000D-07	0.377D-11	0.833D-07	0.126D-14	0.167D-07	0.493D+06
1.000D-07	1.000D-08	0.377D-12	0.833D-08	0.126D-16	0.167D-08	0.493D+06
1.000D-07	1.000D-09	0.377D-13	0.833D-09	0.126D-18	0.167D-09	0.493D+06
1.000D-08	1.000D-04	0.377D-09	0.833D-04	0.126D-10	0.167D-04	0.462D+07
1.000D-08	1.000D-05	0.377D-10	0.833D-05	0.126D-12	0.167D-05	0.490D+07
1.000D-08	1.000D-06	0.377D-11	0.833D-06	0.126D-14	0.167D-06	0.493D+07
1.000D-08	1.000D-07	0.377D-12	0.833D-07	0.126D-16	0.167D-07	0.493D+07
1.000D-08	1.000D-08	0.377D-13	0.833D-08	0.126D-18	0.167D-08	0.493D+07
1.000D-08	1.000D-09	0.377D-14	0.833D-09	0.126D-20	0.167D-09	0.493D+07
1.000D-09	1.000D-04	0.377D-10	0.833D-04	0.126D-12	0.167D-04	0.490D+08
1.000D-09	1.000D-05	0.377D-11	0.833D-05	0.126D-14	0.167D-05	0.493D+08
1.000D-09	1.000D-06	0.377D-12	0.833D-06	0.126D-16	0.167D-06	0.493D+08
1.000D-09	1.000D-07	0.377D-13	0.833D-07	0.126D-18	0.167D-07	0.493D+08
1.000D-09	1.000D-08	0.377D-14	0.833D-08	0.126D-20	0.167D-08	0.493D+08
1.000D-09	1.000D-09	0.377D-15	0.833D-09	0.126D-22	0.167D-09	0.493D+08
1.000D-10	1.000D-04	0.377D-11	0.833D-04	0.126D-14	0.167D-04	0.493D+09
1.000D-10	1.000D-05	0.377D-12	0.833D-05	0.126D-16	0.167D-05	0.493D+09
1.000D-10	1.000D-06	0.377D-13	0.833D-06	0.126D-18	0.167D-06	0.493D+09
1.000D-10	1.000D-07	0.377D-14	0.833D-07	0.126D-20	0.167D-07	0.493D+09
1.000D-10	1.000D-08	0.377D-15	0.833D-08	0.126D-22	0.167D-08	0.493D+09
1.000D-10	1.000D-09	0.377D-16	0.833D-09	0.129D-24	0.167D-09	0.493D+09

Table 5.3: Equilibrium concentrations and partition coefficients of aqueous iodine species according to the net equilibrium,  $3I_2 + 3H_2O = IO_3^- + 5I^- + 6H^+$ , at 100°C with an equilibrium constant of  $2.7 \times 10^{-40}$ . The net equilibrium is a summation of two reactions,  $I_2 + H_2O = HOI + I^- + H^+$  and  $3HOI = IO_3^- + 2I^- + 3H^+$ , with respective equilibrium constants of  $5 \times 10^{-11}$  and  $2.2 \times 10^{-9}$ .

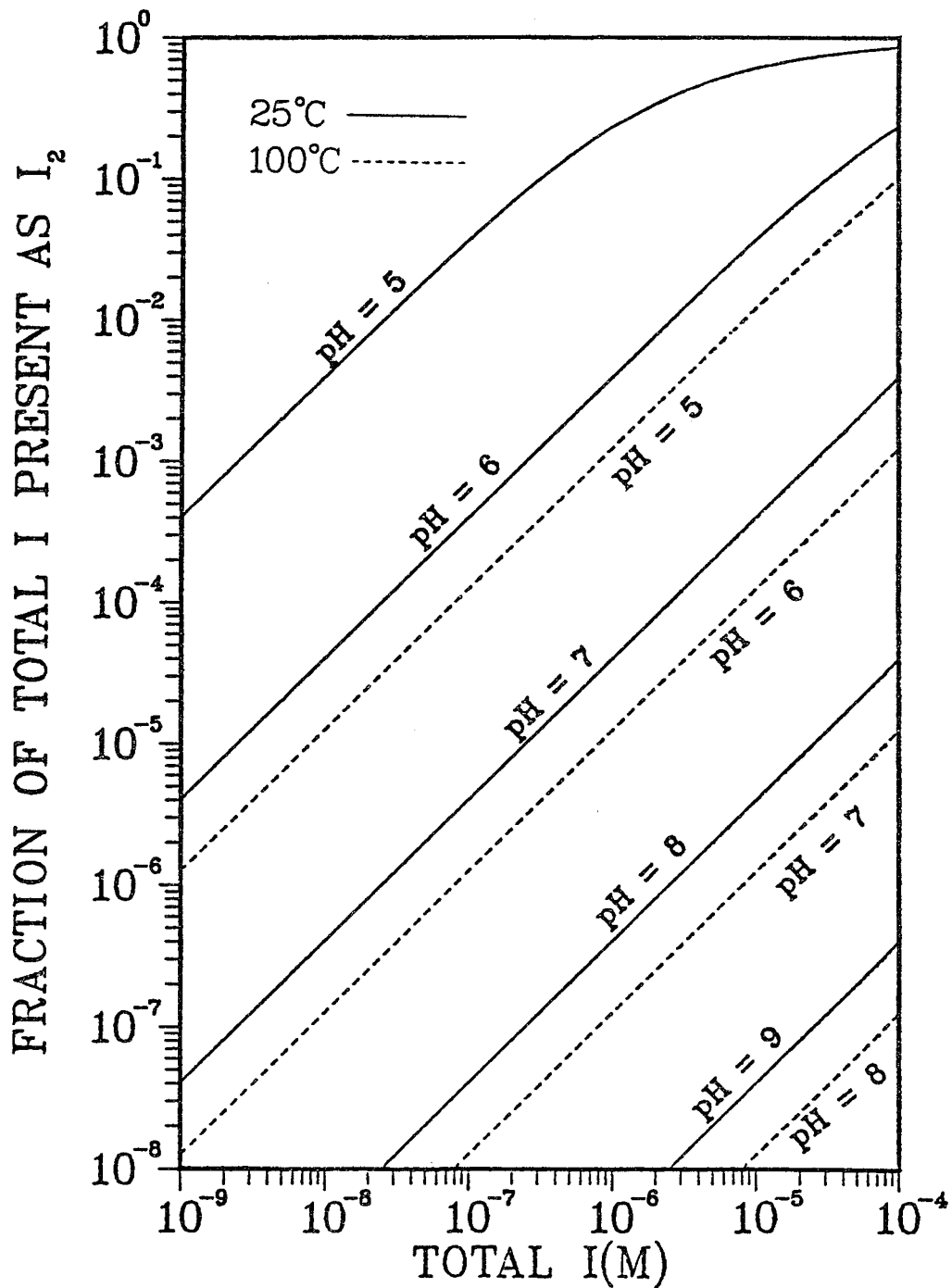


Figure 5.2: The fraction of total iodine that exists as I<sub>2</sub> when a molecular iodine, I<sub>2</sub>, source reacts with water,  $3\text{I}_2 + 3\text{H}_2\text{O} = \text{IO}_3^- + 5\text{I}^- + 6\text{H}^+$ , with equilibrium constants of  $8.1 \times 10^{-48}$  and  $2.7 \times 10^{-40}$  at 25 and 100°C, respectively. Iodine concentrations are moles of iodine atoms per liter.

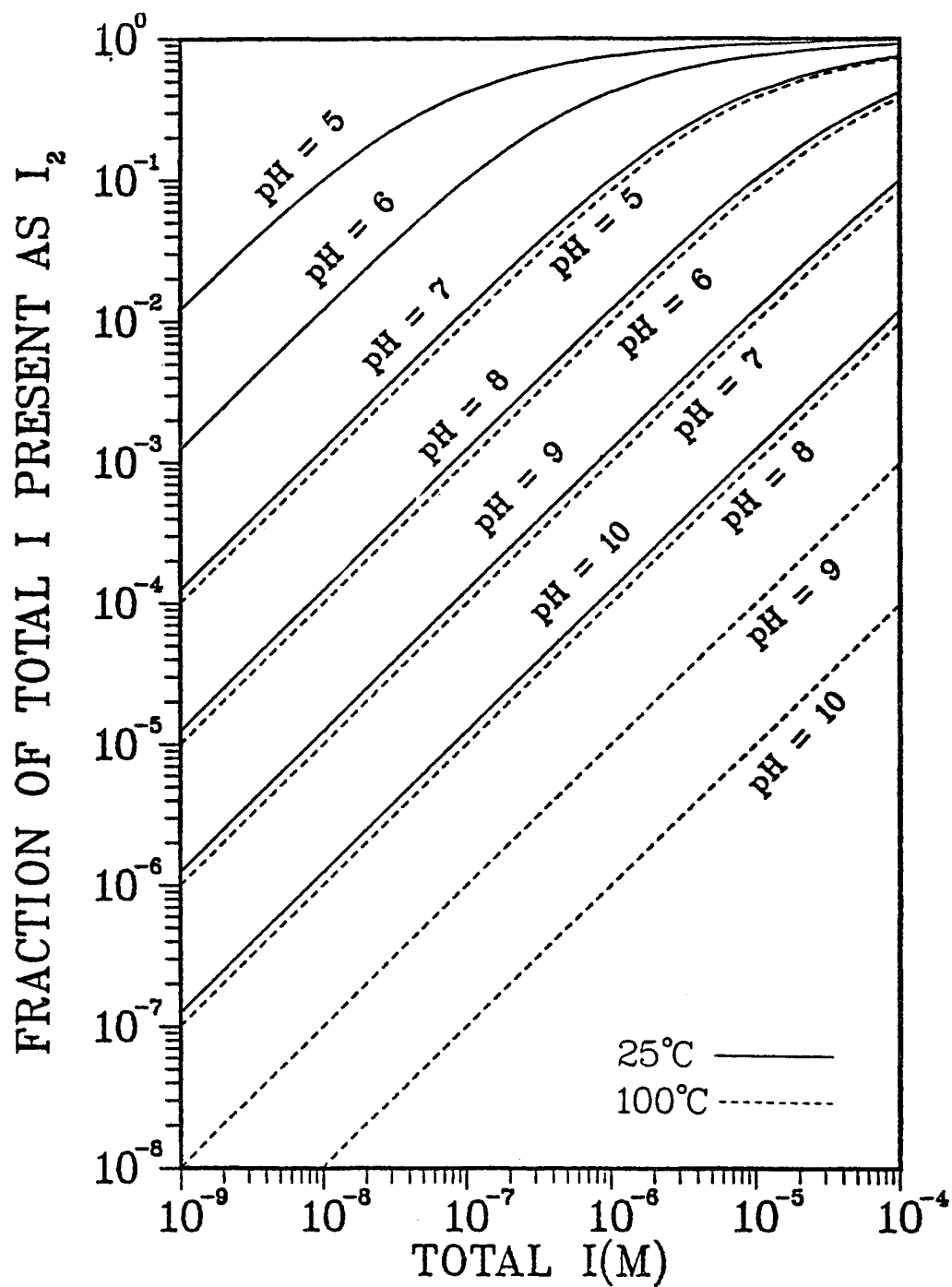


Figure 5.3: The fraction of total iodine that exists as I<sub>2</sub> in aqueous systems when a molecular iodine, I<sub>2</sub>, source reacts with water without forming iodate,  $I_2 + H_2O = HOI + I^- + H^+$ , with equilibrium constants of  $4.04 \times 10^{-13}$  and  $5 \times 10^{-11}$  at 25 and 100°C, respectively.

Table 5.4. Hypothetical concentrations of HOI in aqueous solution at 25° and 100°C when only the first hydrolysis reaction, 5.3, is considered and when the sum of molar concentrations of I<sub>2</sub>, I<sup>-</sup>, and HOI is 10<sup>-5</sup> M

pH	[HOI](25°C)	[HOI](100°C)
5	4.3 x 10 <sup>-7</sup>	3.1 x 10 <sup>-6</sup>
6	1.2 x 10 <sup>-7</sup>	4.6 x 10 <sup>-6</sup>
7	2.9 x 10 <sup>-6</sup>	4.9 x 10 <sup>-6</sup>
8	4.5 x 10 <sup>-6</sup>	4.99 x 10 <sup>-6</sup>
9	4.9 x 10 <sup>-6</sup>	4.999 x 10 <sup>-6</sup>

### 5.3.6 Organic Iodides in Aqueous Systems

Organic iodides in LWR accidents usually are referenced as methyl iodide. This is appropriate because most of the organic iodide associated with a reactor incident is methyl iodide and because methyl iodide is the most volatile organic and hence the most likely to cause iodine release from containment. Several mechanisms by which methyl iodide could be formed in an accident are presented in Appendix C.7. Also discussed there is the point that thermodynamic data indicate that methyl iodide is not a stable or favorable species; i.e., if chemical equilibrium is reached, methyl iodide is not present in significant amounts. However, experimental studies have observed methyl iodide concentrations much higher than the equilibrium quantity of 10<sup>-4</sup>% and it has been concluded that the kinetics of non-equilibrium processes produce organic iodides at higher concentrations.

Methyl iodide reacts with water as



This reaction is essentially irreversible and could occur in liquid or gaseous phases. Several classical chemists chose the above reaction for fundamental kinetic studies because it proceeds unimolecularly to completion at all accessible concentrations and temperatures.<sup>5.38-5.39</sup> Some of that work showed that the maximum methyl iodide concentration, C°, in water at various temperatures follows the expression

$$\log C^\circ = -110.278 + 36.6321 \log T + 4823/T \quad (5.6)$$

This indicates a minimum solubility of 3.5 x 10<sup>-4</sup> M at 23°C.

Modern authors have also studied the hydrolysis of methyl iodide and reported complete reaction with water and with hydroxide.<sup>5.40</sup> This later work also showed that the methyl iodide hydrolysis rate at 100°C is about 4 orders of magnitude greater than at 25°C.

The available information suggests that methyl iodide in an aqueous system eventually would convert quantitatively to methanol and iodide. However, the very low gaseous methyl iodide concentration in the TMI containment remained constant until that atmosphere was released and renewed. Then the methyl iodide concentration in that containment

increased almost to the previous level and appears to again maintain a steady state. This suggests that a process to produce methyl iodide, perhaps one of those in Appendix C.7, is generating  $\text{CH}_3\text{I}$  at a rate equal to the rate of reaction (5.5).

### 5.3.7 Radiation Chemistry of Aqueous Iodide Systems

Textbooks hardly acknowledge this subject, and specific information in the literature is sparse. Because of high water to iodine ratios in LWR accident conditions ( $>10^5$ ), the major effect of radiation on aqueous iodine chemistry is expected to result from reactions of the iodine species with water radiolysis products. Based on discussions in the previous sections the significant interactions will be those with iodide ( $\text{I}^-$ ), iodate ( $\text{IO}_3^-$ ), and molecular iodine ( $\text{I}_2$ ).

A recent review of this subject by Sellers<sup>5.43</sup> included most literature through 1976, and identified nine iodine species that exist as intermediates in the reactions of  $\text{I}^-$ ,  $\text{IO}_3^-$ , and  $\text{I}_2$  with the various water radiation products. There were no conclusions about steady-state iodine species for any particular conditions. Two other publications reported observed effects of gamma radiation on aqueous  $10^{-6}$  to  $10^{-3}$  M iodide solutions and measured oxidized iodine products after irradiation.<sup>5.44,5.45</sup> Lin<sup>5.44,5.45</sup> concluded that iodide was oxidized to iodate by a mechanism that involves an intermediate, probably HOI.

Lin<sup>5.45</sup> also reported the results of iodine analysis of BWR coolant. The fission product iodine in the coolant during reactor operation was 60–90% iodide,  $\text{I}^-$ , and the remainder was iodate,  $\text{IO}_3^-$ . Only traces of  $\text{I}_2$  or organic iodide were found. During reactor shutdown the iodide to iodate ratio,  $\text{I}^-/\text{IO}_3^-$ , decreased markedly because of radiolytic oxidation of  $\text{I}^-$  to  $\text{IO}_3^-$ . However, the trace amounts of  $\text{I}_2$  or organic iodide did not noticeably increase during reactor shutdown and radiolytic oxidation.

The radiolytic oxidation of iodide to iodate was observed during gamma radiolysis of pharmaceutical sodium iodide.<sup>5.47</sup> Various parameters were studied and the presence of hydrogen peroxide was observed as a reducing agent. Removal of oxygen with nitrogen almost completely eliminated radiolytic oxidation of iodide.

### 5.3.8 Partitioning of Iodine Species Between Aqueous and Gaseous Phases

The most important property of iodine species in the aqueous phases of an LWR accident is vapor pressure, i.e., the quantity of the species that will transfer from the aqueous to the gaseous state. The equilibrium concentration of a species in solution divided by that in the gas phase is the species partition coefficient. Ionic iodine species,  $\text{I}^-$  and  $\text{IO}_3^-$ , in aqueous solution have essentially zero vapor pressure or infinite partition coefficients. On the other hand, molecular species,  $\text{I}_2$ , and  $\text{CH}_3\text{I}$ , (and possibly HOI) have appreciable vapor pressures and account for most vapor phase iodine.

The total partition coefficient when more than one species coexist will be the ratio of the sum of the aqueous phase concentrations to the gas phase concentrations, i.e.,

$$\frac{\Sigma [I] \text{ aqueous}}{\Sigma [I] \text{ vapor}} = \frac{[I^-]_a + [IO_3^-]_a + [HOI]_a + [I_2]_a + [CH_3I]_a}{[HOI]_v + [I_2]_v + [CH_3I]_v} \quad (5.7)$$

Thus, the iodine partition coefficient for the aqueous system in an LWR accident is determined primarily by the iodine oxidation states in the water, i.e., the aqueous iodine chemistry.

A theoretical analysis of iodine partition coefficients was done by Eggleton<sup>5.34</sup> with consideration of all known reactions in water including oxidation and reduction. He concluded that partition coefficients for molecular iodine species without consideration of iodide, iodate or other species in water at 25 and 100°C are 83 and 9.1, respectively. He indicated that the partition coefficient for HOI at 25°C would be several thousand but Kabat<sup>5.40,5.41</sup> later indicated that a more conservative value of a few hundred is better for the HOI partition coefficient. Partition coefficients for CH<sub>3</sub>I generally are not included when considering iodine partition coefficients, but they appear to be in the range of 1 to 10.

We have considered equilibrium aqueous systems where the I<sub>2</sub>-H<sub>2</sub>O reactions have produced HOI, I<sup>-</sup> and IO<sub>3</sub><sup>-</sup>. We then calculated total iodine partition coefficients for solutions at 25 and 100°C with total iodine concentrations from 10<sup>-9</sup> to 10<sup>-4</sup> M and pH values of 5 to 10. To simplify the calculations and to be conservative, the partition coefficient for HOI was assumed to be only 2 times that for I<sub>2</sub>. (The real coefficient for HOI could be >10 times that for I<sub>2</sub>.) Trends in the total iodine partition coefficients are shown in Fig. (5.4). These data indicate that an aqueous iodine solution at 25°C with pH of 7 and total iodine of 10<sup>-6</sup> M would be in equilibrium with gaseous iodine concentration of ~10<sup>-12</sup> M. Similar data at 100°C are shown also in Fig. (5.4). At 100°C the gaseous iodine concentration corresponding to the above solution would be only ~2 x 10<sup>-12</sup>, i.e., the increasing temperature does not greatly increase the total iodine partition coefficient. This is because greater fractions of the total iodine at 100°C exists as the nonvolatile ionic species. Total iodine partition coefficients given in figures 5.4 and 5.5 are generally lower than those given by Eggleton, because the data herein consider that the HOI species is one-half as volatile as the I<sub>2</sub> species.

Partition coefficients were also calculated for a hypothetical static iodine solution where only the first hydrolysis reaction (5.3) was considered. These hypothetical values are shown in Fig. (5.5) and should represent the highest possible iodine partition coefficients for aqueous iodine systems.

Most aqueous systems in reactor accidents will be in contact with a gaseous volume that contains low levels of methyl iodide. That methyl iodide concentration will approach a steady state level as the generation and loss rates equalize. Therefore, the effect of the gaseous methyl iodide concentration on the total partition coefficient will be the direct addition of that concentration to the corresponding gas phase concentrations of I<sub>2</sub> and HOI. A steady state gas phase of methyl iodide at 10<sup>-11</sup> M, about that at TMI, above an aqueous system of 10<sup>-6</sup> M iodine at 25°C with a pH of 8 will decrease the partition coefficient from 1.8 x 10<sup>7</sup>, Fig. 5.2, to about 10<sup>5</sup>.

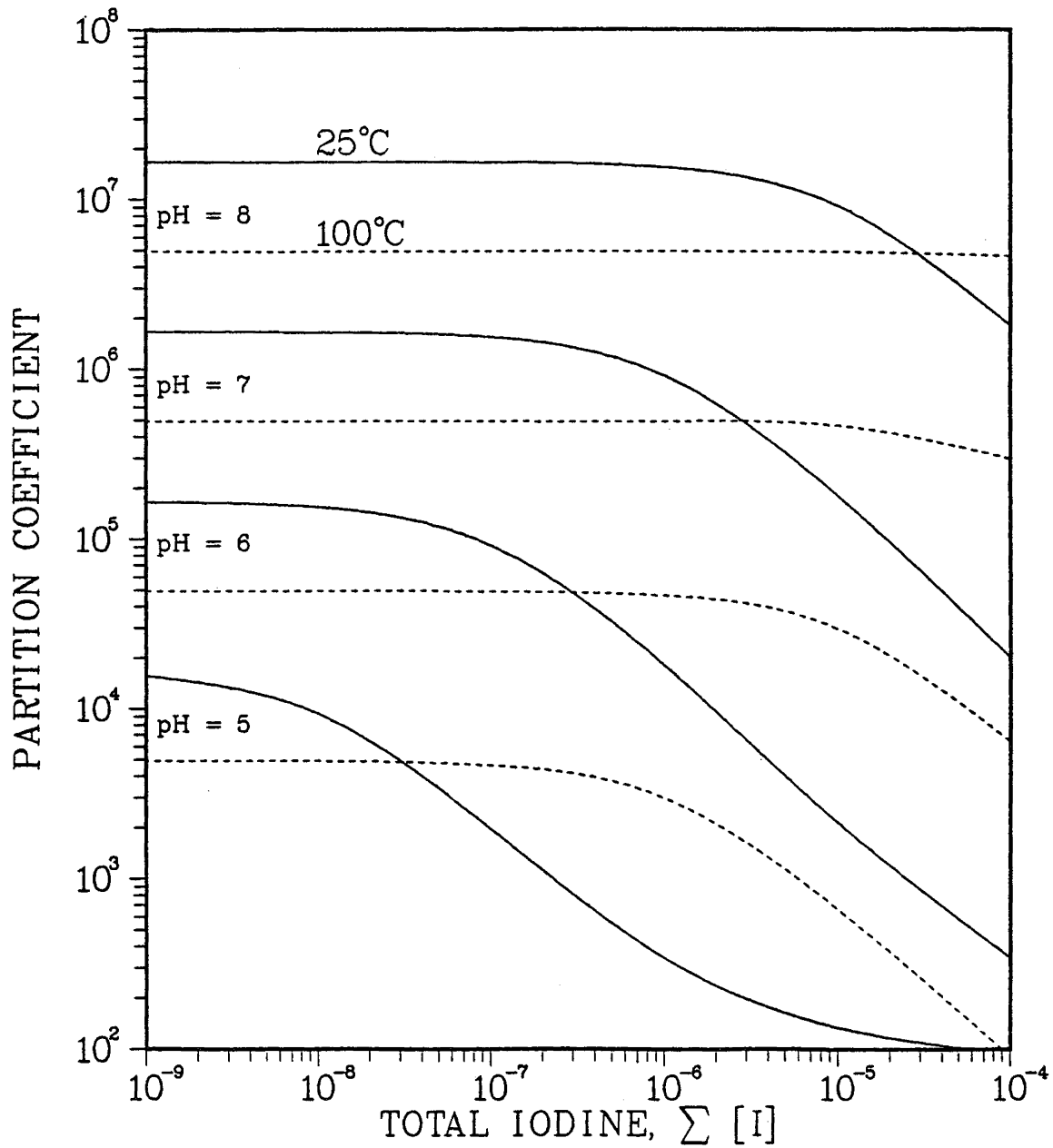


Figure 5.4: Partition Coefficients for Aqueous Iodine Systems at Equilibrium. A molecular iodine,  $I_2$ , source reacts with water:  $3I_2 + 3H_2O + IO_3^- + 5I^- + 6H^+$ .

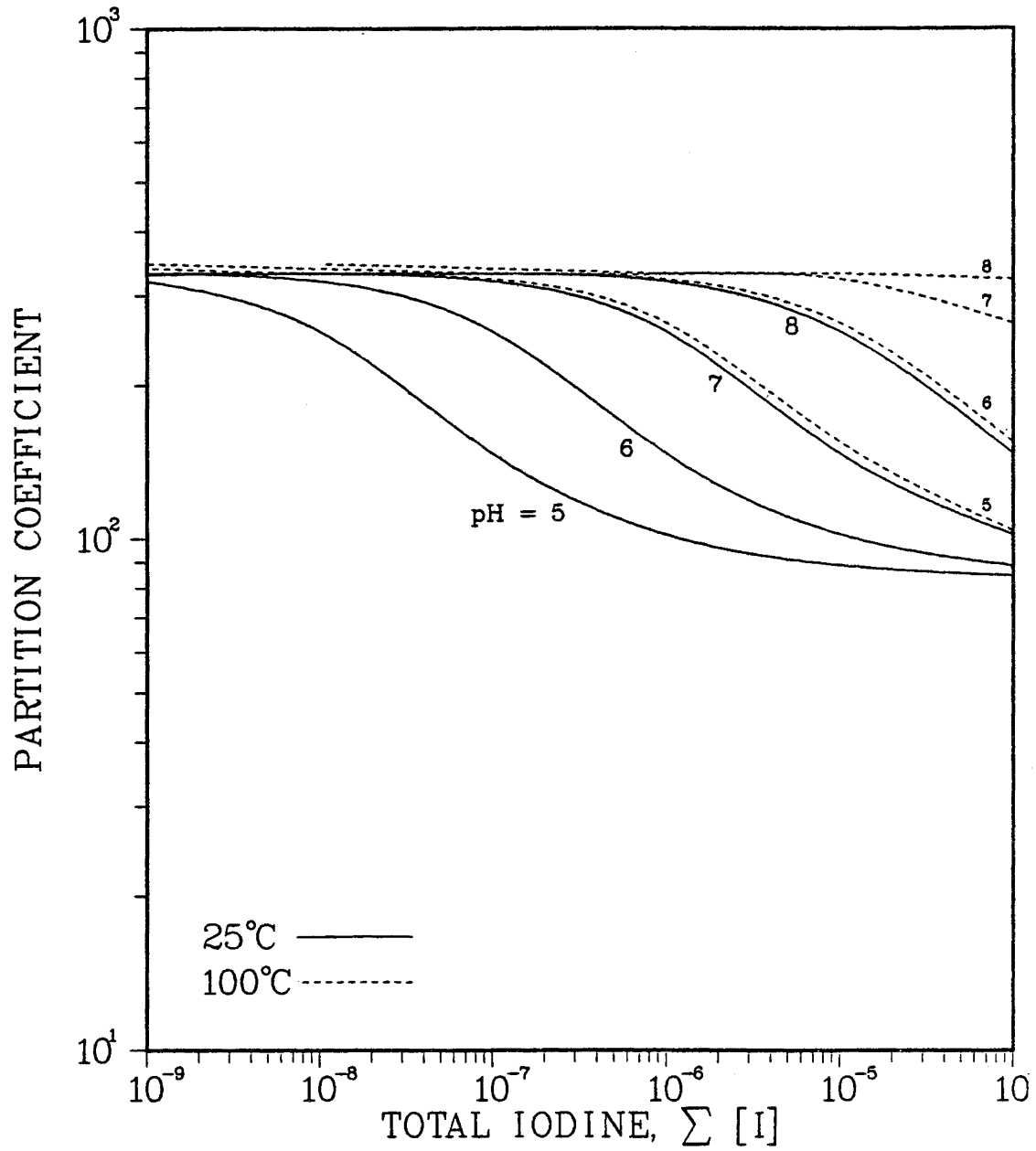


Figure 5.5: Partition coefficients for aqueous iodine systems before iodate formation begins. A molecular iodine,  $I_2$ , source reacts with water:  $I_2 + H_2O = HOI + I^- + H^+$ .

The calculated partition coefficients in this paper have assumed an initial iodine source of molecular iodine,  $I_2$ , dissolved in water and reacted with water to produce the equilibrium concentrations of iodine species. It should be obvious that solutions where the only iodine species is iodide,  $I^-$ , will have essentially infinite partition coefficients.

#### 5.3.9 A Less Conservative Assessment of Organic Iodide Formation (WASH-1233)

Gas phase formation of organic iodide could occur in the volume above an aqueous system and therefore the following discussion is included in this chapter. In their review of organic iodide formation Postma and Zavadoski<sup>5.37</sup> (WASH-1233) summarized the literature at the time and drew conclusions about the extent of conversion of  $I_2$  to organic iodide following a nuclear accident. The study was directed toward licensing, and a very conservative approach was taken, leading to upper bounds estimates. In Appendix C.9, summarized here, their report is reevaluated in a manner intended to be more realistic and less conservative.

Any estimate of organic iodide formation is highly tentative because the basic chemical mechanisms leading to organic iodides are not defined and the significant independent variables are not even known. Unfortunately, nearly all experimental data have been acquired for conditions far removed from those expected following an accident, and the uncertainty about how to extrapolate or interpolate the data casts serious doubt on any such estimate. The model chosen for extrapolation is of much more significance than is the data itself.

Organic iodide formation was divided into two parts, one that is observed in the absence of radiation and the other resulting from radiation effects. The first was estimated using a statistical treatment of a number of experiments in various containment vessel models at Oak Ridge, Idaho, Battelle Northwest, and in the UK. In WASH-1233 the upper bounds line for all this data was used, giving a clearly unrealistic estimate of organic iodide of "less than 1%" at the anticipated iodine concentration of  $100 \text{ mg/m}^3$ . The "realistic" estimate derived here was made by moving a line of the same slope down to represent the experimental data for the larger experimental vessels, and the conversion to organic iodide is 0.02%, some 50-fold smaller.

The second part, that from radiation was estimated in WASH-1233 by interpolation between two sets of data, one in methane-iodine-water mixtures and the other in mixtures also containing air or oxygen, with iodine concentration as the independent variable, and applying the resulting G value to the expected accident conditions. The conversion to organic iodide was "no more than 2.2%." The estimates made here are based on extrapolation of data in methane-iodine-water-air or oxygen mixtures with the  $O_2/I_2$  ratio being the independent variable, and of data in methane-iodine mixtures with  $CH_4/I_2$  being the independent variable. The former would be appropriate for a reaction of methyl free radicals with either  $O_2$  or  $I_2$ , the two in competition. The resulting values are less than 0.01% under projected postaccident conditions. A maximum equilibrium concentration can also be estimated from the suggested G values for formation and decomposition,  $<0.004$  vs. 20, giving  $<0.02\%$ . A very approximate estimate of 0.01% is suggested.

Based on these considerations, the conversion of  $I_2$  to organic iodide is estimated to be in the vicinity of 0.03% under conditions in the range of interest; this is a factor of about 100 lower than the conservative estimate in WASH-1233. In view of this low value, other mechanisms should also be examined. To the extent that the iodine source is iodide rather than  $I_2$ , even this small value should be further reduced. There is a clear need for experimental studies under conditions more appropriate to reactor accidents, and for basic work to identify the chemical mechanisms for formation of organic iodide. With the information available, it is not possible to derive a firm prediction of organic iodide formation and the large disparity between this assessment and the previous one indicates the extent of uncertainty.

References

- 5.1 Sallach, R. A., "Chemistry of Fission Products Elements in High Temperature Steam. I. Thermodynamic Calculations of Vapor Composition", SAND81-0534/1, Sandia National Laboratories, Albuquerque, NM (In preparation)
- 5.2 Barin, I., Knacke, O., "Thermodynamic Properties of Inorganic Substances", Springer-Verlag 1973
- 5.3 Mills, K. C., "Thermodynamic Data for Inorganic Sulphides, Selenides and Tellurides", London Butterworths 1974
- 5.4 D. R. Stull et al., JANAF Thermochemical Tables (The Dow Chemical Company, Midland, MI)
- 5.5 Private communication, T. B. Lindemer, Oak Ridge National Laboratory, Oak Ridge, Tenn. (Feb. 1981)
- 5.6 Feber, R. C. "Thermodynamic Data for Selected Gas Impurities in the Primary Coolant of High-Temperature Gas-Cooled Reactors", LA-NUREG-6635, Los Alamos Scientific Laboratory, Los Alamos, NM
- 5.7 Venugopalan, M. and Jones, R. A., "Chemistry of Dissociated Water Vapor and Related Systems", Interscience 1968
- 5.8 Gotzmann, O., Johnson, C. E. and Fee, D. C., "Attack of Stainless Steel by Liquid and Vaporized CsOH", J. of Nucl. Matl. 74, 68-75 (1978)
- 5.9 Gerlach, T. M., "Evaluation of volcanic gas analyses from Kilauea Volcano", J. Volcanology and Geothermal Research, v. 7, 295-317, 1980; Randich, E. and Gerlach, T. M., "The calculation and use of CVD phase diagrams with applications to the Ti-B-Cl-H system 1200 K-800 K", J. of Thin Solid Films, (in press)
- 5.10 White, W. B., Johnson, S. M., and Dantzig, G. B., "Chemical equilibrium in complex mixtures", J. of Chem. Physics, v. 28, 751-755, 1958
- 5.11 Van Zeggeren, F. and Storey, S. H., "The computation of chemical equilibria", Cambridge Univ. Press (1970)
- 5.12 Malinauskas, A. P., Gooch Jr., H. H. and Redman, J. D., "The Interaction of Tellurium Dioxide and Water Vapor", Nucl. Appl. and Tech., 8 p. 52 (1970)

References

- 5.13. F. A. Cotton and G. Wilkinson, Advanced Inorganic Chemistry, Interscience Publishers, New York (1966).
- 5.14. W. M. Latimer, The Oxidation States of the Elements and their Potentials in Aqueous Solutions, Prentice-Hall, Inc., New York, (1953).
- 5.15. R. C. Weast, editor, Handbook of Chemistry and Physics, 57th ed., CRC Press (1976-1977).
- 5.16. M. Pouboix, Atlas of Electrochemical Equilibria in Aqueous Solutions, Pergamon Press, Cebelcor, Brussels.
- 5.17. D. J. Turner, "Water Chemistry of Nuclear Reactor Systems," BNes, London (1978).
- 5.18. W. Eguchi, M. Adachi, and M. Yoneda, J. Chem. Eng. Jap. 6 389 (1973).
- 5.19. W. C. Broy and E. L. Connally, J. Am. Chem. Soc., 33, 1485 (1911).
- 5.20. G. Hariguchi and H. Hagiwara, Bull. Inst. Phys. Chem. Research (Japan), 22, 661 (1943).
- 5.21. T. L. Allen and R. M. Keefer, J. Am. Chem. Soc., 77, 2957 (1955).
- 5.22. D. Haimovich and A. Treinin, Nature, 207, 185 (1965).
- 5.23. D. Haimovich and A. Treinin, J. Phys. Chem., 71, 1967).
- 5.24. D. Amichai and A. Treinin, J. Phys. Chem., 74, 830 (1970).
- 5.25. M. Anbar and I. Dostrovsky, J. Chem. Soc., 1105 (1954).
- 5.26. J. F. Osilvie, Can. J. Spectrosc., 19(6), 171 (1974).
- 5.27. L. M. Toth, J. T. Bell, S. R. Buxton, H. A. Friedman, D. W. Fuller, and M. R. Billings, "Chemistry of the KALC Process," ORNL/TM-5656, Oak Ridge National Laboratory (1976).
- 5.28. V. Sammet, Zeit. Phys. Chem., 53, 641 (1965).
- 5.29. W. O. Lundberg, C. S. Vestling, and J. E. Ahlberg, J. Am. Chem. Soc., 59, 264 (1937).
- 5.30. I. M. Kalthoff, and V. A. Stenger, "Volumetric Analysis," Vol. II, 2nd ed., Interscience, New York (1947).
- 5.31. M. Eigen and K. Kurtin, J. Am. Chem. Soc., 84, 1355 (1962).
- 5.32. Y. Miyake, W. Eguchi, and M. Adachi, J. Nucl. Sci. Technol., 16, 371 (1979).
- 5.33. E. Abel and K. Hilferding, Zeit. fur Physical Chemie., 136, 186 (1928).
- 5.34. A. E. J. Eggleton, A Theoretical Examination of Iodine-Water Partition Coefficients, AERE-R-4887 (1967).
- 5.35. R. H. Barnes, J. F. Kircher, and C. W. Townley, Chemical Equilibrium Studies of Organic-Iodide Formation Under Nuclear-Reactor-Accident Conditions, BMI-1781, Battelle-Columbus, Columbus, Ohio (1966).
- 5.36. R. H. Barney, J. L. McFarling, J. F. Kircher, and C. W. Townley, Analytical Studies of Methyl Iodide Formation Under Nuclear-Reactor-Accident Conditions, BMI-1816, Battelle-Columbus, Columbus, Ohio (1967).
- 5.37. A. K. Postma and R. W. Zavadoski, Review of Organic Iodide Formation Under Accident Conditions in Water-Cooled Reactors, WASH-1233 (1972).
- 5.38. E. A. Moelwyn-Hughes, Royal Soc. London Proc. Ser. A, 164, 295 (1938).

- 5.39. D. N. Glew and E. A. Moelwyn-Hughes, Discussions Faraday Soc., 15, 150 (1953).
- 5.40. M. Adachi, W. Eguchi, and T. Haoka, J. Chem. Eng. of Japan, 7, 364 (1974).
- 5.41. F. H. Sweeton, R. E. Mesmer, and C. F. Baes, Jr., J. Solution Chemistry 3, 191 (1974).
- 5.42. I. G. Draganic and Z. D. Draganic, The Radiation Chemistry of Water, Academic Press, New York-London (1971).
- 5.43. R. M. Sellers, A Review of the Radiation Chemistry of Iodine Compounds in Aqueous Solution, Central Electricity Generating Board, London EC4P-4EB, GB7704552 (1977).
- 5.44. C. C. Lin, J. Inorg. Nucl. Chem., 42, 1101 (1980).
- 5.45. C. C. Lin, J. Inorg. Nucl. Chem., 42, 1093 (1980).
- 5.46. G. Czapski, J. Jortner, and G. Stein, J. Phys. Chem., 63, 1769 (1959).
- 5.47. L. P. Shubnyakova, V. T. Kharlamov, and A. K. Pikaev, Translation UDC541.15, Khimiya Vysakikh Energii, 10, 49 (1976).
- 5.48. R. P. Bell and E. Gelles, J. Chem. Soc. (London), 1951, 2734 (1951).
- 5.49. L. C. Watson, A. R. Bancroft, and C. W. Hoelke, Iodine Containment by Dousing in NPD-II, CRCE-979 (1960).
- 5.50. M. J. Kabat, "Testing and Evaluation of Absorbers for Gaseous Penetrative Forms of Iodine," Proc. 13th AEC Air Cleaning Conf., 765 (1974).
- 5.51. M. J. Kabat, "Chemical Behavior of Radioiodine under Loss of Coolant Accident Conditions," Proc. 16th DOE Nuclear Air Cleaning Conf. (1980).
- 5.52. T. I. Shaw and L. H. N. Cooper, Nature, 180, 250 (1957).
- 5.53. K. Sugawara and K. Terada, Nature, 182, 250 (1958).
- 5.54. J. K. Johannesson, Nature, 182, 251 (1958).
- 5.55. Y. Miyake and S. Tsunogai, J. Geophysical Research, 68, 3989 (1963).
- 5.56. R. A. Barkley and T. G. Thompson, Deep Sea Research, 7, 24 (1960).
- 5.57. S. Tsunogai and T. Sase, Deep Sea Research, 16, 489 (1969).
- 5.58. S. Tsunogai, Deep Sea Research, 18, 913 (1971).
- 5.59. V. W. Truesdale, Deep Sea Research, 21, 761 (1974).
- 5.60. G. T. F. Wong and P. G. Brewer, Geochemica et Cosmochemica Acta, 41, 151 (1977).
- 5.61. C. H. Li and C. F. White, J. Am. Chem. Soc., 65, 335 (1943).
- 5.62. T. R. Thomas, D. T. Pence, and R. A. Hasty, J. Inorg. Nucl. Chem., 42, 183 (1980).

## 6. FISSION PRODUCT TRANSPORT IN PRIMARY SYSTEM TO CONTAINMENT

The pathway for transport of fission products and other materials from the fuel to the containment building consists of various portions of the primary system prior to meltthrough of the reactor pressure vessel. As they move along this pathway, fission products may be deposited to an extent dependent on the accident sequence and the thermal-hydraulic conditions along the flow path. In order to assess the importance of this deposition and to evaluate the extent to which it is affected by fission product chemical and physical form, transport calculations have been made for various assumed accident sequences and various assumed source terms.

### 6.1 The TRAP-MELT Code

It is possible to make some general statements regarding retention of radionuclides in the primary system under various hypothetical accident sequences, but quantitative estimates can only be made through the use of numerical simulation.

The TRAP-MELT code (6.1) is a dynamic numerical model which calculates radionuclide transport through, and retention in LWR primary systems under accident conditions leading to core melt. Essentially, the code considers a system of an appropriate number of control volumes that are connected by fluid flow in a way determined by the accident sequence. In each of the control volumes radionuclide species can exist in either particulate or gaseous form. These species are assumed to be well mixed within each volume and to transport with the hydrodynamic flow between control volumes. Mass transfer coefficients describe the rates of transport of each species between the physical forms and to surfaces within the volumes.

TRAP-MELT presently considers the following physico-chemical processes:

- arbitrary source terms for radionuclide species within the system
- condensation and evaporation of nuclide vapors
- particle deposition by diffusion from laminar and turbulent flow regimes
- vapor mass transfer to surfaces by sorption processes
- inertial deposition of large particles from turbulent flow
- thermophoresis of particles, assumed to be in thermal equilibrium with the surrounding gas

It should be clear that a great deal of information is required for the model to be able to mechanistically predict the rates of the above processes. One must, first of all, know the core's fission product inventory at the time of release. This can be calculated with the aid of the ORIGEN code (6.2) as was noted in Chapter 2. Then, given the core temperatures and coolant water levels for the hypothesized accident, one must estimate the rates of release of the various fission products from the core and the duration of the release. The thermal-hydraulic conditions in the primary

system, which will be responsible for transport of the released material through the primary system, must be determined. This can be accomplished with the aid of one of the versions of RELAP or TRAC up to the point of severe fuel damage. There are currently no computer codes available that predict the distribution of fluid and surface temperatures within the reactor coolant system during core melting. In this study results of MARCH code (6.3) analyses were extended with the use of hand calculations to estimate these conditions. The source rates of the various fission products, their relevant chemical and physical properties, and the thermal-hydraulic conditions calculated above can then be used in the TRAP-MELT code to predict the retention of the various species in different parts of the primary system. This code predicts a release rate from the primary system which, in turn, serves as input to codes such as CORRAL, NAUA, HAARM-3 and QUICK which predict the removal of fission products from the containment atmosphere. Figure 6-1 illustrates the relationships of the various codes used in estimating radionuclide release to the environment under accident conditions.

## 6.2 Uncertainties Associated with TRAP-MELT Predictions

The TRAP-MELT code requires extensive input data in the form of thermal hydraulic data for the accident under consideration. These include steam mass flow rates, steam and surface temperatures, steam qualities, pressures, etc., as functions of time. A simulation code which is capable of predicting the thermal-hydraulic data throughout the reactor coolant system in a melt-down accident to support TRAP-MELT analyses does not currently exist. It also requires input data on initial conditions, in the form of mass by species and location in the primary system, and source data for both fission products and the structural materials which will comprise the majority of the aerosol mass.

A frequently underemphasized fact regarding the predictions obtained from the TRAP and other codes is that any errors in the specification of the source rates in an accident sequence will propagate through the model in a complex manner. In Chapter 4, data from fission product release experiments were used with predictions of the transient temperature history of the fuel to estimate the release of radioactive and structural materials as a function of time for two core meltdown sequences. This is a significant improvement over the state-of-the-art at the time of the Reactor Safety Study in which it was concluded that "thermal analyses of core meltdown provide only generalized data on core temperature profiles, geometry changes, and melt behavior versus time. This, combined with uncertainties which exist in fission product properties at very high temperatures, argues against construction of a highly mechanistic model to calculate fission product release during the melt-down phase. Therefore, in this work [WASH-1400], fission product release is treated as being simply proportional to the fraction of the core melted." (6.4) Although it is now possible to undertake a more detailed modeling of the transient behavior of the release of materials from over-heated fuel, significant uncertainties exist in the data describing release rate coefficients as a function of temperature, the chemical and physical forms of the released material, and in the modeling of the time-temperature history of the fuel. In the TRAP analyses in this chapter, the fission product and aerosol releases are treated as being proportional to time since core melt initiation for the sequences involving a melt. Comparison of this linear input of fission products and structural materials with the

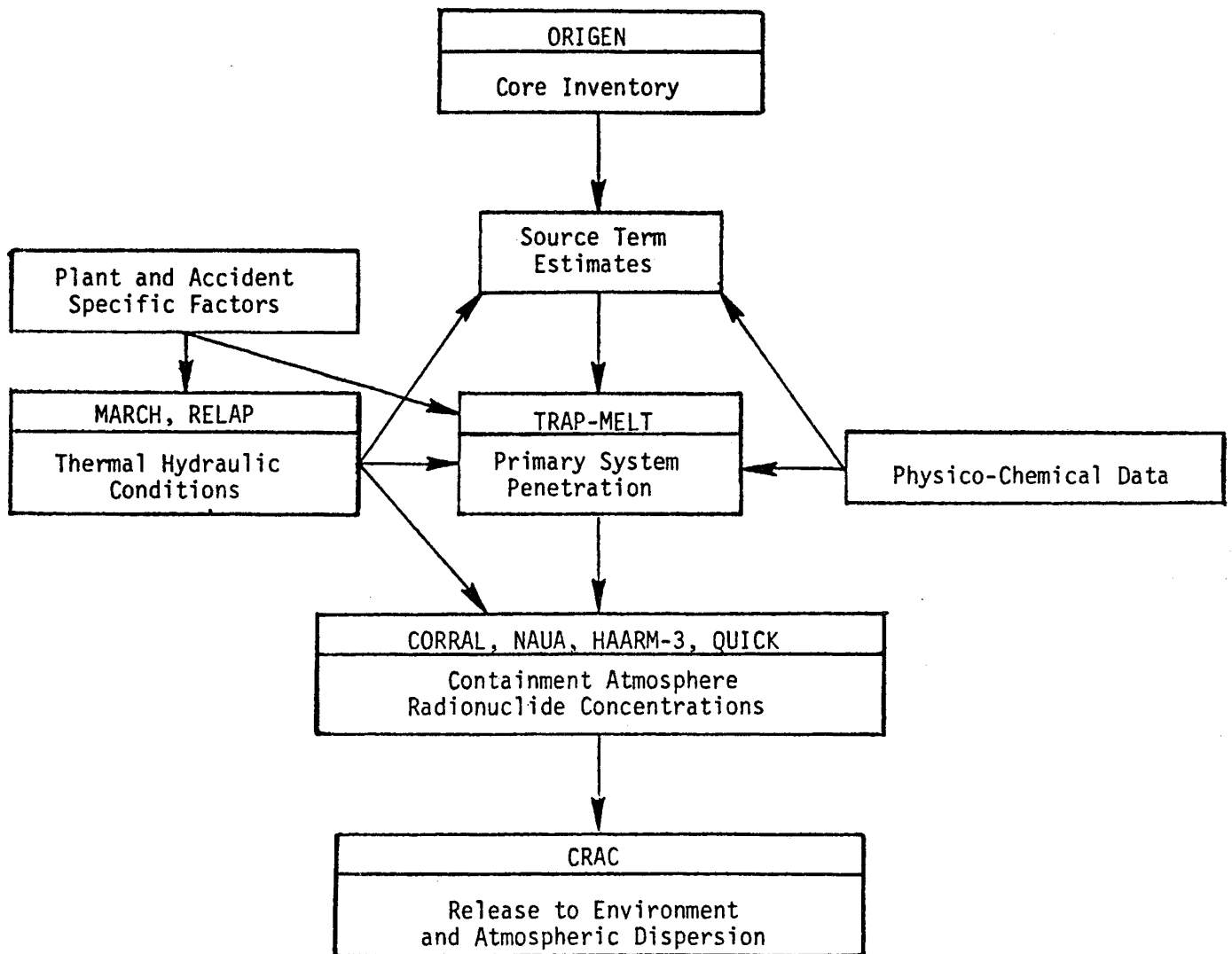


FIGURE 6-1. FLOW DIAGRAM OF RELATIONSHIPS AMONG RISK ASSESMENT CODES

rates presented in Chapter 4 indicates that there is not a large discrepancy between the two sets of source terms. This is especially true since the source term in the TRAP analyses considers only that portion of the accident from initiation of core melt to failure of the pressure vessel for the severe core damage sequences. A potential difficulty with the source term used in the TRAP runs is that if the various vapors and particulate matter are released at different times during the melt, the opportunity for interaction will be greatly reduced from that which pertains to the case where the species are released simultaneously. It should be kept in mind, though, that the core does not heat up uniformly as the melt progresses. Because of the temperature differences which exist between points within the core, the release rate for each fission product will have a range of values throughout the core at any given time. The net effect of this is that materials are co-emitted from the core, in spite of the fact that they are emitted at different temperatures.

The aerosol source term employed in the TRAP code does not include a mechanistic model of homogeneous nucleation and subsequent condensation on the aerosol particles. The number of low vapor pressure species which will nucleate, the concentration gradients which one would find near the sources of these species, and the extremely complicated temperature and flow fields which would exist near a melting core make construction of such a model impractical. What is done, instead, is to permit the user to specify the mass source rate of "aerosol" and its distribution parameters. This aerosol mass includes those species which have vapor pressures so low that they cannot exist in the vapor state except at extremely high temperatures. This group includes the fuel rod cladding, structural material, the fuel itself, and various fission products which comprise only a small portion of the aerosol mass. The use of a user specified initial particle size distribution is a source of uncertainty in the model predictions, but the aerosol's behavior is not sharply dependent on the initially assumed parameters, provided that they are selected within reasonable bounds. A potentially important source of uncertainty in the model is that certain species may remain in vapor form for some portion of their transit through the primary system under certain conditions. If this should occur, it will change the aerosol mass source rate and may significantly alter the aerosol dynamics in the primary system. But at the present time there is not available sufficiently detailed thermal hydraulic information for the core region to evaluate this possibility.

The source rates of the aerosol particles may be an important determinant of radionuclide penetration of the primary system. If the iodine is released in the elemental form it is not expected to interact significantly with the particles. But if released as CsI, it is possible for the iodine to condense on the particles under appropriate temperature conditions due to the much lower vapor pressure of CsI. Further, vapor forms of iodine will transport readily in the gas phase to surfaces (liquid or solid) where their uptake is dependent on solubilities and adsorption. In contrast, particulate forms of iodine will not diffuse nearly as fast in the gas phase but would be expected to dissolve readily at water surfaces or attach to solid surfaces. The depletion of iodine, then will be dependent on chemical form and the depletion rate will be controlled by different physical mechanisms for different iodine forms.

In any attempt to analyze a "real-world" type of problem simplifications are required in order to reduce the system under consideration to manageable proportions, while still retaining the essential features of the problem intact. A number of assumptions are made in order to be able to analyze the primary system of a damaged reactor using the TRAP-MELT code. The major assumptions relevant to the analyses presented in this chapter are the following:

## 6.5

- The source term used assumes a constant mass input rate for each species, all species are co-emitted from the core, particles nucleate very near the core and nowhere else in the system, the particles are of homogeneous composition, and the initial aerosol has a user supplied size distribution.

- No removal mechanisms are operative in the core region.

- Aerosol coagulation is not considered in these analyses (this is discussed further in Section 6.3.2.2.1).

- Fission product retention in the primary system is neglected after the core leaves the pressure vessel.

- Iodine is present as either CsI or I<sub>2</sub> and does not change chemical species in the vapor state.

- The primary system above the core is dry for all core meltdown sequences.

- Chemical reactions are not considered.

- Radioactive decay of fission products is not considered. Clearly, there can be situations in the primary system which contradict some of the above assumptions, and in these cases the results of TRAP analyses must be reviewed carefully to assess the impact of the violated assumptions. Nevertheless, the TRAP-MELT analyses presented below represent the current state of the art in assessing fission product transport in the reactor primary system.

### 6.3 TRAP-MELT Accident Analyses

Under normal operating conditions the physical barriers to fission product release are comprised of the fuel matrix, the cladding, the reactor primary coolant system, and the reactor containment. All of the accidents considered in this document have one essential feature in common, namely the overheating of the core sufficient to result in rupture of the cladding of at least some of the fuel rods. The time period considered in the TRAP analyses for sequences involving minor or no fuel damage begins with the cladding rupture and ends with recovery of the core.

For an accident sequence which results in extensive melting of the core, the time frame of interest begins with melt initiation and ends with failure of the reactor pressure vessel due to meltthrough. One can reasonably assume that there will be no fission product retention in the primary system after the core itself has left the pressure vessel. It is also assumed in the results presented below, that any radionuclides suspended in the gaseous phase at the time of pressure vessel failure will be swept into the containment with insignificant attenuation.

#### 6.3.1 Sequences Involving Minor or No Fuel Damage

Condition I through IV events as defined in Chapter 3 involve minor or no fuel damage. For all but Condition IV, the fuel would not be damaged and the source of radioactive materials available for release from the reactor coolant system would be the inventory of radioactive nuclides in the coolant water. This inventory can be increased somewhat during a transient event through a phenomenon called spiking in which leaking fuel pins release additional radioactive materials to the coolant. In Condition IV events, particularly in

## 6.6

pipe break accidents resulting in loss of coolant, the core can become uncovered and some damage can occur to the fuel before the ECC system recovers it and restores cooling. This type of event has been selected for examination here to illustrate the effects of having water interactions with the iodine forms prior to their release into the containment. The specific accident examined is a large pipe break in the cold-leg of a PWR.

During the period the core is uncovered and heating up, temperatures should not exceed approximately 2200°F. The cladding would be expected to rupture, however, in the range 1400-2000°F so that fission products which exist in vapor form at these temperatures would be released into the primary system. The source rate used in the TRAP analyses of this accident is given in Appendix D. This is the only accident to be considered in this chapter which does not lead to severe core damage.

The flow paths to the containment for the fission products and relevant system temperatures in this accident are also illustrated in Appendix D. Several input parameters were varied in the simulation of the accident to assess the importance of various uncertainties to which the TRAP results are subject. Among these parameters were the steam flow rate and the temperatures of primary system surfaces, which were calculated by the RELAP-WREM code.

Under the baseline conditions shown in Figure D.1 in the Appendix, the TRAP code predicts that 53 percent of the elemental iodine released from the core would escape the primary system and enter the containment. It must be pointed out that the plant geometry and accident specifications assumed for the simulation allow 25 percent of the flow through the primary system to escape the system without encountering any of the ECC water. This flow contains nearly half of the total iodine which reaches the containment. The predicted effect of an increase in the steam flow rate over that used in the base case simulation is shown in Figure 6.2. At this higher flow rate, the residence time of the iodine in the primary system is shortened and, as a result, the opportunity for iodine removal by the ECC system is reduced. Conversely, lower flow rates would permit more time for mass transfer to occur, and smaller fractions of the iodine would be released to the containment atmosphere.

While only a fraction of the elemental iodine released from the core was predicted to be deposited on the surfaces in the system, it is instructive to examine what effect a change in surface temperatures would cause in the TRAP calculations. A decrease in temperature to 350°F from the 500°F used in the base case simulation would permit retention of approximately five times as much elemental iodine. This still represents only  $10^{-3}$  of the amount released from the core, however. The uncertainties in residence times (flow rates) and system temperatures will be seen to impact on predictions of retention for all types of accident sequences analyzed in this chapter.

The fraction of the iodine released from the fuel which was calculated to escape the reactor coolant system ranged from 53 percent for the baseline case, to 67 percent for the steam flow rate increased by 1.5, to 82 percent for the case where the radius of the ECC spray droplets assumed to form at the point of ECC water injection was doubled (this inhibits vapor transfer to the water).

In order to examine the potential for retention in the primary system of iodine released in the form of CsI, two extreme cases were examined. In the first case, it was assumed that the CsI would be released from the core

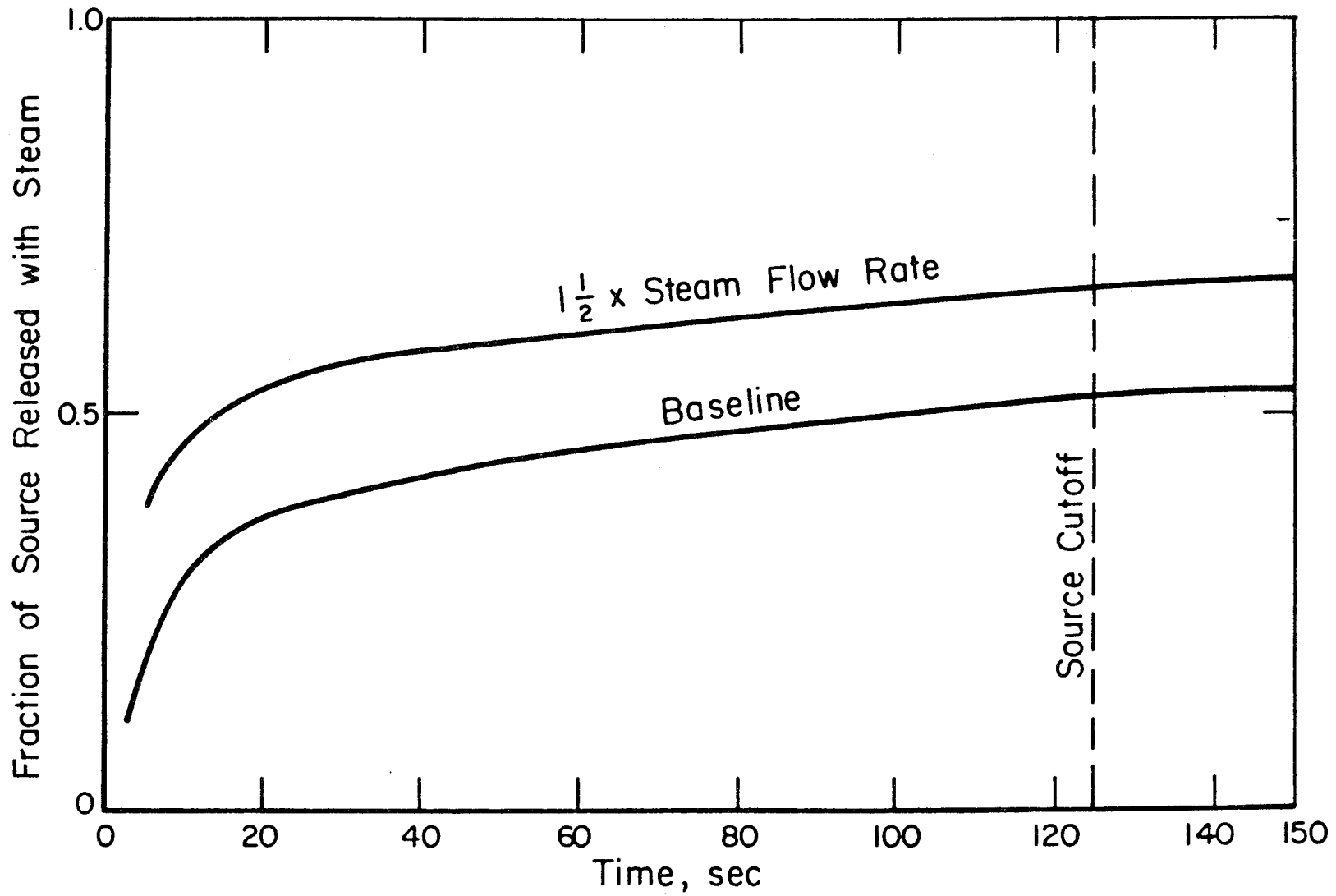


FIGURE 6-2. INFLUENCE OF STEAM FLOW RATE ON IODINE ESCAPE FROM PRIMARY SYSTEM IN A TERMINATED LOCA IN A PWR

in the absence of a simultaneous source of particles. The TRAP analyses show that the system temperatures permit nearly complete condensation of CsI on the internal surfaces of the primary system. The fractions of the CsI retained varied from 99.2 percent for the baseline case to 98.9 percent for the case with the increased steam flow rate. Vapor deposition is clearly the mechanism of prime importance for CsI retention under the above type of accident scenario.

Based upon experiments at ORNL, however, it appears that as much as 0.02% of the fuel could be ejected from the rods as they rupture (6.5). The released material would be in the form of particles ranging in diameter from ten to hundreds of micrometers. The second case examined considers the suspended particulate surface available for CsI condensation.

One might expect that the lower gas phase temperatures relative to the surface temperatures in this scenario could lead to condensation of CsI on the particles and less retention in the primary system. The particles considered here are much larger than those considered elsewhere in this chapter since they come from a much different source. The large size of these particles would cause them to have a settling velocity on the order of a few centimeters per second, which would lead to their partial removal from the gas stream. A potentially more important effect of their large size is that their increased inertia, relative to submicron particles, would allow droplets formed from the ECC water to remove them from the gas stream with high efficiency. The flow pattern of the ECC fluid near the point of injection would have to be well characterized to accurately estimate its effectiveness in removing particles from the gas stream. But qualitative comparison of the relaxation time of these large particles with the characteristic time of the droplets' radial displacements leads one to conclude that the particles should be removed with high efficiency. Approximately 25 percent of the flow would be expected to go out the broken loop and escape to the containment without passing through a region of ECC injection.

Rather than attempt to model the scrubbing of particles by the ECC fluid this case was analyzed using TRAP to examine the CsI and particle behavior if the system were dry. From these results one can make judgements regarding the additional reduction in iodine emissions, which could be brought about by the ECC. In this dry case, even in the presence of the particles, approximately 95 percent of the iodine released as CsI deposits onto the surfaces of the steam generators where the surface temperatures are 500°F and the gas temperature is 450°F. Almost the entire remaining 5 percent is still in the vapor phase. Interestingly, the large particles are removed from the gas stream fairly well, even without the action of the ECC. The TRAP analysis indicates that 81 percent of the particulate mass released from the fuel pins is retained in the primary system, principally in the steam generators.

### 6.3.2 Severe Core Damage Sequences

For accident sequences in which failures of engineered safety features compound the initiating event, it is possible to have more severe core damage than for accidents that fall within the design basis envelope of the plant. These sequences can be subdivided into two categories: degraded core sequences, and sequences leading to a complete core melt.

### 6.3.2.1 Degraded Core Sequences

Accidents in which the ECC system partially operates or has delayed operation could result in extensive core damage without progressing to full core meltdown. Because the potential is not as great in the limited core damage accidents to produce conditions that would threaten the integrity of the containment building, the offsite consequences would in general be expected to be comparatively small. In some sequences, a dry pathway could exist from the core to the containment during the period of fission product release from the fuel. If, however, an accident sequence does not progress to full core meltdown, it is an implicit requirement that cooling water must have been available in the latter stages of the accident to arrest core damage. Thus, the amount of radioactive material released directly to the containment atmosphere would not be as great as in comparable full core meltdown accidents. In many cases, as for the TMI accident, the release from the fuel would have to pass through a water filled environment before reaching the containment.

#### 6.3.2.1.1 Stuck Open Relief Valve, Partial ECC Operation

The behavior of fission product transport in the reactor coolant system has been considered for two types of degraded core sequences. The first sequence is a TMI-like accident. The purpose of reviewing this sequence is not to represent what actually happened at TMI but rather to provide some insights into the behavior of a class of sequences of the TMI type. It is assumed for this example that the steam generators provide inadequate heat removal from the primary system during the early stages of the accident coincident with a stuck open primary system relief valve. The supply of makeup water is inadequate to balance the loss out of the valve. The water level decreases in the primary system uncovering the core and, as the core heats up, fission products are released from the fuel. If the pressurizer is full of water during the release period, as was the case for the TMI accident, the fission products will be dissolved in or be captured by the water before being released to the containment regardless of chemical form. For this reason, the release of fission products to the containment atmosphere would be small in this accident scenario.

#### 6.3.2.1.2 Large Pipe Break, Delayed ECC Injection (AD-1/2)

The other type of degraded core sequence considered here is a pipe break accident in a PWR with delayed operation of the ECC system. The electric powered ECC pumps are assumed to be inoperative for the first 16 minutes of the accident. The core begins to melt 5.5 minutes into the accident. The pumps are then assumed to operate, rapidly covering the core and arresting the amount of fuel melting at approximately 50 percent of the core. Prior to the ECC operation, primary system conditions would be essentially the same as for the first portion of accident sequence AD which is discussed below. For this reason, separate TRAP analyses were not performed for this degraded core sequence. If the iodine is released

in elemental form, over 99 percent will be released to the containment. As shown in Table 6.1, 18 percent of the CsI emitted from the core region will be deposited from the vapor to primary system surfaces, whereas only about 6 percent of the particulate mass is retained in the primary. But, after ECC injection is initiated any further release of radioactive nuclides would be into a water environment. The contaminated water would subsequently spill onto the containment floor. Most of the iodine deposited on the surfaces of the vessel and piping during the first phase of the accident would be dissolved in the cooling water following ECC operation and would also be carried to the floor of the containment building, where subsequent offgassing could occur.

### 6.3.2.2 Core Meltdown Sequences

During accident sequences which lead to a complete core melt much higher releases of the core fission product inventory are possible than for the sequences discussed above. Estimates of the rates and amounts of the various products released to the primary system under assumed accident conditions have been discussed in Chapter 4. Damage to the primary system is also a part of many accidents which result in a melt and this will reduce the effectiveness of the primary system as a barrier to fission product release to the containment. TRAP-MELT analyses have been performed for a number of such sequences for PWRs and BWRs for this report.

Since the main concern of this chapter is the release of iodine from the primary system, and since there is some uncertainty regarding the chemical forms in which the iodine will occur in the primary system, the TRAP analyses performed cover a range of possibilities. In one, all of the released iodine was taken to be in the form  $I_2$ , which interacts hardly at all with the dry surfaces of the primary system. In the other, the iodine was assumed to be in the form of CsI.

#### 6.3.2.2.1 Transient with Loss of Heat Removal (PWR)

There are several different conditions under which the TMLB' accident sequence has been analyzed using TRAP for this report. These are: the base case, a low particulate source case, a large size particulate source case, and a case using somewhat different estimates of the pertinent thermal hydraulic conditions. In addition to these cases the results of a recently completed sensitivity study of the TRAP code will be briefly summarized. The specific geometric parameters, source rates, and thermal hydraulic conditions employed in the simulations to be presented below are given in Appendix D. It should be pointed out here that due to uncertainties regarding the physical arrangement and the water levels in the pressurizer quench tank, no credit is taken in these TRAP analyses for the possible retention of  $I_2$  or CsI in this water.

Base Case (TMLB'-1). In the base case, and in all other TMLB' sequences simulated, the retention of  $I_2$  in the primary system was found to be less than 0.1 percent of the released mass. This species is predicted to remain in the vapor state throughout the accident duration.

The retention of CsI in the primary system is found to be higher and somewhat variable, depending upon the specific primary system conditions. For the base case conditions, Table 6.1 indicates the TRAP analysis shows 6.9 percent of the released CsI mass to be retained on the surfaces of the primary system, predominantly as adsorbed vapor. Almost the entire remainder of the CsI is predicted to be adsorbed on the suspended particle surfaces. This material is expected to be released to the containment atmosphere with little further attenuation.

Large Size Particle Source (TMBL'-2). There is some uncertainty regarding the size of the primary particles emitted from the core region (primary here connotes particles before vapor and steam condensation occurs on their surfaces). The particles' initial size would certainly be expected to increase due to the coagulation engendered by the high number concentrations at the point of release. For spherical particles, a factor of ten increase in particle radius requires a three order of magnitude reduction in particle number concentration. If coagulation is proceeding at a rate sufficient to bring about such concentration reductions, the largest portion of the change will occur very near the core region and can be approximated by changing the particle source characteristics.

Gravitational and turbulent coagulation can greatly enhance the rate of particle growth compared to purely Brownian coagulation. These mechanisms are relatively more important for larger particles, with gravitational agglomeration becoming equal in importance to Brownian for particles about  $0.5 \mu\text{m}$  in diameter. Gravitational agglomeration is much more important than turbulent for the conditions examined in this Chapter. This is true because low flow rate conditions give rise to higher aerosol concentrations, and the coagulation rate is proportioned to the square of the aerosol number concentration. These low flow rate conditions place the flow through the primary system well within the laminar regime. It should also be kept in mind that the intensity of turbulence required for turbulent agglomeration to become important is much higher than what is predicted to exist in the primary system with the possible exception of some highly localized transient conditions.

To assess the importance of gravitational and Brownian agglomeration within the primary system, analyses have been performed using the QUICK code, which is a mechanistic aerosol dynamics code and is described more fully in Chapter 7 of this report. The simulations performed using this code indicate the growth of the aerosol particles and their removal via settling as functions of time. Thus, if one considers an initial aerosol concentration and distribution similar to that emitted from the molten core, the QUICK code can predict the extent to which agglomeration and settling will have modified the distribution at any time as it transits the primary system. The parameters which are then required to predict the extent of retention in the primary system are the initial mass concentration and the residence time of the aerosol in the primary system.

These two parameters vary a great deal from one accident sequence to another, as well as within the course of a given sequence. Typical values of initial aerosol mass concentrations and residence times, calculated by the TRAP-MELT code are plotted in Figure 6-3. A constant input rate of aerosol mass was used for all accidents considered. It is apparent

TABLE 6.1. SUMMARY OF TRAP PREDICTIONS OF IODINE DISTRIBUTION AMONG THE FOUR STATES AT THE END OF THE ACCIDENTS CONSIDERED (SEE APPENDIX D FOR MORE DETAIL)

Case	t <sub>f</sub> (s)	I <sub>2</sub> Released to Containment <sup>(a)</sup> (%)	CsI Released to Containment		CsI Retained in Primary			
			Vapor <sup>(b)</sup> (%)	Suspended Particles <sup>(c)</sup> (%)	Deposited <sup>(d)</sup> Vapor		Deposited <sup>(e)</sup> Particles	
					(%)	Control Volumes	(%)	Control Volumes
TMLB'-1	1320	>99	0.4	92.6	6.2	2	0.7	2, 4
TMLB'-2	1320	>99	0.4	92.8	6.3	2	0.5	4, 2
TMLB'-3	1320	>99	4.3	86.1	9.3	2	0.3	4, 2
TMLB'-4	1320	>99	22.5	40.2	37.1	2	0.1	2, 4, 3
AD-1/2	600	>99	1.3	80.2	18.0	2	0.3	3, 4, 2
AD-1	900	>99	10.8	70.7	16.6	3, 2, 4	1.6	3, 4
AD-2	900	>99	11.5	53.7	33.9	3, 4, 2	0.6	3, 4
AD-3	900	>99	12.4	26.2	61.1	3, 4, 2	0.1	5, 3, 2
AD-4	600	>99	11.3	22.8	51.9	7, 4, 3	13.8	5, 7
AD*	800	>99	86.1	13.6	0	NA	0.1	2
TC	3025	95	8.6	44.6	45.9	2	0.7	3
AE	6050	>99	24.2	64.6	10.6	2	0.3	2, 3

(a) Percent of I<sub>2</sub> mass released from fuel which escapes to containment.

(b) Percent of CsI mass released from fuel remaining in vapor state.

(c) Percent of same deposited on surfaces of suspended particles.

(d) Percent of same deposited on primary system surfaces from vapor state.

(e) Percent of same deposited on system surfaces via particle deposition mechanisms.

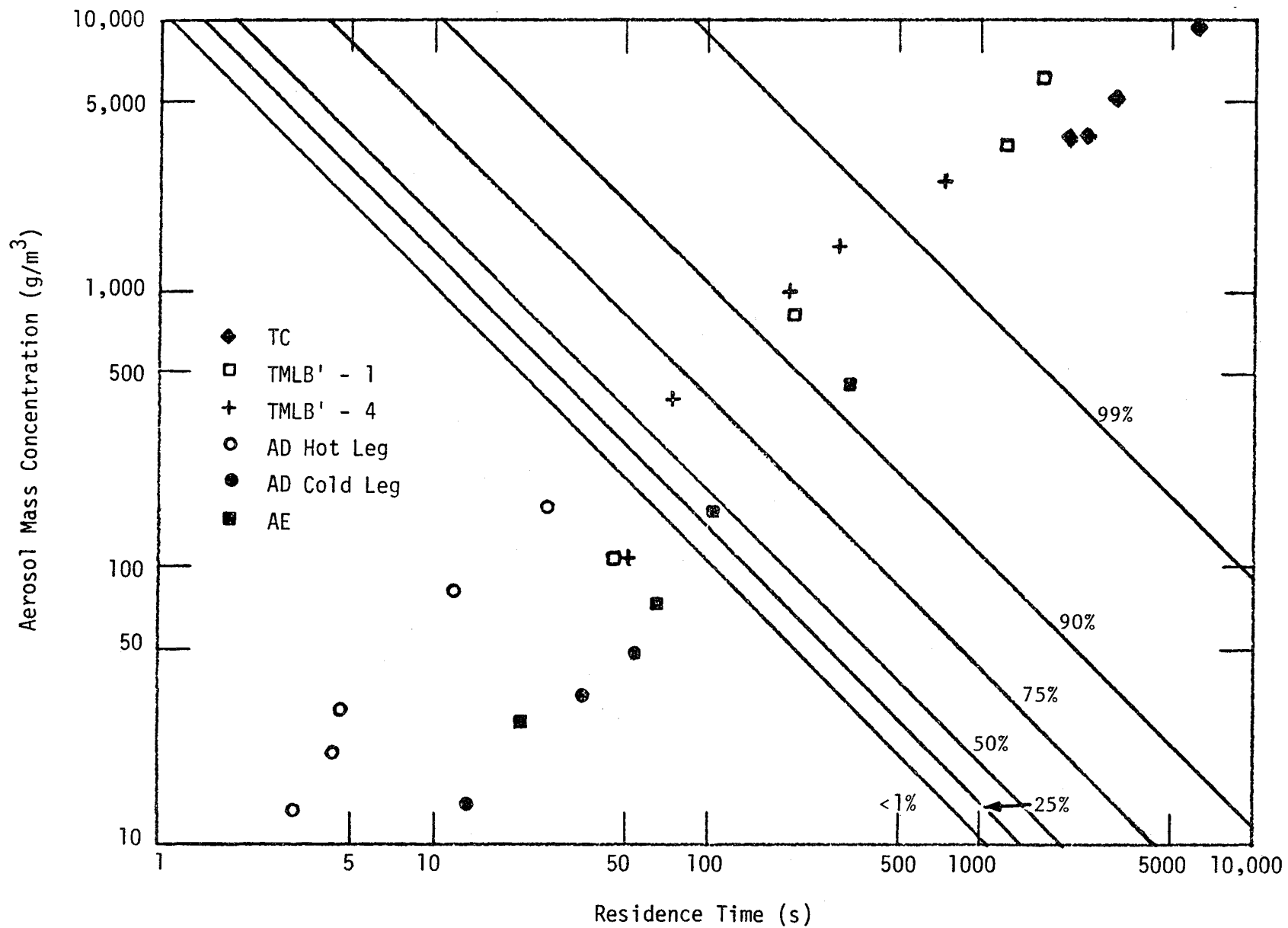


FIGURE 6-3. AEROSOL MASS CONCENTRATION REDUCTION PREDICTED BY 'QUICK' CODE FOR INITIAL MASS CONCENTRATIONS AND RESIDENCE TIMES (LINES). POINTS REPRESENT 'TRAP-MELT' CALCULATIONS FOR VARIOUS SEQUENCES.

that a wide range of conditions is pertinent to the sequences considered in this chapter, and our conclusions regarding aerosol behavior must reflect this fact.

QUICK analyses were performed using initial mass concentrations to cover the range observed in the TRAP-MELT simulations: 35 g/m<sup>3</sup>, 350 g/m<sup>3</sup>, and 3.5 kg/m<sup>3</sup>. The initial aerosol distribution employed had a  $\sigma_g$  of 2.0 and a value of 0.1  $\mu\text{m}$  for the median radius. The results of the QUICK analyses performed indicate those sets of conditions under which agglomeration should be of great importance, and those for which it is not. The lines on the figure are lines of constant mass reduction, i.e., any combination of initial aerosol mass concentration and residence time which falls on a given line will be attenuated in the primary system by the amount indicated on the line. Thus there are sequences, such as AD, which have shorter residence times and lower aerosol concentrations, so that retention in the primary system should be less than 1% of the mass emitted from the core, and there are other sequences, such as TMLB', which has high enough residence times and aerosol concentrations that 99% or more of the initial aerosol mass should be retained in the primary system. Clearly, the importance of agglomeration, as a contributor to particle retention, depends upon the specific sequence and time during the sequence which are under consideration.

Even for those sequences in which 99% or more of the aerosol mass is retained in the core region, some fraction of the smaller particles will be transported through the primary system with the potential for release into the containment. This aerosol can interact with CsI or other vapors, and can be retained in the primary system via deposition mechanisms other than gravitational settling. These particles are predicted to have grown due to coagulation, and there is also the possibility that condensation of fission products of intermediate volatility, such as CsI and CsOH may cause the particles to grow. The increase in radius due to condensation of fission products, however, should be quite small due to the relatively small amount of mass available for condensation on the particles.

Due to these uncertainties associated with the particle size, the effect of an increase in the initial particle size was investigated using TRAP-MELT by selecting a value of 1.0  $\mu\text{m}$  for the count median radius compared with the 0.1  $\mu\text{m}$  used in the base case. The results obtained for iodine and CsI retention are nearly indistinguishable from the base case results, as is indicated in Table 6.1.

Weak Particle Source (TMLB'-3). The QUICK analyses have indicated that for certain sequences, TMLB' in particular, the aerosol mass concentration may be greatly attenuated in the primary system. By far the greatest portion of this reduction in aerosol loading occurs very near the particle source. So the result of coagulation and settling is to effectively reduce the source of particles. This was examined in the TRAP-MELT analyses by lowering the particle mass source rate from 208 q/s, as used in the base case, to 1.4 g/s. The resulting predicted distribution of iodine among the four "states" in Table 6.1 is altered only slightly by the reduced amount of available particle surface area for CsI condensation. The slightly lower amount of CsI deposited on particle surfaces leaves more in the vapor phase, subject to the vapor deposition mechanisms, but there is not a significant difference in the degree of attenuation of CsI provided by the primary system in this case.

Altered Thermal Hydraulic Conditions (TMLB'-4). Because there is a range of values of thermal hydraulic parameters which may be relevant for a given accident sequence, the TMLB' sequence has been analyzed with TRAP using two independently generated sets of thermal hydraulic input. These may be compared in detail in Appendix D. The major difference in the two sets of data is that the fluid temperatures in the TMLB'-4 case are sufficiently high so that the CsI vapor deposition on the particle surfaces is hindered. This is due to the fact that the particles are in thermal equilibrium with the steam, and the CsI vapor pressure at this temperature is higher than in the TMLB'-1 case. Since a greater portion of the released CsI remains in the vapor state, there is more opportunity for its deposition on the internal surfaces of the primary system, especially in the upper plenum, whose surface is cool enough to permit some vapor condensation.

This result is reflected in the TRAP predictions shown in Table 6.1, which indicates that in this case just over 37 percent of the released CsI will be retained on the surfaces of the primary system. The difference between these results and those for the base case demonstrate the need for accurate thermal hydraulic conditions for fission product transport analyses.

TMLB' Sensitivity Study Results. A recently completed study determined the response of the TRAP model for iodine retention in the primary system to changes in various input parameters. The results of the study will be discussed separately for I<sub>2</sub> and then for CsI.

The input variables relevant for I<sub>2</sub> retention studies were the I<sub>2</sub> deposition velocity (range: from 0.2 to 5.0 times the base case value), fluid flow rates (range: approximately  $\pm 25$  percent of the base case values), and surface temperatures in the primary system (range: varies due to different time profiles for the temperatures but maximum difference is less than a factor of 2). The dominant variable for the retention of I<sub>2</sub> was the deposition velocity, as the three cases showing greatest retention all employed the high value for this parameter. The largest fractional retention of I<sub>2</sub> was  $8.41 \times 10^{-3}$  of the released mass and occurred for the low flow rate, low temperature case. The highest retention was  $1.14 \times 10^{-3}$  for the low flow, high temperature case, and the

third highest retention occurred for the low temperature, high flow case, retaining  $7.02 \times 10^{-4}$ . This trend is what one would expect based on residence time and vapor pressure considerations. In any event though, the retention of  $I_2$  in the primary system is seen to be minimal.

The sensitivity study results for CsI in the primary system also reflect the strong influence of residence time and surface temperatures on retention. The results for this species, however, are somewhat confounded by source strength variations, since some lower source rates may not generate a sufficient amount of material to surpass the vapor pressure at the surface temperatures of interest. The maximum fractional retention of CsI in the primary system found in the sensitivity study was 12.8 percent of the released mass. The thermal hydraulics for this case include slightly lower flow rates and system temperatures than those used in the base case above.

To summarize the iodine retention expected for the TMLB' sequence,  $I_2$  is released to the containment with no more than 0.1 percent attenuation, whereas approximately 6 to 40 percent of the released CsI is retained, depending primarily upon the thermal hydraulic conditions for the specific accident.

#### 6.3.2.2.2 Large Pipe Break with Failure of Emergency Core Cooling (PWR)

The AD (cold leg) accident sequence was selected for examination in this chapter because it is both a relatively fast accident and quite different from the TMLB' discussed above. The flow paths and geometry, as well as a summary of the temperatures of the system are shown in Appendix D. As for the previous core melt sequence, a number of variations on the base case were examined. And, as was true for the TMLB' accidents, the molecular  $I_2$  was predicted to penetrate the primary system with almost no attenuation.

Base Case (AD-1). The results for the base case AD cold leg sequence, with respect to CsI retention, are not strikingly different than for the TMLB' sequence in spite of the differences in the accident sequences' characteristics. Table 6.1 indicates that just under 20 percent of the CsI will be retained in the primary system for this case, most of this via vapor deposition on surfaces. At the end of this accident sequence, almost 11 percent of the CsI is predicted to be in the vapor form, although the detailed table in Appendix D shows that this value is smaller during the course of the accident. This increase in the amount of CsI in the vapor state is due to heating of primary system surfaces and the accompanying evaporation of previously deposited vapor.

Large Particle Source (AD-2). For the TRAP analysis which assumed an initial size of  $1.0 \mu\text{m}$ , the differences from the base case are more pronounced here than for TMLB', as shown in Table 6.1. For a fixed mass input rate, an increase in primary particle size requires a reduction in particle number concentration. Consequently there is less particle surface area available in the primary system to serve as condensation sites for the CsI. Clearly, the result here is that less mass is deposited on the particles,

and more on the system surfaces than in the base case. The reason that this effect is more pronounced than for the TMLB' cases is to be found in the thermal-hydraulics, which are such as to permit relatively more condensation on system surfaces for the AD than for the TMLB' sequence.

Weak Particle Source (AD-3). This case, with a particle source rate of only 1.4 g/s, demonstrates essentially the same effect as was shown in the above case. The reduced source strength obviously reduces the amount of surface area available, by even more than the larger size particle source. The results shown in the table indicate a correspondingly larger shift of CsI from that condensed on the particles to that condensed on the system surfaces. These results clearly indicate the importance of having an accurate assessment of the particle source rate to determine the release fraction of fission product iodine from the primary system.

Altered Thermal Hydraulic Conditions (AD-4). Using the same source rates as the base case, but slightly different thermal hydraulic conditions can also shift the distribution of CsI among the various states. The shift to higher deposition on the system surfaces shown for this case relative to the base case is due primarily to two differences in the thermal hydraulics, namely the cooler temperatures of the steam generators in this case, and the somewhat longer residence time of the CsI in the lower plenum while it is relatively cool. The thermal hydraulics for this case are summarized in Appendix D.

The results shown for the above simulations of AD (cold leg) accidents indicate that variations in the source particulate characteristics, and fairly small variations in the input thermal hydraulic conditions can have substantial influence on the CsI retention which TRAP predicts. The range in the retention shown here is from approximately 18 percent to over 60 percent of the CsI which leaves the core region.

AD (Hot Leg)-AD\*. The AD accident sequence which is initiated by a pipe break in one of the hot legs is similar to the AD (cold leg) accident, but the flow path to the containment is much more direct (see Appendix D). One expects in this case to have less attenuation of the fission products which are released due to the reduced opportunity for deposition on primary system surfaces. This expectation is realized in the results of TRAP shown in Table 6.1, where 85 percent of the CsI released will exit the primary system in the vapor state, and none is deposited on the surfaces. It is interesting to note that during the course of this accident sequence, TRAP predicts up to 17 percent retention of the CsI on the upper plenum surfaces. But as the temperatures in this control volume increase, the material is driven off the surfaces and ultimately released to the containment. This situation may be repeated, to a lesser extent, in other accidents which have CsI plated out on the primary surfaces, in that the primary system will then serve as a low level source of CsI so long as the surface temperatures are elevated.

Other Pipe Breaks. TRAP analyses were performed for other accidents initiated by pipe breaks in the primary system. The sequences S<sub>2</sub>D and AD were simulated for a pipe break occurring in the surge line to the pressurizer. The results of these simulations are not presented in summary Table 6.1, since the TRAP code requires extensive computing time for these accidents.

The reason for this is that very high flow rates through the system (consisting of the core, upper plenum, and a length of pipe) are predicted by the thermal hydraulics code, and as a result the mass through-put rates for the control volumes are quite high. Of course, these high mass flow rates lead to short residence times in the system. During the eight or nine minutes of the accidents for which TRAP could be run, up to 18 percent of the released CsI is predicted to be deposited in the upper plenum and the pipe, but, as seen for the AD (hot leg), as the temperatures rise during this type of accident scenario, the deposited material will very likely be reevolved and escape to the containment atmosphere.

#### 6.3.2.2.3 Transient with Failure to Scram (BWR)

The flow paths, control volume parameters, and summary of system temperatures during this sequence (TC) are shown in Appendix D. Nearly all of the expected CsI retention is predicted by TRAP to occur in the steam separators, and nearly all of the  $I_2$  retention occurs in the steam dryers. It should be pointed out that this is the only sequence examined in this chapter which exhibited as much as 1 percent  $I_2$  retention in the primary system, the value here being 5.4 percent.

The majority of the CsI is split almost equally between that deposited on particle surfaces and that which is deposited on the surfaces in the steam separators. As was shown for the AD sequences above, this split can be influenced greatly by the source rate of particulate matter, its initial size, and the thermal hydraulics of the system. Results obtained in a recently completed sensitivity study achieved predictions of as much as 83 percent retention of CsI in the system for conditions with low flow rates and surface temperatures. It is also of interest that up to 19 percent of the released  $I_2$  was predicted to be retained in this study for low flow and temperature conditions, albeit with an increased deposition velocity for the  $I_2$ .

#### 6.3.2.2.4 Large Pipe Break with Failure of the ECC (BWR)

The AE sequence, whose flow paths, control volume parameters, and system temperatures are indicated in Appendix D, is predicted to permit little reduction of the amounts of the fission products released from the core. The results indicated for the end of the sequence in Table 6.1 do not change very much during the course of this accident as can be seen in the table in Appendix D. It is interesting to note that even though the temperatures in the steam separators (where nearly all the CsI deposition occurs) are less hot than for the TC case, there is considerably less vapor deposition on the surfaces of the system in this case. The reason for this is to be found in the flow rates, which are predicted to be nearly an order of magnitude greater at times for the AE case, thus reducing residence times in the system. Once again, the significant amount of deposition on particulate surfaces indicates that the fraction of CsI retained in the primary system will depend greatly on the particle source characteristics.

#### 6.4 Effects of Iodine Species Distribution

The discussion in Chapter 5 dealt in detail with the distribution of fission product iodine among the species CsI, I, and HI. The results of the analyses performed indicate that CsI becomes the dominant species at higher fission product concentrations, lower temperatures, and in more reducing atmospheres. The implications of those results, in light of anticipated primary system conditions during a melt are that (1) in the immediate vicinity of the molten core, the high fission product concentrations and the highly reducing nature of the gas favor formation of CsI, but the very high temperatures here may shift the equilibrium to more elemental iodine and (2) as the gas leaves the core region and is diluted and becomes less reducing, the temperature is lowered such that the majority (90 percent or more) of the iodine would be found in the form of CsI well before the fission products enter the containment. An exception to this is possible for the case of a hot leg break in which the gas temperatures are still quite high at the point of the break. But for the accidents of this type examined for this chapter, the temperatures were never high enough to shift the iodine from CsI. Thus, the results presented in this chapter for CsI penetration of the primary system under the accident sequences examined characterize the bulk of the fission product iodine released from the core. This conclusion is, of course, subject to the uncertainties regarding the primary system atmosphere as discussed in the previous chapter.

#### 6.5 Primary System Retention of Other Fission Products

While the focus of this chapter is on the behavior of iodine released from the fuel during an accident, it is worth noting that the principles governing penetration of the primary system by forms of iodine will also determine the extent of retention of other fission products. For the accident sequences in which water is present in the primary system and able to contact the fission products, the solubility of the fission products becomes an important determinant of their retention. For the more severe accidents in which liquid water is not present in the flowpath, the vapor pressures of the fission products become the parameters of major concern. This implies that the chemical forms of the fission products are known, and as shown in Chapter 4, this is not always a straightforward matter. Without detailed information on the concentrations of the various fission products, their chemical forms and reactions, and their vapor pressures as functions of system conditions one can only make broad generalizations regarding their behavior in the primary system.

The non-iodine fission products may be classified into three groups according to their vapor pressures under accident conditions. The highly volatile species<sup>(1)</sup>, such as the noble gases, would be expected to behave much like the I<sub>2</sub> analyzed here. Thus, they would experience almost no attenuation in the primary system. At the other extreme are the fission products of extremely low vapor pressure<sup>(2)</sup>. These materials will recondense as particulate matter subsequent to their release from the core and remain in particulate form during transport through the primary system. The retention of these

particulate species in the primary system is determined by the various aerosol processes.

The final category of fission products is those with intermediate vapor pressures<sup>(3)</sup> such as CsI, whose behavior has been discussed at length in this chapter. The fate of these species is determined by the temperatures which are attained in their transit through the primary system. In general, lower surface temperatures favor vapor deposition on the walls and thereby cause retention in the primary system, but lowered gas stream (and particle) temperatures will enhance deposition on the particles and permit relatively more penetration of the primary system. Tellurium represents a fission product of considerable importance in risk assessment since it is a precursor of iodine and is present in the core at levels similar to iodine. This nuclide, and a number of others, should receive detailed attention in the near future. At the present time, more cannot be said regarding fission product retention without detailed consideration of the physical and chemical properties of the individual species and the thermal-hydraulic conditions in specific accident sequences.

References

- 6.1 Jordan, H., J. A. Gieseke, and P. Baybutt, "TRAP-MELT Users Manual", NUREG/CR-0632, BMI-2017 (February 1979). \*
- 6.2 Bell, M. J., "ORIGEN - The ORNL Isotope Generation and Depletion Code", ORNL-4628 (May 1973).
- 6.3 Wooton, R. O., and H. I. Avci, "MARCH (Meltdown Accident Response Characteristics) Code Description and User's Manual", NUREG/CR-1711, BMI-2017 (February 1979). \*
- 6.4 Reactor Safety Study, An Assessment of Accident Risks in U.S. Commercial Nuclear Power Plants, WASH-1400 (NUREG-75/014), October 1975.\*\*
- 6.5 Lorenz, R. A., J. L. Collins, A. P. Malinauskas, O. L. Kirkland, R. L. Towns, "Fission Product Release from Highly Irradiated Fuel", NUREG/CR-0722 (February 1980). \*

\*Available for purchase from the NRC/GPO Sales Program, U.S. Nuclear Regulatory Commission, Washington, DC 20555, and/or the National Technical Information Service, Springfield, VA 22161.

\*\*Available free upon written request to the Division of Technical Information and Document Control, U.S. Nuclear Regulatory Commission, Washington, DC 20555.



## 7. FISSION PRODUCT TRANSPORT THROUGH THE CONTAINMENT

Fission products will enter the containment on release from the reactor coolant circuit, will be transported and deposited within the containment, and will then be transported to the environment through leak paths or a failed containment. The amount of radioactive material released to the ambient atmosphere would be largely dependent on attenuation of radionuclides within the containment, and subsequent release from the containment is dependent on the containment conditions as specified by the assumed accident sequence. Therefore, specific accident sequences have been used to demonstrate major effects of containment conditions and to identify the impact of assumptions regarding the physical and chemical nature of the iodine source term. In addition, effects of assumed conditions and uncertainties in rate controlling variables have been analyzed in a parametric fashion to illustrate how release to the environment is affected by deviations from best estimate conditions.

Radionuclides introduced into the containment building are subject to various natural and engineered removal processes. The important natural processes are: radionuclide phase change, vapor sorption, transport due to convective flow, diffusion of vapors and particles to the containment walls, and the sedimentation, thermophoresis, diffusio-phoresis, and agglomeration of aerosol particles. The engineered safety systems that are either designed to or have some capability for reducing the concentration level in the containment building include for example, aqueous sprays, recirculating and once-through filters, pressure suppression pools and ice condensers. To the extent that these mechanisms are included in available computer codes or are available individually, calculations based on these mechanisms are used to estimate transport and deposition in the containment. Discussion of the effectiveness of engineered safety features is provided in Chapter 8 of this report.

### 7.1 Transport and Deposition Rate Processes

#### 7.1.1 Vapor Species

The vapor attenuation mechanisms that must be modeled to permit predictions of elemental iodine behavior in the containment are natural deposition on surfaces and removal by sprays, filters, suppression pools and ice-beds.

Natural Deposition on Surfaces. Typically, the concept of a deposition coefficient is used to quantify the deposition rate of a radionuclide from the bulk of the well-mixed volume to the containment surface. The deposition coefficient has units of reciprocal time and is calculated using mass transfer correlations. Natural convection due to temperature differences between the bulk fluid and the containment surface is assumed to provide the gradient for the transfer of iodine vapor to the walls upon which it is deposited. Correlations for natural deposition of iodine on surfaces have been obtained from the Containment Systems Experiments (7.1). The principal questions about the use of these correlations in modelling transport conditions in an actual containment relate to the scalability of the correlations from the relatively small experimental facility. The correlations currently used in the CORRAL-2 code (7.2) are presented in Appendix E.

Spray Removal of Iodine. The removal of iodine by containment sprays is modeled as a mass transfer process from an infinite medium of steam to a spherical water droplet. As for natural deposition, mass transfer as a first order rate process is used for spray removal. In the Containment Systems Experiments, the effectiveness of spray removal of iodine vapor was examined for spray water with a variety of additives. The correlations presented in Appendix E were developed from these experimental data.

Vapor Removal by Filters. In general, the effectiveness of filters in removing iodine from a gas stream is determined experimentally and characterized by a decontamination factor. The empirically determined decontamination factor is used in the analyses.

Pool Scrubbing. Usually pool scrubbing is treated by the use of a decontamination factor in computer codes which model radioactivity behavior in the containment. Some experimental data do exist for iodine transport from rising vapor bubbles in pools.(7.3) The results are sensitive, however, to the manner in which the bubbles are formed, the bubble size, bubble velocity, bubble interactions (for example, attachment of bubbles to each other to form rafts), pool depth and bubble composition. A model for vapor transport from a bubble is presented in Appendix E.

Ice-Bed Filtering. Experimental data have been obtained by Westinghouse Electric Company (7.4) for elemental iodine decontamination in ice beds. The fraction of air mixed with the steam was found to have a major influence on the decontamination factor for iodine. The effect of different additives to the ice on the amount of iodine retention was also investigated.

### 7.1.2 Particulate Species

To evaluate attenuation of particulate species, one must consider particle growth by agglomeration and by vapor condensation on the particles, deposition by natural processes onto surfaces, and removal by engineered safety features such as sprays, filters, suppression pools, and ice bed condensers.

Aerosol Agglomeration. Depending on accident conditions and characteristics of the radionuclides in the containment, significant aerosols agglomeration can take place. While agglomeration processes do not alter the overall mass, they reduce the number concentration and increase the size of the aerosol particles. This change in size will affect the efficiency of particle removal by sprays or filters and will enhance loss by sedimentation. It is important to note that agglomeration will occur between solid particles and small water droplets condensed from steam as well as just among the solid particles. The basic mechanisms for agglomeration and procedures for solving the governing equations are well established in the HAARM-3, QUICK and NAUA codes used for calculations in this chapter. The equations governing aerosol agglomeration are described in Appendix E.

Aerosol Deposition Mechanisms. Mathematical descriptions of aerosol deposition mechanisms such as gravitational settling, diffusional deposition on walls, thermophoresis, and diffusiophoresis are available. Assuming the various deposition mechanisms to be independent, the change in particle concentration is taken as being equal to the sum of removal rate constants

(having velocity units) multiplied by the particle concentration and deposition surface area. The removal rate constants are determined for each removal mechanism depending on the physical processes involved. These are described further in Appendix E.

Engineered Safety Systems. Particulate radionuclides can be removed by engineered safety features such as containment sprays, filter system and pool scrubbing. For sprays the nuclide concentration change is modeled in terms of the particulate laden gas volume swept by a drop as it falls and an efficiency of collection for particles contained in this swept volume. The mechanisms considered for collection are impaction and interception which both lead to higher collection efficiencies for larger particles.

In the case of filter and pool scrubbing the rate of particle removal is usually given in terms of an overall removal efficiency. The particle removal rate is then the product of efficiency, flow rate through the filter or pool, and airborne concentration. Detailed methods for calculating removal by bubbling through pools are described in Appendix E.

Leakage Flow. Containment radionuclide concentration can be significantly affected by escape of gases from the containment to the atmosphere, particularly if containment failure modes are to be considered. The effect of such leakage on the suspended aerosol is determined by the product of leak rate and airborne concentration. In the absence of large leaks as typified by a failed containment, leakage has little effect on airborne concentration because other removal mechanisms predominate.

Condensation. Water vapor may condense on radionuclide aerosol particles present in the containment atmosphere as supersaturated steam mixes and cools, or as the entire containment atmosphere cools. Condensation of water vapor will lead to growth and perhaps changes in agglomerate shape. The rate of condensation is described in terms of a simple model where the change in droplet size is governed by thermodynamic functions and the degree of supersaturation.

## 7.2 Computer Models

A number of computer models that calculate size dependent aerosol and vapor behavior within reactor containments are currently available. As a part of assessing the current state of the technology on fission product iodine, a brief review of these existing computer codes will be made in this section.

There exist two computer codes, CORRAL-2 and NAUA, which have been developed exclusively for describing radionuclide transport within LWR containments. In addition there are the codes such as HAARM-3 and QUICK which were originally developed for calculating aerosol behavior in LMFBR containments but can be utilized for LWR containments under conditions without excessive steam condensation. These and some related codes are described briefly below.

## 7.4

Two codes currently being developed in the United States which can be expected to improve the existing capability for predicting radionuclide transport in LWR containment buildings. The TRAP-MELT code described in the preceding chapter is under development to improve its capabilities and extend its application to the containment. The code is to describe radionuclide transport behavior in a thoroughly mechanistic fashion. A new code is also being developed to replace the CORRAL-2 code. While still primarily intended to be a systems code and not reliant strictly on basic mechanisms, the CORRAL-3 code will improve on many of the current limitations of CORRAL-2 in the treatment of transport mechanisms.

### 7.2.1 NAUA Code

The NAUA computer model (developed at KFK in Germany) calculates aerosol behavior in an LWR containment. It assumes that aerosol concentration in a containment is uniformly distributed and calculates results for aerosol generation, deposition, and leakage processes.(7.5) The mechanisms included in the code are steam condensation on particles, agglomeration due to gravitational and Brownian motion, gravitational settling on the floor, diffusion to walls, and leakage out to the environment. Due to uncertainties in some of the physical parameters an experimental program intended to provide data for code improvements is continuing. Turbulent agglomeration of particles, multiple compartments, aerosol particle removal by sprays and fission product vapors are not included in the NAUA code. Application of the code is dependent on detailed thermal conditions in the containment which control the condensation process.

### 7.2.2 CORRAL-2 Code

The CORRAL-2 computer code permits calculations of fission product removal by natural and engineered processes in multicompartment containments.(7.2) A total of 15 compartments and four types of fission products (noble gases, elemental iodine, organic iodides, and aerosols) can be considered. Sources of radioactive materials can be time dependent so as to accommodate gap, melt, vaporization and oxidation releases. The code is empirical in nature with the particle sizes fixed within the code such that the sedimentation loss model using these fixed sizes provides a prediction of the observed attenuation in CSE experiments. Similarly, spray removal efficiencies have been selected to model the CSE washout results. Although not mechanistic in nature the code is based on an experimental simulation of accident conditions which permitted processes such as particle agglomeration and steam condensation on walls and particles. Since it is largely not mechanistic in nature, the validity of extending the CORRAL-2 code to various containment scales and geometries, and to a variety of accident conditions is dependent on the CSE having properly simulated all other conditions. It is to be expected that deviations between CORRAL-2 calculations and actual iodine vapor or particle behavior would be greater as assumed accident conditions (such as aerosol source rate, spray characteristics, vessel size and steam injection rates) deviate from the conditions employed in CSE experiments.

## 7.5

A limitation of the CORRAL-2 code regards its applicability for cases where airborne mass concentrations of aerosols are high and agglomeration becomes a controlling factor. The CSE concentrations of aerosol mass were well below those anticipated for some accident conditions. The CORRAL-2 code is best suited for cases where there is steam condensation in the containment.

Even though there should be excellent agreement between CORRAL-2 calculations and the CSE data (the rate constants used in the code were derived from the data), a thorough analysis of the extent of agreement seems warranted. Such evaluations would provide a more complete understanding of CORRAL-2 capabilities.

### 7.2.3 HAARM and QUICK Codes

The HAARM-3 code has been developed for describing aerosol behavior within LMFBR containments.(7.6) The aerosol behavior processes included in the code are Brownian, gravitational and turbulent coagulation; gravitational, diffusional and thermophoretic deposition on surfaces; particle removal by filtration; and leakage to the environment. The most important assumptions employed in the code are that aerosol concentration is spatially homogeneous throughout the containment and that the size distribution on the aerosol particles remains log-normal. No provisions for a multiple compartmented containment or for vapor phase nuclide behavior are provided, nor can the code account for water vapor condensation on particles.

The QUICK computer code has been developed independently for describing aerosol behavior primarily in LMFBR containments.(7.7) Although the same processes are included as used in the HAARM-3 code no simplifying assumptions are made regarding the aerosol particle size distribution and a numerical solution technique different from that used in HAARM-3 was utilized. Again no capabilities for handling fission product vapor, water condensation, or multiple compartments are included. A related code designated ZONE is an extension of QUICK.(7.8) In the ZONE computer codes, the containment is divided into three conceptual compartments which are interconnected by convective flows. Fission products in vapor form and fission product or steam condensation are not included.

### 7.2.4 Other Codes

The PARADISEKO-IIIb computer code (essentially the NAUA code without steam condensation) calculates the aerosol behavior in an LMFBR containment. The aerosol behavior mechanisms included in the code are Brownian and gravitational agglomeration, gravitational, thermophoretic and diffusional deposition and leakage.

Other computer codes which calculate airborne radionuclide behavior include ABC-2 and AEROSIM, both of which are similar to PARADISEKO-IIIb in that all these codes are concerned with aerosol behavior primarily in LMFBR containments. The MAEROS code has recently been completed and in addition to the basic aerosol behavior mechanisms, maintains an accounting of particle composition as a function of size when there are sources of more than one aerosol material.

The computer codes discussed above can be compared in terms of the radionuclide behavior mechanisms and capabilities, and these are shown in Table 7.1.

### 7.3 Experimental Evaluations of Transport in Containment

Predictions of airborne radionuclide transport as vapor or particles are made with a variety of computer codes. The adequacy of such predictions can be assessed in terms of the extent to which the computer codes are able to model experiments which provide measurements of the transport and deposition of radionuclides. Comparisons among codes and experimental results for aerosol behavior experiments along with extensive comparisons between the HAARM-3 code and experiments are available (7.9-7.14) for dry conditions, as are reasonably extensive comparisons of a variety of codes with selected experiments. (7.5, 7.15) In general, the aerosol behavior codes [HAARM-3, HAA-3B, NAUA (or PARDISEKO-IIIb), ABC-2, AEROSIM and QUICK codes] have been compared with experimental determinations of the behavior of aerosols under dry conditions. The CORRAL code was developed by empirically fitting experimental results for the behavior of aerosol and vapor iodine forms in a steam and fog-filled CSE vessel with and without spray removal. In the CORRAL code development program, experimental studies of iodine vapor removal from a variety of vessels were also taken into account. A modified version of the HAA-3B code was also used successfully to predict spray removal of aerosols. (7.16) From this extensive collection of comparisons of codes and data, the current state of technology can be assessed in terms of the agreement between predicted and experimental results, the ranges over which experimental results are available for code verification, and the uncertainties in the data and predictions.

#### 7.3.1 Available Experimental Results

Experimental data have been used both to develop and to verify the various transport and deposition codes. For the behavior of molecular iodine, data obtained in a number of experiments performed in a variety of test vessels were used to determine values for natural deposition velocities onto stainless steel and painted surfaces, and to determine washout coefficients during spraying. Figure 7.1 illustrates the ranges of molecular iodine concentrations used in experiments plotted against the volume of the experimental vessels. Also shown in the figure for comparison are maximum possible iodine concentrations in reactors calculated as the total inventory mass of iodine down to 0.02 percent of this mass divided by the containment volume. This then represents an approximate range of maximum values for a range of accidents. Because removal processes operate simultaneously with the source, concentrations would most likely be somewhat lower than these maximum possible values.

It is seen in Figure 7.1 that a wide and fairly representative range of concentrations were used in the experimental studies. Further, for some experiments the vessel sizes have been near the same size as reactor containment. It should be noted that the use of containment volume in this comparison is not meant to imply that volume is a true scaling parameter. Surface to volume or floor area to volume are probably more meaningful scaling parameters in most cases.

TABLE 7.1. COMPARISON OF CONTAINMENT CODES

Code	Reactor Type	Containment Compartment	Radionuclide Form	Radionuclide Mechanisms Include	Mechanism Not Included
CORRAL-2	LWR	Multi	Vapor, Aerosol	Deposition, Spraying	(Mainly Empirical, not mechanistic)
HAARM and QUICK	LMFBR	Single	Aerosol	Deposition, Agglomeration, Filtration	Condensation, Vapor Species
NAUA	LWR	Single	Aerosol	Condensation, Agglomeration, Deposition	Vapor Species
PARDISEKO and AEROSIM	LMFBR	Single	Aerosol	Deposition, Agglomeration	Condensation, Vapor Species

Experiments on dry aerosol behavior in enclosed vessels are summarized in Figure 7.2. Since many aerosol behavior experiments have involved sodium oxides, these data are also included and identified. For comparison, reactor containments with estimated total particle mass injections of 3000 kg down to 0.5 percent of this value are shown. These represent the estimated range of maximum values for airborne particulate concentrations. Because the aerosol behavior codes are largely mechanistic in nature, the experimental data have been used in basically a verification mode in which disagreements between data and predictions served as the impetus for improving the theoretical bases of the codes rather than in adjusting parameters to force a fit between code and experiment.

### 7.3.2 Comparisons of Predictions with Experimental Results

As noted previously, extensive comparisons between predicted and experimental aerosol behavior have been reported in the literature. An example of such a comparison is presented as Figure 7.3 where the HAARM-3 and QUICK code predictions of airborne mass concentrations are compared with measured concentrations for  $UO_2$  particles in NSPP Experiment 204. Although the agreement shown is quite good, the use of measured or alternate choices of input parameters describing agglomerate properties would be expected to improve the agreement. Figure 7.3 illustrates the type of agreement usually achieved with an a priori calculation. Similar comparisons are not available for vapor behavior and would be less meaningful since the predictive models employ rate constants derived from the available data.

An excellent review of the state of the art for analyzing nuclear aerosol behavior has been recently prepared (7.5) and additional data and advances were the subject of a technical conference.(7.15) Based on these recent analyses of the topic which include comparisons between predictions and experiments, several pertinent conclusions have been reached:

- Integral aerosol tests (without steam) extend over a range of vessel volumes to  $850 \text{ m}^3$ , mass concentration to  $>20 \text{ g/m}^3$  for uranium oxides, and vessel heights to 20 m. Mass concentrations are generally overpredicted (compared to experiments) but are within a factor of 10 for time-dependent sources. By starting the prediction at the end of the source period using experimental values at that point, the predictions follow the measured concentration decline with time to within a factor of about two.
- Mixtures of aerosols formed from even markedly different materials will coagglomerate and exhibit mixture aerosol behavior. However, there are scant experimental data that combine fission products,  $UO_2$ , concrete, clad, and structural aerosols.
- Homogeneously nucleated aerosols of  $U_3O_8$  and  $UO_2$  have sub-micron mean aerodynamic sizes. However, the model predictions are not very sensitive to the initial mean size below about  $0.1 \text{ }\mu\text{m}$  because of rapid agglomeration at the concentrations of interest.

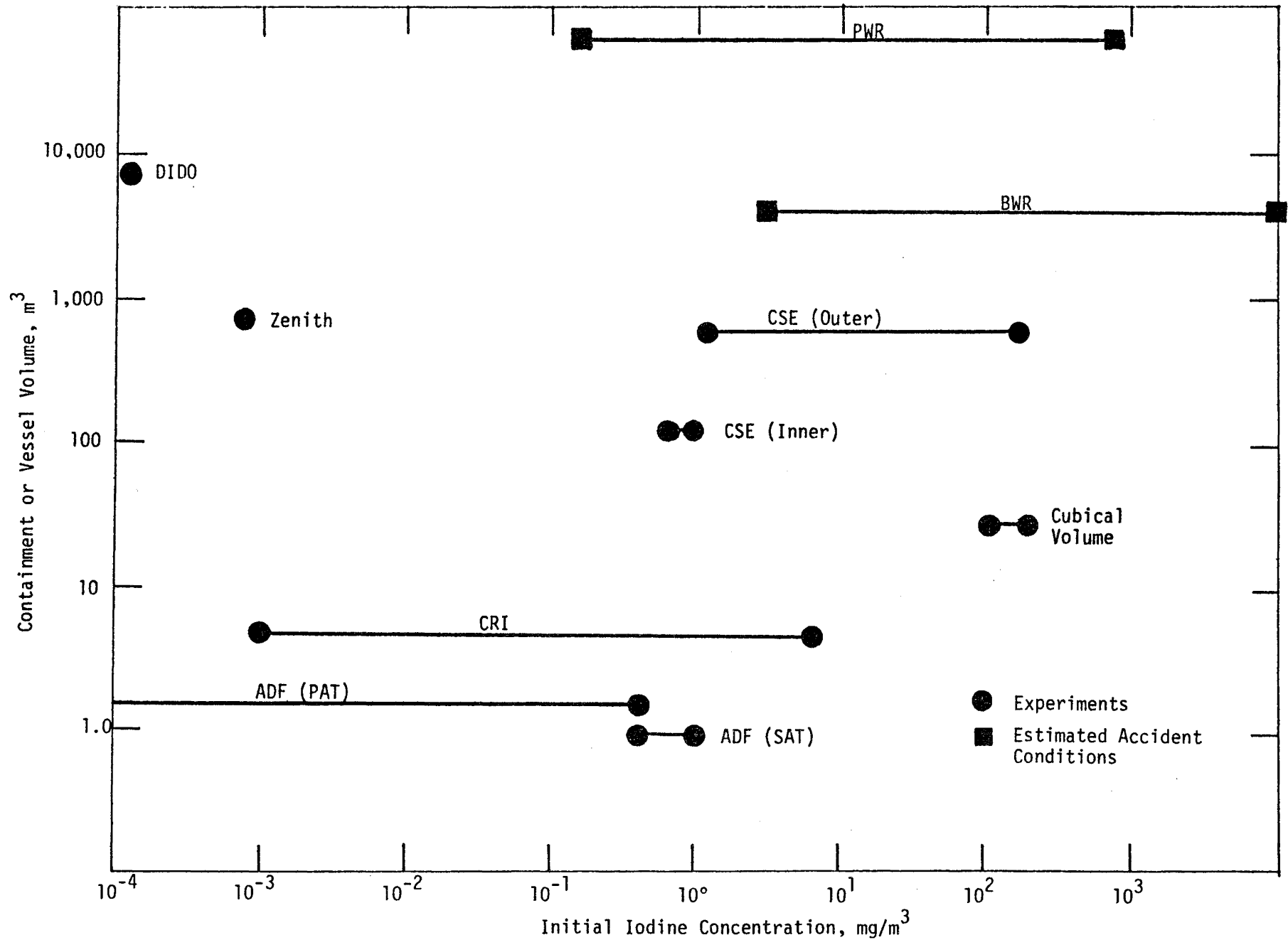
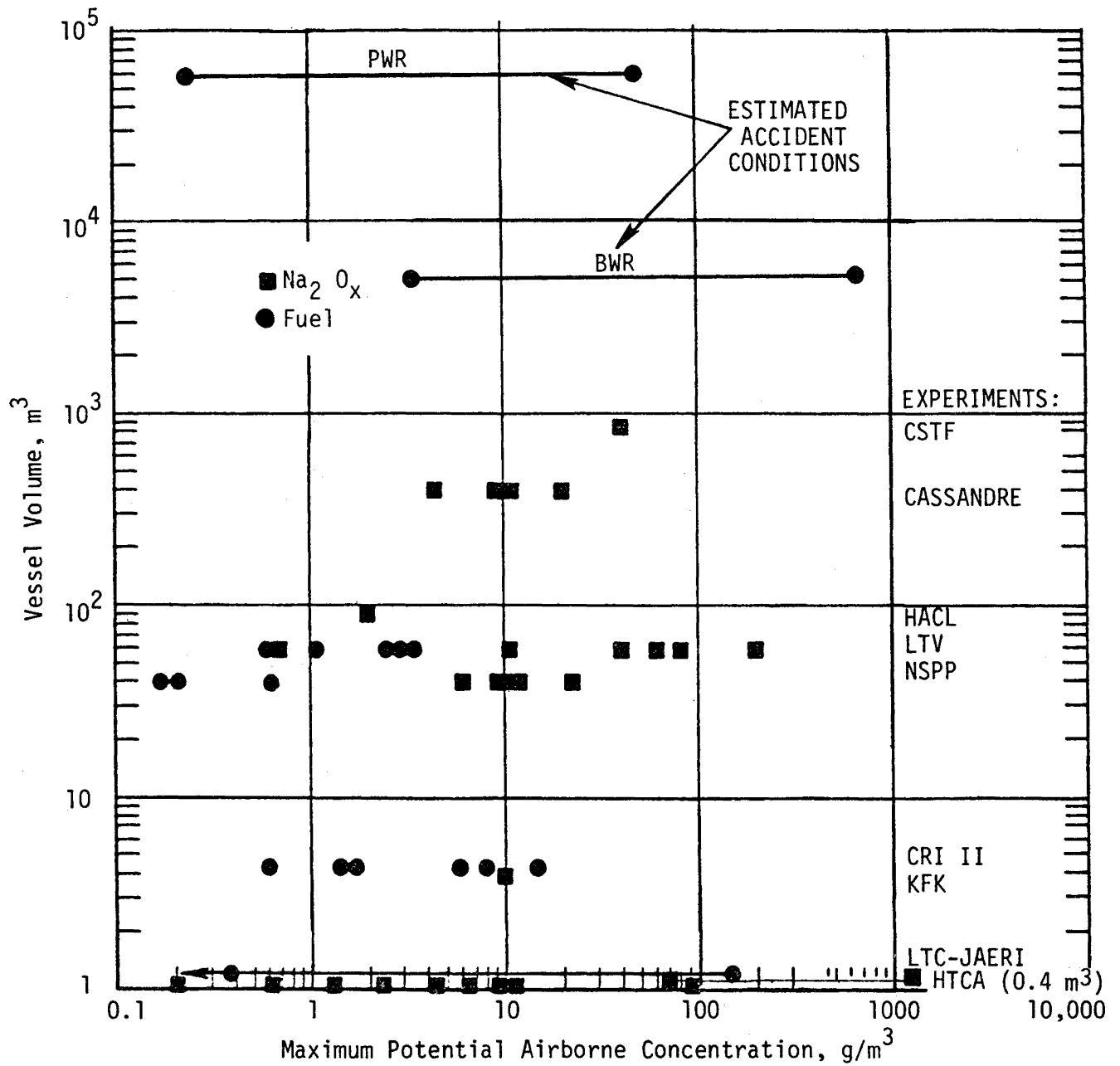


FIGURE 7.1. ESTIMATED ACCIDENT AND EXPERIMENTAL CONDITIONS FOR IODINE VAPOR TRANSPORT





## 7.12

Most of the data base for validation of nuclear aerosol models has been developed in the absence of steam. Within a containment environment, steam condensation on particles can enhance settling and the condensing of steam onto vessel surfaces can enhance plateout.

Under high concentration conditions ( $\sim 200 \text{ g/m}^3$ ),  $\text{UO}_2$  aerosols have been observed to grow to average sizes as large as  $40 \text{ }\mu\text{m}$  in small vessels (horizontal cylinder 1 m in diameter) with some particles as large as  $300 \text{ }\mu\text{m}$ . These very large particles found in high concentration experiments are also predicted by the QUICK code for similar cases. Aerosols released within the primary containment or at the initial release point into the secondary containment could exist temporarily at these high concentrations. The growth and aerosol behavior in general under these conditions should depend on the geometry (confinement volume, surface area, and height), aerosol physical processes (source rates, agglomeration, plateout, and fallout), and the residence times. Proper accounting for these allow the present models to predict the observed high concentration behavior.

### 7.4 Fission Product Behavior in Severe Core Damage Sequences

In this section results are presented for analyses which were performed to examine the transport of fission products in the containment building for a variety of severe core damage sequences. Accidents involving minor core damage were not investigated because, as illustrated in Chapter 6, the amount of radioactive material released to the containment atmosphere would be comparatively small. The purpose of the analyses was to investigate the effect of fission product chemical form on release to the environment and the effectiveness of safety features in the retention of radioactive materials within the containment. Principal emphasis in the analyses has been on iodine behavior, although some insights into the behavior of other fission products can be inferred from the results.

In Chapter 6 it was shown that some radioactive materials released from the fuel may be retained within the reactor coolant system depending upon the conditions for a particular accident sequence. In this chapter, no credit is assumed for attenuation in the primary system so that the potential for retention in the containment can be identified separately. In order to obtain a best estimate of the release to the environment in an accident sequence, the effects of the primary system and containment would have to be superimposed.

The analyses that are presented were performed with the HAARM-3 and CORRAL-2 codes. More cases were examined with CORRAL-2 because of the broader applicability of this code to a variety of LWR accident sequences and containment design features. Recognizing the limitations in the rigor with which the CORRAL-2 code treats some transport processes, results of a number of sensitivity studies and comparison calculations among additional computer codes are presented in Section 7.5. The thermal-hydraulic behavior in the accidents is based on analyses performed with the MARCH computer code (7.16). The MARCH code represents a major improvement over the thermal-hydraulic analyses performed in the Reactor Safety Study. It should be recognized, however, that there are significant uncertainties in the ability of existing computer codes to predict the physical processes of core meltdown accidents and that these processes can have a major influence on radionuclide transport and deposition. The timing and mode of containment failure in particular affect the predicted retention of radioactive material in an accident sequence.

#### 7.4.1 Source Terms and Bases for Calculations

In the calculations for both the degraded core sequences and the core meltdown sequences which are described in subsequent sections of this chapter, a common baseline source term for both iodine and other species was used. The source terms for radionuclide release from the fuel as given in Chapter 4 were simplified for use in the containment analyses, and in general are listed in Table 7.2. The iodine form was chosen as being either totally  $I_2$  vapor or totally CsI. For the CORRAL-2 calculations identified as being for  $^{137}CsI$ , the CsI was assumed to be in particulate form because of its low vapor pressure at the temperatures of interest. The mechanisms and logic for this choice of forms were discussed in Chapter 6. It was further assumed that the CsI distributed with a constant mass fraction among particles of all sizes. The timing for CsI release from the fuel was taken to be the same as that for  $I_2$  vapor. All sources ( $I_2$ , CsI and particulate) used with the CORRAL-2 code were at a constant input rate for the melt release and an exponentially decreasing rate (half time 30 min) for the vaporization source. Of the core inventory of iodine, 90 percent was assumed to be released during the melt phase (either as  $I_2$  or as CsI) with the balance released for the vaporization phase. For the total aerosol calculation in CORRAL-2 800 kg (72%) was released in the melt phase and 310 kg (28%) in the vaporization phase.

No additional sources for  $I_2$  vapor or aerosol mass were considered, nor were transformations among chemical forms. Therefore, postulated methods of formation for  $I_2$  from CsI through chemical formations in the containment were neglected. Such transformations have been suggested to result from  $H_2$  deflagration or radiation exposure of compounds formed with atmospheric constituents such as  $CO_2$ .

The total particulate release or aerosol source was taken to have the total values shown in Table 7.2. However to evaluate the effects of source term, the maximum value for each phase of the release was scaled up or down proportionately for parametric calculations. The initial mass median diameter of particles entering the containment was taken as  $0.1 \mu m$  and the distribution of the particles was assumed log normal with a geometric standard deviation of 1.5. All radionuclides were assumed to be distributed with a constant mass fraction among all particle sizes.

The timing of the aerosol releases to give the total amounts listed in Table 7.2 varied with the accident sequence being considered and was determined by the thermal hydraulic conditions calculated. The melt release of aerosol mass was assumed to occur at a linearly increasing rate with the total input being that shown in Table 7.2. After a time period specified chiefly by thermal hydraulics during which there is no source, the vaporization release is then assumed to occur over a two-hour time period at a constant rate sufficient to provide the total vaporization release. In all cases where the total aerosol mass was varied parametrically, the ratio of melt to vaporization release excluding concrete degradation products was held approximately constant.

The timing of each accident sequence which governed the calculations is presented in Appendix E as Table E.3. Also included there are Tables E.4 and E.5 which specify the system geometries and spray rates used in the calculations.

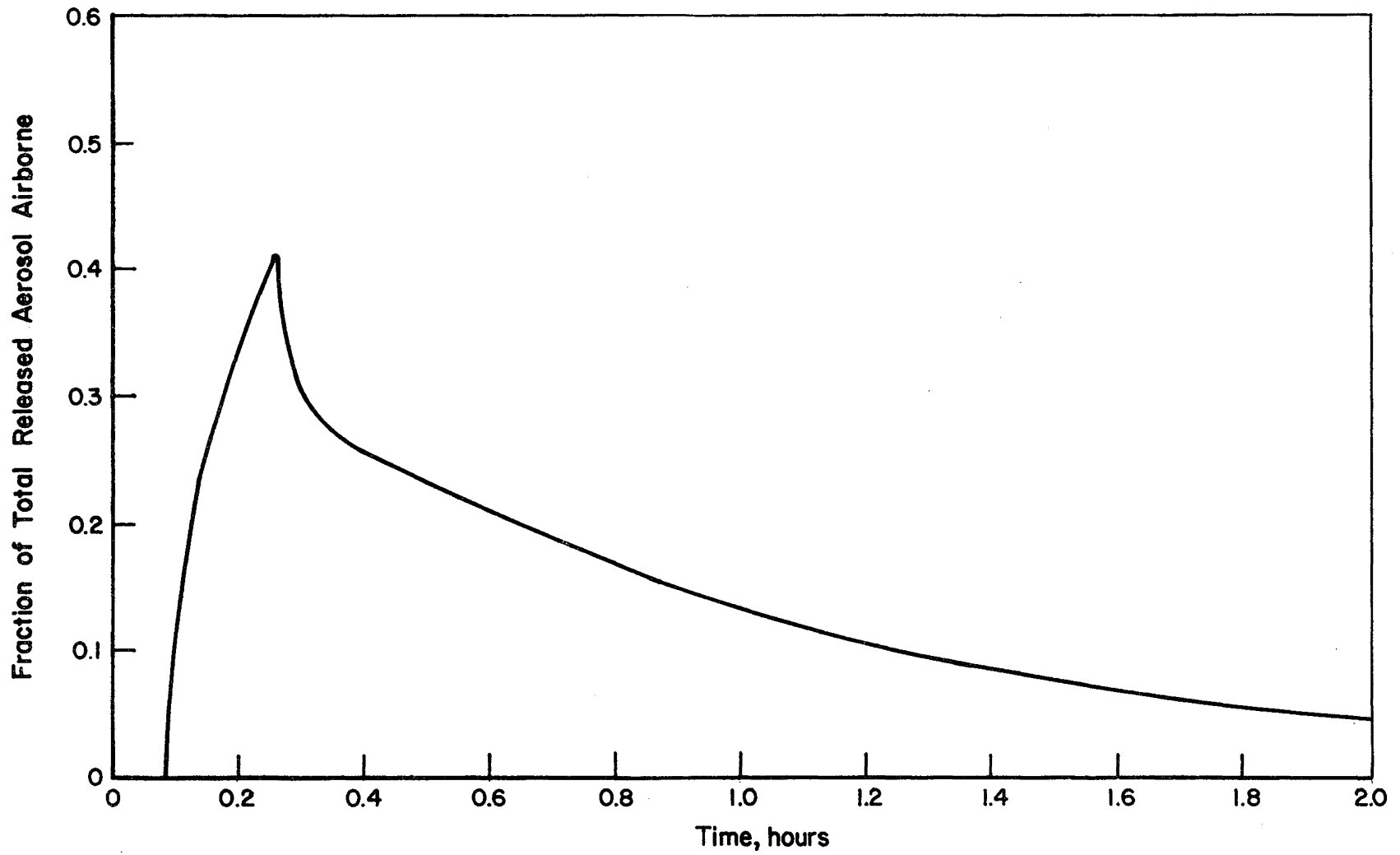
#### 7.4.2 Degraded Core Sequences

Because degraded core sequences involve partial performance of safety systems, a complete spectrum of accident conditions can be hypothesized. Two sequences of this type are examined in this report, one involving a dry pathway to containment and the other a pathway which is water filled.

Large Pipe Break, Delayed ECC Injection. This sequence is very similar to the core meltdown case AD except that the emergency core cooling system is assumed to operate after a 16 minute delay, leading to arresting of core heatup with approximately one half of the core molten. In this accident the containment spray system would be operational and would aid in the removal of radioactive material from the containment atmosphere. In Figure 7.4, the airborne fraction of the total aerosol released to the containment building is shown as a function of time. Consistent with the release assumptions given in Table 7.2 for full core meltdown accidents, the total aerosol source to the containment would be approximately 400 kg in this accident sequence. The amount of iodine which is predicted to be released from the containment building is a very small fraction of the initial core inventory of iodine regardless of the chemical form. These results are tabulated in Table 7.3.

Stuck-Open Relief Valve, Partial ECC Performance. This sequence is intended to be similar in character to the TMI accident in that: fission products pass into a water-filled volume before leaving the reactor coolant system, a large volume of contaminated water is dumped onto the containment floor, and some leakage exists into the auxiliary building from the letdown system.

Assuming that 20 percent of the core inventory of iodine was released to the floor of the containment building in 500,000 gallons of water, the amount of iodine that would become airborne in equilibrium with the iodine in the water can be estimated. As discussed in Chapter 5, the minimum partition coefficient between water and air would be  $10^5$  for elemental iodine under the anticipated accident conditions. If the chemical form of the iodine were elemental, then the fraction of the core inventory that would become airborne in the containment would be  $6 \times 10^{-5}$  of the initial core inventory. For a leak rate of 0.1 volume percent per day, the total I-131 that would leak from the containment would be  $7 \times 10^{-7}$  of the initial core inventory after accounting for the radioactive decay. Since the containment pressure would be near atmospheric pressure, there would be no driving force for leakage and the total release of iodine would actually be much less than this. If the chemical form of the iodine were cesium iodide, even less would be expected to be released from the water on the containment floor to the containment atmosphere and subsequently to the environment. However experience in actual accidents and experiments indicates that the airborne concentration of iodine would not be as low as predicted by assuming that the chemical form is elemental iodine or cesium iodide because of the existence of the more volatile form, methyl iodide. It can therefore be expected that methyl iodide would be the dominant form of iodine leaked from the containment building regardless of the initial chemical form of the iodine.



7.15

FIGURE 7.4. LARGE PIPE BREAK WITH DELAYED ECC INJECTION

TABLE 7.2. SOURCE TERMS FOR FULL CORE MELTDOWN<sup>(a)</sup>

Accident Phase	Fission Product Iodine (Fraction of Initial Core Inventory)	Total Aerosol (kg)
Melt Release	0.9 <sup>(b)</sup>	800
Vaporization Release	0.1	310
Total	1.0	1110

(a) These release fractions were used irrespective of the chemical form of iodine. The small differences in CORRAL-2 results for CsI and total particulate are only due to differences in the timing of release. The same source terms for total particulate were used in the HAARM-3 and CORRAL-2 analyses.

(b) Includes gap release component.

TABLE 7.3. SUMMARY OF PREDICTED RELEASES IN ACCIDENTS INVOLVING SEVERE CORE DAMAGE

Reactor	Sequence	Containment Failure Mode	Decontamination Factor	Fraction of Core Inventory Leaked <sup>(a)</sup>		Fraction of Particle Source Leaked <sup>(a)</sup>		
				CORRAL-2		CORRAL-2	HAARM-3	
				Elemental Iodine	Cesium Iodide	Total Particulate	Total Particulate	
<b>PWR</b>								
Large, High Pressure	Large Pipe Break, Delayed ECC	None	--	$1.0 \times 10^{-6}$	$7.0 \times 10^{-6}$	$1.0 \times 10^{-5}$	--	
Large, High Pressure	S <sub>2</sub> D	Basemat Melthrough	--	$1.1 \times 10^{-5}$	$2.6 \times 10^{-4}$	$2.4 \times 10^{-4}$	--	
Large, High Pressure	TMLB'	Overpressure	--	$4.1 \times 10^{-1}$	$4.9 \times 10^{-1}$	$3.8 \times 10^{-1}$	$5.3 \times 10^{-1}$	
Large, High Pressure	TMLB'	Basemat Melthrough	--	$3.3 \times 10^{-4}$	$1.1 \times 10^{-3}$	$9.6 \times 10^{-4}$	$8.6 \times 10^{-4}$	
Large, High Pressure with Filter	S <sub>2</sub> D	Basemat Melthrough	--	$1.4 \times 10^{-4}$	$1.5 \times 10^{-4}$	$1.2 \times 10^{-4}$	$2.0 \times 10^{-4}$	
General Ice Condenser	V	Bypass	--	$3.6 \times 10^{-1}$	$3.2 \times 10^{-1}$	$3.1 \times 10^{-1}$	--	7.17
	AD	Hydrogen Combustion	2	$4.2 \times 10^{-3}$	$1.7 \times 10^{-2}$	$4.3 \times 10^{-2}$	--	
			10	$1.6 \times 10^{-3}$	$3.2 \times 10^{-3}$	$8.5 \times 10^{-3}$	--	
			10	$1.0 \times 10^{-1}$	$3.3 \times 10^{-1}$	$2.8 \times 10^{-1}$	--	
Ice Condenser	TMLB'	Overpressure	2	$1.0 \times 10^{-1}$	$3.3 \times 10^{-1}$	$2.8 \times 10^{-1}$	--	
			10	$5.6 \times 10^{-2}$	$1.4 \times 10^{-1}$	$1.4 \times 10^{-1}$	--	
Ice Condenser	S <sub>2</sub> HF	Overpressure	1	$1.6 \times 10^{-1}$	$6.5 \times 10^{-1}$	$5.6 \times 10^{-1}$	$6.8 \times 10^{-1}$	
<b>BWR</b>								
Mark I	AE	Overpressure, Flow Through Annulus	10	$4.7 \times 10^{-3}$	$9.0 \times 10^{-3}$	$8.5 \times 10^{-3}$	--	
			100	$6.4 \times 10^{-4}$	$9.0 \times 10^{-4}$	$8.5 \times 10^{-4}$	--	
			1000	$6.5 \times 10^{-5}$	$8.9 \times 10^{-5}$	$8.5 \times 10^{-5}$	--	
Mark I	TC	Overpressure, Flow Through Annulus	1	$6.2 \times 10^{-2}$	$1.2 \times 10^{-1}$	$1.2 \times 10^{-1}$	--	
			10	$5.6 \times 10^{-3}$	$1.2 \times 10^{-2}$	$1.2 \times 10^{-2}$	--	
Mark I	TW	Overpressure, Direct Release	1	$7.2 \times 10^{-1}$	$7.7 \times 10^{-1}$	$6.5 \times 10^{-1}$	$7.2 \times 10^{-1}$ (b)	
			10	$7.2 \times 10^{-2}$	$7.7 \times 10^{-2}$	$6.5 \times 10^{-2}$	--	
Mark III	TQUV	Overpressure	100	$1.1 \times 10^{-3}$	$7.3 \times 10^{-3}$	$9.3 \times 10^{-3}$	--	
			1000	$2.1 \times 10^{-4}$	$5.3 \times 10^{-3}$	$7.1 \times 10^{-3}$	--	

(a) Assumes a constant leak rate of one volume percent per day with no attenuation along leak path up to point of containment failure if such occurs.

(b) Calculation performed with the QUICK code.

Assuming that 5 percent of the core inventory of iodine was retained in the water in the reactor primary system, some iodine would be transported to the auxiliary system through the letdown system. For a leak rate of 10 gallons per hour, 0.017 percent of the core inventory of iodine would be leaked to the auxiliary building per day and, accounting for decay, the total I-131 transferred would be 0.2 percent of the initial core inventory. Some of this iodine would be released from the water to the auxiliary building atmosphere depending on the chemical form. Experiments in the Containment Systems Experiment (7.17) program demonstrated that for elemental iodine, only a small fraction would be reevolved once dissolved in borated water. If the iodine were in the form of cesium iodide before entering into solution in the leaked water, essentially none would be expected to be evolved to the air in the auxiliary building.

One of the reasons for diverting the letdown flow from the reactor coolant system is to degasify the reactor coolant. The gases stripped from coolant water are then piped to waste gas decay tanks for storage. Any leaks in this system would provide another pathway for noble gases and possibly iodine to be released to the atmosphere of the auxiliary building. As discussed previously for the containment building, at the low airborne concentration of iodine which would be expected in the auxiliary building a significant percentage of the iodine would be expected to be organic. The atmosphere of the auxiliary building is vented through a filter to the environment. Because the filter is less efficient in removing organic iodine than other forms, the principal form of iodine released to the environment would probably be methyl iodide as was the case at Three Mile Island. This would represent only a small percentage of the iodine actually transferred to the auxiliary building. Although bounding estimates can be made for the quantity of methyl iodide produced in an accident, as discussed in Chapter 5, there are no mechanistic models available which attempt to predict the amount quantitatively as a function of the existing environmental conditions.

#### 7.4.3 Core Meltdown Sequences

Results from analyses of a number of core meltdown sequences using the HAARM-3 and CORRAL-2 codes are presented in this section of the report. The nomenclature which is used to represent specific accident sequences is described in Appendix A. The sequences were selected to cover a broad range of potential conditions within the containment and to demonstrate the effects of different containment designs and engineered safety features on fission product behavior. The source terms for radioactive materials and aerosol production which were used in the codes are presented in Table 7.2. In the HAARM-3 analyses the transport of the total aerosol mass released from the fuel and concrete was calculated. In the CORRAL-2 analyses it was also possible to follow the behavior of the iodine fission product explicitly. The fractions of iodine released during the melting and vaporization phases were based on the WASH-1400 release fractions. The values assumed for the release of iodine and total aerosol mass are in good agreement with Chapter 4 analyses.

#### 7.4.3.1 Large Volume, High Pressure Design (PWR)

In these containment types, the large volume and high design pressure capability enable the containment to withstand the pressure increase resulting from depressurization of the primary system fluid. Containment spray systems would then operate to condense steam and reduce the pressure in the containment to atmospheric. Operation of the spray system would be very effective in reducing the airborne inventory of iodine either as  $I_2$  in vapor form or as cesium iodide in particulate form. Typically, chemical additives are included to enhance the removal of elemental iodine. In some plant designs, internal filters are also included which would remove radioactive material from a recirculating flow of containment air.

Containment Spray System Functional. In Figure 7.5 airborne concentrations are compared for CORRAL-2 analyses of the sequence S<sub>2</sub>D. This is a pipe break accident in which the containment safety systems function to maintain the integrity of the building and to remove radioactive material from the containment atmosphere. Release to the environment results from the expected low level of leakage from the containment building. As illustrated, the airborne concentration of either elemental or particulate iodine would be rapidly decreased by the spray system. Although the CORRAL-2 analysis indicates greater effectiveness of the spray system for elemental iodine, the efficiency with which sprays remove aerosols is very sensitive to the assumed aerosol size distribution. The higher the mass loading and resultant particle size, the more effective the spray system would be. However, Table 7.3 indicates that the predicted release to the environment is small regardless of the principal chemical form.

Containment Safety Systems Not Functional. In some accident sequences, usually of much lower probability, the containment safety systems would not operate. The TMLB' sequence with above-ground failure of the containment is one that was found to be an important contributor to risk in the Reactor Safety Study. In this accident, a transient is initiated by loss of off-site power. Through a combination of assumed failures, the capabilities of the containment to remove heat from the primary system, to operate the sprays and to remove heat from the containment atmosphere are lost. At the time of pressure vessel meltthrough, the release of steam from the vessel and from the interaction of emergency core cooling (accumulator) water with hot core material can produce pressures which threaten containment integrity. Figure 7.6 shows the results of containment transport analyses assuming that the containment fails at this time. The rapid drop in airborne concentration between 4 and 5 hours is the result of containment failure.

In this sequence there is too little time available for natural deposition processes in the containment to be effective in removing much of the radioactive material from the containment atmosphere prior to failure and leakage to the environment. The fraction of the initial core inventory of iodine that was predicted to be released from the containment building is shown in Table 7.3. The release of total particulates predicted by the HAARM-3 and CORRAL-2 analyses are very similar. Further, the assumed chemical form does not appear to make a significant difference in the results for this case.' In interpreting the overall results for the TMLB' sequence, the potential for retention of a significant amount of radioactive material in the reactor

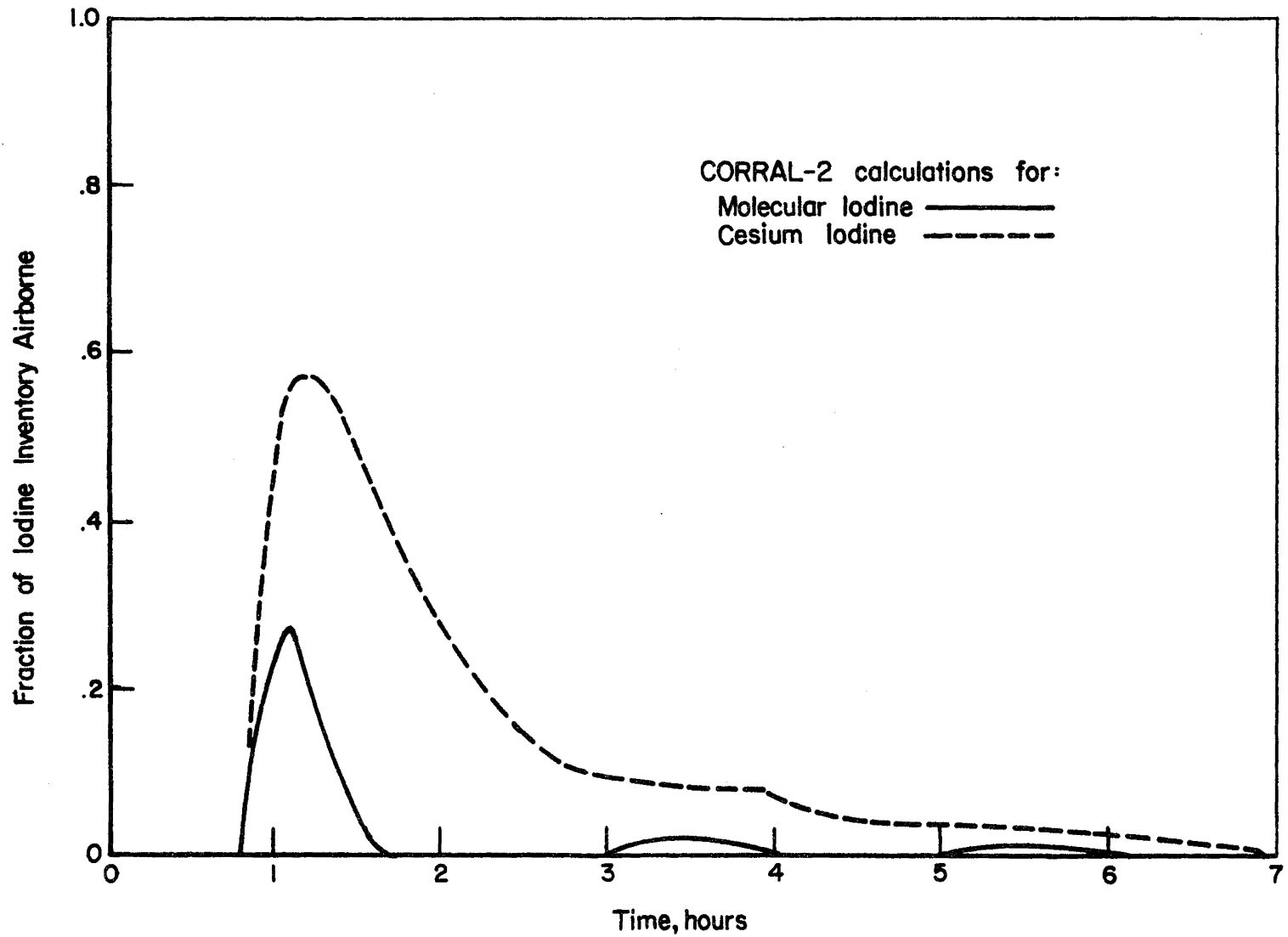


FIGURE 7.5. AIRBORNE CONCENTRATION FOR CASE WITH SPRAYS OPERATIONAL

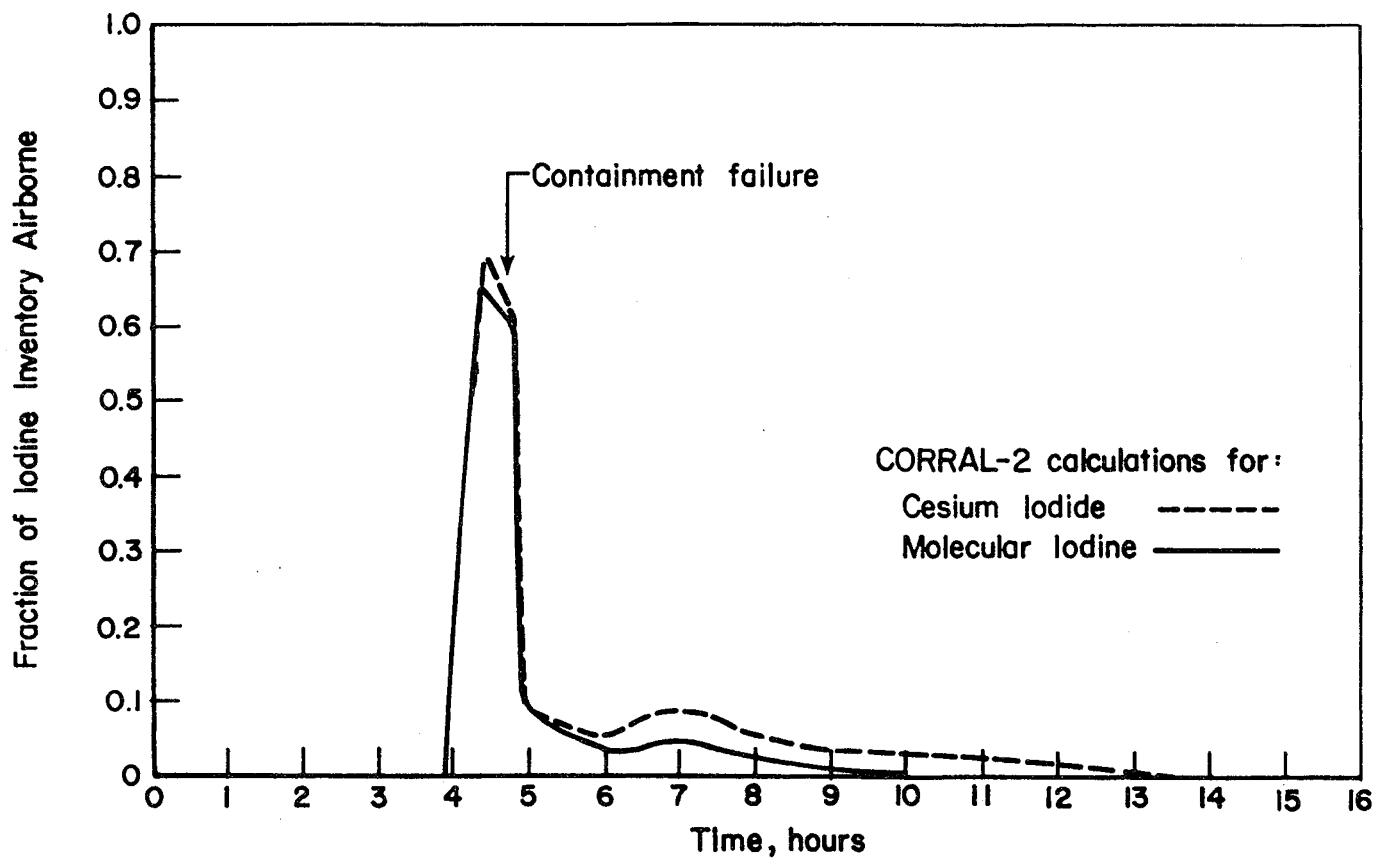
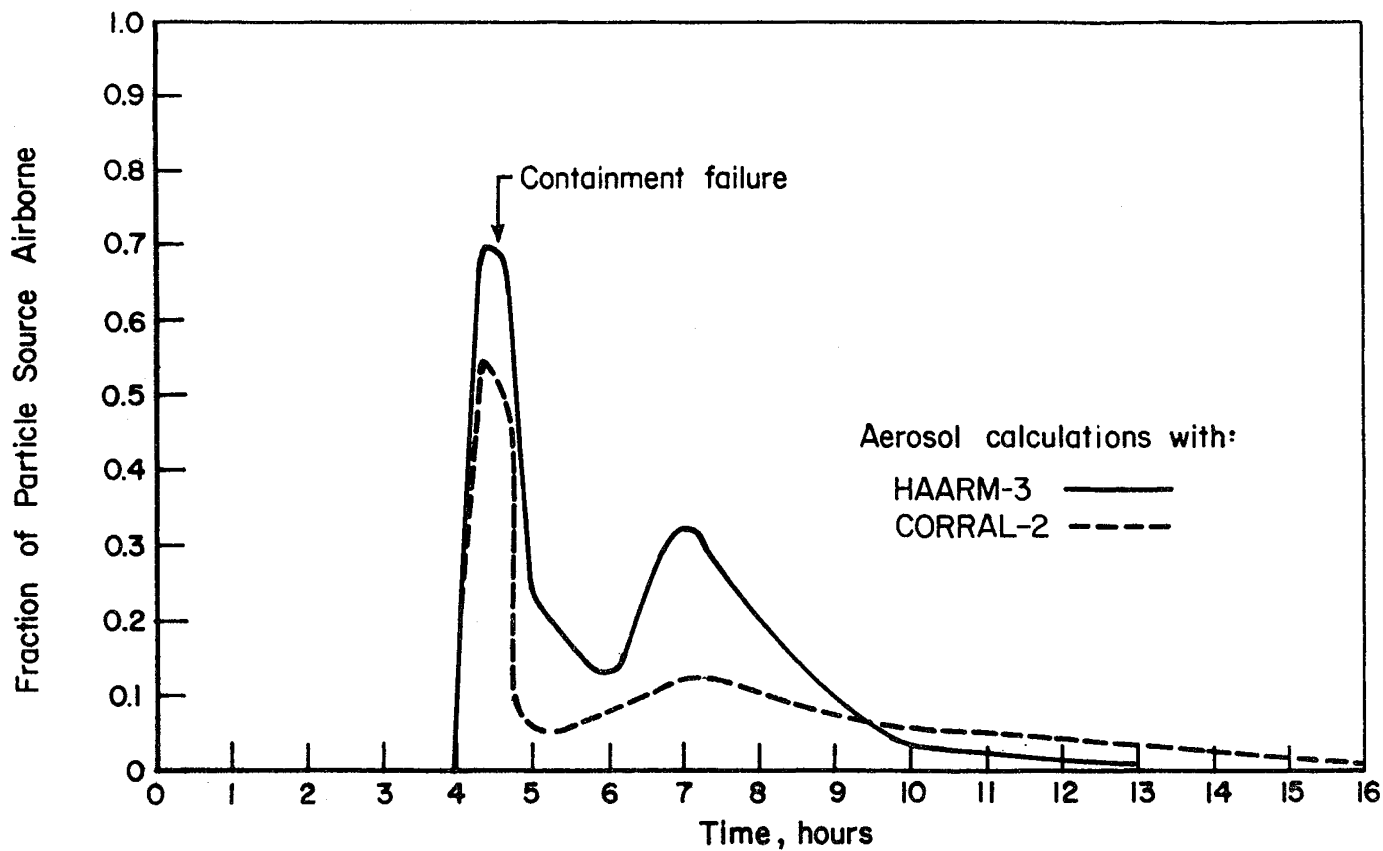


FIGURE 7.6. AIRBORNE CONCENTRATION FOR CASE WITHOUT SAFEGUARDS OPERATIONAL

coolant system must be taken into account. As indicated in Chapter 6, sequences of this type in which core meltdown would occur at high reactor coolant system pressure, could have significant agglomeration occurring. This would not only affect the quantity of mass reaching the containment but could also result in larger initial particle sizes than were assumed in the containment aerosol calculations.

If the containment survives the pressure pulse at the time of pressure vessel meltthrough, the pressure would decrease for a period of time as heat is transferred to the structures in the containment building. A number of hours later the pressure would again rise into the region in which containment failure would be expected. In Section 7.5 the results for a number of different codes are presented for the TMLB' sequence in which it is assumed that the containment does not fail. The effect of containment failure on mass leaked is illustrated in Figure 7.7. In general from the time-dependent decrease of airborne radioactive material the reader can infer the effect of a delay in time to containment failure on the magnitude of leakage to the environment.

Another type of sequence in which containment safety features are not effective is event V in which the release bypasses the containment. Results of CORRAL-2 analyses are provided in Table 7.3. The integrity of the auxiliary building would be lost very early in the accident sequence. Little retention of iodine is predicted to occur in the failed building regardless of chemical form.

Sprays Not Functional/Filtered Recirculation Operational. In some plant designs, the capability of the spray system in reducing airborne radioactivity is augmented by filters on the containment atmosphere cooling system. For accident sequences in which the sprays fail but the containment cooling system operates, the filters would be the principal mode of fission product removal if they are capable of accommodating the aerosol loading (see Chapter 8). In Figure 7.8 results are compared for HAARM-3 and CORRAL-2 analyses under the assumption that the filters are capable of withstanding the imposed aerosol loading. If the filters were to become overloaded, the subsequent falloff of airborne concentration would be less steep. Because of the high filter efficiency for either particulate or elemental iodine and the high flow rate through the coolers, the behavior of airborne iodine is seen to be independent of either the method of analysis or the assumed chemical form.

#### 7.4.3.2 Ice-Condenser Containment Design (PWR)

In this type of plant design, the ice which is used for vapor condensation would also be effective in removing iodine from the containment atmosphere. Because these designs have comparatively small volumes and low design pressures, the gases generated in a core meltdown accident including hydrogen generated from the oxidation of steel would result in a pressure buildup which would eventually result in containment failure. For most accident sequences, fission products released from the core would pass through the ice bed before entering the upper containment volume. In some sequences, however, the ice-bed would be bypassed or the ice would have melted by the time of fuel melting.

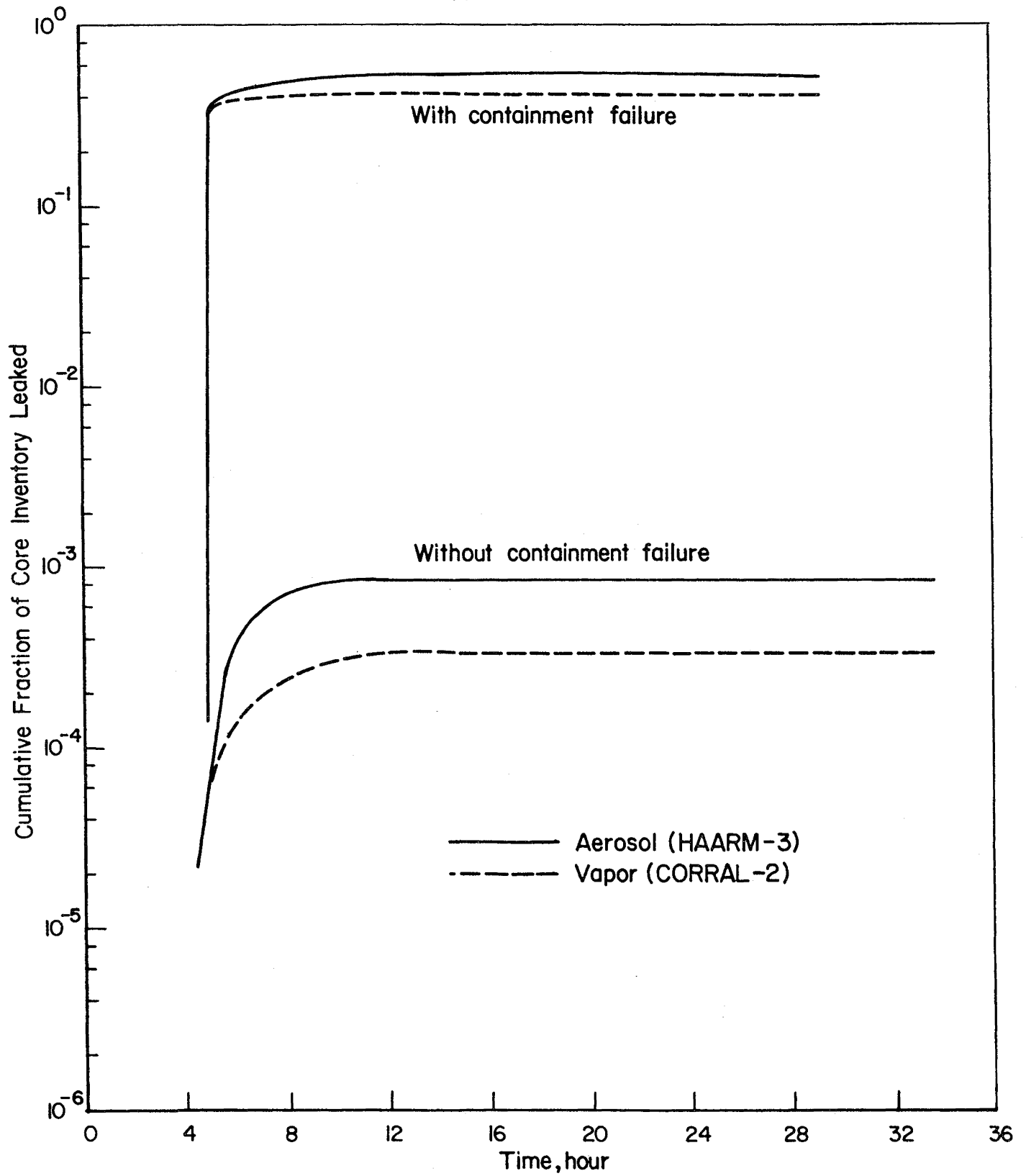


FIGURE 7.7. EFFECT OF CONTAINMENT FAILURE ON MASS LEAKED FROM CONTAINMENT

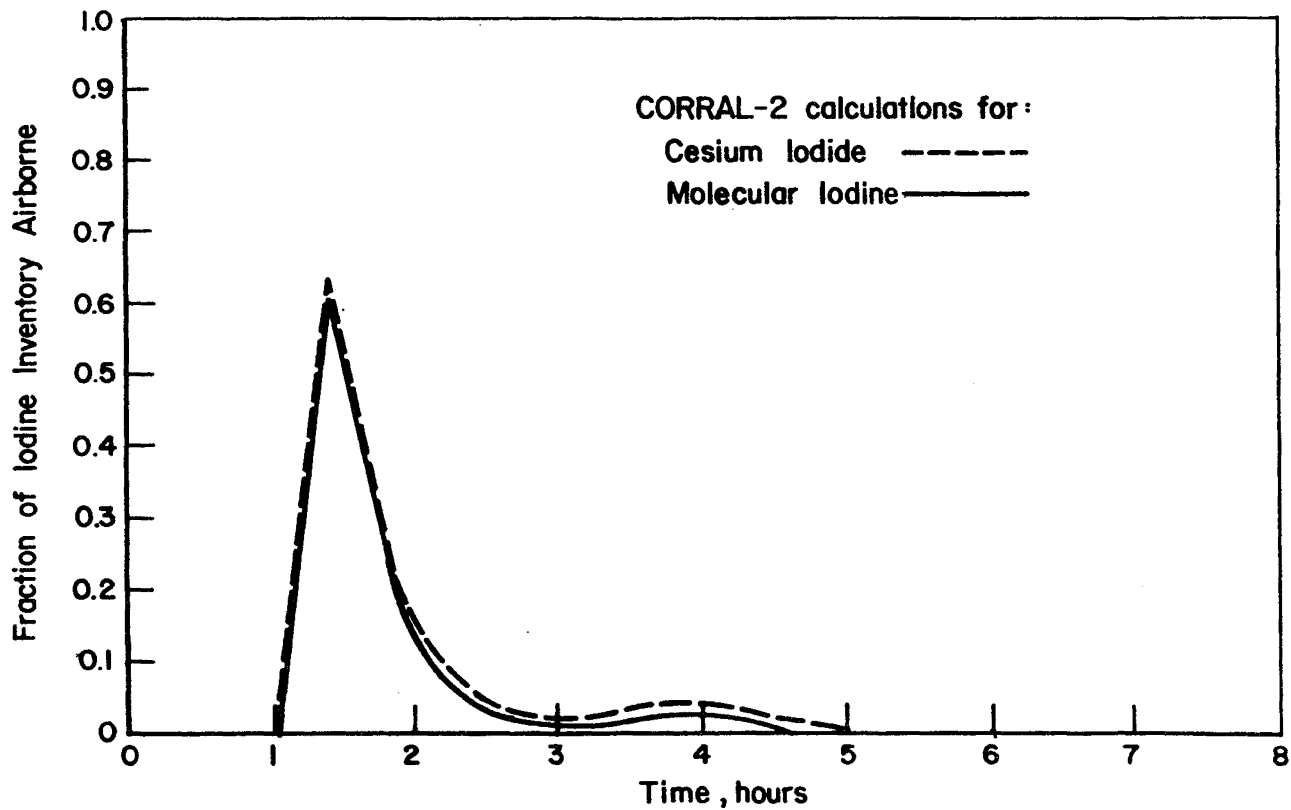
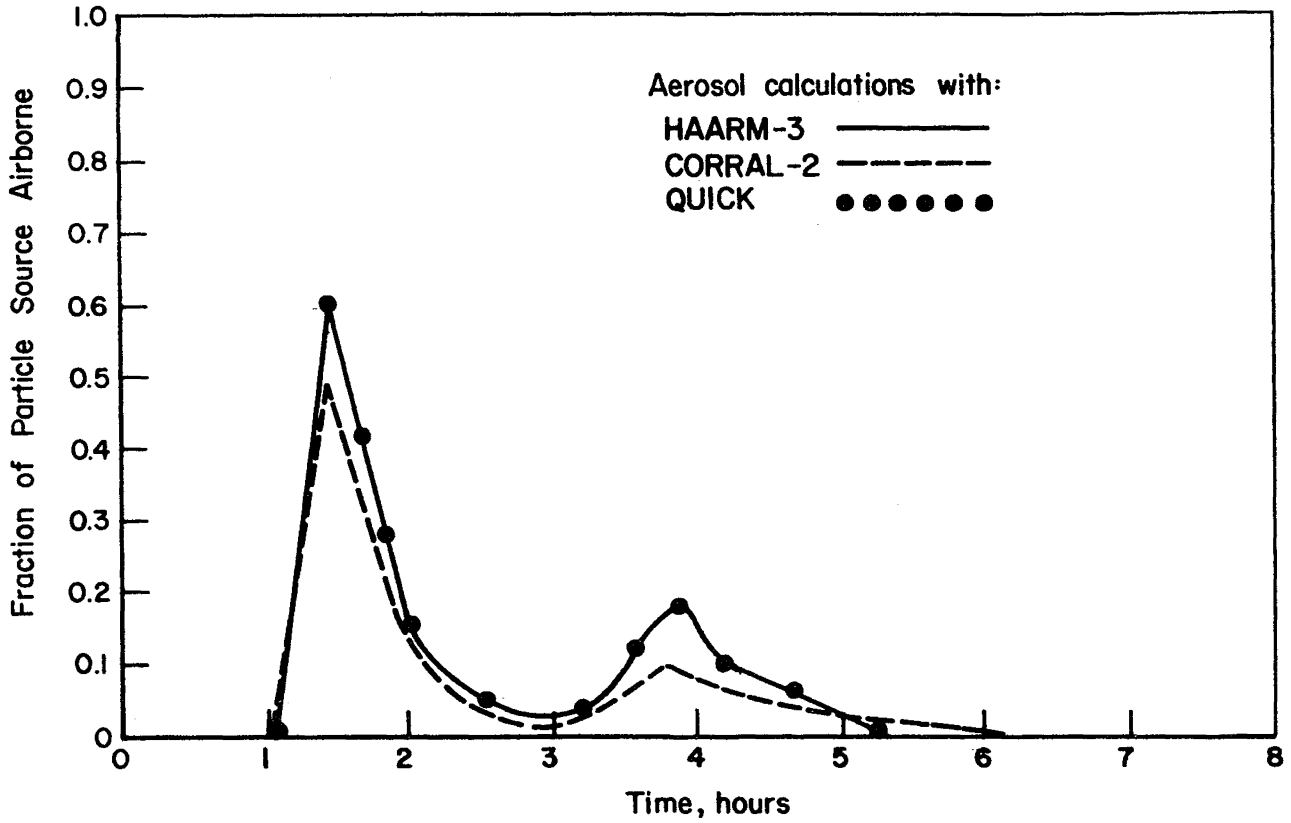


FIGURE 7.8. AIRBORNE CONCENTRATION FOR CASE WITHOUT SPRAYS BUT WITH RECIRCULATION FILTERS

Ice-Bed Functional. The CORRAL-2 code does not model the performance of an ice bed mechanistically. A decontamination factor is input by the user to apply to the flow as it passes through the bed. Westinghouse (7.4) has examined the scrubbing capability of ice beds for elemental iodine experimentally and found the decontamination factor to be very sensitive to the mass fractions of steam and non-condensable gases passing through the bed. There is no directly relevant empirical data for aerosol decontamination. Two cases were examined with the ice bed functional. For the AD sequence the containment was predicted to fail as the result of rapid hydrogen combustion. Nevertheless the release fractions from containment were calculated to be comparatively small. For the TMLB' sequence neither the spray system in the upper containment compartment nor the fans, that recirculate flow back to the lower compartment and through the ice beds, would be operational. Both sequences were examined parametrically for decontamination factors of 2 and 10. The fraction of radioactive material which leaves the reactor coolant system that is released from the containment to the environment is substantially larger for the TMLB' sequence. Analyses presented in Chapter 6 indicate, however, that significant retention of radioactive material would be expected in the reactor coolant system for this accident sequence.

Ice-Bed Not Functional. In the S<sub>2</sub>HF sequence the ice would have been melted and the spray system in the upper containment volume would be inoperative at the time of core meltdown. The results in Table 7.3 indicate that the natural deposition processes would provide only limited containment of iodine for this sequence particularly if in the form of aerosols.

#### 7.4.3.3 Pressure Suppression Containment Design (BWR)

The three basic designs for BWR containments involve the use of large water pools to condense steam released from the reactor coolant system in an accident. In addition to suppressing the pressure rise from the released steam, the water pool can act as a filter for radioactive materials. Because of the small volumes of the Mark I and II designs and the low design pressure of the Mark III design, the containment building cannot withstand the production of non-condensable gases in a core meltdown accident without failure.

Suppression Functional. For most core-melt accident sequences, the suppression pool would be expected to be subcooled during the melt period. As a result the pool would be effective in condensing steam and in removing fission products from the gases leaving the drywell. Some time would also be required for the pressure in containment to rise to the failure level, during which natural deposition could take place. The CORRAL-2 code does not model decontamination in suppression pools. Decontamination factors for the suppression pools were therefore treated parametrically for all of the sequences analyzed (see Appendix E). For the sequence AE in a Mark I design, decontamination factors of 10, 100, and 1000 were assumed. Following failure of the containment, a further decontamination is calculated as the gases flow up the narrow annular region between the wall of the drywell and the adjoining structural wall. The results in Table 7.3 indicate that the consequences of this sequence would be comparatively small. Direct comparisons between the results for the two different chemical forms of iodine assumed are not appropriate because decontamination in the suppression pool, which was treated the same for both forms, is the principal retention mechanism.

CORRAL-2 results are also presented in Table 7.3 for sequence TQUV in a Mark III containment design. Decontamination factors of 100 and 1000 were assumed for the suppression pool. Although the releases for this sequence are greater than for the previous case, the consequences would still be comparatively small.

Because of the importance of the suppression pool in these accident sequences, it cannot be inferred from the CORRAL-2 analyses which of the assumed chemical forms for iodine is the more conservative.

Suppression Not Functional. In some accident sequences, the suppression pool would be boiling at the time of fission product release from the fuel. The amount of decontamination that could occur in the pool is quite uncertain, particularly since there is some possibility of containment failure occurring in the region of the suppression pool. Two sequences of this type have been examined: TC, in which the suppression pool is rapidly heated as the result of failure to shutdown the reactor, and TW, in which the system for cooling the suppression pool fails. Both sequences were analyzed for a specific plant design with a Mark I type of containment. Based on analyses presented in WASH-1400, it was assumed in the analyses that failure of the Mark I containment design would occur in the suppression pool area and that water loss would impair the decontamination capability of the pool. Decontamination factors were treated parametrically with values of 1 and 10 for both sequences. In the TC sequence examined, the flowpath after containment failure was up the annular region external to the drywell and through the failed secondary containment to the environment. The containment failure mode examined for the TW sequence involved the most adverse failure location, which results in a direct release to the environment. The results in Table 7.3 indicate that the quantity of radioactive material released in these sequences can be quite large.

The principal uncertainties affecting the magnitude of release appear to relate to the mode of containment failure and its subsequent impact on the performance of engineered safety features and to the amount of retention of fission products that would occur within the reactor coolant system. The location of containment failure and the response of engineered systems is expected to be very plant design dependent. For example, in later plants, coolant injection pumps have been designed to pump saturated water, which significantly decreases the likelihood of core meltdown in a TW sequence. Similarly the likelihood of containment failure in a location which would defeat the decontamination capability of the suppression pool in a Mark III design appears to be very small.

In all of the sequences examined for the Mark I design, failure of the containment building would immediately result in failure of the surrounding secondary containment building. The Standby Gas Treatment System in the secondary containment building would therefore be expected to have little value in limiting the consequences of a core meltdown accident.

## 7.5 Uncertainties and Parametric Studies

Calculational procedures employed to predict radionuclide transport and deposition are all based on assumptions regarding specific rate mechanisms, interactions among competing mechanisms and physical properties. For example, uncertainties exist in constants used in rate expressions and it is of interest to know the importance of such uncertainties on the resulting predictions of radionuclide transport. In a similar fashion, uncertainties exist in the assumed or predicted accident conditions. In this case variations in the assumed conditions can also be related to the effects of different conditions on transport predictions, i.e., to how the predicted results would differ if the accident conditions were different. In this section the importance of such uncertainties, changing conditions, or altered assumptions are discussed.

### 7.5.1 Particulate Transport and Deposition

Based on special calculations performed with the HAARM-3, QUICK, NAUA and CORRAL-2 codes for the specific accident sequences considered in this report as well as on code predictions available in the literature, the effects of major parameters, accident sequence, and importantly, source characteristics can be assessed. Although fission product behavior in a containment is discussed in general terms for all possible core meltdown accident sequences, the TMLB' sequence was selected for specific discussion. This particular accident sequence has relatively dry conditions and is regarded as one of the most likely cases that lead to a very high rate of leakage to the environment since no safety features are assumed to operate because of loss of electric power. Assumed leak rate and the calculated aerosol mass released to the outside atmosphere in each run are listed in Table 7.4. Since the listed calculations did not use the same leak rate, the leaked aerosol mass per unit leak rate (i.e., 1 percent per day) has additionally been shown. The results show that a decrease in the aerosol mass from 2000 kg to 1000 kg causes the leaked mass to decrease by about 30 percent. In order to demonstrate this effect, the calculated leaked masses have been calculated further using HAARM-3 as a function of source amount. The results are shown in Figure 7.9. It is seen that while leaked mass increases linearly with increasing source when aerosol source mass is small, the leaked mass starts deviating from linearity at a source of about 500 kg apparently due to the increased amount of mass deposited in the containment.

In Table 7.4, the role of steam source on aerosol behavior mechanisms as predicted by the NAUA code is seen to be that of reducing the airborne mass concentration. It is postulated that the small difference of about 20 percent between the dry case and the steam source case for TMLB' was due to the rather short period of condensation predicted by the thermal hydraulic calculations. The NAUA calculations also show that with forced temperature decrease as might be expected with spray injection, the aerosol concentration decreased markedly causing the leaked mass to be reduced accordingly. With such a forced temperature decrease, the condensation mechanism is enhanced thereby enhancing aerosol deposition. The effect of steam condensation in the containment needs to be more extensively investigated and calculations performed for additional accident sequences. The effects of condensation could be more significant for sequences other than TMLB'.

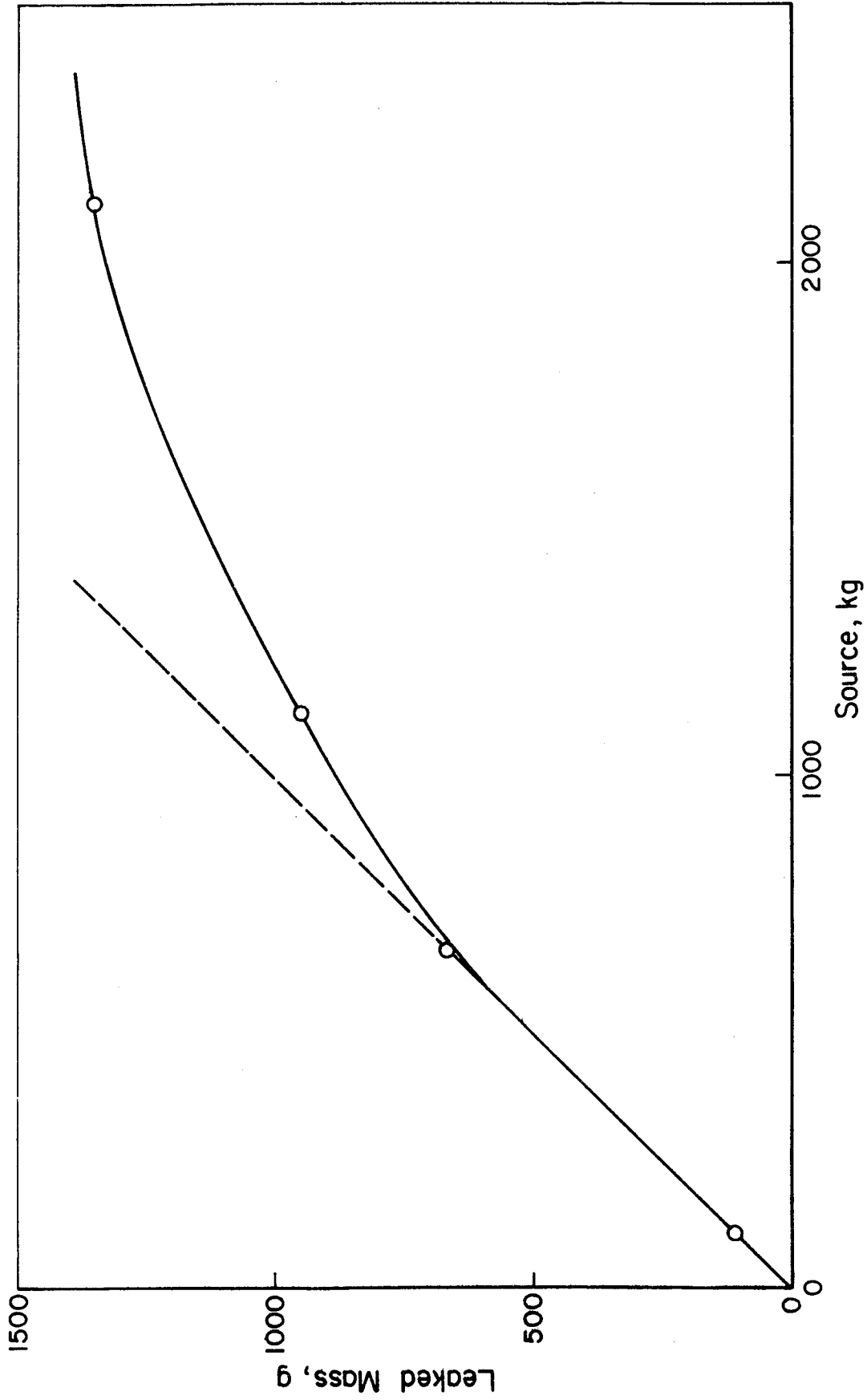


FIGURE 7.9. EFFECT OF PARTICLE SOURCE ON MASS LEAKED FROM CONTAINMENT

TABLE 7.4. COMPUTER CALCULATION RESULTS FOR HYPOTHETICAL ACCIDENT CONDITIONS

Release Type	Reactor Size	Code	Total Released Fuel Aerosol Mass kg	Assumed Leak Rate percent/day	Leaked Aerosol Mass g <sup>(a)</sup>	Leaked Aerosol Mass Per Leak Rate g/(percent/day) <sup>(a)</sup>
AB	1300 MWe	NAUA-3	2000	0.25	1186 (1146)	4744 (4584)
			1000	0.25	754 (711)	3016 (2844)
			100	0.25	172 (156)	688 (624)
			1000 <sup>(b)</sup>	0.25	(239)	(956)
Constant Source Release	650 MWe	NAUA-3	1000	0.1	120	1200
		HAARM-3	1000	0.1	140	1400
		AEROSIM	1000	0.1	90	900
TMLB'	775 MWe	HAARM-3	2000	1.0	1350	1350
			1000	1.0	960	960
TMLB'	775 MWe	CORRAL-2	2000	1.0	2090	2090
			1000	1.0	1070	1070
TMLB'	775 MWe	NAUA-3	2000	1.0	2162	2162
			1000	1.0	1511	1511
		NAUA-4	2000	1.0	1437	1437
			1000		1061 (796) <sup>(c)</sup>	1061 (796) <sup>(c)</sup>

(a) Values in parentheses were calculated with steam condensation considered and except as noted in footnote (c), assume steam input into the containment of 15 kg/sec.

(b) This case assumed a forced temperature.

(c) Steam input and containment thermal conditions were taken from MARCH calculations.

It is also seen in Table 7.4 that there exist considerable discrepancies among the calculated leaked aerosol masses depending on the choice of code even with identical source terms. Differences in the input data such as temperature and pressure, aerosol size distribution parameters, and reactor size as well as the mechanisms and models employed in the codes are considered to be the reasons.

Figures 7.10 and 7.11 compare the airborne particulate concentrations calculated by HAARM-3 and QUICK. The accident sequence TMLB' with aerosol sources of 1000 kg and 2000 kg were used for the comparison. It is seen that there is good agreement between the two calculated results. In order to compare calculations made with other codes, calculated results for the TMLB', 1000 kg source as obtained with the HAARM-3, QUICK, NAUA-3 and CORRAL-2 codes are included in Figure 7.12. The fraction of airborne mass to the total aerosol introduced was used for the comparison. Reasonable agreement exists among the results obtained with the various codes and it is seen that at the peak concentration, the highest concentration is about 1.5 times the lowest. There are, however, significant differences in the time dependent behavior of the concentration. Figure 7.13 shows suspended mass concentrations for various sources ranging from 100 to 4000 kg as calculated with the HAARM-3 code. It can be observed that as the source rate was varied by 40 fold, the resulting maximum concentration ranged from 1.5 to 60  $\mu\text{g}/\text{cc}$  which shows roughly the same proportion.

#### 7.5.2 MARCH/CORRAL-2 Uncertainty Analyses

Recognizing that many of the models are not well validated in the codes that are used to analyze the thermal-hydraulic behavior and the transport of radioactivity in core meltdown accidents, uncertainty analyses have been performed for the MARCH/CORRAL-2 computer codes. Table 7.5 provides the 90 percent confidence interval obtained from these analyses for iodine in the molecular and particulate forms for two of the high consequence core meltdown accidents that were found to be major contributors to risk in the Reactor Safety Study. It should be recognized that these analyses do not account for any retention that could occur in the reactor coolant system. Since the uncertainty analysis was made for a limited set of parameter and model variations, it is expected that the true uncertainty interval is broader than shown in this table. The principal source of the uncertainties shown for the fraction of iodine released to the environment was found to be the uncertainty in the deposition mechanisms in the containment. The uncertainty results which are presented do not account for uncertainties in the retention of radioactive material in the reactor coolant system.

TABLE 7.5. UNCERTAINTY SPREAD FOR PREDICTED RELEASE FRACTIONS

Assumed Form of Iodine	Fraction of Core Inventory Leaked					
	PWR, TMLB'			BWR, TC		
	Lower*	Mean	Upper*	Lower*	Mean	Upper*
Elemental	0.05	0.18	0.30	0.001	0.08	0.16
Particulate	0.10	0.38	0.66	0.06	0.25	0.43

\*90 percent confidence interval.

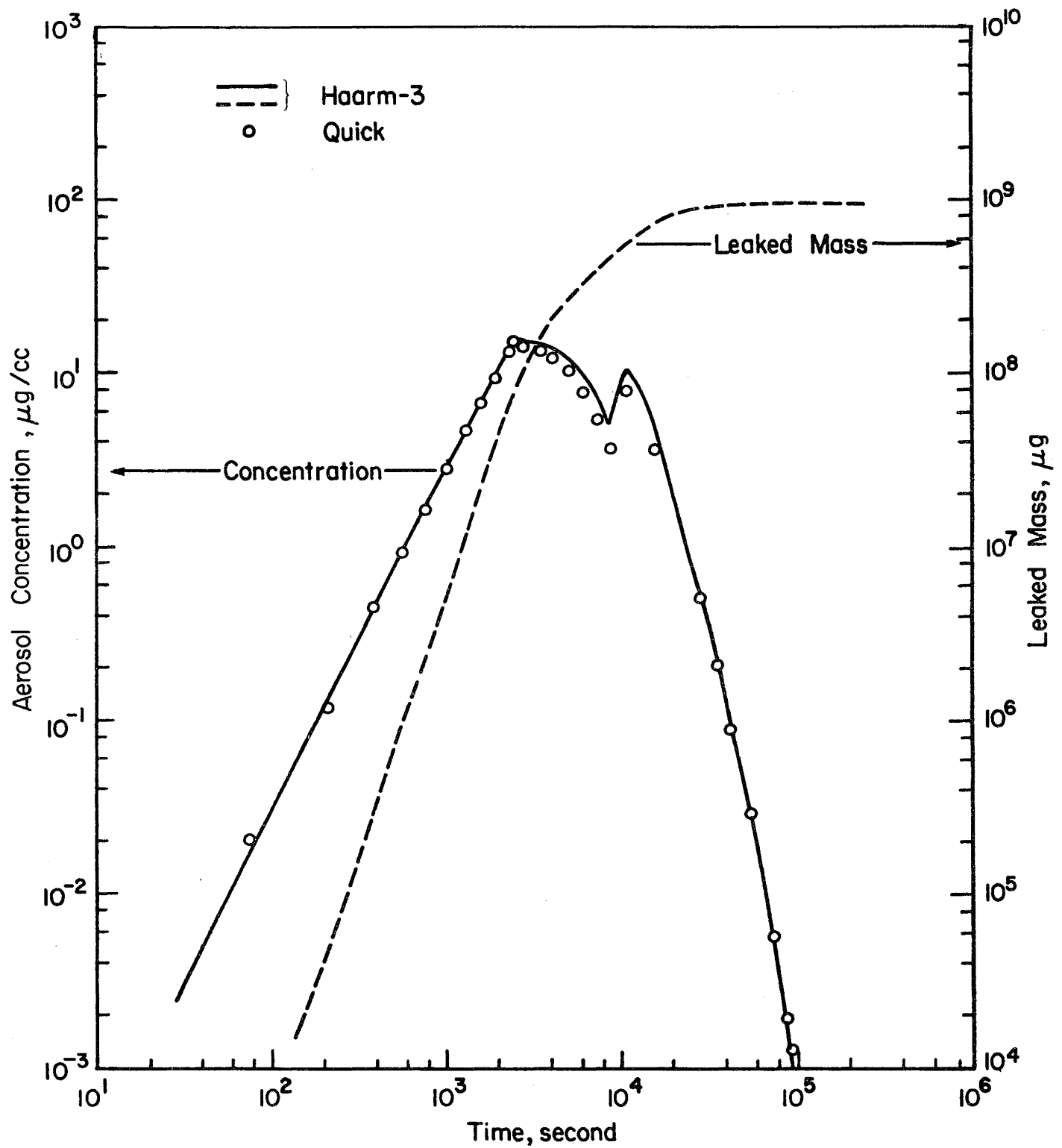


FIGURE 7.10. AIRBORNE AEROSOL CONCENTRATIONS PREDICTED FOR TMLB' WITH 1000 kg AEROSOL SOURCE

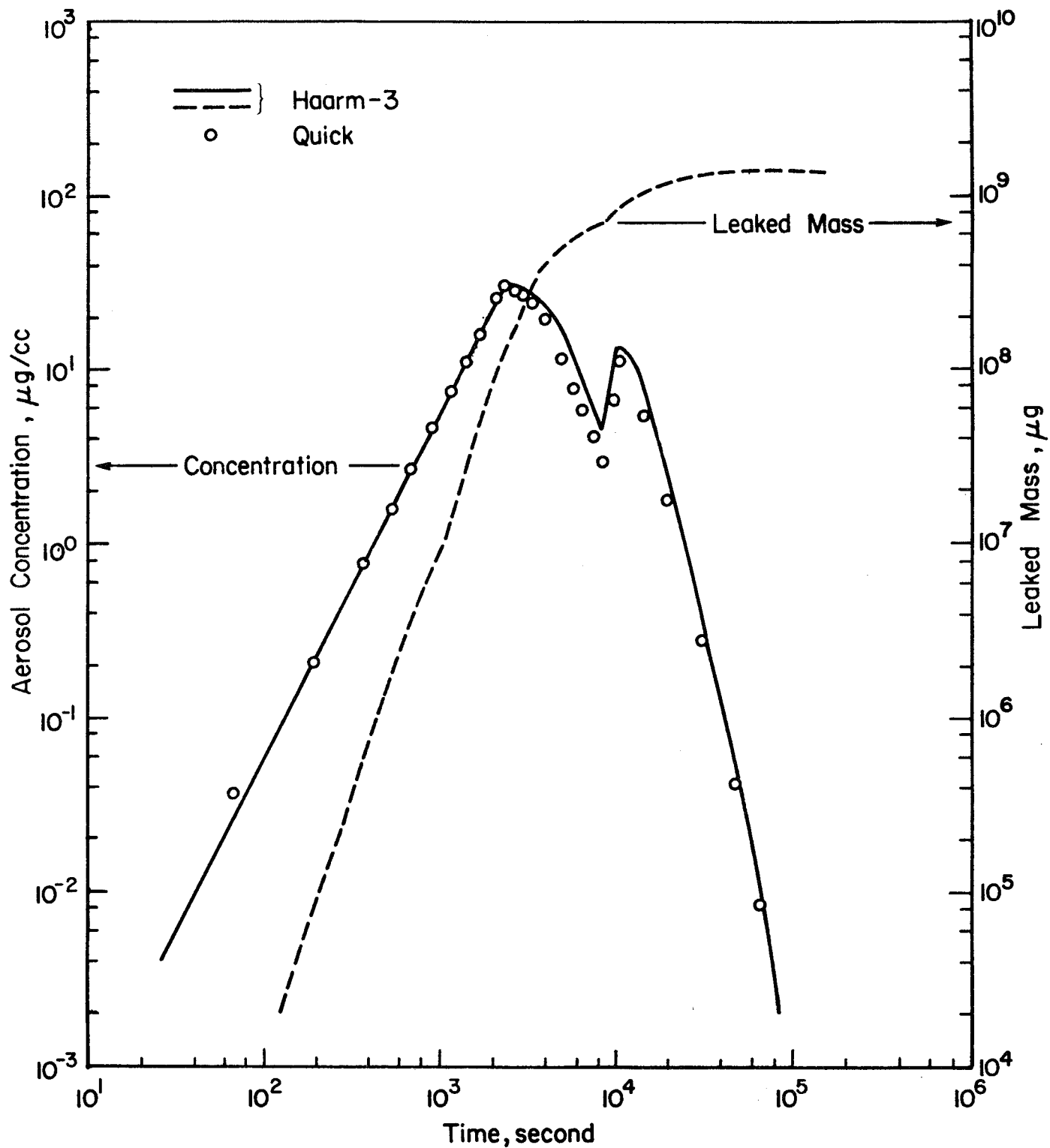


FIGURE 7.11. AIRBORNE AEROSOL CONCENTRATIONS PREDICTED FOR TMLB' WITH 2000 kg AEROSOL SOURCE

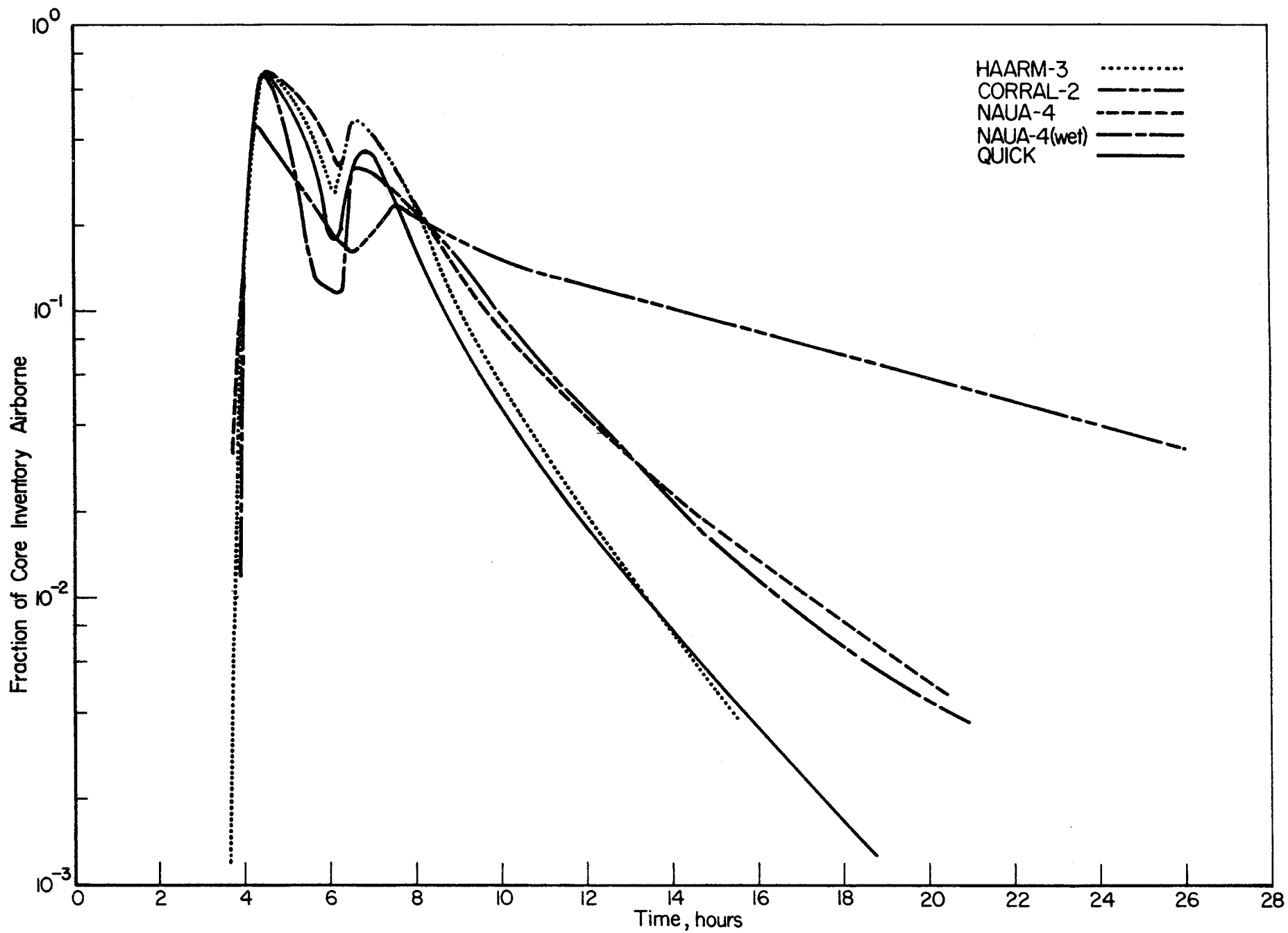


FIGURE 7.12. COMPARISON AMONG HAARM-3, CORRAL-2, NAUA-4 AND QUICK FOR TOTAL AIRBORNE PARTICULATE

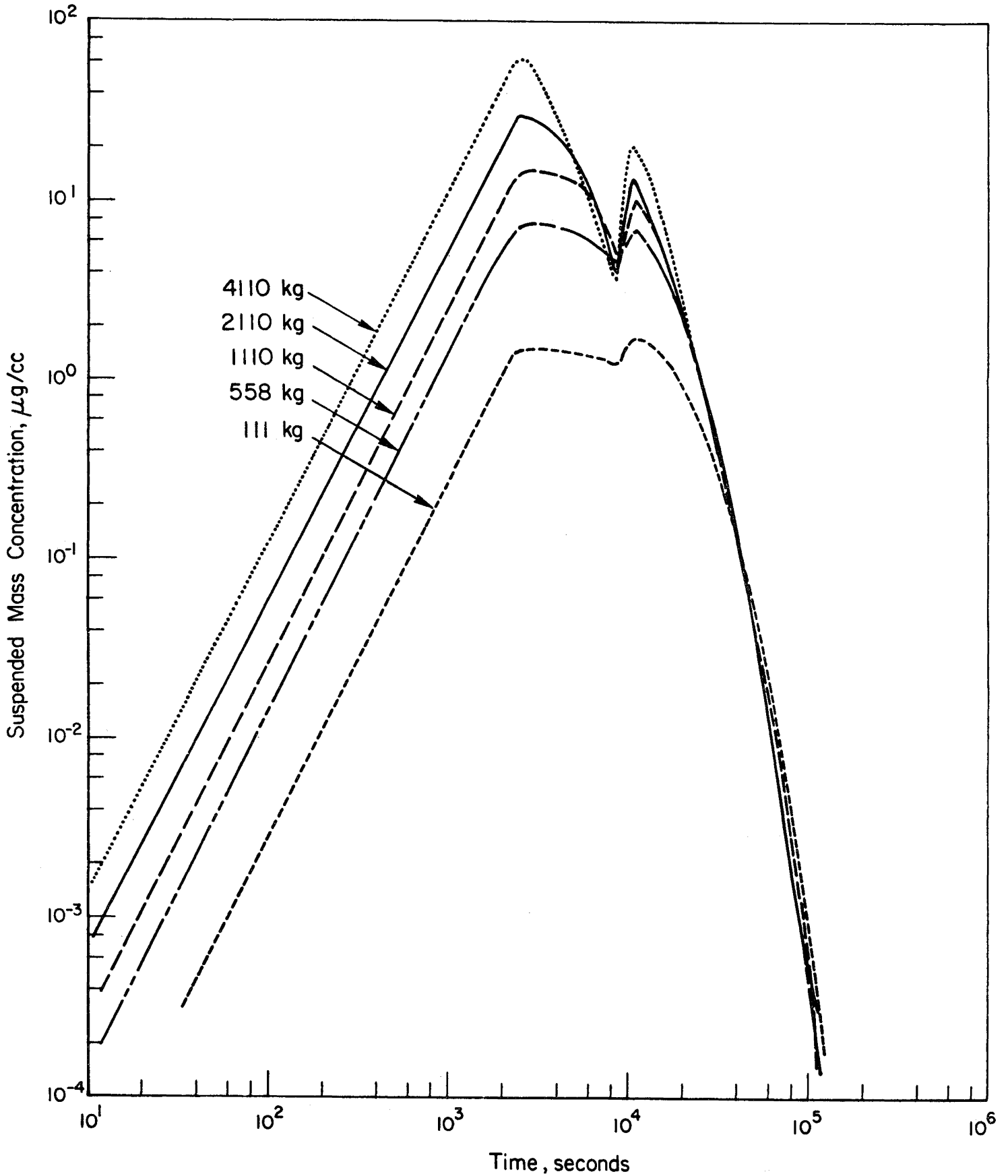


FIGURE 7.13. EFFECTS OF SOURCE AEROSOL ON AIRBORNE CONCENTRATION, HAARM-3 CODE CALCULATIONS

### 7.5.3 Distribution of Fission Products

It is of importance and interest in nuclear reactor safety analysis to examine how aerosol particulates are distributed at various phases of an accident. In general, the total amount of source particulates may be divided into those airborne, leaked outside the containment, deposited on the walls, and settled on the floor. The distribution among these locations depends upon aerosol behavior mechanisms which take place in the containment. In order to examine these effects, the distribution of aerosol among the various locations was analyzed for the TMLB' case without containment failure using the HAARM-3 computer code. Since aerosol behavior mechanisms are expected to be governed by source amount, distributions of the aerosols at two different times were calculated for different source amounts. The results are shown in Table 7.6. Fractions of each amount in percent are shown in Figures 7.14 and 7.15. It is seen from Figure 7.14 that at 3 hours after the source initiation, a considerable amount of particulates remains suspended. As the source rate for aerosol increases, the relative amount of mass airborne is seen to decrease. This can be attributed to the fact that particles agglomerate to become large and settle to the floor at a faster rate when the source rate and hence airborne concentration is greater. As shown in Figure 7.15, very little remains suspended at 50 hours after the source initiation. The amount settled on floor is seen to be relatively large with increasing source amount.

### 7.6 Radionuclide Transport Through the Containment Barrier

Radionuclides airborne as gases, vapors or particles within the containment are expected to be emitted to the ambient atmosphere by leakage through the containment structure. The amount of material leaked will be dependent on the concentration of airborne radionuclides, the reactor type, the assumed accident sequence, and attenuation along the leak path.

For accident sequences in which the containment remains intact, transport through the containment barrier occurs along small leak paths with flows corresponding to the design leak rate. Higher leak rates may be possible if partial containment failure occurs resulting from stresses arising during the accident. For the design leak rate it is likely that if aerosols are present, plugging of leak paths will occur. However, experiments in the Markiven full-scale containment have indicated increased gas leakage following primary blowdown.

Morewitz, et al.(7.19) reviewed the data on aerosol plugging and Vaughan(7.20) has correlated the data with a simple model,

$$\bar{m} = KD^3,$$

where  $\bar{m}$  is the total mass that leaks through a leakage path before it plugs, D is the duct diameter ( $LW^2$  is used instead of D if the leak is through a slit of cross section LxW), and K is a constant  $\approx 50$  g/cc

TABLE 7.6. DISTRIBUTION OF AEROSOL PARTICULATES FOR TMLB' AS CALCULATED BY HAARM-3

Time	Source kg	Distribution, kg			
		Floor	Wall	Airborne	Leaked
3 hrs	111	16.6	2.5	91.5	0.083
	558	196.2	8.5	352.0	0.354
	1110	571.4	11.5	523.5	0.577
	2110	1415.0	13.5	673.8	0.867
50 hrs	111	77.8	32.7	$8.4 \times 10^{-5}$	0.2
	558	495.5	60.9	$3.1 \times 10^{-4}$	0.7
	1110	1038.0	67.6	$4.2 \times 10^{-6}$	1.0
	2110	2019.0	83.2	$6.4 \times 10^{-4}$	1.4

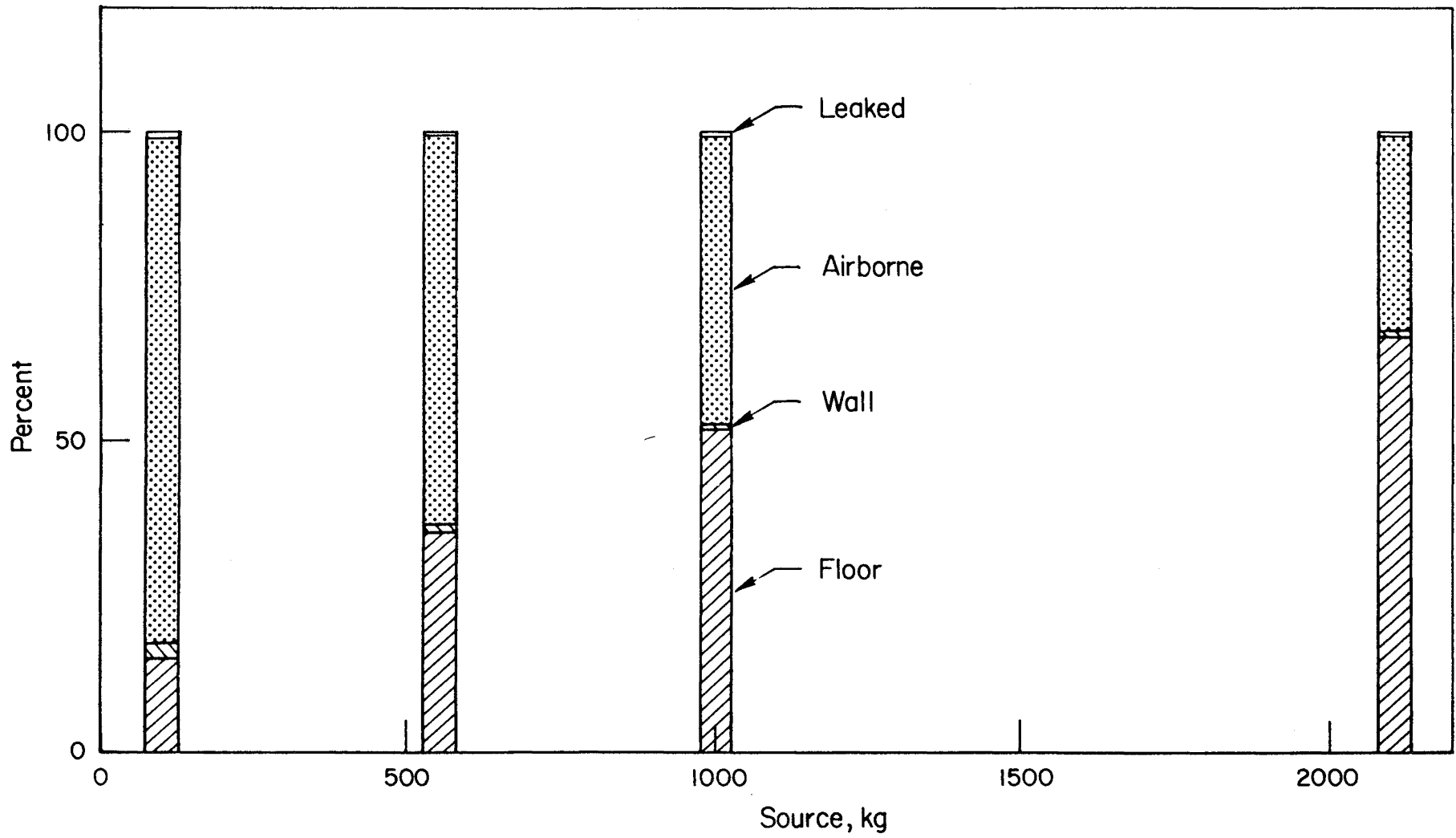
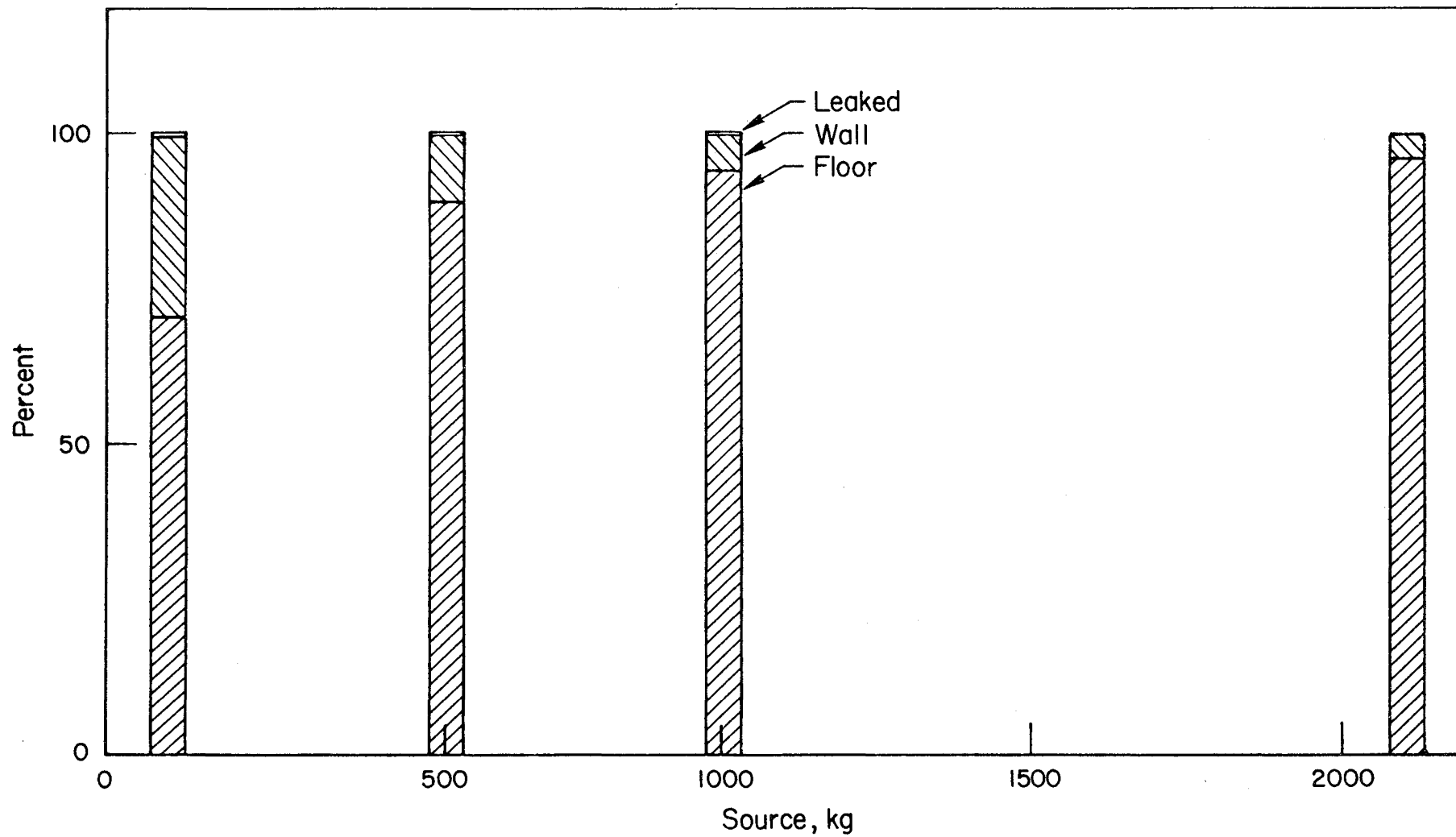


FIGURE 7.14. DISTRIBUTION OF PARTICULATE MASS AFTER 3 HOURS AS CALCULATED BY HAARM-3 FOR TMLB'



7.38

FIGURE 7.15. DISTRIBUTION OF PARTICULATE MASS AFTER 50 HOURS AS CALCULATED BY HAARM-3 FOR TMLB'

This correlation has been shown to be applicable for a wide range of aerosol types, leak rates, and duct diameters up to as big as 30 cm. Realizing that some attenuation by deposition along the leak path will occur and applying this correlation to leak path dimensions commensurate with a design leak rate of 0.1 volume percent per day indicates that quite small amounts of aerosol will be leaked before plugging will occur.

Examination of the results of accident sequences presented in Table 7.3 indicates, however, that the environmental release of radioactive materials through the design leak rate is very small in comparison to the release that occurs after failure of the containment in severe accident sequences. Although it is possible that some attenuation could occur along the leak path following containment failure, in general the mode and location of containment failure is so uncertain that retention cannot be assured. In the Mark I design the annulus external to the drywell presented a well-characterized pathway that would be followed by escaping gases for certain containment failure locations. In most cases, however, transport behavior in failed containments and buildings external to the containment is quite speculative.

### 7.7 Radionuclide Transport Outside the Containment

Once gases, vapors, or particles are emitted into the ambient air from a stack, vent, or leak, they mix in the same manner as the atmosphere into which they are dispersed except for particles large enough to have a net settling force in air. Particulate matter, if it is of a size small enough to remain suspended in the air more than a few seconds will mix within the atmosphere in the same fashion as gases. The emitted materials will undergo vertical dispersion, crosswind dispersion, and transport with the wind as controlled by the atmospheric stability, wind speed, wind direction, and the local turbulence set up by elevated structures, vegetation, or topography. During their residence in the air the gases and particles may undergo chemical and physical transformation before they are ultimately removed by dry deposition or by precipitation scavenging.

Mathematical dispersion models are routinely used to predict the ambient concentrations of radioactive materials released into the air. Currently, the most popular type of models, the gaussian type, portrays the plume as having an elliptic cross section which expands with distance downwind in response to the atmospheric turbulence. Source parameters including emission rate, source height, exit velocity and plume buoyancy are parameters required for insertion into the models' controlling equation. Standard empirical dispersion coefficients and wind speed are the other parameters needed for calculations. Models can predict short-term (one-hour or less) ambient concentrations with a single set of parameters, or longer term concentrations when the joint frequency of wind speed, wind direction and atmospheric stabilities are available for longer periods. Variations on the standard model can handle instantaneous releases, topographic influences, and downwash of the plume caused by flow over obstacles. Other algorithms can be used with the dispersion model to depict radiological decay, chemical transformation, dry deposition and deposition by precipitation. Dry deposition is given in terms of deposition velocities derived from experimental studies and precipitation scavenging is based on a combination of experimental results and theoretical analyses. In a few cases attenuation can be

calculated as a function of aerosol particle size. Such capabilities need improvement and expanded use since the most significant property of the emitted radionuclides determined by the accident sequence is probably the particle size.

Particle size would be expected to be a major factor in controlling both the dry deposition and precipitation scavenging of particulate releases. For example, if particle sizes are greater than about 10 to 20  $\mu\text{m}$ , loss from the plume by dry deposition could significantly exceed that predicted by currently assumed deposition velocities. If iodine is released from the containment in a form associated with large particles, there could be considerable attenuation and further analyses of such effects seem warranted as better predictions of aerosol properties in the containment become available.

### 7.8 Effect of Radionuclide Source on Release From Containment

In Chapter 6 the influence of the assumed chemical form of iodine on the predicted release to the containment atmosphere was investigated. In this chapter the same types of comparisons were made for the transport and deposition of iodine in the atmosphere of the containment building. In general, the analyses indicated that the behavior of elemental and particulate iodine would not be dramatically different. For most sequences, less retention was predicted with the CORRAL-2 code for particulate iodine than for elemental iodine. The differences were well within the uncertainties of the analysis techniques, however.

In some instances relevant data could not be found to evaluate the comparative behavior of the two iodine forms. This was particularly true of the potential for iodine retention in suppression pools and ice beds. Although some data were identified for elemental iodine behavior in pools and ice beds, directly relevant data for particulates are not available.

Although it is recognized that iodine could be released from the reactor coolant system as cesium iodide and subsequently oxidized to the elemental form due to conditions in the containment, this effect was not examined directly in this chapter.

The source term for release of radionuclides and other materials as described in Chapter 4 indicates that the composition of the released material varies with time. Most notable is the early time release of iodine and cesium relative to much of the less volatile materials. This means that for particulate releases, the composition of airborne materials, the deposited material, and the leaked mass will each have different compositions and these compositions will vary with time.

References

- 7.1 Hilliard, R. K., and L. F. Coleman, "Natural Transport Effects on Fission Product Behavior In the Containment System Experiment", BNWL-1457, Battelle, Pacific Northwest Laboratories, Richland, WA 99352, June 15, 1973.
- 7.2 Reactor Safety Study, WASH-1400, Appendix VII (1975).\*
- 7.3 Dadillon, J., and Geisse, G., "Diffusion de l'Iode a Travers l'Eau Experience Piree", CEA-R3199 (1967).
- 7.4 Malinowski, D. D., "Iodine Removal in the Ice Condenser System", WCAP-7426 (March 1970).
- 7.5 "Nuclear Aerosols in Reactor Safety", CSNI/SOAR No. 1 (June 1979).
- 7.6 Gieseke, J. A., K. W. Lee, and L. D. Reed, "HAARM-3 Users Manual", BMI-NUREG-1991 (January 5, 1978).
- 7.7 Gieseke, J. A., H. Jordan, and K. W. Lee, "Aerosol Measurements and Modeling for FRS, Quarterly, January-March, 1979", NUREG/CR-1165, BMI-2037 (January 1980).\*\*
- 7.8 Jordan, H., P. M. Schumacher, J. A. Gieseke, and K. W. Lee, "Multiple Zone Aerosol Behavior Model", NUREG/CR-1294, BMI-2042 (January 1980).\*\*
- 7.9 Gieseke, J. A., K. W. Lee, H. Jordan, P. M. Schumacher, and E. W. Schmidt, "Aerosol Measurements and Modeling for Fast Reactor Safety", NUREG/CR-1776, BMI-2060 (October 1980).\*\*
- 7.10 Gieseke, J. A., R. C. Behn, A. S. Chace, and L. D. Reed, "Analytic Studies of Aerosol Behavior Predictions for Fast Reactor Safety", BMI-1932 (March 18, 1975).
- 7.11 Gieseke, J. A., and L. D. Reed, "Aerosol Behavior Modeling for Fast Reactor Safety: FY 1975 Annual Report", BMI-X-662 (October 1975).
- 7.12 Gieseke, J. A., L. D. Reed, E. W. Schmidt, and H. Jordan, "Aerosol Measurements and Modeling for Fast Reactor Safety: Annual Report for FY1976 and FY1976T", BMI-NUREG-1963 (December 1976).
- 7.13 Gieseke, J. A., H. Jordan, K. W. Lee, B. Vaishnavi, and L. D. Reed, "Aerosol Measurements and Modeling for Fast Reactor Safety: Annual Report for FY1977", BMI-NUREG-1989 (December 23, 1977).
- 7.14 Gieseke, J. A., K. W. Lee, H. Jordan, and L. D. Reed, "Aerosol Measurements and Modeling for Fast Reactor Safety", NUREG/CR-0676, BMI-2021 (February 1979).
- 7.15 Kress, T. S. (ed.), "Proceedings of the CSNI Specialists Meeting on Nuclear Aerosols in Reactor Safety", NUREG/CR-1724, ORNL/NUREG/TM-404, CSNI-45 (October 1980).\*\*

- 7.16 Postma, A. K., R. L. Ritzman, J. A. Gieseke, and E. W. Schmidt, "Models for Predicting the Removal of Airborne Contaminants by Reactor Containment Sprays", BNWL-B-417 (June 27, 1975).
- 7.17 Postma, A. K., L. F. Coleman, and R. K. Hilliard, "Iodine Removal from Containment Atmospheres by Boric Acid Spray", BNP-100 (July 1970).
- 7.18 Schoeck, W., Private Communications (March 1981).
- 7.19 Morewitz, H. A., et al., "Annual Technical Progress Report, LMFBR Safety Program, Government Fiscal Year 1977", AI-DOE-13210 (1977).
- 7.20 Vaughan, E. U., "Aerosol Leakage Model, Quarterly Progress Report, LMFBR Safety Program October-December 1977", AI-DOE-13723 (1978).

\*Available free upon written request to the Division of Technical Information and Document Control, U.S. Nuclear Regulatory Commission, Washington, DC 20555.

\*\*Available for purchase from the NRC/GPO Sales Program, U.S. Nuclear Regulatory Commission, Washington, DC 20555, and/or the National Technical Information Service, Springfield, VA 22161.

## 8. ENGINEERED SAFETY FEATURE EFFECTIVENESS

Engineered Safety Feature (ESF) systems are included in plant designs for the purpose of mitigating the consequences of postulated accidents. These systems perform the desired function by containing contaminants, by reducing pressure driving forces, or by removing contaminants from fluids which could leak to the outside environment.

Engineered safety features represent the safety-designer's last opportunity to affect the quantity and form of fission products prior to their release to the environment. The effects of various engineered safety features on the fission product release to the environment have been included in the analysis of the previous chapter. This chapter addresses the effectiveness of various ESF's under a range of accident conditions.

### 8.1 Engineered Safety Features and Their Design Basis

The engineered safety feature most important to the control and mitigation of fission product releases is the reactor containment. The reactor containment, in conjunction with related containment systems (e.g., enclosure or shield building, penetration rooms, etc.), is the outermost of several sequential barriers protecting against uncontrolled releases of radioactive material from the reactor core. Although numerous other safety considerations, including normal operating requirements, enter into the design bases for the containment, the retention of fission products following accidental release from the previous fission product barrier (i.e., the primary coolant pressure boundary) is the primary design basis for containment isolation and leak-tightness. This aspect of containment design will be addressed in this chapter under the title "Containment Leakage Requirements."

Current generation nuclear power plants include a number of safety systems designed to function in conjunction with the reactor containment by removing fission products from the containment atmosphere (containment spray and spray additive systems, recirculation filter systems), by reducing containment pressure and airborne contaminants (pressure suppression pools, ice condenser systems), and by filtering the air within likely leakage paths from the containment (main steam isolation valve leakage control systems, standby gas treatment systems, auxiliary building filtration systems.)

The design basis for ESF safety systems have been formulated to reflect two requirements: (1) the ability to perform the required degree of cleanup and pressure suppression to achieve the criteria of 10 CFR 100 and (2) the ability to operate under postulated accident conditions. These design requirements have been quantified by postulating Design Basis Accidents.

The Design Basis Accident (DBA) used by the NRC staff in evaluating ESF systems is defined in Regulatory Guides 1.3 and 1.4 (ref. 8.1) to include the following:

- a. Twenty-five percent of the equilibrium radioactive iodine inventory developed from maximum full power operation of the core should be

## 8.2

assumed to be available for leakage from the primary reactor containment. Of this 25%, it is assumed that 91% is in the form of elemental iodine, 5% is assumed to be present in particulate form, and 4% is assumed to be present as organic iodides.

- b. One hundred percent of the equilibrium radioactive noble gas inventory developed from maximum full power operation of the core should be assumed to be immediately available for leakage from the reactor containment.

The temperature and pressure environment for the ESF's are those corresponding to a large loss-of-coolant accident (LOCA). The design basis radiation environment corresponds to the 100% noble gas and 25% iodine source term for the containment atmosphere. Another 25% of the iodine and 1% of all solid (non-gaseous) fission products are added as the radiation source term for liquids in the primary coolant system or the containment sump (ref. 8.2). Throughout the DBA the containment is assumed to maintain its integrity, so that the demonstrated design basis leak rate of containment is not exceeded during the accident. The solid fission products are assumed to remain in the water phase within the containment, and neither aerosol formation, nor leakage of the solids are assumed.

These assumptions were intended to provide a conservative design basis for engineered safety features. The large noble gas and iodine source terms were postulated as an upper bound of the release of these fission products for any accident considered credible. In lieu of detailed analyses of the release of all fission products, conservative assumptions concerning the iodine source term, and additional conservatisms in the ESF evaluation methods were considered to provide an adequate safety margin in the design of these systems.

Certain ESF systems have been the subject of specific Regulatory Guides which list additional factors which must be considered in their design. For example, Regulatory Guide 1.52 (ref. 8.3) deals with air filtration and adsorption systems which may be used in the primary containment and auxiliary systems of light water power plants. Typical requirements described in this Regulatory Guide include the following:

- " Maximum temperatures and pressures for systems used inside containment are 280°F and 60 psi and for secondary systems are ~ 1 atm and 180°F.
- " Pressure surges caused by the blowdown of the reactor coolant system must not damage the system.
- " The maximum iodine loading on activated carbon is 2.5 mg I/g carbon.
- " The installed system shall have a demonstrated DOP removal efficiency of 99.95% in order to warrant a 99% removal efficiency for accident dose evaluations.

In summary, ESF systems have been designed on the basis of an airborne source term of 100% of the noble gas inventory and 25% of the iodine inventory

of the reactor core, postulated to occur in conjunction with a large LOCA. The large iodine source term serves as a surrogate for other fission products which would also be released under these accident conditions.

## 8.2 Loadings Imposed by Representative Accidents

In order to provide a realistic assessment of the performance of ESF systems when challenged by the radioactive source terms defined in this study, a number of representative accident sequences have been selected to identify source term characteristics and environmental conditions.

It should be noted here that severe accidents are expected to impose loads which are well beyond the design basis, and for this reason one would not expect ESF's to perform as desired for severe accidents. Severe accidents are considered herein in order to identify, on a best-estimate basis, the extent to which ESF systems provide appreciable benefits for a spectrum of accidents beyond the design basis.

The loadings imposed on ESFs by various accident sequences are identified below. One of the parameters affecting the performance of several ESFs is the fraction of iodine present in the form of organic iodides, such as  $\text{CH}_3\text{I}$ . This iodine compound was the predominant form of iodine found in the containment atmosphere following the TMI-2 accident. As described above, Regulatory Guides 1.3 and 1.4 specify that 4% of the iodine initially released to the containment should be assumed to be in the organic form. The basic considerations concerning methyl iodide formation are discussed in Chapter 5 of this report. Although considerable uncertainties concerning the relative size of this parameter remain, the absolute magnitude of the methyl iodide presence can be expected to be considerably lower than the regulatory guide values, at least during the early phases of the accident sequences analysed.

### 8.2.1 Accidents in PWR's with Large, High Pressure Containment Buildings

Several accident sequences have been analyzed in this study to examine fission product behavior in PWRs with large, high pressure containments. Key parameters which characterize the radioactive source term, the thermal conditions imposed on the containment, and the occurrence of key events are summarized in Table 8.1.

Important aspects of containment parameters are discussed as follows for each accident sequence.

In accidents with minor or no fuel damage, the environmental conditions are less severe than those commonly used as a design basis for ESF systems. On the other hand, the low fission product release from the primary coolant system suggests that a lesser degree of mitigation by ESF's would be required to meet offsite dose criteria. Accidents in this category, therefore, do not challenge the ESF's, and can be considered well within the design basis envelope.

For the TMI-type sequence, environment conditions are nominal, and the airborne source term is minimal. Therefore, similar to the first sequence, this accident sequence does not provide a challenge to the performance of the

Table 8.1 Containment Parameters Used to Evaluate ESF's in PWR's Using a Large High Pressure Containment

Containment Parameter	Terminated LOCA	TMI Type	Terminated AD	Severe S <sub>2</sub> D	Severe TMLB'	Severe TMLB'	Severe S <sub>2</sub> D
Spray Operation?	Yes	No	Yes	Yes	No	No	No
Recirc. Filter Operation	No	Yes	No	No	No	No	Yes
Hydrogen Burn	No	Yes	No	No	No	No	No
Steam Explosion	No	No	No	No	No	No	No
Time of Containment Failure, hr	None	None	None	None	4.7	None	None
Peak Atm. Temp., °C	120*	40*	120*	255	160	190	140
Peak Atm. Press., MPa Absolute	0.376*	0.14*	0.376*	0.26	0.68	0.68	0.21
Aerosol Mass Released, kg	<1*	<1*	400*	1110	1110	1110	1110
Peak Aerosol Conc., g/m <sup>3</sup>	<1x10 <sup>-4</sup> *	<1x10 <sup>-4</sup> *	3.1*	9.6	12.2	11.3	10.9
Iodine Release, Fract. of Core Inventory <sup>(a)</sup>	<2x10 <sup>-3</sup>	<6x10 <sup>-4</sup>	0.50*	1.0	1.0	1.0	1.0
Iodine Form:							
Fraction CsI	0.99-1.0*	0.99-1.0*	0.99-1.0*	0.99-1.0*	0.99-1.0*	0.99-1.0*	0.99-1.0*
Fraction I <sub>2</sub>	0-0.01*	0-0.01*	0-0.01*	0-0.01*	0-0.01*	0-0.01*	0-0.01*

(a) Iodine released as aerosol or gas to the containment atmosphere

\* Numerical value for this parameter was assumed for purposes of evaluating ESF's only. See Chapters 6 and 7 for the detailed analyses for these parameters.

ESF's in the containment. Similar to TMI-2 this accident scenario includes the consideration of a leakage path to the environment via contaminated liquid pumped to the auxiliary building. Iodine and noble gases would be the dominant fission products released. Because iodine is predicted in this study to be present mainly as CsI, little would be evolved to the gas phase. For purposes of evaluating auxiliary building filters, it would have to be assumed that all iodine present as organic iodides would enter the atmosphere of the auxiliary building.

The terminated AD sequence was selected to yield a realistic fission product source term for an accident with a degree of core damage roughly equivalent to the one implied in Regulatory Guides for the DBA. The major difference between this sequence and the DBA is the relatively large aerosol concentration estimated for the containment atmosphere.

In the first core melt accident sequence S<sup>2</sup>D, a molten core releases large quantities of aerosol to the containment atmosphere. For the high aerosol concentrations indicated ( $\sim 10$  g/m<sup>3</sup>), relatively large particles would result from agglomeration. Because iodine is present mainly as CsI, it would be attached to the particulate mass. Another important feature of this sequence is the relatively high temperatures in containment. The higher-than design temperature could affect the leak-tightness of the containment.

The two TMLB' sequences are similar except that in the first, containment is assumed to fail at 4.7 hr as a result of overpressure; whereas in the second TMLB' sequence the containment is assumed to fail via basemat meltthrough at a later time. Electric power is not available for these two sequences so only passive ESF's are available. High aerosol mass concentrations indicated for these sequences suggests that relatively large particles would be formed by coagulation, which would lead to significant depletion of airborne radionuclides by settling.

The last sequence, S<sub>2</sub>D, used a reference plant design which includes a recirculating filter system. Sprays were assumed not to operate because the containment pressure does not reach the level required for automatic actuation in a small pipe break accident. The high aerosol mass concentrations indicated for this sequence would be expected to severely challenge the filter system.

#### 8.2.2 Sequences for PWR Ice Condensers and BWR Pressure Suppression Containments

Three severe accident sequences have been selected for a PWR ice condenser containment and four severe accident sequences have been postulated for BWR's. DBA-type sequences were not included because it was anticipated that source term characteristics for these cases would be similar to those defined for the large, high pressure PWR containment (Table 8.1). Containment parameters and key accident assumptions are summarized in Table 8.2 for ice condenser and pressure suppression containments.

Important aspects of the selected sequences are discussed in the following paragraphs.

Table 8.2 Containment Parameters Used to Evaluate ESF's in PWR Ice Condensers and BWR Pressure Suppression Containments

Containment Parameters	Ice Condenser TMLB <sup>1</sup>	Ice Condenser S <sub>2</sub> HF	Ice Condenser AD	Mark I Pool AE	Mark I Pool TC	Mark I Pool TW	Mark III Pool TQUV
Spray Operation (PWR)	No	up to 1.9 hr	up to 1.1 hr	--	--	--	--
Ice Available (PWR)	Yes	No	Yes	--	--	--	--
Pool Subcooled (BWR)	--	--	--	Yes	No	No	Yes
Hydrogen Burn	No	No	At 1.1 hr	No	No	No	No
Time of Containment Failure, hr	4.0	3.15	1.1	0.81	1.5	55.3	6.7
Steam Explosion	No	No	No	No	No	No	No
Peak Atm. Temp., °C	137	212	253	417	592	262	440
Peak Atm. Press., MPa Absolute	0.29	0.29	0.29	1.21	1.21*	1.21*	0.31
Aerosol Mass Released, kg	1110	1110	1110	1110	1110	1110	1110
Peak Aerosol Conc., g/m <sup>3</sup>	15.2	19.5	11.6	40.9	55	10	12.9
Iodine Release, Fract. of Core Inventory <sup>(a)</sup>	1.0	1.0	1.0	1.0	1.0	1.0	1.0
Iodine Form:							
Fraction CsI	0.99-1.0*	0.99-1.0*	0.99-1.0*	0.99-1.0*	0.99-1.0*	0.99-1.0*	0.99-1.0*
Fraction I <sub>2</sub>	0-0.01*	0-0.01*	0-0.01*	0-0.01*	0-0.01*	0-0.01*	0-0.01*
Leak Path for Mark I	--	--	--	Annulus	Annulus	Direct	--

(a) Iodine released as aerosol or gas to the containment atmosphere

\*Numerical value for this parameter was assumed for purposes of evaluating ESF's only. See Chapters 6 and 7 for the detailed analyses for these parameters.

The first severe accident sequence for the ice condenser containment, TMLB', involves total loss of electric power and containment failure by overpressure. The ice bed is available to condense steam and scrub fission products. Relatively large particles would be formed by agglomeration of the high aerosol mass concentrations indicated in Table 8.2 ( $15 \text{ g/m}^3$ ). Iodine attached to the aerosol would be efficiently trapped by the ice.

In the second sequence, S<sub>2</sub>HF, a delayed melt allows fission products to be released after ice has melted. Also, failure of the spray system leads to overpressure and containment failure of 3.15 hr. High aerosol mass concentrations ( $19.5 \text{ g/m}^3$ ) would result in large particles being formed by agglomeration. Iodine is predominately present as CsI, so would be attached to the particulate mass.

The AD sequence for the ice condenser involves a hydrogen burn at 1.1 hr which fails the containment. Sprays are assumed to fail as at the time of containment failure. Scrubbing by both sprays and the ice bed were effective up to the time of containment failure.

The first sequence listed in Table 8.2 for the Mark I BWR, AE, involves failure of the containment due to overpressure. The leak path is through the annulus and then into the reactor building. The high steam flow rate into the secondary containment building is expected to fail walls and ductwork, thereby prevent effective operation of the SGTS. Very high aerosol concentrations are indicated for this sequence, resulting in large particles which would be effectively removed by deposition on the surfaces which form the annulus.

In the TC sequence, reactor shutdown does not occur, and the pool is at the boiling temperature at the time of fission product release. Very high aerosol concentrations projected for this sequence would result in large particles which would be subject to capture in the boiling pool and in the annulus. The SGTS would not be effective because the steam flow rate through the reactor building as a result of containment failure would result in failure of the leakage control function of the reactor building.

In the last sequence for the Mark I BWR, TW, containment failure is delayed to 54 hrs. Again the pool is at the boiling point when containment failure occurs. The leak path to the environment for this sequence bypasses the annulus, going directly from the wet-well to the outside environment. Another notable feature of this sequence is the high temperature,  $592^\circ\text{C}$ , indicated in Table 8.2. This temperature is much higher than the design value and could degrade leak-tightness prior to gross containment failure.

In addition, structural analysis indicates that the containment failure can occur in the region of the suppression pool which could limit its decontamination capabilities for the TW and TC sequences.

The final BWR sequence, TQUV, applies to a Mark III suppression-type containment. Notable features of the assumed sequence are that the pool is subcooled, and that the containment fails at 6.7 hours due to overpressure.

One unique LOCA sequence was considered to evaluate ESF systems. Event V involves a failure of the check valves between the reactor coolant system and a low pressure fluid system resulting in a leak pathway (which bypasses containment) directly into the auxiliary building. The blowdown rate is postulated high enough to challenge the structural integrity of the walls of the auxiliary building. Released fission products would enter the auxiliary building and a fraction would be released to the atmosphere through the failures caused by the blowdown.

### 8.3 Comparison of Accident Loads with the Capabilities of Selected Engineered Safety Feature Systems

In this section, the performance of ESF systems will be evaluated for source terms obtained from realistic analyses of specific accident sequences. The accident spectrum includes both accidents within the design basis envelop and severe accidents. Because some severe accidents are expected to impose loads which are well beyond the design basis for the ESF's, one would not expect that ESF's would perform as desired for severe accidents. On the other hand it is important to know how well the various ESF's would perform when challenged by a realistically estimated source term for both DBA-type accidents and a spectrum of more severe accidents.

#### 8.3.1 PWR Containment Sprays

Containment sprays remove heat from the containment atmosphere as well as scrub airborne radioactivity. The cooling process is quite independent of aerosols and gases present. Therefore the cooling process would be performed as designed regardless of the radioactive source term.

In several accident sequences, mechanical events prevent successful spray operation. For example in TMLB sequences electric power is not available to drive spray pumps. In event V, the dominant leak path is through the auxiliary building and spray operation is irrelevant. If a steam explosion occurred when the molten core drops into the reactor cavity there is the potential for ejected core debris to plug the sump, thereby preventing continued spray operation, or for missiles generated by the steam explosion to damage the spray piping.

For sequences where containment sprays operate, the issue is whether airborne radioactivity would be effectively removed. For the cases involving limited core damage, the aerosol concentration is low, and nearly all of the iodine is predicted to be airborne as an aerosol. The washout rate of aerosols is strongly dependent on particle size. For the dilute aerosols which would be present in the non-severe sequences, particle sizes would probably be smaller than approximately two micrometers, aerodynamic mass median diameter (AMMD). These small particles are predicted to be removed less rapidly than elemental iodine by containment sprays.

In all severe accident sequences, the overheated core produces copious quantities of aerosol mass, and the resulting high mass concentrations are predicted to favor the formation of relatively large particles through agglomeration. The large particles would be removed by sprays at a rate comparable to

that for elemental iodine. The dominant iodine specie, CsI, would be attached to the particulate mass and would therefore be effectively scrubbed by sprays.

Many spray systems incorporate chemical additive systems to enhance the absorption of elemental iodine. These systems add sodium hydroxide, or hydrazine to spray water to convert iodine to the ionic form, iodide ion, which is non-volatile. If iodine were airborne as CsI, the iodine would enter water as the iodide, and no chemical dosing system would be needed. The overall iodine removal effectiveness of the containment spray system without any additives, however, would be limited by the fraction which is assumed to be in the elemental form.

### 8.3.2 Containment Recirculating Filter Systems (PWR)

Filter systems are included as part of the Containment Air Recirculation System in some of the earlier PWRs to trap fission product iodine within the containment atmosphere following an accident. Filter systems of this type are not included in later PWRs.

These filter systems employ in series: moisture separators to remove water droplets, prefilters to remove large aerosol particles, HEPA filters for final removal of small aerosol particles, activated carbon (charcoal) adsorbers to trap iodine in the gaseous form, and fans to move air through the system. During normal operations the filter systems are not exposed to air flow; all of the recirculated air passes through the cooling section. In the event of an accident, the air flow is divided into two parts with about 30% passing through the filter system and the remainder through the cooling section.

Air Recirculation Cooling Systems (containing the filter systems) serve to complement and backup the function of the Containment Spray Systems. The filter systems are intended primarily for trapping of elemental and organic iodines and not for trapping large quantities of aerosol material. One HEPA filter (of 0.47 m<sup>3</sup>/s rating) will trap a nominal 1 kg of aerosol material before the increased pressure drop across the filter will overcome the air motive force produced by the fan; at this point the filter is effectively "plugged" and the air flow through the filter (and the activated carbon adsorber immediately downstream) will be reduced drastically.

This type of filter system would be expected to operate in a satisfactory manner and to accomplish its intended purpose during accident sequences involving limited core damage where the aerosol mass release to containment is small. Under accident sequences involving core melt where the released aerosol mass is high (above 500 kg) the HEPA filters would operate only a matter of minutes before accumulating the 1 kg of material needed to effectively stop air flow.

### 8.3.3 Auxiliary Building Filter System (PWR)

Filter systems of this type are intended to treat exhaust air from equipment areas and volumes outside of containment where the potential for small quantities of airborne radioactive material exists during accident situations as a result of normal leakage from fluid systems processing contaminated material outside the containment.

Typically, these systems employ trains having in series: prefilters, HEPA filters, activated carbon adsorbers, final HEPA filters, and a fan. The size of the system varies substantially from plant to plant and ranges from 5 to 30,000 cfm capacity.

In use during accident situations these systems would be exposed to small quantities of particulate aerosol and radioiodine in the various forms. When applied in the intended mode these systems will provide high trapping efficiencies for all forms of iodine and nominal amounts of particulate aerosol. The experiences at TMI illustrates the need for systems of this type and their value in handling radioiodine released in a manner, and into areas, not anticipated.

As discussed previously, fission products could enter the auxiliary building through the letdown system. In Chapter 7, it was postulated that as much as 0.2% of the core inventory of iodine could enter the auxiliary building. Filter systems designed with HEPA and charcoal traps would easily accommodate this iodine source term.

Event V involves a LOCA in which the discharge point is in the auxiliary building. The high steam flow rates are expected to challenge the structural integrity of the auxiliary building walls, thereby potentially creating a direct pathway to the environment. The pressure transient associated with the blowdown might also fail the ventilation filter system. The damage to the auxiliary building itself would probably be sufficient to prevent effective operation of the auxiliary building filters, and it is concluded that the filters would not mitigate the consequences of an event V accident.

#### 8.3.4 MSIV Leakage Control System (BWR)

In BWR plants, ventilation control systems are provided to trap gas-borne contaminants leaked past the inboard main steam isolation valve. The main steam isolation valve (MSIV) leakage control system provides benefit under design basis accident conditions where little radioactive material is leaked to the environs by other pathways.

As presently designed, the MSIV control systems would trap particulate fission products as efficiently as elemental iodine. Iodine and other fission products are predicted to be present as particles, hence would be efficiently removed by HEPA filtration alone. The charcoal beds of current designs would easily trap the small quantities of elemental iodine and organic iodides predicted to accompany the CsI aerosol for accident sequences involving limited core damage.

Containment failure is predicted for all of the severe accident sequences identified for the BWR in Table 8.2. Fission product leakage through the breach in the containment would be much greater than the small quantity leaked past isolation valves.

#### 8.3.5 Pressure Suppression Pools (BWR)

Pressure suppression pools are designed to condense steam following loss of coolant accidents, thereby reducing containment pressure.

Although the pressure suppression pool is not designed as a fission product removal system, a byproduct of the pressure suppression process is the scrubbing of contaminants from the steam entering the suppression pool.

The ability of the pool to suppress pressure is dependent on the availability of cool water. Cool water is expected to be available in all non-severe accidents, and in severe accidents where pool cooling is functional. Accident sequences TC and TW are typical of those where the pool becomes saturated and thereby loses its ability to condense steam. In other severe sequences the containment may fail by overpressure even though the pool is subcooled. For these cases overpressures are caused by either a hydrogen burn or by the accumulation of non-condensable gases.

The fission product scrubbing efficiency of the pool is expected to be different for CsI particles than for elemental iodine. Based on analyses of analogous phenomena in PWR steam generators following tube rupture accidents, it is expected that particles smaller than approximately 2 micrometers would be less efficiently removed than elemental iodine. Larger particles would be removed more efficiently. Therefore for accidents where the aerosol concentration is low, scrubbing of CsI and other particulate fission products would be less effective than the scrubbing of elemental iodine. On the other hand, for severe accident sequences, where high aerosol concentrations would produce relatively large particles, the suppression pool would effectively trap CsI and other particulates.

Scrubbing efficiency depends on many parameters, including pool temperature. For subcooled pools, the steam content of the gas stream would be reduced, and condensing conditions are known to favor particle capture and gas scrubbing. If the pool is allowed to warm to the saturation temperature, then evaporation will occur into the gas stream, and scrubbing efficiency will be reduced. Unfortunately, the present data base on pool scrubbing is not sufficient to permit a quantitative prediction of the influence of pool temperature on scrubbing efficiency.

### 8.3.6 Secondary Containment and Standby Gas Treatment Systems

The standby gas treatment system (SGTS) is a ventilation control system that traps contaminants leaked from the primary containment, and collected in a secondary containment structure. For BWRs (other than the "Mark III" containment), the secondary containment is the reactor building. A similar concept is employed for some PWR containment designs, which include an outer concrete shield building surrounding a steel shell primary containment, or an enclosure building which may surround either the entire steel-lined reinforced concrete primary containment, or those portions of the primary containment containing the containment penetrations.

The secondary containment air space which may be a narrow annulus adjacent to the primary containment boundary, is exhausted to the environment via the SGTS, thereby filtering any leakage from the primary containment which has entered the secondary air space.

A typical SGTS filter train includes in series: moisture separators, heater, prefilter, HEPA filter, charcoal trap, and a final HEPA filter. This train would be expected to achieve very high efficiencies for particulate contaminants (99.99%), whereas a somewhat lower efficiency would be obtained for elemental iodine and methyl iodide. Noble gases are not retained effectively by this system, although some reduction by decay would occur during the additional hold-up time in the secondary containment.

For non-severe accident sequences, where iodine and other fission products would be present mainly in the form of a dilute aerosol, the SGTS would efficiently trap all fission products entering the secondary containment except noble gases.

The SGTS requires electric power for fan operation, hence would be unavailable for sequences which assume total loss of power occurs. Also, it is possible that failure of the wetwell could occur in such a manner that the main flow path bypasses the SGTS. For these sequences the SGTS would provide no benefit regardless of the composition of the fission product source term.

In severe accidents where containment failure allows venting through the reactor building (AE), the secondary containment structures would quickly fail as a result of overpressurization, thereby rendering the SGTS ineffective.

#### 8.3.7 Pressure Suppression by Ice (PWR)

The ice condenser is very similar in concept to the suppression pool of a BWR. The main function of the ice is to condense steam, but it is expected that significant scrubbing of contaminants would also occur in the ice. Since the ice bed is passive, it will perform its condensing function unless the ice melts (such as in sequence S<sub>2</sub>HF) prior to the termination of large steam releases.

For design basis accident sequences, the ice beds would condense steam and perform a degree of scrubbing. A limited amount of data is available to demonstrate the elemental iodine removal effectiveness of ice containing sodium hydroxide (ref. 8.5). Very little information on particle scrubbing in an ice bed is available, and for this reason subjective judgments were relied on to evaluate scrubbing by ice. Based on a comparison of the physical processes involved in aerosol scrubbing by ice beds with those of the containment spray, filters, and suppression pools, it is expected that fine aerosol particles would be removed less effectively than coarse aerosols.

For iodine present as CsI, scrubbing of fine particle aerosols would be less efficient than the effectiveness predicted for elemental iodine removal. Scrubbing efficiency could be comparable to that for elemental iodine under accident conditions where fission products would be associated with large aerosol particles.

#### 8.3.8 Containment Leakage Requirements

In the past, the allowable leak rate for containment systems has been based on the airborne concentrations of iodine and noble gases in the containment

atmosphere and on downwind dispersion and dose calculations. If one assumes that dispersion and dose predictions are fixed parameters, then the airborne fission product concentrations determine the leakage requirements.

For accidents where iodine is airborne as a dilute aerosol, the depletion rate by either plateout or ESF operation would be smaller than for elemental iodine. On the other hand, realistic estimates of iodine released from the core indicate substantial retention of iodine in the primary system. For the terminated AD sequence, the average iodine concentration for a 2-hour period would tend to be higher than predicted for a Regulatory Guide source term because CsI aerosol is less easily removed than is elemental iodine in this sequence.

Most core melt accident sequences lead to failure of the containment. Up to the time of failure the containment would effectively retain all fission products. Once the containment is breached, the release is not affected by pre-accident building leak rates.

#### 8.4 Summary and Conclusions Regarding the Performance of Engineered Safety Feature Systems

Eight ESF systems were studied in order to determine their performance when challenged by the fission product source terms defined in this study. A spectrum of accident sequences was considered ranging from terminated LOCAs for which essentially no core damage is postulated to severe core melt accidents which lead to containment failure.

Existing ESF systems were designed using iodine and noble gases source terms defined in Regulatory Guides. A key objective of this study was to evaluate how the systems would perform with realistically-chosen source terms. While it was recognized that severe accidents would impose loads which are well beyond the design basis, such accidents were considered to help identify those ESFs which provide appreciable benefits for a spectrum of accidents.

The work completed supports the following conclusions and summary statements regarding the performance of ESF systems:

##### 8.4.1 Containment Sprays

Containment sprays would perform their pressure suppression function for most accident sequences. Scrubbing of particulate iodine would be less rapid than for elemental iodine in accident sequences involving limited core damage where the mean particle size would be relatively small, but for severe accidents with relatively larger aerosol particles, spray washout would be comparable to what has been predicted for elemental iodine.

##### 8.4.2 Containment Recirculating Filter Systems

Containment recirculating filter systems would perform effectively only for accident sequence wherein aerosol loadings are minimal. Under most severe accident conditions, the attendant high aerosol concentrations in the containment atmosphere would plug the filters, rendering the system inoperative within a few minutes.

#### 8.4.3 Auxiliary Building Filter Systems

Filter trains of current design would effectively trap the modest quantity of fission products transported to the auxiliary building via leakage from fluid systems outside containment. For event V, where the blowdown occurs in the auxiliary building, the filter system would not significantly mitigate the release of radioactive materials as a result of failure of auxiliary building walls and ventilation system duct work.

#### 8.4.4 MSIV Leakage Control System (BWR)

This BWR system would control the leakage of radioactive materials for the design basis accident conditions and under degraded core conditions for accidents where electric power was available. This system would offer little benefit for accidents where the dominant leakage paths to the environment bypass the main steam line.

#### 8.4.5 Pressure Suppression Pools (BWR)

Pressure suppression pools would perform the steam condensation function for many severe accident sequences. The amount of decontamination in pressure suppression pools is a function of the fraction of non-condensable gases in the bubble, bubble size, and pool depth. Under most conditions, the decontamination of iodine passing through the pool should be substantial. The scrubbing effectiveness for aerosols would depend upon the size of the particles, with larger particles being removed more effectively. The particle size itself would depend upon the degree of agglomeration and condensation in the reactor coolant system or drywell.

#### 8.4.6 Standby Gas Treatment System (BWR)

The SGTS would effectively trap contaminants which leak from the primary containment provided that reasonable containment integrity is maintained. The system would be ineffective for most severe accidents because of damage to the secondary containment or reactor building, and leak paths which bypass the SGTS.

#### 8.4.7 Pressure Suppression by Ice (PWR)

Pressure suppression by ice beds would be effective for a number of accident sequences including many severe accident sequences. The ice condenser system with ice containing sodium hydroxide has been demonstrated to be effective for elemental iodine removal. Its effectiveness for scrubbing of aerosols is difficult to quantify without further study. Based on analyses of analogous heat and mass transfer phenomena, larger aerosol particles are expected to be removed more effectively than smaller particle aerosols.

#### 8.4.8 Containment Leakage Requirements

Limitations on containment leakage have significance primarily for sequences in which containment integrity is maintained. For most core melt accident sequences, some type of breach in containment is encountered, and the release of radioactive material is not greatly affected by pre-accident leak requirements.

References

- 8.1 Assumptions Used for Evaluating the Potential Radiological Consequences of a Loss of Coolant Accident for Boiling Water Reactors. Regulatory Guide 1.3, Revision 2, June 1974. Directorate of Regulatory Standards, USAEC, and Assumptions Used for Evaluating the Potential Radiological Consequences of a Loss of Coolant Accident for Pressurized Water Reactors. Regulatory Guide 1.4, Revision 2, June 1974, Division of Reactor Standards, USAEC.
- 8.2 Control of Combustible Gas Concentrations in Containment Following a LOCA, Regulatory Guide 1.7, Rev. 1, September 76, Office of Standards Development, USNRC.
- 8.3 Design, Testing, and Maintenance Criteria for Atmospheric Cleanup System Air Filtration and Adsorption Units of Light-Water-Cooled Nuclear Power Plants. Regulatory Guide 1.52, June 1973, Directorate of Regulatory Standards, USAEC.
- 8.4 J. D. McCormack, et al. "Loading Capacity of Various Filters for Sodium Oxide/Hydroxide Aerosols," Proceedings of the 15th DOE Nuclear Air Cleaning Conference, CONF-780819, Boston, MA, pp. 1018-1043, August 7-10, 1978.
- 8.5 D. D. Malinowski, "Iodine Removal in the Ice Condenser System," WCAP-7426, Westinghouse Nuclear Energy Systems Division, March 1970.



APPENDIX A  
GENERAL DESCRIPTION OF CORE MELTDOWN ACCIDENT SEQUENCES

A.1 PRESSURIZED WATER REACTOR ACCIDENTS

A number of possible core meltdown sequences have been identified in which the conditions vary substantially under which fuel melting and fission produce release would occur. In order to simplify the discussion of these sequences, they have been categorized into groups of sequences for which the expected behavior in the reactor vessel and reactor cavity is generally similar. The thermal and chemical environment is described as the fuel heats and as the fission products are released and transported to the containment volume. The description of these categories is further divided into two time periods: Stage 1, prior to melt-through of the lower head of the reactor vessel, and Stage 2, when at least part of the core is attacking the concrete basemat. Sequences which would typically be assigned to each category are identified using the nomenclature of the Reactor Safety Study (A.1) as described in Tables A-1 and A-2.

After the fission products have been released to the containment atmosphere, subsequent behavior, (e.g., deposition, change in chemical form and release to the environment) will depend upon conditions in the containment. These conditions will in turn depend upon the type of containment design for the plant and the operability of certain engineered safety features for each accident sequence.

A.1.1 Conditions in the Primary System  
and Reactor Cavity

Category 1. Transients Without Secondary Heat  
Removal and Feed/Bleed Capability

In this type of sequence, heat cannot be adequately removed from the primary system. As a result, the primary system pressure rises to the relief valve setpoint. Water is boiled away faster than cooling water can be provided (if available).

Typical Sequences. TMLB', TML, TKQ.

Stage 1

Modes of Release. As water boils away and the core is uncovered, fuel heats and becomes molten in the range 2100-2800°C. Fission products and structural materials are vaporized and released from the fuel region above the grid plate. After fuel slumps into the lower plenum, it is quenched or partially quenched. Since the system is at high pressure, it is unlikely that, prior to failure of the lower head, fuel in the lower plenum would reach temperatures higher than those achieved earlier in the accident.

TABLE A-1. KEY TO PWR ACCIDENT SEQUENCE SYMBOLS

- 
- A - Intermediate to large loss of coolant accident (LOCA).
  - B - Failure of electric power to engineered safety features (ESF).
  - B' - Failure to recover either onsite or offsite electric power within about 1 to 3 hours following an initiating transient which is a loss of offsite AC power.
  - C - Failure of the containment spray injection system.
  - D - Failure of the emergency core cooling injection system.
  - F - Failure of the containment spray recirculation system.
  - G - Failure of the containment heat removal system.
  - H - Failure of the emergency core cooling recirculation system.
  - K - Failure of the reactor protection system.
  - L - Failure of the secondary system steam relief valves and the auxiliary feedwater system.
  - M - Failure of the secondary system steam relief valves and the power conversion system.
  - Q - Failure of the primary system safety relief valves to reclose after opening.
  - R - Massive rupture of the reactor vessel.
  - S<sub>1</sub> - A small LOCA with an equivalent diameter of about 2 to 6 inches.
  - S<sub>2</sub> - A small LOCA with an equivalent diameter of about 1/2 to 2 inches.
  - T - Transient event.
  - V - Low pressure injection system check valve failure.
-

TABLE A-2. KEY TO BWR ACCIDENT SEQUENCE SYMBOLS

- 
- A - Rupture of reactor coolant boundary with an equivalent diameter of greater than six inches.
  - B - Failure of electric power to engineered safety features.
  - C - Failure of the reactor protection system.
  - D - Failure of vapor suppression.
  - E - Failure of emergency core cooling injection.
  - F - Failure of emergency core cooling functionality.
  - G - Failure of containment isolation to limit leakage to less than 100 volume percent per day.
  - H - Failure of core spray recirculation system.
  - I - Failure of low pressure recirculation system.
  - J - Failure of high pressure service water system.
  - M - Failure of safety/relief valves to open.
  - P - Failure of safety/relief valves to reclose after opening.
  - Q - Failure of normal feedwater system to provide core make-up water.
  - S<sub>1</sub> - Small pipe break with an equivalent diameter of about 2"-6".
  - S<sub>2</sub> - Small pipe break with an equivalent diameter of about 1/2"-2".
  - T - Transient event.
  - U - Failure of high pressure coolant injection or reactor core isolation cooling system to provide core make-up water.
  - V - Failure of low pressure emergency core cooling system to provide core make-up water.
  - W - Failure to remove residual core heat.
-

## A.4

Transport Pathways. 1. Core--upper plenum--hot leg--pressurizer--drain tank--containment.

Pathway Conditions. Radioactivity would be released into a reducing environment of hydrogen and superheated steam at temperatures  $\sim 2000^{\circ}\text{C}$ . Surfaces in the pathway would be cooler and the gas temperature would drop rapidly downstream. During the initial stages of release, the pressurizer could contain a significant quantity of saturated water which would drain back into the core resulting in quenching, delayed melting, and the re-evolution of fission products trapped earlier in the accident. The pressurizer should be empty during most of the melting period. The reactor coolant drain tank would contain some saturated water during the release period. Whether the flow is released above or beneath the water surface is uncertain.

Entry Conditions Into Containment. The mixture of hydrogen and steam would probably be at saturation or slightly superheated.

### Stage 2

Modes of Release. Fuel remaining in the vessel following head failure would continue to heatup and release radioactive material. (The fraction of fuel remaining is very uncertain). Fuel on the basemat would also release some of the less volatile fission products. A source of volatile fission products would be unmelted fuel falling out of the vessel at the time of vessel failure. If the vessel is pressurized at the time of melthrough, some fuel could be swept out of the reactor cavity into the containment building.

Transport Pathways. 1. Core--lower plenum--reactor cavity--containment.  
2. Core--upper plenum--hot leg--steam generator--cold leg--downcomer--reactor cavity--containment.  
3. Basemat--reactor cavity--containment.  
4. Containment.

Pathway Conditions. Flow through the primary system should be quite slow, driven by convection and gas expansion, and portions of the pathway may be at steel melting temperature. The composition should be hydrogen, steam, and fission product gases. The atmosphere of the reactor cavity will be determined by the decomposition of concrete: hydrogen, steam,  $\text{CO}$ , and  $\text{CO}_2$ . Air in the cavity at the time of lower head failure would be expelled by steam as the primary system depressurizes. For a dry cavity, the temperature would be in the range of  $1200\text{--}2200^{\circ}\text{C}$ . In some accident sequences and system designs, water may continually enter the cavity reducing the temperature of the atmosphere and perhaps covering the core debris.

Entry Conditions to Containment. Same as conditions in reactor cavity.

Category 2. Pipe Break Accidents  
With ECC Failures

In these sequences, inadequate cooling water is supplied to balance the water leaving the breach in the primary system. Depending on the size of the break, the system pressure may or may not be elevated during core meltdown. In the special case of a rod ejection accident, some fuel failure and fission product release could occur prior to core uncover.

Typical Sequences. (A,S<sub>1</sub>,S<sub>2</sub>)B; (A,S<sub>1</sub>,S<sub>2</sub>)D; (A,S<sub>1</sub>,S<sub>2</sub>)H;  
 S<sub>2</sub>C, V.

Stage 1

Modes of Release. As water boils away and the core is uncovered, fuel heats and becomes molten in the range 2100-2800°C. Fission products and structural materials are vaporized and released from the fuel region above the grid plate. After fuel slumps into the lower plenum, it is quenched or partially quenched. Additional release of fission products may occur as the fuel reheats prior to failure of the lower head.

Transport Pathways. 1. Core--break location--containment.

Pathway Conditions. Radioactivity would be released into a superheated steam-hydrogen environment at temperatures ~2000°C. Surfaces in the pathway would be cooler and the gas temperatures would drop rapidly downstream to as low as 260°C. For most accident sequences, the pathway to release from the primary system would be expected to be dry. For a large pipe break or breaks at multiple points in the primary system, the possibility of some air ingress cannot be completely ruled out but appears quite unlikely. In cases of partial ECC performance (in combination with breaks on the cold leg side of the steam generator, or hot leg injection) ECC water could mix with the stream of gases from the hot core as it exits the primary system.

Entry Conditions Into Containment. Depending upon the length of the pathway, the mixture of hydrogen, steam, and fission products could be at temperatures from 260°C to 1500°C as it enters the containment. A flame could form on the exiting jet as it is exposed to oxygen in the containment atmosphere.

Stage 2

Modes of Release. Fuel remaining in the vessel following head failure would continue to heatup and release fission products. Fuel on the basemat would also continue to release some of the less volatile fission products.

Transport Pathways. 1. Core--primary system breach--containment.  
 2. Basemat--reactor cavity--containment.  
 3. Basemat--reactor vessel--primary system breach--containment.

Pathway Conditions. Conditions in the reactor cavity would be determined by the decomposition of concrete. Air, originally in the cavity, would be swept out following head failure by steam generation and the gases produced from the concrete. Constituents of the atmosphere would be hydrogen, steam, carbon monoxide, and carbon dioxide. If significant quantities of water drain into the reactor cavity (such as with sprays operating), the temperature in the cavity atmosphere would remain in the neighborhood of 100°C. For sequences in which there is no water in the cavity or the water is boiled away, the temperature would be in the range of 1200-2200°C. The amount of flow from the cavity through the vessel would be limited by the size of the break. The composition of gases in the vessel would probably be similar to those in the reactor cavity. The temperature of gases in the vessel would be quite hot, however, as long as fuel remained in the vessel.

Entry Conditions Into Containment. Depending on the location of the break, gases leaving the break could be as high as 1500°C and could burn spontaneously as oxygen is encountered in the containment atmosphere. The temperature of gases leaving the reactor cavity could be as high as 2000°C. If water were continually entering the cavity, however, the temperature of the exiting gases would be cooler.

### Category 3. Vessel Rupture

The emergency core cooling system (ECCS) is designed to protect against a range of failures in the primary system piping up to and including the largest piping diameter. Depending on the size and location of the breach in the vessel, the ECCS might not be able to prevent meltdown. Vessel failure is expected to be an unlikely event. However, vessel failure could result from crack growth beyond a critical size, severe overcooling accidents, overpressurization by rapidly liquid-filling the system (as in a transient without scram) or by the generation of an internal pressure pulse in a severe reactivity excursion accident.

Typical Sequences. R, TK.

Stage 1

Modes of Release. As in Category 2.

Transport Pathways. As in Category 2, except that fuel could be directly exposed to the cavity or containment atmosphere.

## A.7

Pathway Conditions. Conditions would be very similar to those described for Category 2. For a severe rupture, fuel could be directly exposed to air circulating in the reactor cavity or to the containment atmosphere during heatup.

Entry Conditions Into Containment. As in Category 2.

### Stage 2

Modes of Release. As in Category 2.

Transport Pathways. As in Category 2.

Pathway Conditions. As in Category 2. Because of the reaction of the core with concrete it is less likely that fuel would be exposed to oxygen in this stage of the accident. Gas composition within the cavity should be determined by the products of reaction with the concrete.

Entry Conditions Into Containment. As in Category 2.

### Variation in Conditions in the Event of a Steam Explosion

In the Reactor Safety Study(A.1), consideration was given to the possibility of a molten fuel coolant interaction of sufficient severity to fail the upper head of the vessel and to damage the containment boundary. Since the Study, considerable experimental research has been performed which has provided evidence that such an outcome is very unlikely.

The possibility of a molten fuel coolant interaction of sufficient severity to fail the vessel and result in the expulsion of some fuel into the containment cannot be discounted, however. In addition, if there were water in the reactor cavity at the time of vessel melt-through, a molten fuel coolant interaction could occur which could expel material from the reactor cavity. In the event that small particles of fuel were dispersed in the containment atmosphere, oxidation of the fuel could occur resulting in the enhanced release of some fission products, in particular ruthenium. The fraction of the fuel that was dispersed would probably be coolable in the settled configuration and would not participate in attack of the concrete.

### A.1.2 Containment Conditions

LOCA Bypassing Containment. In the Reactor Safety Study, a potential accident sequence was identified in which a loss of coolant accident could occur outside of the containment building. In the V sequence, two check valves in the low pressure injection system are assumed to fail, subjecting parts of the low pressure system which is designed to 600 psi to the full primary system pressure of 2200 psi. The system is illustrated in Figure A-1. A more detailed description of the accident is provided on pp. I.47-I.48 of the Reactor Safety Study.

Under the imposed pressure loading, the low pressure system would be expected to fail. Detailed analyses have not been performed to predict the location and nature of the failure. It is likely, however, that a rupture of the low pressure system would occur in the safeguards building at a rate characteristic of an intermediate size break (approximately 100,000 lb/minute). Since the design pressure of the safeguards building is low, it would be expected to fail in the first minute of the accident leaving a large breach to the environment.

Although it is possible that the high pressure injection system would be operated to delay core meltdown, the failure in the low pressure system would be expected to incapacitate both the low pressure injection system and the low pressure recirculation system. Indeed, with the rupture outside of the containment, there would be no water in the sump to be recirculated if the recirculation system were operable.

Core meltdown and fission product behavior in the primary system would behave in the same manner as described for Category 2 accidents, except that in Stage 1 the release would be to the safeguards building rather than to the containment. In the most likely scenario, there would be no emergency core cooling water flowing in the low pressure piping at the time of core melting. The fission products would be released to the atmosphere of the safeguards building in a mixture of hydrogen and superheated steam. For gas generation rates consistent with decay heat, the residence time in the safeguards building would only be a few minutes before release to the environment.

Large, High Pressure Containment. The large, high pressure containment design is the more typical variation in containment design for the pressurized water reactor. The safety features of interest are sprays and air coolers. In some designs, cooling is dependent on spray operation. If cooling is functioning in a meltdown accident sequence, the containment pressure would be near atmospheric and the temperature would be at or below saturation during the core melting period. With time, sufficient hydrogen would be released for combustible conditions to be achieved. One or more deflagration events could occur during the accident.

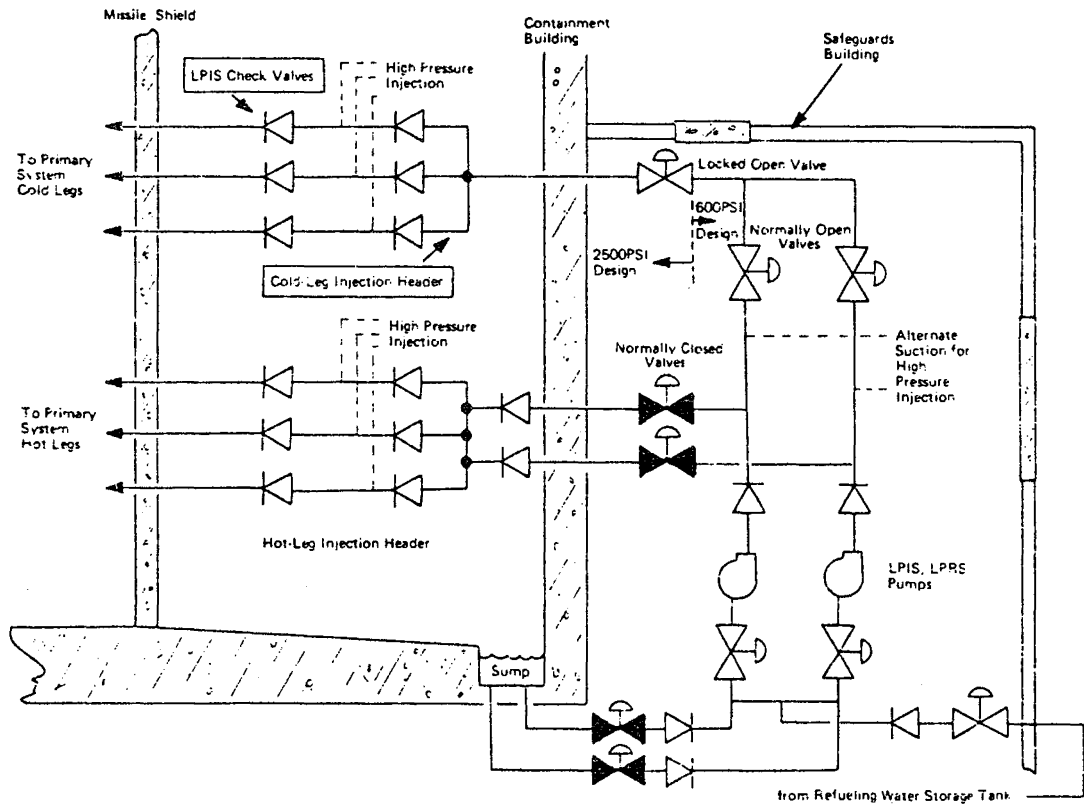


FIGURE A.1 Low Pressure Recirculation System Schematic Diagram

For most sequences in which containment cooling is not functioning, the containment pressure would be elevated and the temperature would be saturated at the steam partial pressure during the period of fission product release. In some cases, the quantity of steam in the atmosphere would be high enough to suppress hydrogen flammability. In other sequences, however, a hydrogen deflagration event would be possible at least during some phases of the accident.

In the Reactor Safety Study, some sequences were identified in which containment failure was predicted to precede core meltdown. For example, in the S<sub>2</sub>C sequence, loss of ability to remove heat from the containment atmosphere would lead to a steady increase in containment pressure which would eventually result in containment failure. Depressurization of the containment building would lead to cavitation and failure of the emergency core cooling pumps with subsequent fuel uncover and meltdown. The conditions in the containment at the time of fission product release would depend upon the mode of containment failure. For a localized failure in containment, the pressure could be elevated ranging from atmospheric pressure to the containment failure pressure, depending on the size of the leak. The atmosphere would primarily be composed of steam and hydrogen at a temperature approximately equal to saturation at the steam partial pressure. The amount of air would be depleted due to release from containment. If the failure mode of the containment were massive, air circulation into the containment would be expected. The pressure in containment would be near atmospheric. Although temperatures could be very hot near the point of the break in the primary system, sharp temperature gradients would exist in the containment atmosphere determined by the circulation patterns of incoming air. Since there is great uncertainty in the mode of containment failure, the latter assumption is usually made in analyzing this type of sequence. However, it should be recognized that the size of the breach in the containment can affect not only the conditions in the containment but also the time available for deposition. The results of the analyses can therefore be quite sensitive to the assumed failure mode.

Ice Condenser Design. Since the ice-condenser is a passive safety feature, it would be expected to function in most meltdown sequences. The ice would not only be effective in condensing steam but would act as a filter for fission products. After some time period, however, the ice would be completely consumed. The timing of core meltdown, relative to the availability of ice, is therefore critical in determining the amount of decontamination available. The volume of the containment is comparatively small so that flammable conditions can be readily achieved in the upper compartment. Whether or not flammable conditions would occur in the lower compartment depends on whether or not recirculation fans are operating.

## A.2 BOILING WATER REACTOR ACCIDENTS

There are three basic containment designs for boiling water reactors in the United States called Mark I, Mark II, and Mark III. Each uses a suppression pool to condense water vapor under accident conditions. The reactor vessel is contained within a drywell. If the pressure rises in the drywell, it can be relieved into a wetwell consisting of a liquid space and a gas space. If the pressure should rise in the reactor coolant system, steam can be discharged directly to the suppression pool from relief valves through discharge lines. For convenience, the discussion of expected behavior in BWR accident sequences is divided into two regions of the containment. In Section A.2.1 conditions are described for the reactor coolant system and the drywell. Although there are differences in reactor coolant systems and drywell design among BWR plants, they are sufficiently similar that for the purposes of this discussion the behavior can be described generically, without reference to the specific type of containment design. In Section A.2.2 conditions in the balance of the containment, the suppression pool and vapor space (outer containment volume in the Mark III design), are described. In this section the differences in behavior within the three types of containemtn design are identified. As in the PWR sequences, the accident period is divided into two stages, before and after melthrough of the lower head. Conditions in the wetwell will be described depending on the operability of safety features and the location of the failure in containment when it occurs.

### A.2.1 Conditions in the Reactor Coolant System and Drywell

#### Category 1. Transients With a Makeup Water/Heatload Imbalance

In the event that insufficient water is provided to remove heat from the reactor core, pressure will rise in the reactor vessel to the relief valve setpoint. As more water is boiled out of the system than replenished, the core would become uncovered and would heat up. The imbalance can result either because the core power is too high, such as in the case of failure to shutdown reactor power, or when the capacity of the coolant makeup systems is reduced, such as the result of pump cavitation following containment failure. Typically, meltdown would occur at elevated pressure in the reactor coolant system unless the automatic depressurization system is activated.

Typical Sequences. TC, TW, TQUV, TPE, TPI.

## Stage 1

Modes of Release. As in Category 1 for the PWR.

Transport Pathways. 1. Core--steam separators--outer annulus--discharge line--suppression pool.  
2. Core--steam separators--steam dryers--upper vessel head--outer annulus--discharge line--suppression pool.

Pathway Conditions. Fission products would be released into a reducing environment of hydrogen and superheated steam at temperatures of  $\sim 2000^{\circ}\text{C}$ . Surface temperatures and fluid temperatures would decrease rapidly downstream. Most of the flow would bypass the steam dryers.

## Stage 2

Modes of Release. Fuel remaining in the vessel following failure of the lower head would continue to heatup and release fission products. Fuel attacking the basemat would continue to release some of the less volatile fission products.

Transport Pathways. 1. Core--lower plenum--drywell.  
2. Core--steam separators--outer annulus--jet pumps--lower plenum--drywell.  
3. Basemat--drywell.

Pathway Conditions. As long as fuel remains in the vessel, temperatures would be very hot. Release from the vessel would be slow, driven by thermal expansion of hydrogen and steam and the release of fission gases. The source of gases to the drywell would be composed of the decomposition products of concrete attack:  $\text{CO}$ ,  $\text{CO}_2$ , hydrogen, and steam.

Category 2. Pipe Break Accidents  
With ECC Failure

In these sequences, inadequate emergency cooling water is supplied to balance the loss of water from the break. Depending on the size of the break and the operability of the automatic depressurization system, the system pressure may be high or reduced during core melting.

Typical Sequences.  $(A_1, S_1, S_2)E$ ;  $(A, S_1, S_2)J$ ;  $(A, S_1, S_2)I$ .

## Stage 1

Modes of Release. Same as Category 2 for PWR.

Transport Pathways. 1. Core--steam separators--outer annulus--break location--drywell.

Pathway Conditions. Fission products would be released into a reducing environment of hydrogen and superheated steam at temperatures  $\sim 2000^{\circ}\text{C}$ . Temperatures in the steam separators would also be very hot. However, surface temperatures and gas temperatures would decrease rapidly with distance downstream. If the core spray system is operating (but at a rate insufficient to cool the core), complex patterns of trapping of fission product in the water with subsequent reevolution in the core region could result. In other examples of degraded ECC performance, it is possible that the stream of gases leaving the core could mix with cooling water near the break location as they exit the vessel. In the event of complete ECC failure, the pathway to containment would be dry.

## Stage 2

Modes of Release. Same as Category 2 for PWR.

Transport Pathways. 1. Core--steam separators--outer annulus--break location--drywell.  
2. Basemat--drywell.

Pathway Conditions. Some flow might enter the failed bottom head but the composition should be primarily the gases from concrete decomposition. If the drywell is not inerted, there is some possibility for entraining air into the vessel. The amount of oxygen would be expected to be very small in comparison to the quantities of hydrogen and steam. The temperature in the vessel would be very hot. The gases coming off the concrete would be in the range of  $1200\text{-}2200^{\circ}\text{C}$ .

Category 3. Vessel Rupture

A severe breach in the reactor vessel is considered to be a very unlikely occurrence. Such an accident could result from the undetected growth of a flaw beyond a critical size, from a severe overcooling transient, from a rapid pressurization transient, or from a pressure pulse generated in a severe reactivity insertion accident. The forces generated as the result of vessel rupture could be large enough to fail the integrity of the drywell and to allow air inleakage. A direct pathway for fission product release to the environment would also be provided.

Typical Sequences. R.

## Stage 1

Modes of Release. As in Category 2.

Transport Pathways. As in Category 2 except that fuel could be directly exposed to the drywell atmosphere.

Pathway Conditions. Conditions could be very similar to those described for Category 2. For a severe rupture, fuel could be directly exposed to the drywell atmosphere. Depending upon the containment design and the nature of the accident, the drywell atmosphere could be inert, steam-filled, air-filled, or a combination of the above.

## Stage 2

Modes of Release. As in Category 2.

Transport Pathways. As in Category 2 except that fuel could be directly exposed to the drywell atmosphere.

Pathway Conditions. Conditions in the vessel would be very hot as long as fuel remains in the vessel. The composition of gases in the vessel and in the drywell would be dominated by the products of concrete decomposition. The temperature in the drywell could be in the range of 1200-2200°C.

Variation in Conditions in the Event  
of a Steam Explosion

A steam explosion in a BWR accident sequence would have similar consequences to those described for PWR accidents. Failure of the drywell could result in air ingress. If the integrity of the drywell survived the pressure pulse and missiles produced in the accident, the fuel would not be exposed to air for inerted containment designs or for accidents in which the air had been driven to the suppression pool earlier in the accident.

A.2.2 Conditions in the Wetwell

The three types of BWR containment designs are similar in concept. Some differences in the designs can influence the conditions in the containment volumes during accident sequences, however. The responses of the Mark I and Mark II designs would be nearly the same for most accidents. The current intent of the NRC is to have all Mark I and II plants inerted. Up until the time of failure of containment, an oxidizing atmosphere would not, therefore, exist in the drywell. It should be recognized, however, that in some sequences, such as TW, containment failure would precede core meltdown and that air ingress cannot be precluded. One major

difference in accident behavior between Mark I and Mark II designs relates to the location of the suppression pools. For the Mark II design, the molten core would penetrate into the suppression pool in the Stage 2 time period. The Mark III design is in many respects more similar to the PWR ice condenser design than to the other BWR designs. In this design, the vapor space above the suppression pool is actually an outer containment volume.

While the drywell is intact, the suppression pool can be an effective scrubber of fission products as well as condenser of steam for each of the designs. Gases released from the vessel during an accident would either be discharged directly to the suppression pool or, having been released to the drywell, would flow through vent pipes into the pool. Even if the water in the suppression pool is saturated, the pool may still have some effectiveness in removing fission products from the gas stream prior to release to the wetwell vapor space.

Once the containment boundary fails, the subsequent pathway of release of fission products to the environment and the amount of retention in the pathway would be sensitive to the location of failure. For the Mark I design, failure could occur either in the drywell or the torus. Failure in the drywell would lead to bypassing of the suppression pool for the remainder of the accident. Whether or not failure in the torus region would also prevent further scrubbing by the pool would depend upon the type of failure. Following failure in the drywell or torus, fission products either travel up the narrow annular space surrounding the drywell before release to the operating floor of the secondary containment, or are released to lower compartments of the secondary containment building or directly to the environment depending upon the mode and location of failure.

Because of the small volumes of the BWR designs, hydrogen generation presents a considerable problem as a non-condensable gas which is predicted to eventually lead to failure of the containment by overpressurization. Since the Mark I and II designs will probably be operated in an inerted mode in the future, hydrogen deflagration would in general not be possible for these designs. Since the containment volume is small and the suppression pool will in general be expected to suppress the release of steam to the outer containment volume, flammable conditions could be expected by the end of Stage 1 for most accident sequences in the Mark III design.

## REFERENCES

- A.1 "Reactor Safety Study, An Assessment of Accident Risks in U.S. Commercial Nuclear Power Plants", WASH-1400 (October, 1975).



## B.1

### Appendix B. Aerosol Release Calculations

#### In-Primary Vessel Release

The rate of release of fission products and other aerosol material from heated and melting fuel is assumed to be proportional to the concentration,

$$dM_x/dt = -k_x(T)M_x \quad (B.1)$$

where  $M_x$  is the mass of material  $x$  in the mixture and  $k_x$  is a fractional release rate coefficient assumed to be a function of temperature only.

The fractional release rates used in this study are shown in Fig. 4.3. For calculational purposes, the fractional release coefficients of Fig. 4.3 were approximated by equations of the form

$$k(T) = Ae^{BT} \quad (B.2)$$

where the constants,  $A$  and  $B$ , were different for each element and, for the fission products, two different sets were used - for temperatures up to 2200°C and for temperatures greater than 2200°C. The values used in this study are shown in Table B.1.

Substitution of Equation B.2 into B.1 gives

$$dM_x/dt = -A_x e^{B_x T} M_x \quad (B.3)$$

For ease of computation, the temperature of any given finite core region is assumed to increase linearly with time,  $T = a + bt$ , so that Eq. (B.3) becomes

$$dM_x/dt = -A_x e^{B_x(a + bt)} M_x \quad (B.4)$$

The solution to Eq. (B.4) is

$$\frac{M_x - M_{0x}}{M_{0x}} = \left\{ 1 - \exp \left[ \frac{K_x}{C_x} (1 - e^{C_x t}) \right] \right\} \quad (B.5)$$

where  $M_{0x}$  is the initial mass inventory of element  $x$

and  $K_x$  is  $A_x e^{B_x a}$

$C_x$  is  $B_x b$  .

Equation (B.5) can be used to predict the time-release from any region of the core presuming the temperature history of that region is known.

B.2

Table B.1. Approximations of the fraction release coefficient  $k = Ae^{BT}$

Element	1000°C <T ≤ 2200°C		T > 2200°C	
	A	B	A	B
Uranium (UO <sub>2</sub> )	10 <sup>-14</sup>	.00768	same	same
Clad (Zr, Sn)	4.6 x 10 <sup>-14</sup>	.00768	same	same
Structure (Fe)	3.2 x 10 <sup>-11</sup>	.00576	same	same
Ru	1.36 x 10 <sup>-11</sup>	.00768	8.49 x 10 <sup>-7</sup>	.00262
Zr	8.3 x 10 <sup>-10</sup>	.00622	1.44 x 10 <sup>-5</sup>	.00173
Ba	7.28 x 10 <sup>-11</sup>	.00677	6.40 x 10 <sup>-7</sup>	.00377
Sb	1.0 x 10 <sup>-8</sup>	.00667	1.55 x 10 <sup>-6</sup>	.00303
Te, Ag	2.96 x 10 <sup>-8</sup>	.00677	1.17 x 10 <sup>-5</sup>	.00404
Cs, I	1.65 x 10 <sup>-7</sup>	.00667	1.89 x 10 <sup>-5</sup>	.00451

The total release is the sum of the releases from the various finite regions of the core.

The application of the above model to sequences AB and S<sub>2</sub>C were made as follows. The temperature history developed by MARCH as shown on Tables C.2 and C.3 were approximated by first plotting the fraction of the core above 1000°C (~1900°F on the Tables) as a function of time along with the fraction above 2200°C (~4000°F) as shown on Figs. B.1 and B.2 for AB and S<sub>2</sub>C respectively. As seen on these figures, the rate at which the core parts are heated to 1000°C is the slope of the 1000°C line (or approximately 10%/min for AB and 2%/min for S<sub>2</sub>C. The average heat-up rate from 1000°C to 2800°C is approximated by dividing (2800-1000) by the average time difference between the two lines which gave ~250°C/min for AB and ~80°C/min for S<sub>2</sub>C.

Consequently, in Eq. B.5, "a" is 1000°C and "b" is 250°C/min for AB and 80°C/min for S<sub>2</sub>C. In this application of Eq. B.5, the core was divided into 10 finite regions heating up to 1000°C at a rate of 10%/min for AB and 2%/min for S<sub>2</sub>C. Consequently, in AB each finite region in order is delayed by 1 minute before the release calculation starts. That is, Region 2 starts releasing 1 minute after Region 1, Region 3 starts two minutes after Region 1, etc. For S<sub>2</sub>C, since the rate is 2%/min, the delay between regions is 5 minutes. Consequently the total fractional release (fraction of total core inventory) for the 10 finite regions is calculated for the AB and S<sub>2</sub>C sequences respectively by

$$\text{Total fractional release} = \begin{cases} 1/10 \sum_{i=0}^9 (\text{fractional release of first element})_{t-i} \\ 1/10 \sum_{i=0}^9 (\text{fractional release of first element})_{t-5i} \end{cases}$$

Table B.2. Fraction of core within 200°F temperature interval as function of time for Sequence AB, Temperature, °F + 100

Time (min)	300	500	700	900	1100	1300	1500	1700	1900	2100	2300	2500	2700	2900	3100	3300	3500	3700	3900	>4000	
1	.333	.033	.217	.150	.117	.067	.050	.033													
2	.25	.05	.083	.183	.167	.100	.083	.033	.017	.033											
3	.167	.083	.033	.117	.150	.150	.100	.100	.017	.033	.017	.033									
4	.167	.017	.05	.067	.150	.133	.100	.083	.083	.067	.017	.017	.017	0	0	.033					
5	.133	.033	.05	.033	.083	.117	.100	.133	.067	.067	.05	.033	0	.017	.033	0	.017	.017			.017
6	.083	.067	.033	.033	.067	.067	.117	.083	.100	.050	.067	.050	.017	.067	0	0	.017	.017			.083
7	.083	.050	.033	.033	.050	.050	.117	.050	.083	.083	.033	.050	.033	.033	.033	0	.050	0	.017		.177
8	.083	.017	.050	.033	.033	.067	.017	.100	.050	.083	.067	.067	.033	.017	.017	.017	.017	.067	0		.167
9	.083	0	.050	.017	.033	.050	.050	.050	.083	.017	.050	.100	.17	.083	0	.017	.017	.033	.017		.233
10	.033	.050	.033	.033	.017	.033	.050	.017	.033	.033	.050	.050	.017	.083	.050	0	.017	.017	.033	.017	.300
11	0	.083	.017	.033	.033	0	.050	.033	.017	.067	.017	.050	.033	.050	.033	.050	0	.033	.033		.367
12	0	.067	.017	.033	.017	.017	.017	.067	0	.033	.050	.017	.033	.033	.067	.017	.050	0	.017		.450
13	0	.050	.017	.033	.017	.017	0	.033	.033	0	.033	.033	.033	.033	.033	.033	.033	.050	0		.517
14	0	.017	.033	.017	.017	.017	0	0	0	.03	.017	.033	.050	0	.033	.050	.033	.033	.050		.567
15	0	.017	.017	.017	0	0	0	0	0	0	0	.017	.017	.033	.033	.017	.033	.050	0		.733
16	0	.017	0	.017	0	0	.017	0	0	0	0	.017	.017	.017	.033	.017	.033	.050	.033		.733
17	0	0	.017	0	.017	0	0	0	0	0	0	0	.017	.017	.017	.050	.033	.033	.050		.750
18	0	0	.017	0	0	.017	0	0	0	0	0	0	.017	.017	.017	.050	.017	.017	.050		.783
19	0	0	.017	0	0	0	0	0	0	0	0	0	.017	.017	0	.017	.067	.033	.017		.817
20	0	0	.017	0	0	0	0	0	0	0	0	0	0	.017	.017	.017	.050	.017	.017		.850

Table B.3. Fraction of core within 200°F temperature interval as function of time for S<sub>2</sub>C,  
Temperature, °F + 100

Time (min) from start of acci- dent	300	500	700	900	1100	1300	1500	1700	1900	2100	2300	2500	2700	2900	3100	3300	3500	3700	3900	>4000
1825	0	1.00																		
1835	0	.95	.05																	
1846	0	.517	.333	.150																
1857	0	.333	.100	.250	.200	.083	.033													
1867	0	.25	.033	.083	.200	.150	.133	.083	.017	.017	.033									
1877	.083	.083	.050	.050	.083	.117	.133	.083	.067	.050	.017	.017	.017	.017	.033	0	0	0	0	.100
1887	.083	.017	.050	.050	.033	.067	.033	.067	.067	.033	.033	.017	.050	.017	.017	.033	0	0	0	.333
1898	0	.067	.050	.033	.017	.033	.017	.050	0	.033	0	.033	.050	.017	.033	.017	0	0	0	.550
1908	0	.017	.050	.050	.017	0	.017	0	0	.033	.033	0	.033	0	.017	.033	0	0	.017	.683
1918	0	0	.050	.017	.017	.017	0	0	0	0	0	.033	.017	0	.017	.017	.017	.017	0	.783
1928	0	0	.017	.017	.017	0	.017	0	0	0	0	0	.017	.017	.017	.033	.017	0	.017	.833

ORNL-DWG 81-173

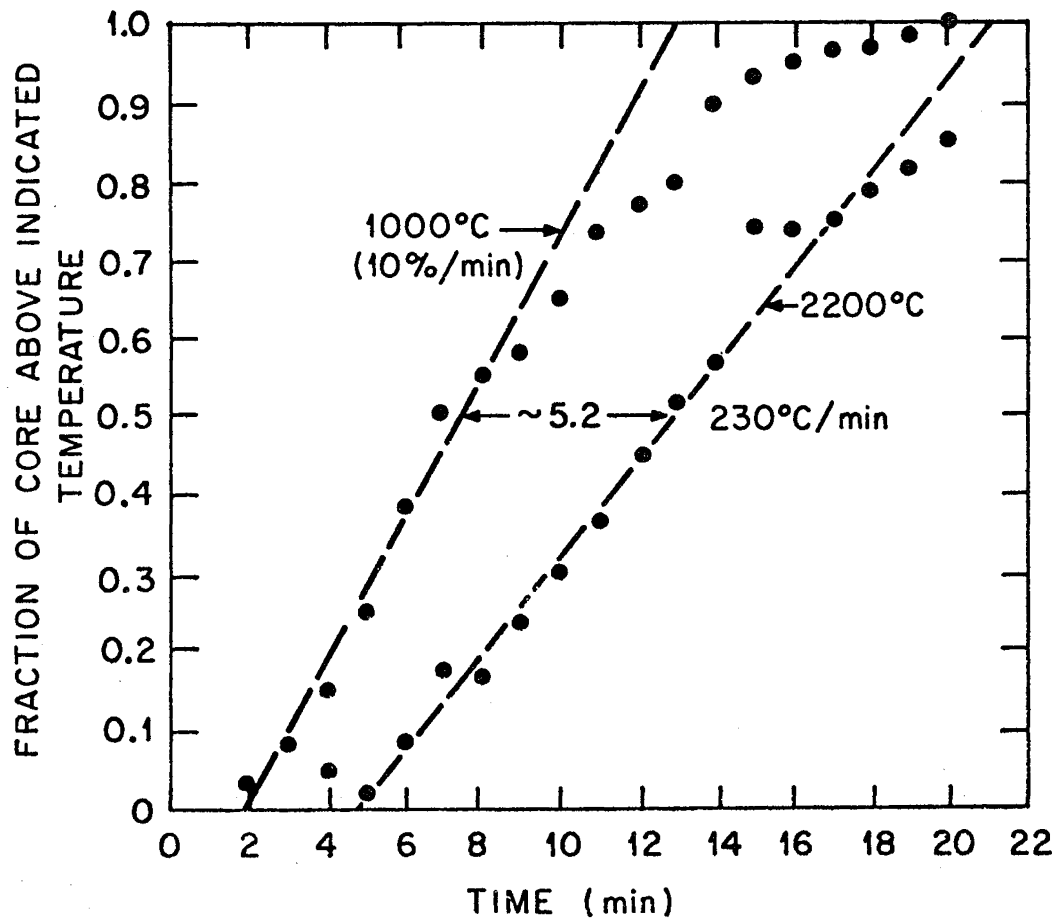


Fig. B.1. MARCH results for AB sequence.

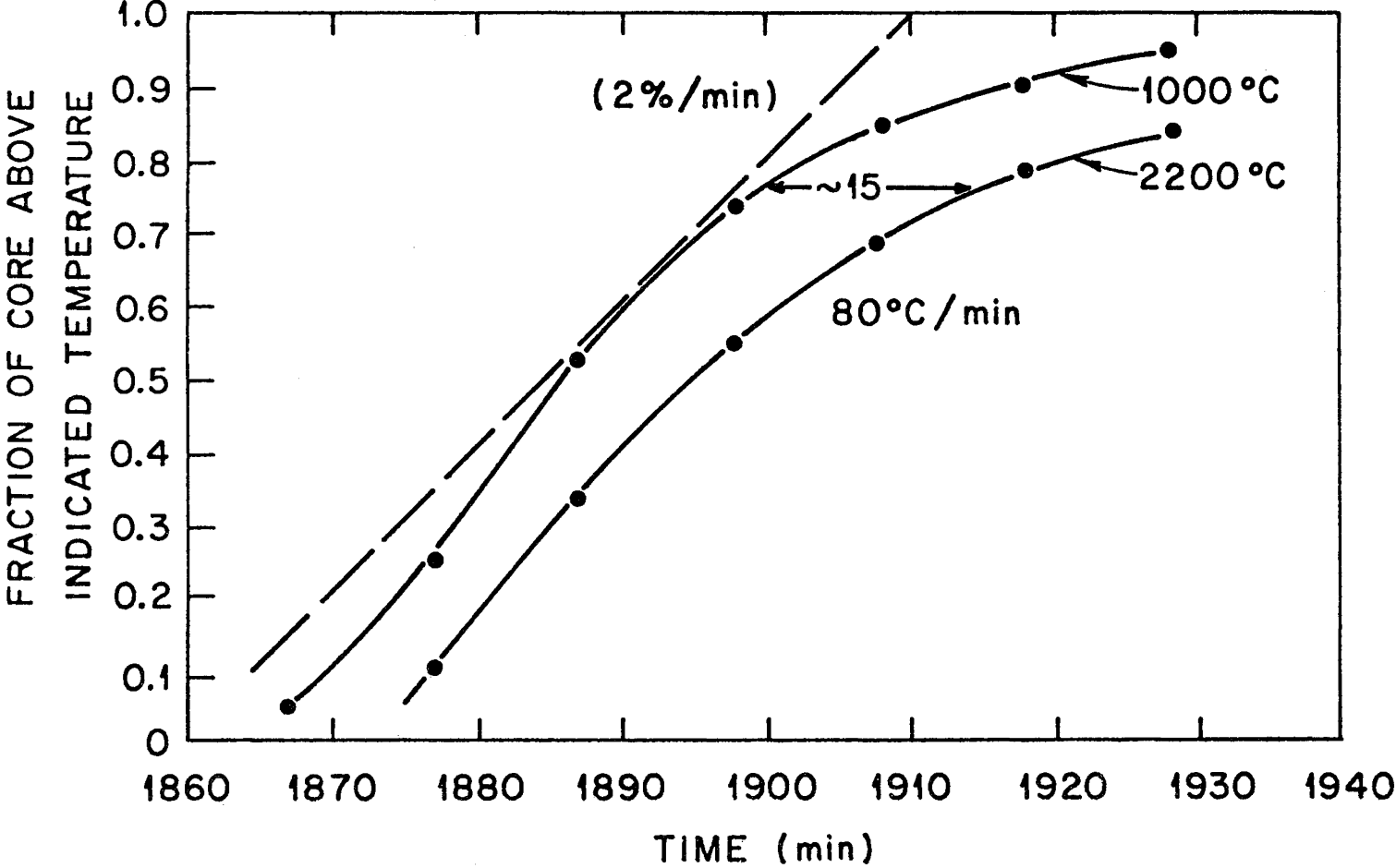


Fig. B.2. MARCH results for S<sub>2</sub>C sequence.

## B.7

The results of this calculation are shown on Fig. B.3 for AB and on Fig. B.4 for S<sub>2</sub>C.

To determine the total mass released, it is necessary to specify the inventories of each element. For the estimates in Section 4.3, the inventories used were the following, appropriate for a typical 1100 Mw PWR:

UO <sub>2</sub>	. . . . .	10 <sup>5</sup> kg
Zr (clad)	. . . . .	2.0 x 10 <sup>4</sup> kg
Sn (clad)	. . . . .	300 kg
Fe (structure)	. . . . .	2.5 x 10 <sup>3</sup> kg (in core) 2.5 x 10 <sup>4</sup> kg (core + bottom structure)
I (F.P.)	. . . . .	18 kg
Cs (F.P.)	. . . . .	255 kg
Ba, Sr, Mo (F.P.)	. . . . .	416 kg
Noble metals (F.P.)	. . . . .	318 kg
Zr (F.P.)	. . . . .	276 kg

### Release from Fuel Melt/Concrete Interactions (Vaporization Release)

As identified in the Reactor Safety Study, the other major source of airborne materials that can be introduced into the secondary containment is the vigorous interaction that occurs when molten core materials penetrate the primary vessel and contact the concrete in the basemat of the cavity housing the primary vessel. Currently, core-melt/concrete release experiments and analyses are being conducted at Sandia National Laboratory and preliminary results have recently been reported.<sup>(4.26)</sup> In these tests, Sandia observed that large quantities of aerosols are produced. The thermal decomposition of the concrete produces large quantities of gas which sparges through the melt and, at the high melt temperatures, produces aerosols. They made the following observations:

1. Aerosol generation rate at a fixed temperature is linearly proportional to the superficial velocity of gas sparging through the melt;
2. Aerosol generation rate is a sharp function of melt temperature;
3. Aerosol generation rate is not strongly dependent on concrete type;
4. The aerosol is composed mostly of non-fuel material;
5. The aerosol particle size distribution is sharply peaked at a mean aerodynamic particle size of 2 μm.

Sandia developed a preliminary correlation based on data from one small scale transient corium/concrete interactions test and two larger scale sustained stainless steel/concrete tests. The model gives the rate of aerosol release from the surface of a molten pool interacting with concrete as being

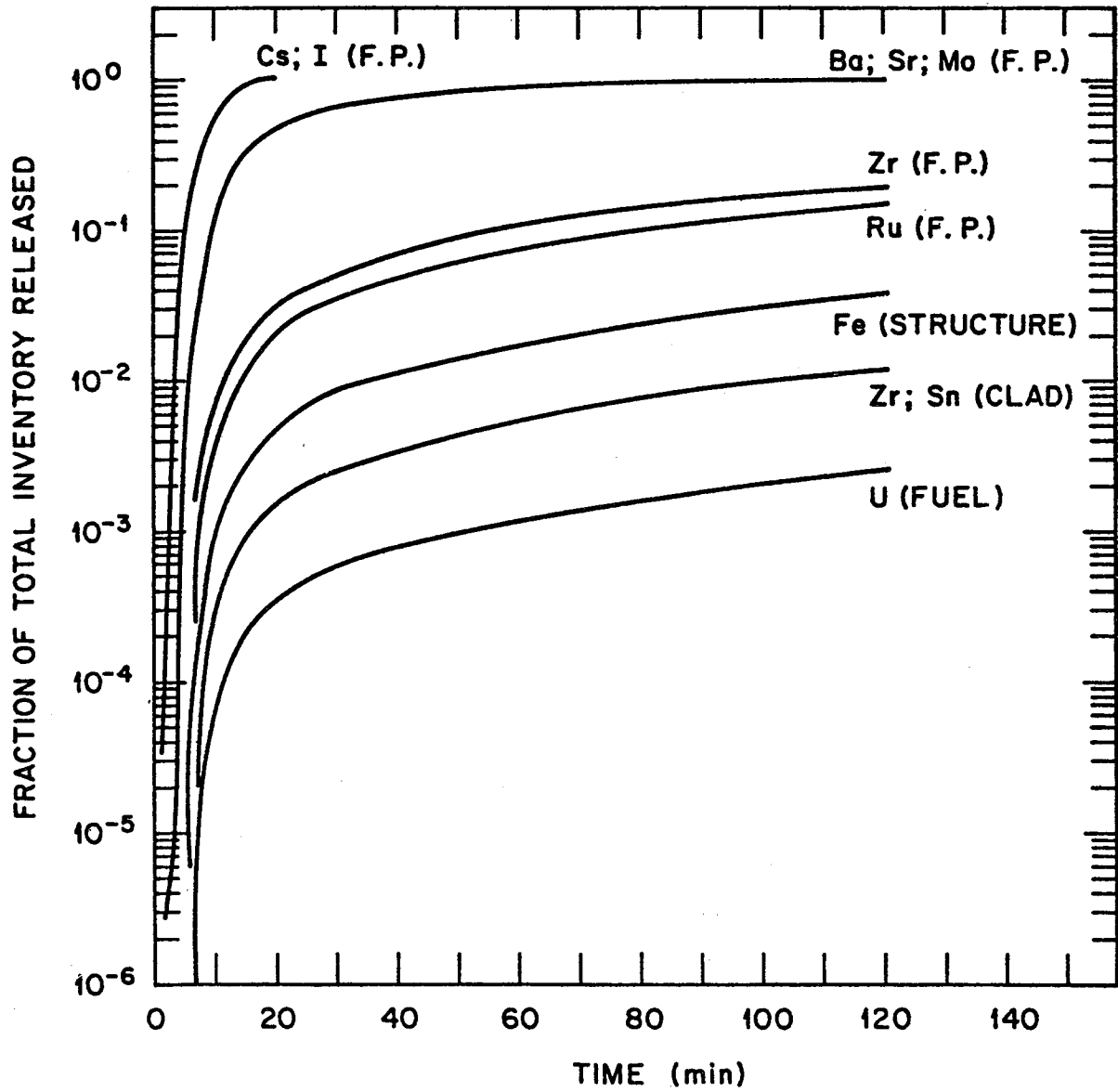


Fig. B.3. Aerosol source term for AB sequence.

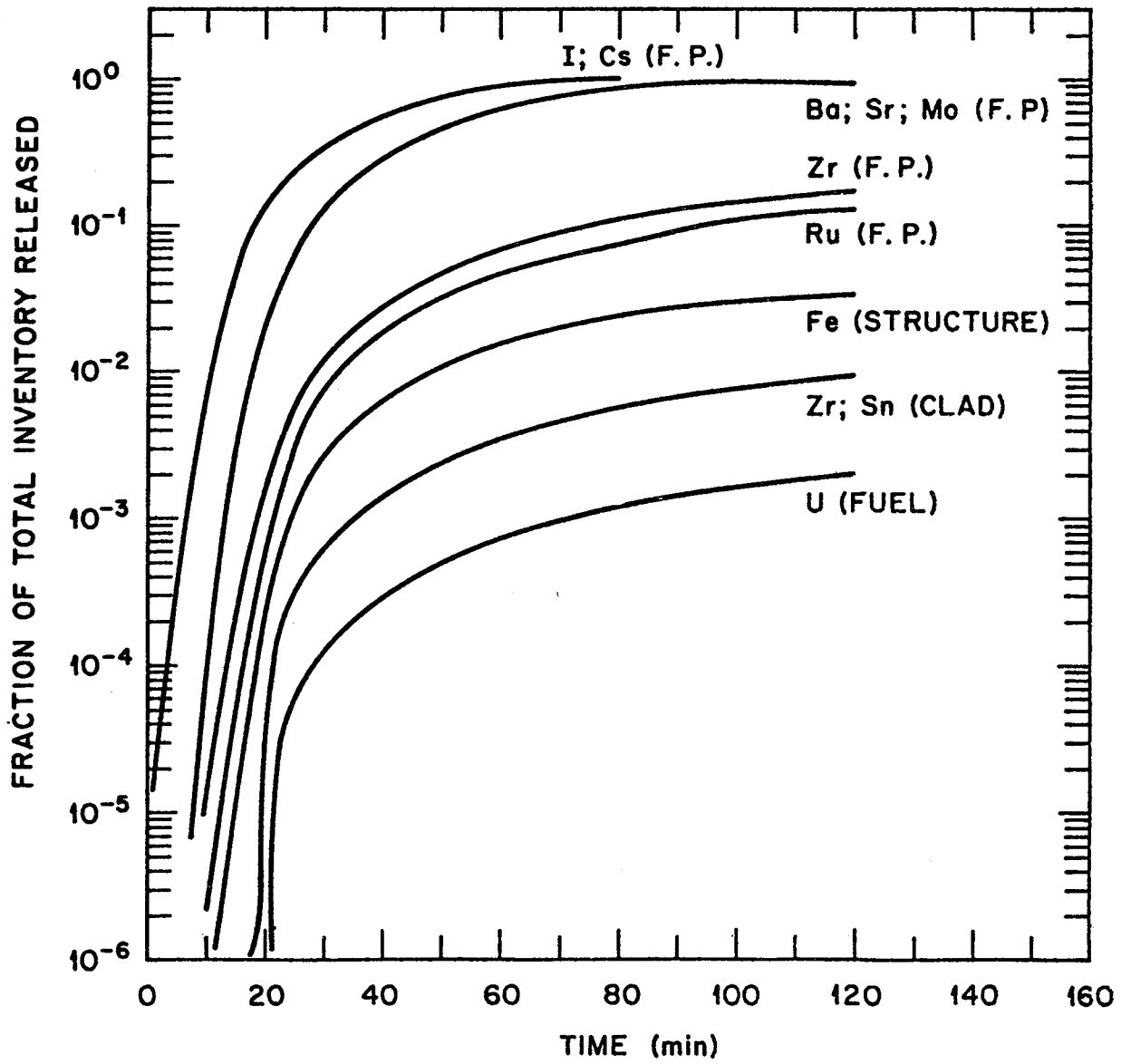


Fig. B.4. Aerosol source term for  $S_2C$  sequence

## B.10

$$dM/dt = C_a A_S V_S \quad (B.6)$$

where  $C_a$  is the aerosol concentration in the plume rising above the melt,

$A_S$  is the melt surface area (plume cross section),  
and  $V_S$  is the superficial gas velocity.

The concentration,  $C_a$ , was empirically related to the melt temperature and the superficial gas velocity as

$$C_a = A_0 \exp(-E/RT)(\beta V_S + \alpha)$$

where  $A_0$ ,  $E$ ,  $\beta$ , and  $\alpha$  are empirical constants,

$$E/R = 19,000$$

$$\beta = 24$$

$$\alpha = 3.3$$

$$A_0 = 10^4$$

$$R = 1.987 \text{ cal/mole}$$

$$T = \text{melt temperature } (^{\circ}\text{K})$$

$$V_S = \text{superficial gas velocity at STP (m/s)}.$$

The concentration values given by this equation are shown in Table B.4 as a function of temperature and superficial gas velocity.

To utilize this correlation along with Eq. B.6 for estimating aerosol release, it is necessary to specify the melt surface area,  $A_S$ ; the melt temperature,  $T$ , and the superficial gas velocity,  $V_S$ . The superficial gas velocity depends on the heat transfer from the melt to the concrete,  $q$ , according to

$$V_S = \psi q / h_{\text{eff}}$$

where  $\psi$  is the volume of gas per unit mass of concrete and  $h_{\text{eff}}$  is the effective heat of ablation. Consequently, to estimate the release requires knowledge of the melt geometry and a thermal analysis of the melt/concrete interaction to determine the heat exchange and the transient temperatures. Such models are presently under development by Karlsruhe (WECHSL code)<sup>(4.27)</sup> and Sandia (CORCON code).<sup>(4.28)</sup> The WECHSL code was utilized in the Zion/Indian Point Study [Reference 4.26] along with the above preliminary model to determine release quantities for a variety of accident sequences as shown in Table B.5. For the AB sequence, which had the highest calculated release of ~510 kg, the calculated release is shown as a function of time in Fig. B.5.

Because (1) the release model is preliminary and based on limited data, (2) there is considerable disagreement between WECHSL and CORCON on the thermal analysis, and (3) the aerosol production is strongly dependent on the initial temperature of the melt, these release estimates must be

## B.11

Table B.4. Aerosol concentration ( $\text{g}/\text{m}^3$ )  
 $[A] = \exp(-19000/T(24V + 3.3))1000$

Superficial gas velocity (m/s)

Temperature (K)	0.1	0.3	0.5	0.7	0.9
1573	0.32	0.60	0.87	1.14	1.41
1723	0.93	1.71	2.49	3.27	4.05
1873	2.24	4.13	6.01	7.90	9.79
2023	4.75	8.76	12.76	16.76	20.76
2173	9.09	16.74	24.40	32.05	39.71
2323	15.99	29.45	42.91	56.37	69.83
2473	26.25	48.36	70.47	92.58	114.69
2623	40.74	7505	109.35	143.66	177.97
2773	60.28	111.04	161.81	212.57	263.33
2923	85.68	157.83	229.99	302.14	374.29

V = superficial gas velocity at STP (m/s)

T = absolute temperature (K)

A = aerosol concentration ( $\text{g}/\text{m}^3$ )

Mean equivalent, unit dense, spherical particle size =  $2 \mu\text{m}$

Table B.5. Results of Melt/Concrete Interaction Calculations

Sequence	Initial radius (m)	Temperature (K)	Carbonate content	Water above melt (a)	Decay heat	Melt-through (Hr)	Aerosols (Kg)
TMLB'	3.8	2073	medium	yes	ORIGEN	84	(b)
TMLB'	3.8	2073	medium	no	ORIGEN	83	130
TMLB'	3.8	2073	medium	no	BCL	83	(b)
TMLB'	3.8	(c)	high	no	BCL	85	(b)
TMLB'	3.12	2073	high	no	BCL	81	(b)
TMLB'	3.12	2073	medium	no	ORIGEN	81	(b)
AB	3.8	2550	medium	no	ORIGEN	79	208
AB	3.12	2550	high	no	BCL	75	437
AB	3.05	2550	medium	no	ORIGEN	71	485
AB	3.05	2550	high	no	ORIGEN	73	510

NOTES: (a) Water is assumed to boil away quiescently and absorbs all aerosols  
 (b) Not calculated for this run.  
 (c) Oxide temperature 2073K, metal temperature 1684K.

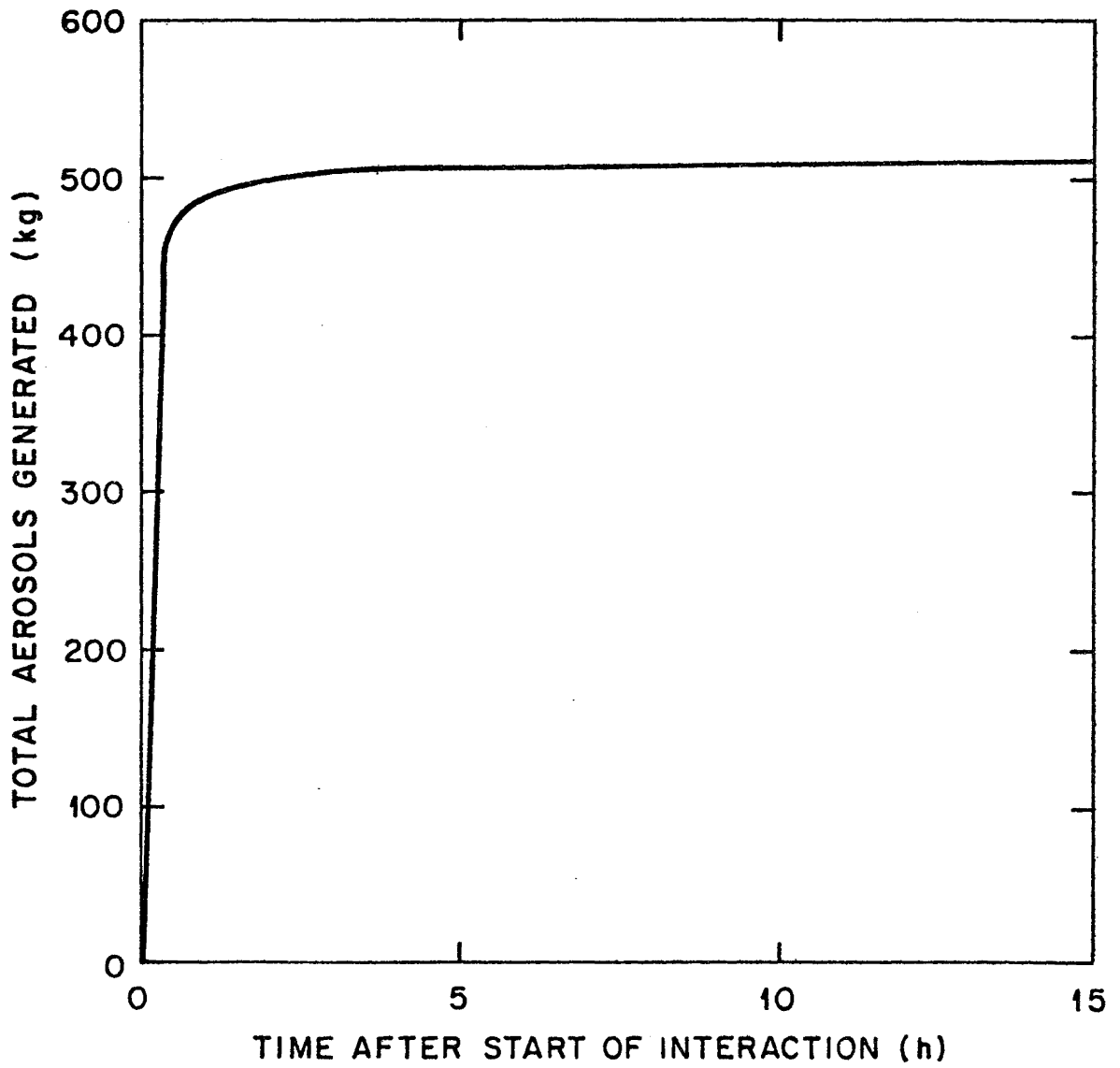


Fig. B.5. Aerosols generated by melt/concrete interaction in sequence AB.

## B.14

considered only as illustrative at this time. For example, if the initial melt temperature in Sequence AB were 2500°C instead of the 2377°C used in Table B.4 and Fig. B.5, the calculated total release would become 1660 kg.

It should also be noted that Sandia reports that these are mostly non-radioactive aerosols coming from the concrete constituents. The solid materials released were identified as being oxides of silicon, calcium, and aluminum and other inorganic oxides. For aerosol transport calculations, the melt/concrete releases can be considered to be made up of spherical particles, 2  $\mu\text{m}$  in mean aerodynamic diameter, with a geometric standard deviation of 2 for a log-normal distribution. The importance of the non-radioactive aerosols is that they serve as scavengers that help remove radioactive aerosols from the containment by co-agglomeration and sedimentation. The radiological threat, however, is posed by the fuel, plutonium, activation, and fission products that are released. It will be important to specify the fraction of these that are entrained in the total released mass.

## APPENDIX C

### CHEMISTRY OF CESIUM AND IODINE

#### C.1 Vapor Phase Chemistry for the Cesium-Iodine-Hydrogen-Oxygen System

Only the iodine-containing species on the Cs-I-H-O system are examined in detail in this appendix. Two chemical regimes for the iodine-containing species were found by the FLUEQU code (see appendix C.4). These chemical regimes are characterized by the stability of different iodine species. In one regime, the dominant iodine species are I and HI while in the other regime CsI is the dominant iodine species. The transition between these two regimes is not easy to delineate because the transition is sensitive to all the system parameters. In general, low temperatures, high pressures, high fission-product concentrations and reducing conditions promote the formation of CsI.

The interplay of the system parameters are illustrated in the paragraphs below.

The limits of parameter variation for the Cs-I-H-O system are:

Temperature: 600C to 2300C

Pressure: 1 bar and 150 bars

Cesium-to-iodine ratio (Cs/I in moles/mole): 10 and 1

Hydrogen to oxygen ratio (H/O in moles/mole): 1.5 to 30

Iodine to water ratio, I(moles)/H<sub>2</sub>O(moles): from  $2 \times 10^{-7}$   
to  $2 \times 10^{-1}$

Fission product concentration has been expressed as a mass ratio (I/H<sub>2</sub>O for instance), rather than as a density (mass/volume). This was an input parameter to the code. System pressure has no effect on concentration expressed in mass ratio but obviously directly affects the concentration expressed in density units. The pressure effects reported here reflect this change in density.

The variations of composition with temperature are shown in Figures C.1, C.2, C.3, and C.4.

In all figures the Cs/I ratio is 10.

As temperature is raised there is a conversion of CsI into other species. The cesium reacts with steam to produce CsOH while iodine appears as I or HI. The temperature at which a 50% conversion of CsI occurs is used to illustrate the stability trends.

As the H/O ratio increases from 1.5 to 30, CsI, is stable

## C.2

to higher temperatures. Figures C.1 a, b, c, and d illustrate this for  $I/H_2O = 2 \times 10^{-7}$ . At an H/O ratio of 1.5 (oxidizing) about 50% of the iodine is present as CsI for a system at 550C and a pressure of 1 bar.

(Corresponding curves for a system pressure of 150 bars are shown as dashed lines. In all cases, increasing the total system pressure increases the stability of CsI and HI at the expense of I.)

As the H/O ratio increases to 2 (pure steam - no excess hydrogen or oxygen) the vapors must be heated to about 820C before 50% the CsI is converted. For an H/O = 3 the corresponding temperature is about 1150C and not much higher for an H/O = 10. For H/O values greater than 2 (reducing) the iodine forms HI with the dissociated iodine from CsI. At higher temperatures both I and HI are formed since in turn HI is becoming unstable.

A single example will be given for the effect on system stability of reducing the Cs/I ratio. For a concentration of  $2 \times 10^{-7}$ , an H/O = 2 and Cs/I = 1, 50% of CsI has dissociated at 620C. Compare this to the dissociation temperature obtained for a Cs/I ratio of 10 which was 820C. Decreasing the ratio of cesium-to-iodine decreases the stability of CsI.

Increasing the  $I/H_2O$  ratio raises the temperature at which conversion of CsI to other species begins. This is illustrated in Figure C.2 a, b, c and d for a concentration of  $2 \times 10^{-5}$  and 1 bar pressure. At an H/O ratio of 1.5, 50% of the CsI is converted at about 1000C (compare with 550C at  $2 \times 10^{-7}$ ). At H/O ratios of 2, 3 and 30 the corresponding temperatures are about 1270C, 1550C and 1560C.

A further increase in  $I/H_2O$  to  $2 \times 10^{-3}$  increases the point at which CsI is 50% converted to 1960C, 2100C, 2160C and about 2040C for H/O values of 1.5, 2, 3 and 30 (Figures C.3 a, b, c and d).

At the maximum concentration,  $2 \times 10^{-1}$  and the maximum temperature, 2300C studied about 90% of the iodine exists as CsI for H/O values from 1.5 to 30 (Figures C.4 a, b, c and d).

### C.2 Condensation on Surfaces: Aerosols and Structures

Fission products may physically condense on any available surface including aerosols and structures. The condensation can occur only if the partial pressure of the vapor species is greater than the vapor pressure of the corresponding condensate.

For various fission product concentrations ( $I/H_2O$  ratios) temperatures can be determined at which the partial pressure equals the vapor pressure for CsOH and CsI. Table C.1 presents typical examples of these temperatures.

### C.3

TABLE C.1

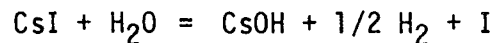
Temperatures at which Partial Pressure Equals Vapor Pressure

I/H <sub>2</sub> O(Cs/I=10)	T <sub>CsOH</sub>	T <sub>CsI</sub>
2 x 10 <sup>-3</sup>	723 C	760 C
2 x 10 <sup>-5</sup>	510 C	555 C
2 x 10 <sup>-7</sup>	371 C	418 C

At temperatures below those in the table, CsOH and CsI will condense on either aerosols or structures. For the above table, the partial pressure of CsOH vapor is assumed to be nine times the partial pressure of CsI vapor (Cs/I = 10). The temperature at which less concentrated CsOH would condense is lower than tabulated.

#### C.3 Chemical Reactions with Surfaces: Aerosol and Structural

No thermodynamic data exist to detail the reaction between CsOH and stainless steel although they do react at elevated temperatures (5.8). Whenever CsOH is removed from the vapor phase, the composition of the vapor will change to reflect the accompanying decrease in the cesium to iodine ratio. This decrease may cause the transfer of the iodine from CsI to other iodine species. Consider the equation



Under most conditions the reaction is shifted to the left hand side. However removal of CsOH from the vapor will cause the reaction to begin to shift to the right hand side. The extent of this shift is determined by the degree to which CsOH is removed from the vapor. If CsOH and stainless steel react very strongly, there may be virtually complete removal of the CsOH from the vapor. This would result in the disappearance of some, maybe all of the CsI vapor.

The chemical reaction with surfaces can be most easily discussed by choosing a specific set of conditions:

Temperature: 1000C

Pressure: 1 bar

H/O ratio: 2.1

I/H<sub>2</sub>O ratio: 2 x 10<sup>-4</sup>

## C.4

At 1000C the vapor pressure of CsOH is about 0.7 bar. Since the reduced vapor pressure of the CsOH, resulting from its reaction with stainless steel is not known, a series of pressures from  $10^{-3}P_{\text{CsOH}}$  to  $10^{-7}P_{\text{CsOH}}$  have been assumed. Table C.2 presents the calculated iodine distribution resulting from the above CsOH pressures. If the CsOH that has reacted with stainless steel exhibits a vapor pressure greater than  $10^{-4}P_{\text{CsOH}}$ , for instance, then all of the iodine in the system remains as CsI vapor. However if the CsOH that has reacted with stainless steel exhibits a vapor pressure of  $10^{-6}P_{\text{CsOH}}$ , then only 60% of the iodine remains as CsI while 24% of the iodine is present as HI and 16% as I.

TABLE C.2

Postulated Conditions for CsOH Reaction with Stainless Steel

(1000C,  $P_{\text{CsOH}} = 0.7$  bar)

	Concentration of species (%)		
	CsI	HI	I
$10^{-3}P_{\text{CsOH}}$	100	0	0
$10^{-4}P_{\text{CsOH}}$	100	0	0
$10^{-5}P_{\text{CsOH}}$	93	5	2
$10^{-6}P_{\text{CsOH}}$	60	24	16
$10^{-7}P_{\text{CsOH}}$	10	64	26

Firm conclusions are not possible until experimental data become available.

### C.4 Notes on FLUEQU

The code FLUEQU was developed by T. M. Gerlach at Sandia National Laboratories as part of the Magma Energy Research Project under funding from the Office of Basic Energy Sciences of the Department of Energy. FLUEQU has been applied extensively in research on magmatic and volcanic gases, and it has also proven useful in the calculation of high temperature chemical vapor deposition phase diagrams (5.9).

FLUEQU is based on method for complex chemical equilibrium calculations originated by White, et al. (5.10) and incorporating improvements discussed in Van Zeggeren and Storey (5.11). The method used is a second order steepest descent technique in which the system free energy is approximated by a quadratic equation obtained by a Taylor's expansion. The resulting parabolic surface is differen-

tiated to obtain its minimum as an approximation to the Gibbs free energy minimum. This point is then used as a starting point for making an improved estimate of the Gibbs free energy minimum, and so on in an iterative fashion until a convergence criterion is satisfied.

FLUEQU is run in an interactive mode on a timesharing system. It has been equipped with several capabilities that allow for rapid exploration of complex gas systems. It can be programmed to run bulk compositions of interest along prespecified temperature-pressure paths or to run along isobars of interest. Nonideality in the gas phase at high pressures is treated in the code by a corresponding state version of the Redlich-Kwong equation.

Selected thermodynamic data for the major vapor species are tabulated below. These data are a) the heat of formation at 298K and b) the "free energy function",  $-(G-H_{298})/T$ , at 298K, 1000K, and 1700K. For code input the latter function, evaluated at 100K internals, was fitted by a six-degree polynomial.

Table C.3  
Selected Thermodynamic Data for  
Major Vapor Species

Vapor (Reference)	$H_f(298)$ [kcal/mole]	$-(G-H_{298})/T$ [Gibbs/moles]		
		298K	1000K	1700K
H <sub>2</sub> O (5.4)	-57.798	45.106	49.382	53.183
O <sub>2</sub> (5.4)	0.0	49.004	52.765	56.013
H <sub>2</sub> (5.4)	0.0	31.207	34.758	37.675
HI (5.4)	+6.30	49.351	52.977	54.079
I (5.4)	+25.54	43.184	45.709	47.737
CsI (5.2)	-28.55	70.156	74.910	78.703
CsI (5.6)	-40.3	65.767	70.353	74.071
CsOH (5.4)	-62.0	60.866	67.177	72.427
Te (5.3)	+50.6	43.64	46.16	48.22
Te <sub>2</sub> (5.3)	+38.33	61.87	66.45	70.35
TeO (5.3)	+17.8	57.50	61.64	65.10
TeO <sub>2</sub> (5.3)	-14.2	65.70	71.72	76.95

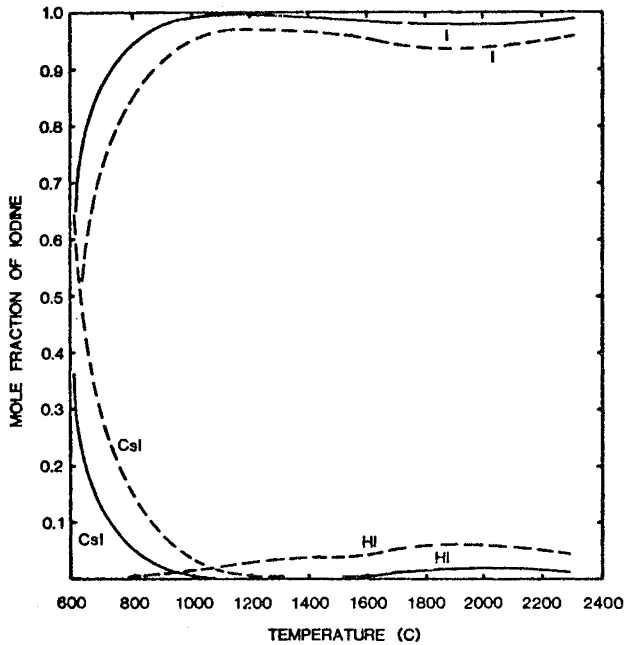


Fig. C.1a  $1/H_2O = 2 \times 10^{-7}$ ;  $H/O = 1.5$ ;  $Cs/I = 10$ ;  
 (—) PRESSURE EQUALS 1 BAR.  
 (---) PRESSURE EQUALS 150 BARS.

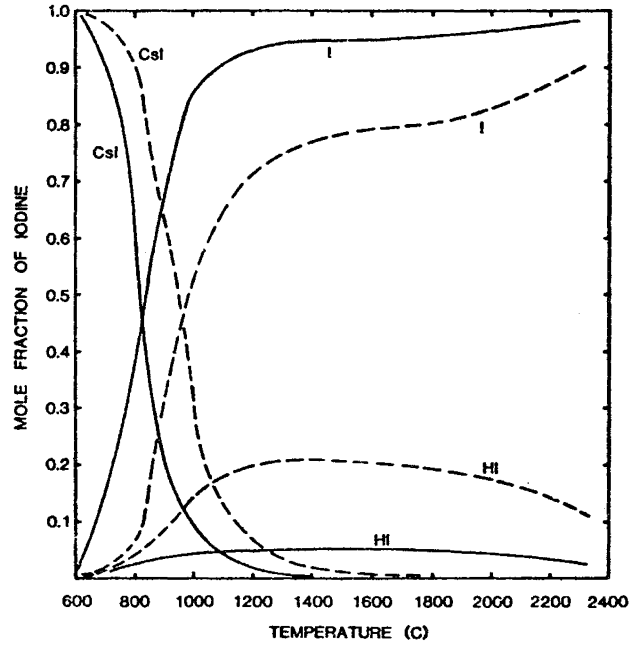


Fig. C.1b  $1/H_2O = 2 \times 10^{-7}$ ;  $H/O = 2.0$ ;  $Cs/I = 10$ ;  
 (—) PRESSURE EQUALS 1 BAR.  
 (---) PRESSURE EQUALS 150 BARS.

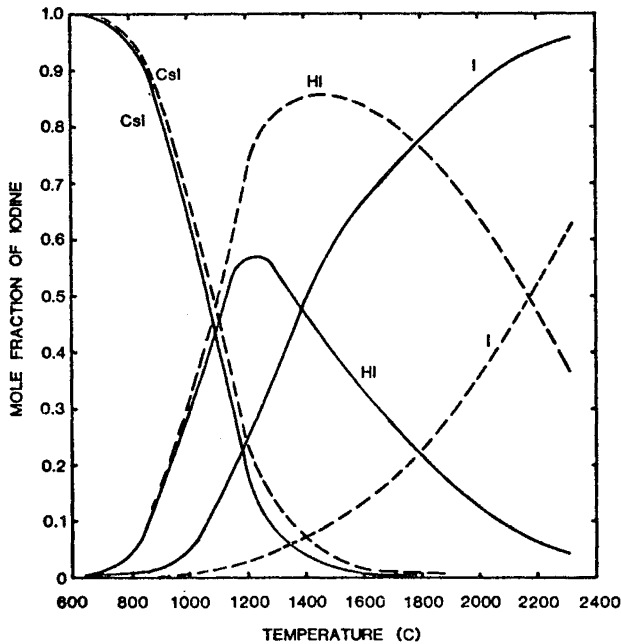


Fig. C.1c  $1/H_2O = 2 \times 10^{-7}$ ;  $H/O = 3.0$ ;  $Cs/I = 10$ ;  
 (—) PRESSURE EQUALS 1 BAR  
 (---) PRESSURE EQUALS 150 BARS.

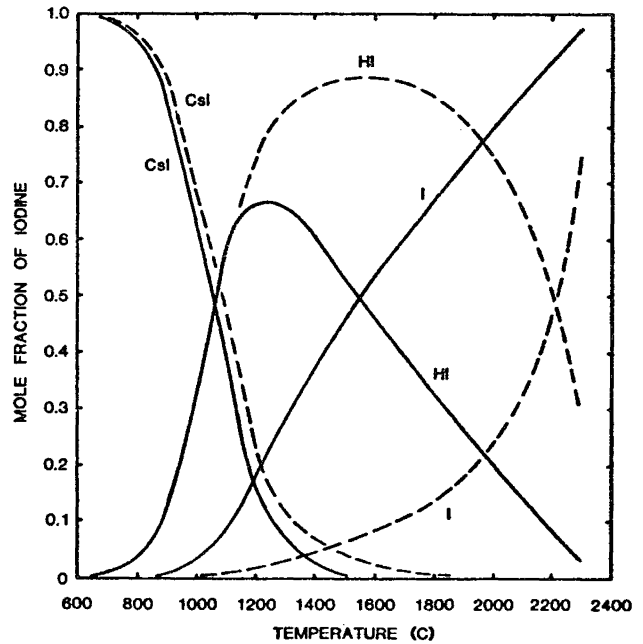


Fig. C.1d  $1/H_2O = 2 \times 10^{-7}$ ;  $H/O = 30$ ;  $Cs/I = 10$ ;  
 (—) PRESSURE EQUALS 1 BAR.  
 (---) PRESSURE EQUALS 150 BARS.

Fig. C.1 Relative abundance of iodine species in the Cesium-Iodine-Hydrogen-Oxygen System for the conditions given

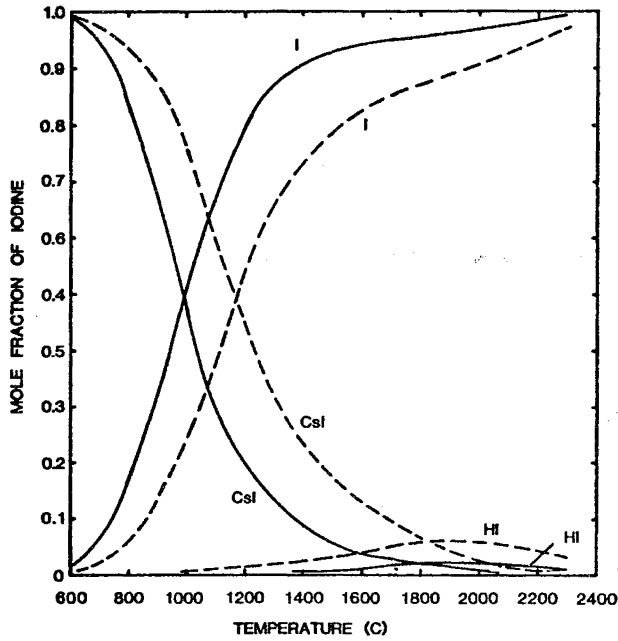


Fig. C.2a  $I/H_2O = 2 \times 10^{-5}$ ;  $H/O = 1.5$ ;  $Cs/I = 10$ ;  
 (—) PRESSURE EQUALS 1 BAR.  
 (---) PRESSURE EQUALS 150 BARS.

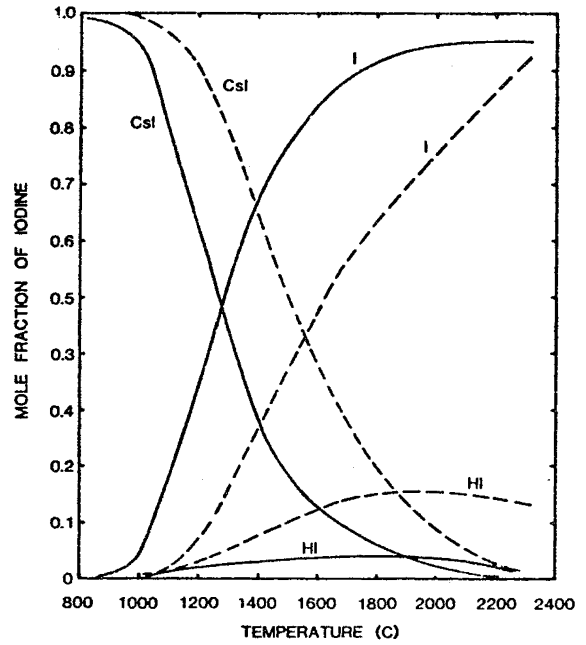


Fig. C.2b  $I/H_2O = 2 \times 10^{-5}$ ;  $H/O = 2.0$ ;  $Cs/I = 10$ ;  
 (—) PRESSURE EQUALS 1 BAR.  
 (---) PRESSURE EQUALS 150 BARS.

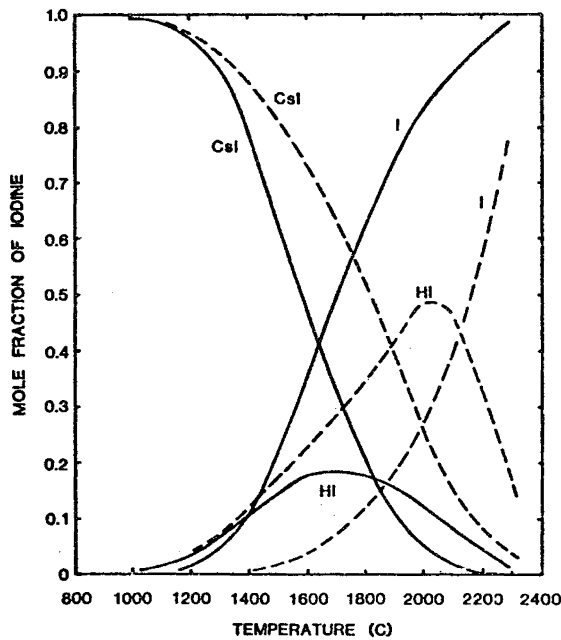


Fig. C.2c  $I/H_2O = 2 \times 10^{-5}$ ;  $H/O = 3.0$ ;  $Cs/I = 10$ ;  
 (—) PRESSURE EQUALS 1 BAR.  
 (---) PRESSURE EQUALS 150 BARS.

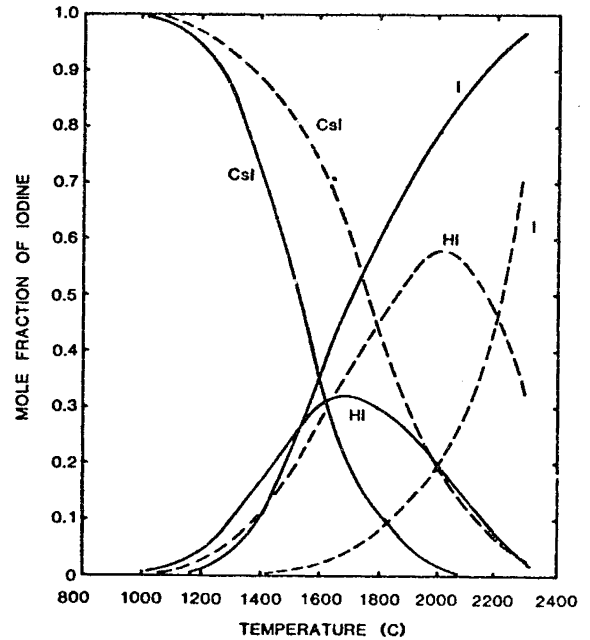


Fig. C.2d  $I/H_2O = 2 \times 10^{-5}$ ;  $H/O = 30$ ;  $Cs/I = 10$ ;  
 (—) PRESSURE EQUALS 1 BAR.  
 (---) PRESSURE EQUALS 150 BARS.

Fig. C.2 Relative abundance of iodine species in the Cesium-Iodine-Hydrogen-Oxygen System for the conditions given

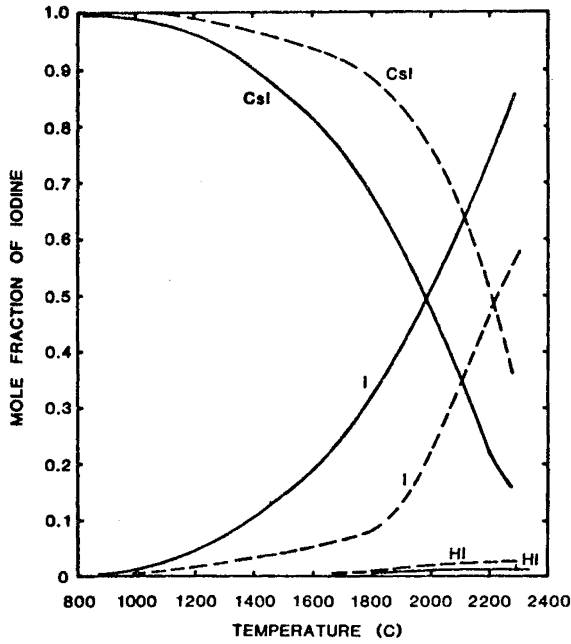


Fig. C.3a  $I/H_2O = 2 \times 10^{-3}$ ;  $H/O = 1.5$ ;  $Cs/I = 10$ ;  
 (—) PRESSURE EQUALS 1 BAR.  
 (---) PRESSURE EQUALS 150 BARS.

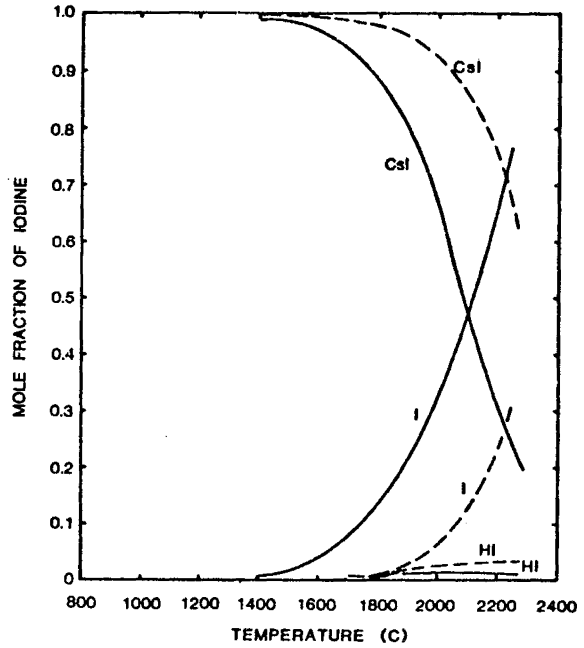


Fig. C.3b  $I/H_2O = 2 \times 10^{-3}$ ;  $H/O = 2.0$ ;  $Cs/I = 10$ ;  
 (—) PRESSURE EQUALS 1 BAR.  
 (---) PRESSURE EQUALS 150 BARS.

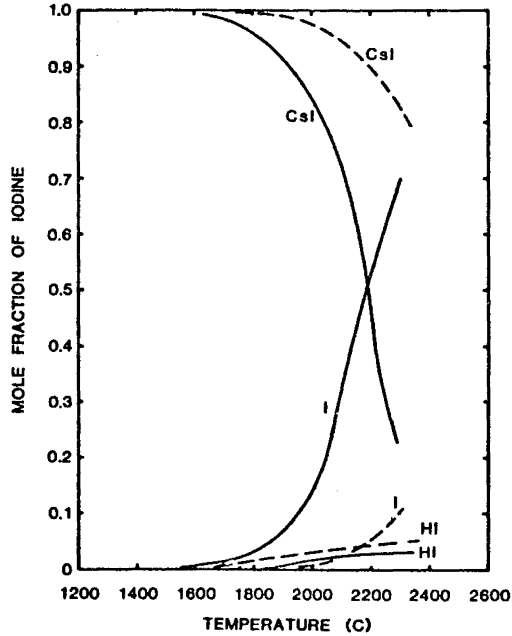


Fig. C.3c  $I/H_2O = 2 \times 10^{-3}$ ;  $H/O = 3.0$ ;  $Cs/I = 10$ ;  
 (—) PRESSURE EQUALS 1 BAR.  
 (---) PRESSURE EQUALS 150 BARS.

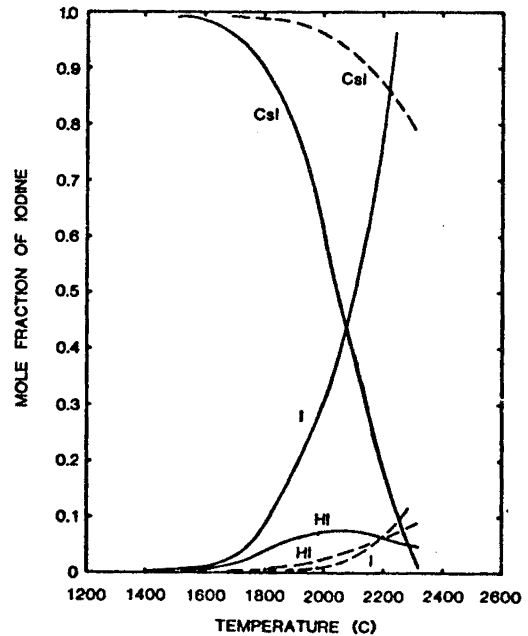


Fig. C.3d  $I/H_2O = 2 \times 10^{-3}$ ;  $H/O = 30$ ;  $Cs/I = 10$ ;  
 (—) PRESSURE EQUALS 1 BAR.  
 (---) PRESSURE EQUALS 150 BARS.

Fig. C.3 Relative abundance of iodine species in the Cesium-Iodine-Hydrogen-Oxygen System for the conditions given

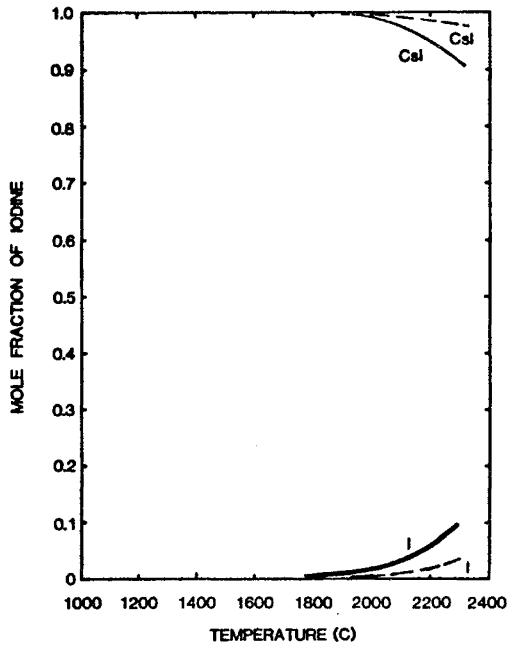


Fig.C.4a  $V/H_2O=2 \times 10^{-1}$ ;  $H/O=1.5$ ;  $Cs/I=10$ ;  
 (—) PRESSURE EQUALS 1 BAR.  
 (---) PRESSURE EQUALS 150 BARS.

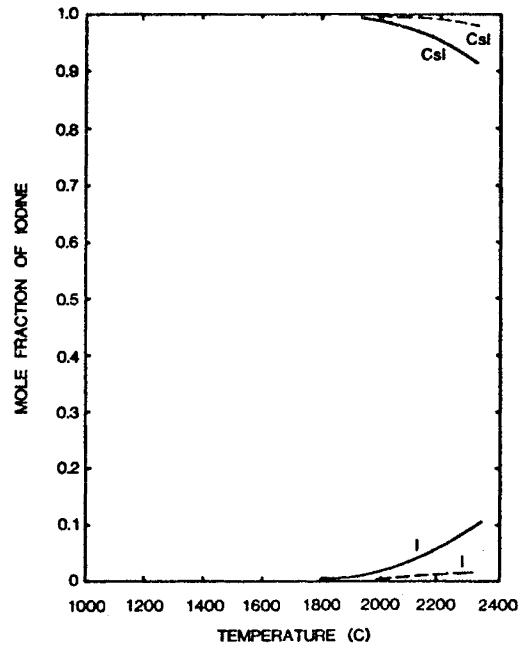


Fig.C.4b  $V/H_2O=2 \times 10^{-1}$ ;  $H/O=2.0$ ;  $Cs/I=10$ ;  
 (—) PRESSURE EQUALS 1 BAR.  
 (---) PRESSURE EQUALS 150 BARS.

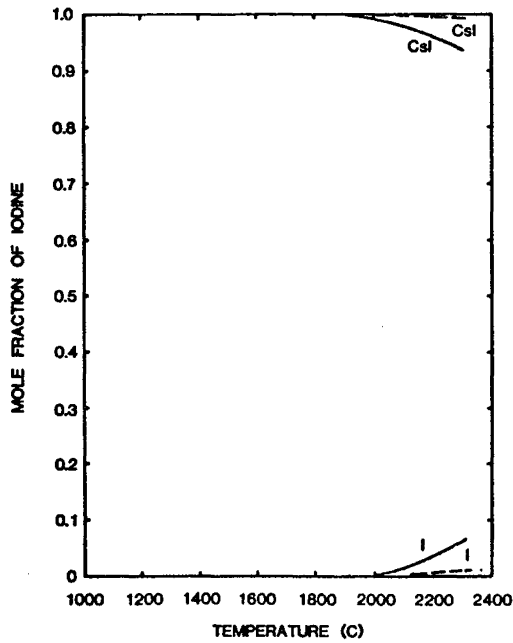


Fig.C.4c  $V/H_2O=2 \times 10^{-1}$ ;  $H/O=3.0$ ;  $Cs/I=10$ ;  
 (—) PRESSURE EQUALS 1 BAR.  
 (---) PRESSURE EQUALS 150 BARS.

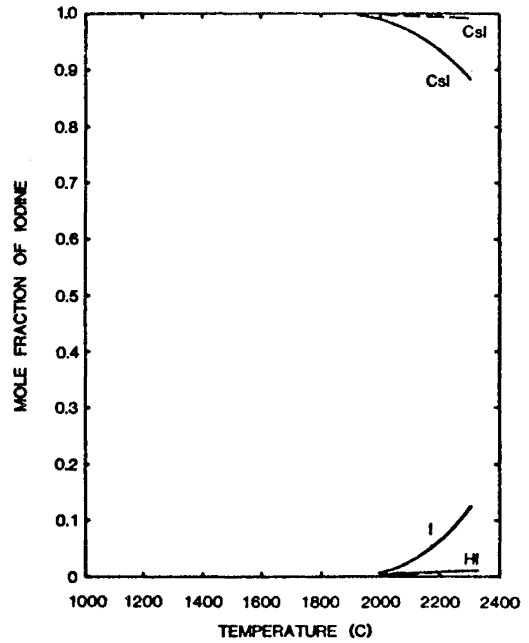


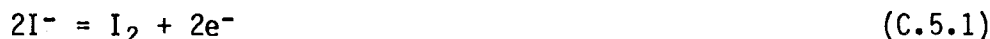
Fig.C.4d  $V/H_2O=2 \times 10^{-1}$ ;  $H/O=30$ ;  $Cs/I=10$ ;  
 (—) PRESSURE EQUALS 1 BAR.  
 (---) PRESSURE EQUALS 150 BARS.

Fig. C.4 Relative abundance of iodine species in the Cesium-Iodine-Hydrogen-Oxygen System for the conditions given

Appendix C.5 Redox Reactions of Iodine Species

Iodine can exist theoretically in all oxidation states between -1 and +7. In aqueous solutions the -1, 0, and +5 states ( $I^-$ ,  $I_2$ , and  $IO_3^-$ , respectively) are predominant, and redox reactions generally include these three states with suggestions that the +1 and +3 states exist as intermediate species. Standard redox potentials for iodine species may be found in inorganic chemistry texts<sup>5.13</sup> and in chemical handbooks.<sup>5.15</sup> Such tabulated data do not always specify standard states, care must be taken to select proper potentials for calculating aqueous system equilibrium constants.

For example, the footnote under the tabulated data in Cotton and Wilkinson<sup>5.13</sup> implies that those potentials may be used for aqueous solutions. Also, potentials for iodine reactions from handbooks can be confusing because of differences in unspecified standard states. As one example, the half cell reaction



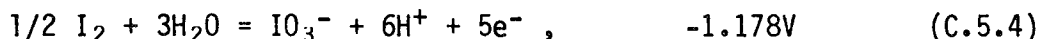
does not give the standard state for  $I_2$  and the potential is frequently given as  $-0.535V$ .<sup>5.13,5.15</sup> That potential is for solid state  $I_2$  at unit activity. The half cell reaction in aqueous solution is



and the potential is  $-0.621$  where the standard states for both  $I^-$  and  $I_2$  are 1 molal. Another example that is important to this work is the half cell reaction,



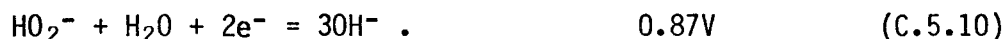
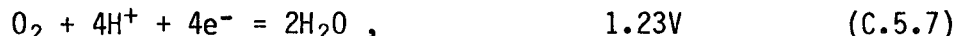
where the potential for the aqueous system is  $-1.178 V$ . The potential for the reaction with solid state  $I_2$  is  $-1.195 V$ . The aqueous system potentials must be used when calculating aqueous system equilibrium constants from the half cell potentials, i.e.,



The calculated equilibrium constant for (C.5.6) from redox potentials is then,  $\exp [-0.557 \times 96484 \times 5 \div 8.284 \div 298]$  or  $5.37 \times 10^{-48}$ . (Relationships of cell potentials, reaction free energies and equilibrium constants are discussed in the last part of this appendix. Improper selection or usage of the potentials could indicate an equilibrium constant as small as  $9.74 \times 10^{-57}$ , i.e., in error by nine orders of magnitude. Perhaps the best electrochemical data for aqueous systems are given by Poubaix<sup>5.16</sup> where the standard states are easily recognized.

## C.11

Other redox potentials that must be considered in iodine-water chemistry are:



Combinations of these reactions lead to redox potentials for iodine reactions with oxygen, etc. For example, the addition of reactions (C.5.2) and (C.5.7) is



and the equilibrium constant, calculated from the cell potential is  $2.6 \times 10^{23}$ . This indicates that oxygen will oxidize iodide to molecular iodine in water. Also, the reaction of molecular iodine with oxygen can be examined by adding equations (C.5.3) and (C.5.7) to derive an equation for that reaction,



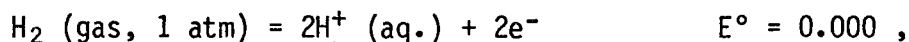
with an equilibrium constant of  $9.4 \times 10^{16}$ . Furthermore, combining equations (C.5.11) and (C.5.12) gives



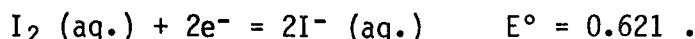
with an equilibrium constant of  $8.9 \times 10^{15}$ . This indicates that iodide can be oxidized to molecular  $\text{I}_2$  and that  $\text{I}_2$  can be further oxidized to the very stable iodate,  $\text{IO}_3^-$ .

### Thermodynamic Calculations

Relative stabilities of iodine species are given by half-cell redox potentials,  $E^\circ$ . This relative potential energy in volts is that required for removal or addition of an electron from or to a species; it is relative to the voltage for removal of an electron from a standard state hydrogen molecule with the formation of aqueous protons. That standard voltage is assigned a value of zero. Examples of half-cell reactions are



and



The half-cell voltage is directly related to the free energy of formation of a species by the relationship,

## C.12

$$F^\circ (\text{Cal}) = -23,060 \cdot n \cdot E^\circ ,$$

where  $n$  is the number of involved electrons. Half-cell reactions and potentials may be added to examine the feasibility of reactions. For example, the above reactions may be added as



The positive cell potential indicates that the reaction proceeds as written with standard state conditions. The free energy change for the reaction  $\Delta F^\circ$  may be calculated as

$$\Delta F^\circ = -23,060 \cdot n \cdot E^\circ (\text{cell}) .$$

Furthermore, the equilibrium constant,  $K$ , for the reaction is related to the free energy change by the standard thermodynamic relationship,

$$\Delta F^\circ = -RT \ln K .$$

The equilibrium constant may then be calculated directly from the cell potential as

$$K = \exp (23,060 \cdot n \cdot E / RT) .$$

For the above reaction,  $\Delta F^\circ = -28.6 \text{ kcal}$ , and at  $25^\circ\text{C}$ ,  $K = 1.0 \times 10^{21}$ .

Appendix C.6. Iodine Hydrolysis

Iodide and iodate salts dissolve in water and produce generally stable solutions that contain essentially all of the iodine in solution. However, some reactions can convert portions of these species to molecular iodine,  $I_2$ . Then the iodine-water chemistry becomes significant just as if the iodine source were molecular iodine.

Molecular iodine,  $I_2$ , is soluble in water, 0.0013 M at 25°C, and rapidly reacts with water according to the reaction,



and textbooks report an equilibrium constant of  $2 \times 10^{-13}$ . This value was computed from standard redox potentials<sup>5.13</sup> and is close to other published constants. Turner<sup>5.17</sup> has plotted the published equilibrium constants<sup>5.18-5.21</sup> for the 0 to 40°C range in the Arrhenius form, and applied least squares analyses to determine, the heat of reaction,  $\Delta H^\circ = 14.17 \text{ kcal mole}^{-1}$ , and the entropy change,  $\Delta S^\circ = -8.95 \text{ cal deg}^{-1} \text{ mole}^{-1}$ . From these results one can calculate the free energy and the "best" constant at 25°C for reaction (C.6.1) to be  $\Delta F^\circ = 16.84 \text{ kcal/mole}$  and  $K = 4.04 \times 10^{-13}$ . The positive enthalpy and free energy for the reaction suggests that the reaction is more pronounced at higher temperatures, and Turner has estimated the equilibrium constants to about 300°C.

Hypoiodous acid, HOI, is generally accepted to be an intermediate species in the iodine hydrolysis. However, static and equilibrium concentrations are questioned, and the direct observation of HOI has not been confirmed. The hypoiodite ion,  $OI^-$ , has been fairly well established based on the results of A. Treinin, et al<sup>5.22-5.24</sup>. Comparison of Treinin's spectrum at 365 nm with those reported for  $OCl^-$  and  $OBr^-$  shows a spectral trend in the hypohalite species.

<u>Species</u>	<u>Band Location</u>	<u>Band Intensity</u>
		<u>Molar Absorbitivity</u>
$OCl^-$	290 nm	360
$OBr^-$	331	326
$OI^-$	365	32

The unusually low value for the  $OI^-$  molar absorbitivity probably reflects error in measuring the concentration of the  $OI^-$  species. A similar trend is apparent for the corresponding values that have been reported<sup>5.25</sup> for the hypochlorous and hypobronous acids:

HOCl	240	90
HOBr	260	92

This indicates that HOI may have an absorption band at ~280 nm which could be used for analytical purposes.

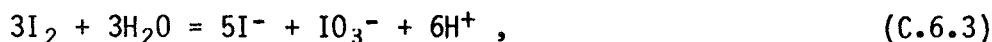
Force constants and observed vibrational frequencies for HOF, HOCl, HOBr, and HOI have also been reported.<sup>5.26</sup> Also, a band at 250 nm was observed

when  $I_2$  with 0-160 ppm  $H_2O$  was studied in liquid carbon dioxide.<sup>5.27</sup> Even though the higher temperatures and lower pH of LWR systems make the existence of HOI in neutral solutions doubtful, there appears to be a means to identify  $OI^-$ , and the acid form, HOI, probably can be observed spectrophotometrically.

Hypoidous acid, HOI, is not stable because of disproportionation generally described by



The equilibrium constant is about  $10^{-13}$  but has not been measured directly.<sup>5.13</sup> The net reaction for the hydrolysis of iodine is then the sum of reactions (C.6.2) and (C.6.1);



and the equilibrium constant is small. Latimer<sup>5.14</sup> gives the Gibbs Free Energy of formation ( $\Delta F^\circ$ ) for all components at 25°C in equation (C.6.3), from which one can calculate 64.29 kcal/mole for the reaction, and the corresponding equilibrium constant is  $4.78 \times 10^{-48}$ . Turner<sup>5.17</sup> has plotted the literature values<sup>5.14, 5.28-5.30</sup> for the equilibrium constant for equation (C.6.3) in Arrhenius form and determined  $\Delta H^\circ$  to be 75.66 kcal/mole and  $\Delta S$  to be 39.2 cal/deg·mole. The  $\Delta F^\circ$  at 25°C is then 64.21 kcal/mole, and the calculated equilibrium constant  $K = 8.09 \times 10^{-48}$ , somewhat higher and probably more accurate than the previous value calculated from Latimer's data.

The "best" values of equilibrium constants for Reactions (C.6.1) and (C.6.3) at 25°C are concluded to be respectively,  $4.04 \times 10^{-13}$  and  $8.09 \times 10^{-48}$ , because these values are based on all of the known literature. On this basis, the best thermodynamic values for the intermediate equation (C.6.2) are then  $\Delta F^\circ = 13.47$  kcal/mole and  $K = 1.23 \times 10^{-10}$ . Another approach to equation (C.6.2) is to calculate the free energy of the reaction from the free energies of formation of the components,<sup>5.14</sup> 13.55 kcal/mole, from which  $K$  is  $1.06 \times 10^{-10}$ . It is apparent that the textbook values<sup>5.13</sup> for reaction (C.6.2) are in error.

A cursory evaluation of the small equilibrium constant,  $8.1 \times 10^{-48}$ , for the net hydrolysis reaction (C.6.3) can give an erroneous implication that the extent of the reaction is low, i.e., the amount of  $I_2$  that reacts is small. However, in a low acid medium such as pH of 6 or greater, the sixth power dependence on the acid concentration begins to dominate the equilibrium. The concentrations of  $I_2$ , HOI,  $I^-$ , and  $IO_3^-$  can be calculated for a given amount of total iodine at equilibrium in a system at a given acidity; under LWR accident conditions the amount of  $I_2$  in an equilibrated system will be a very low percentage of the total iodine. Tables (5.2) and (5.3) give the  $I_2$  and HOI concentrations of iodine species for an aqueous solution at 25°C and 100°C with total iodine concentrations of  $10^{-9}$  to  $10^{-5}$  M over the pH range 5 to 9. The amount of  $I_2$  is low at pH of 6 and essentially insignificant at pH of 8 and higher. This analysis suggests that  $10^{-9}$  to  $10^{-5}$  M solutions of iodine at equilibrium in the pH range of 6 to 9 will exist essentially as the iodide and iodate species.

Equilibrium concentrations of  $I_2$  as fractions of total iodine at pH values from 5 to 10 are shown as functions of total iodine concentration from  $10^{-9}$  to  $10^{-4}$  M in Figure (5.2). For a particular pH greater than six, the  $I_2$  concentration changes with the square of the total iodine concentration. At these conditions, most of the iodine exists as  $I^-$  and  $IO_3^-$  and the real correlation based on equation (C.6.3),

$$[I_2]^3 = \frac{[I^-]^5 [IO_3^-] [H^+]^6}{K},$$

when  $[IO_3^-] = 1/5[I^-]$ , reduces to

$$[I_2] = \frac{[I^-]^2 [H^+]^2}{[5K]^{1/3}}.$$

The equilibrium constant for the hydrolysis reaction (C.6.3) at  $100^\circ\text{C}$  that is calculated from the above thermodynamic values is  $1.28 \times 10^{-36}$ . However, the  $\Delta H$  and  $\Delta S$  may be temperature dependent, and Turner<sup>5.17</sup> recommended that the equilibrium constant be calculated instead by the relationship,

$$\log K = -3.1508 \times 10^4/T + 114.00 - 0.18523 T,$$

which gives  $K = 2.74 \times 10^{-40}$  for  $100^\circ\text{C}$ , some 8 orders of magnitude greater than that at  $25^\circ\text{C}$ . This calculated value probably is the better value to represent the  $100^\circ\text{C}$  system because the thermodynamic quantities,  $\Delta H$  and  $\Delta S$ , include a dependence on temperature. The  $I_2$  concentrations at  $100^\circ\text{C}$ , Table (5.3), are much smaller than at  $25^\circ\text{C}$ , Table (5.2).

The equilibrium constant for reaction (C.6.1) to form the HOI intermediate at  $100^\circ\text{C}$  is estimated to be  $5 \times 10^{-11}$ , or about 2 orders of magnitude greater than that at  $25^\circ\text{C}$ . Then the intermediate HOI concentration at  $100^\circ\text{C}$  and  $\text{pH} = 7$  with  $10^{-6}$  M total iodine would be about  $4 \times 10^{-10}$  M HOI. At  $\text{pH} = 5$ ,  $100^\circ\text{C}$  and with  $10^{-6}$  total iodine, the HOI concentration would be about  $4 \times 10^{-8}$  M, Table (5.3). In equilibrium systems near LWR conditions, the concentration of the intermediate species, HOI, can be about the same at  $100^\circ\text{C}$  as at  $25^\circ\text{C}$ .

There can be periods of time when the aqueous systems in an LWR accident are not at equilibrium. The relative rates of reactions (C.6.1) and (C.6.3) will determine the relative amounts of  $I_2$  and HOI. Although the  $OI^-$  species in base solutions has been observed,<sup>5.22</sup> there are no direct measurements of rates of formation of HOI. However, the measurements of decreasing  $I_2$  and increasing  $I^-$ , along with the assumption that HOI and  $I^-$  form at equal rates, has led to the conclusion that HOI is rapidly formed by iodine hydrolysis, i.e.,  $I_2$  dissolved in water rapidly equilibrates according to equation (C.6.1).<sup>5.31,5.32</sup> On the other hand, reaction (C.6.3) is believed to equilibrate slowly. The rate of iodate

loss by the iodate-iodide,  $\text{IO}_3^- - \text{I}^-$ , reaction has been reported.<sup>5.33</sup> Eggleton<sup>5.34</sup> assumed those rate data to be valid for the reverse reaction (C.6.3) and divided the equilibrium constant by the reverse rate constant to calculate the forward rate constant. Eggleton's analysis on the kinetics for reaction (C.6.3) in the pH range of 5-9, indicated that formation of  $\text{IO}_3^-$  and  $\text{I}^-$  is very slow compared to the formation of HOI, reaction (C.6.1). Other studies on the disproportionation of  $\text{IO}^-$ , the hypoiodite ion,<sup>5.62</sup> generally support the conclusions of Eggleton. Therefore, the possibility exists where the HOI concentration could be considerably greater than those given in Table 5.2 for systems at equilibrium. The maximum concentration for HOI in a static system would be that when reaction (C.6.1) approaches equilibrium but reaction (C.6.2) has not initiated. Such hypothetical maximum HOI concentrations are given in Table 5.4 for 25 and 100°C based only on the equilibrated reaction (C.6.1).

Concentrations of  $\text{I}_2$  that correspond to the maximum HOI concentrations discussed above are plotted against total iodine concentrations in Fig. (5.3). As in Fig. (5.2), the  $\text{I}_2$  concentration is a function of the square of the total iodine except at lower pH and higher total iodine.

Reaction rates for  $\text{I}_2$  hydrolysis are not known to an extent that static concentrations of various iodine species can be estimated. The above calculations only establish limits of concentrations, and the realistic values are somewhere in between.

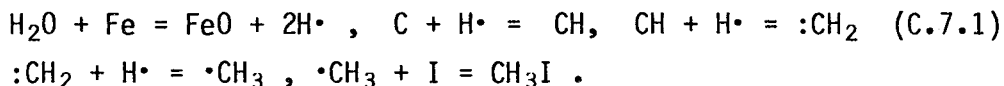
### Appendix C.7. Organic Iodides in Aqueous Systems

Organic iodides in LWR incidents usually are referenced as methyl iodide. This is appropriate because most of the organic iodide associated with a reactor incident is methyl iodide and because methyl iodide is the most volatile organic and hence the most likely to cause iodine release from containment.

#### Formation of Organic Iodide

The source of organic iodide in a reactor incident is not well established. Several possibilities exist and are mentioned here.

1. Methane fragments are produced by interaction of steam with stainless steel, S.S., to produce hydrogen followed by the reaction of hydrogen with the carbon impurity in S.S. Then the methane fragments react with iodine atoms or molecules to form  $\text{CH}_3\text{I}$ .



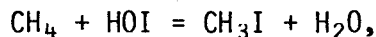
The formation of methyl iodide by this mechanism could proceed, but the  $\text{CH}_3\text{I}$  in the vicinity of the reactor fuel during an accident that also produced hydrogen could be destroyed as



2. The reaction of atmospheric methane in the reactor containment with iodine species. Methane in air and that produced by irradiation of organic materials would be the methane source. Methane will react with molecular iodine and perhaps HOI as



and



but should not react with other iodine species. This gas phase reaction is enhanced by radiation, but the radiation enhancement is greatly reduced by the presence of water and oxygen.

3. The reaction of molecular iodine,  $\text{I}_2$ , with organic compounds and the subsequent fragmentation to yield volatile iodide. Paints and lubricants are the most likely organic compounds,  $\text{RCH}_3$ .



This reaction could occur in aqueous media or as a gas-solid reaction. (R represents any organic radical).

### Theory of CH<sub>3</sub>I Formation

A theoretical study of the formation of methyl iodide in a system of 13 chemical species most likely to be in a reactor accident was reported by Barnes et al.<sup>5.25</sup> Thermodynamic values were used to calculate equilibrium concentrations of various species at various temperatures. The theoretical maximum methyl iodide concentration was at 700°K and represented only 10<sup>-4</sup>% of the total iodine which was 4 x 10<sup>-6</sup> g atoms per liter. At 300°K the methyl iodide percentage was almost three orders of magnitude lower. Therefore, as previously discussed,<sup>5.35-5.37</sup> thermodynamic data indicates that methyl iodide is not a stable or favorable species; i.e., if chemical equilibrium is reached, methyl iodide is not present in significant amounts. However, those same authors also have pointed out that experimental studies have observed methyl iodide concentrations much higher than the equilibrium quantity of 10<sup>-4</sup>% and concluded that the kinetics of non-equilibrium processes produce organic iodides at the higher concentrations. The theoretical considerations with kinetic processes have not given satisfactory comparisons with observed data, and Postma and Zavadoski<sup>5.37</sup> have concluded that theoretical predictions have not had a firm basis for meaningful information on methyl iodide formation.

Most of the above discussion is related primarily to gas phase conditions, and some consideration should be given to aqueous phase chemistry of organic iodides.

### Methyl Iodide-Water Interactions

Methyl iodide reacts with water as



This reaction is essentially irreversible and in aqueous media cannot be a source for the formation of methyl iodide.

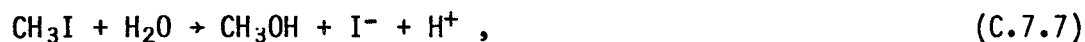
Classical work in developing chemical kinetic theory studied the hydrolysis of methyl iodide.<sup>5.38</sup> Using Reaction C.7.5, Moelwyn-Hughes proved that the activation energy for a chemical reaction generally decreases with increasing temperature. He chose that reaction for kinetic studies in aqueous media because it proceeds unimolecularly to completion at all accessible concentrations and temperatures. Subsequent work by Glew and Moelwyn-Hughes<sup>5.39</sup> showed that the ratio of methyl iodide pressure to methyl iodide concentration in water slightly decreased with an increasing pressure, and that the maximum methyl iodide concentration, C°, in water at various temperatures follows the expression

$$\log C^\circ = -110.278 + 36.6321 \log T + 4823/T \quad (\text{C.7.6})$$

This indicates a minimum solubility of 3.5 x 10<sup>-4</sup> M at 23°C.

The same reaction, C.7.5, was more recently studied by Adachi, Eguchi, and Haoka<sup>5.40</sup> along with the reaction of methyl iodide with dilute

hydroxide solutions. They showed that methyl iodide reacts completely with water or hydroxide to form methanol and iodide with respective reaction rates and rate constants as



$$r_7 = k_7[\text{CH}_3\text{I}] ,$$

and



$$r_8 = k_8[\text{CH}_3\text{I}][\text{OH}^-] ,$$

with  $k_7 = 4.35 \times 10^{16} \exp(-27600/\text{RT}) \text{ hr}^{-1}$  and  $k_8 = 3.20 \times 10^{15} \exp(-22000/\text{RT}) (\text{l/mol}\cdot\text{hr})$ . Pseudo reaction rate constants at 25 and 100°C are given in Table C.4, and indicate that methyl iodide hydrolysis at 100°C will be about 4 orders of magnitude faster than at 25°C. Furthermore, the hydrolysis mechanisms, reactions (C.7.7) and (C.7.8), are indicated to be equally important near a pH of 11, but at lower pH, the reaction (C.7.7) dominates at both temperatures. Reaction halftimes based on these data are 3285 and 0.28 hr at 25 and 100°C, respectively.

Table C.4. Reaction rate constants ( $\text{hr}^{-1}$ ) for methyl iodide reacting with water,  $k_7$ , and hydroxide,  $k_8$ , at 25 and 100°C.

pH	$[\text{OH}^-](25)$	$k_7^a$	$k_8[\text{OH}]^a$	$k_7^b$	$k_8[\text{OH}]^b$
7	$10^{-7}$	$2.11 \times 10^{-4}$	$2.05 \times 10^{-8}$	2.51	$2.29 \times 10^{-4}$
8	$10^{-6}$	$2.11 \times 10^{-4}$	$2.05 \times 10^{-7}$	2.51	$2.29 \times 10^{-3}$
9	$10^{-5}$	$2.11 \times 10^{-4}$	$2.05 \times 10^{-6}$	2.51	$2.29 \times 10^{-2}$
10	$10^{-4}$	$2.11 \times 10^{-4}$	$2.05 \times 10^{-5}$	2.51	$2.29 \times 10^{-1}$
11	$10^{-3}$	$2.11 \times 10^{-4}$	$2.05 \times 10^{-4}$	2.51	2.29

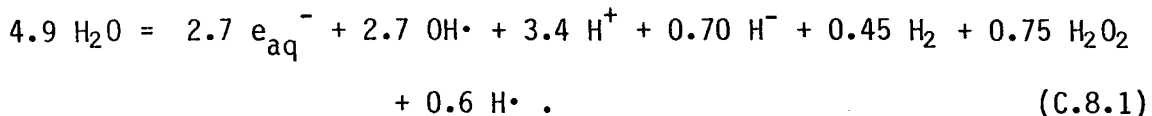
<sup>a</sup>25°C.

<sup>b</sup>100°C. The  $\text{OH}^-$  concentration at 100°C could be as much as seven times greater than at 25°C.<sup>5.41</sup>

The above information suggests that methyl iodide in an aqueous system at 25°C eventually would convert quantitatively to methanol and iodide, and at 100°C that conversion rate would be rather fast. However, the very low methyl iodide concentration in the TMI containment remained constant until that atmosphere was released and renewed. Then the methyl iodide concentration in that containment increased almost to the previous level and appears to again maintain a steady state. This suggests that a process to produce methyl iodide, perhaps one of those above is generating  $\text{CH}_3\text{I}$  at a rate equal to the rate of reaction (C.7.5).

Appendix C.8 Radiation Chemistry of Aqueous Iodide Systems

Textbooks hardly acknowledge this subject, and specific information in the literature is sparse. Because of high water-to-iodine ratios in LWR accident conditions ( $>10^5$ ), the major effect of radiation on aqueous iodine chemistry is expected to result from reactions of the iodine species with water radiolysis products. Those products include reasonably stable compounds and highly active radicals. Such products from the ionizing radiation of water have been summarized quantitatively by the Draganics<sup>5.42</sup> where 100 eV of radiation dissociates 4.9 molecules of water;



Then radiation chemistry of dilute aqueous iodine systems becomes the interaction of iodine species with the products in equation (C.8.1). Furthermore, from the discussions in the previous sections the significant interactions will be those with iodide ( $\text{I}^-$ ), iodate ( $\text{IO}_3^-$ ), and molecular iodine ( $\text{I}_2$ ). Often impurities in the water will scavenge the highly active radicals from the water radiation products, and thus will diminish the radiation effects on iodine species.

A recent review of this subject by Sellers<sup>5.43</sup> includes most literature through 1976. That review summarized much work and identified nine iodine species that exist as intermediates in the reactions of  $\text{I}^-$ ,  $\text{IO}_3^-$ , and  $\text{I}_2$  with the various water radiation products. There were no conclusions about steady-state iodine species for any particular conditions.

Two recent publications have reported observed effects of gamma radiation on aqueous iodine systems.<sup>5.44,5.45</sup> That work concentrated on  $10^{-6}$  to  $10^{-3}$  M iodide solutions and measured oxidized iodine products after irradiation. The initial acid concentrations before irradiation ranged from pH = 2 to 9. Lin<sup>5.44,5.45</sup> concluded that iodide was oxidized to iodate by a mechanism that involves an intermediate, probably HOI. Those data showed that higher fractions of iodide were oxidized to iodate with lower initial iodide concentrations,  $<10^{-5}$  M. Also, significant quantities of  $\text{I}_2$  were produced at the higher acidities, pH  $<5$ , and with larger doses. Acid concentrations after irradiation were not reported, but one would expect some acid change corresponding to the iodide oxidation. The primary mechanism for irradiation oxidation of  $\text{I}^-$  is the reaction of iodide with the hydroxyl radical,<sup>5.46</sup>



The hydroxide ions decrease the acidity, and it would be interesting to know the acid change corresponding to the radiation effects.

Lin<sup>5.45</sup> also reported the results of iodine analysis of BWR coolant. The fission product iodine in the coolant during reactor operation was 60–90% iodide,  $\text{I}^-$ , and the remainder was iodate,  $\text{IO}_3^-$ . These ratios are in

accord with oxidation of  $I^-$  to  $I_2$  followed by hydrolysis, equation (C.8.3). Lin could not measure HOI and indicated that the reported iodide concentration could include HOI. Only traces of  $I_2$  or organic iodide were found. During reactor shutdown the iodide to iodate ratio  $I^-/IO_3^-$  decreased markedly because of radiolytic oxidation of  $I^-$  to  $IO_3^-$ . However, the amounts of  $I_2$  or organic iodide did not noticeably increase during reactor shutdown and radiolytic oxidation.

Some results<sup>5.47</sup> preceding Lin's work were not in complete agreement with Lin.<sup>5.44,5.45</sup> Shubnyakova et al.<sup>5.47</sup> irradiated sodium iodide solutions with  $^{60}Co$  gamma rays at 52 rad/sec to investigate purification of pharmaceutical iodide. They reported that the radiolytic oxidation of iodide increased with radiation dose, decreased with initial pH, increased with oxygen content, and increased with iodide concentration. Those authors also reported the formation of hydrogen peroxide at rates of about 0.07 molecules/100 ev, and that peroxide,  $10^{-2}$  M, added to a  $10^{-6}$  M NaI solution at pH of 7, decreased the radiolytic oxidation of  $I^-$ . Thus, the effect of hydrogen peroxide on the aqueous iodide was as a reducing agent. Another interesting observation was that sparging the solutions with nitrogen to eliminate the oxygen almost completely eliminated the radiolytic oxidation of iodide. This suggests that the addition of oxygen gettering agents such as hydrazine would also reduce radiolytic oxidation.

Appendix C.9 A Reassessment of Organic Iodide Formation Based on a More Realistic Interpretation of WASH-1233

The review paper by Postma and Zavadosky (WASH-1233) concluded that "overall, no more than 3.2% of airborne iodine (airborne mass assumed equal to 25% of maximum core inventory) could be converted to organic iodides during the first two hours following fission product release." The percentage was comprised of two independent parts, (a) "less than 1% of iodine initially airborne" could become organic by nonradiolytic means and (b) "no more than 2.2%" could become organic from radiolytic reactions. These conclusions were based on interpretations that were highly conservative, and the conservatisms are clearly stated. The paper also provides an excellent compilation of available data at the time, and that same data can be used to draw less conservative conclusions with respect to iodine behavior following reactor accidents.

The primary issue is the chemical form of iodine. Most of the data in WASH-1233 was for experiments and tests in which molecular iodine ( $I_2$ ) was the dominant or exclusive chemical form of iodine introduced into the experiment. For reasons stated elsewhere, iodide rather than  $I_2$  is expected to be the form of iodine actually introduced into containment following a reactor accident under nearly all scenarios. Since iodide is much less reactive chemically than is  $I_2$ , with respect to every mechanism considered for forming organic iodides, the generation of organic iodides would be much smaller if iodide indeed is the source term. To the extent that the total iodine released in an accident exists as  $I_2$ , the conclusions of WASH-1233 may be valid but very conservative (see below). However, even on a conservative basis, the 3.2% figure should be reduced by multiplying it by the fraction of the total iodine that is really  $I_2$ . The following discussion will address the hypothetical case in which  $I_2$  is the accident source term.

The secondary issue is the successive elements of conservatism introduced into the analysis of the data in WASH-1233. At some point it is important to make the "best" estimate of the risks -- in this instance, of iodine behavior -- rather than the conservative (upper bounds) estimate; and this report appears to be such a point.

In WASH-1233 the formation of organic iodides is divided generally into two parts, (1) that observed in the absence of radiation, based primarily on a statistical study of a number of experiments in containment vessels and models at four sites (Oak Ridge, Idaho, Battelle Northwest, and the UK), and (2) that estimated to result from radiation effects, estimated from experimental data under conditions not resembling the post-accident environment. There is a large amount of data scatter due to a variety of reasons, but certain definite trends still appear. However, the effects of individual variables are generally not well enough defined to permit one to extrapolate very far with much confidence, and it is really not clear what the independent

variables are. Such data were interpreted conservatively, and in addition, mechanisms leading to destruction of organic iodides were totally excluded. In the estimate presented below, the same data will be examined with the goal of arriving at a value nearer the middle of the range suggested by the data, rather than at the upper extreme, in the hope of arriving at a more realistic assessment of organic iodide generation for the case in which the source term is  $I_2$ .

#### Containment Vessel Experiments

The containment vessel experimental data are summarized in Fig. 2 of WASH-1233 (references to data are to WASH-1233 unless otherwise stated). There is a clear trend for the percent organic iodide to increase as the iodine concentration decreases, and the least squares fit of the data is given. As a conservative estimate, this line is shifted upwards (same slope) to pass through the single data point that gives the highest position for the line. This gives 1% organic iodide at a concentration of 100 mg  $I/m^3$ ; the least squares line for all data is 16 times lower.

Other experimental variables are also significant, but it is not clear that they can be separated from each other. Thus, the volume of the experimental vessel is important, with percent organic iodide being smaller in larger vessels (Fig. 3 and Table 2). All vessels were smaller than real containment buildings. Similarly, there is some trend between studies made at different sites. The Oak Ridge, Idaho, and Hanford data scattered frequently above the British data.

The estimate used here is based on eyeballing a parallel line through the data points for the two larger categories of experimental vessels illustrated in Fig. 3 (including British and some Battelle Northwest data). The resulting line passes through 0.02% organic iodide at 100 mg  $I/m^3$ , or 50-fold lower than the conservative estimate. It is suggested that this is a reasonable, and perhaps still somewhat conservative, value for an actual, full-sized containment building.

It should be mentioned that other factors, not taken into account, suggested a lower amount of organic iodide. Equilibrium calculations (Section 6 of the report) suggest very small formation of organic iodide, and it was stated that no reliable conclusions can be drawn on this basis, given the present state of knowledge. The mechanism leading to formation of organic iodide in these experiments is not understood or even identified. In addition, one significant factor not considered in the review is the hydrolysis of organic iodides. Hydrolysis is reported to be rapid at the elevated temperatures that exist in the containment building for a time following certain accident scenarios. This would tend to reduce the percent organic iodide.

#### Radiolytic Formation

WASH-1233 concluded that the gas phase reaction of iodine with organic material is the dominant factor, compared to aqueous phase reactions or surface effects. This appears to be a reasonable assumption as long as  $I_2$  is really present in the gas phase as the dominant species. If this

is not the case, there will be little organic iodide formed anyway, because the other mechanisms appear capable of yielding only small amounts of organic iodide, as pointed out. Here, the conservative assumptions used in WASH-1233 to estimate organic iodide formation via the gas phases reaction will be examined. However, it should be remembered that, if this reaction does not produce much organic iodide, then the other mechanisms should be reexamined.

As pointed out,  $I_2$  is an excellent scavenger for radicals, so reaction of  $I_2$  with organic radicals formed by radiation effects would be expected. However, other components present in great excess, especially oxygen, will compete with  $I_2$  for reaction with these radicals. Unfortunately, practically all experimental data involve gas compositions very far from those projected for the post-accident containment building, and this is clearly an area where some experimental study would be worthwhile. These considerations are discussed rather well in the reference report.

The estimate of a G value of 0.004, based on Fig. 12, is extremely tenuous. The two plots of G versus the  $I_2$  concentration may not have real significance since each separate set of data (Barnes' results cover a factor of 10 in  $I_2$  concentration and Charamathieu's cover a factor of 100 at a much lower concentration) shows no clear trend with  $I_2$  concentration; thus, the slope of the line probably results from changes in other variables (such as  $CH_4$ ,  $H_2O$ , or  $O_2$  concentration) rather than  $I_2$  concentration. The data also apply to mixtures of  $CH_4$  and  $I_2$  alone, whereas the accident situation involves air and steam with only very small concentrations of  $I_2$  and organic material. Thus, nearly all the radiation is not absorbed initially in the reactants, and  $CH_3I$  formation would be reduced further.

The percent conversion of  $I_2$  to  $CH_3I$  is proportional to the  $CH_4/I_2$  ratio (from data of Fig. 10 and also Table 2 of BMI-1829), and extrapolation via a log-log plot to the reference ratio of about 0.4 and dose of  $3.2 \times 10^6$  rads for accident conditions gives a conversion of 0.008%. The molar concentrations of both  $CH_4$  and  $I_2$  are much lower than for the experimental data, but this extrapolation may still be valid for mixtures of  $CH_4$  and  $I_2$  alone. In the presence of the great excess of steam and air in a containment building, however, an even smaller yield would be expected.

The data in Fig. 11 (and also Table 4 of BMI-1829 by Barnes) may be more useful for estimating the effect of competition from oxygen. There is definite evidence of saturation of methyl iodide production as the oxygen concentration is increased, especially at the highest oxygen concentration (Fig. 11). If the formation mechanism is dominated by reaction of  $CH_3$  radicals with either  $I_2$  or  $O_2$ , the two in competition, and there is also a radiolytic destruction of methyl iodide, then the steady state concentration of  $CH_3I$  (when formation and destruction mechanisms are in balance and the concentration does not change with time) would be

$$[\text{CH}_3\text{I}] = \frac{[\text{CH}_4][\text{I}_2]}{k'[\text{I}_2] + k''[\text{O}_2]} = \frac{[\text{CH}_4]}{k' + k''[\text{O}_2]/[\text{I}_2]}$$

$$[\text{CH}_4]/[\text{CH}_3\text{I}] = k' + k''[\text{O}_2]/[\text{I}_2] .$$

The data in Table 4 of BMI-1829 (also Fig. 11) with air or oxygen present can be used to estimate the values of the k's. The  $\text{O}_2/\text{I}_2$  ratio is not explicitly given in this data, and there is some uncertainty about the exact experimental conditions. By normalizing on the basis of the water vapor being present at 1 atmosphere pressure, the  $\text{I}_2/\text{O}_2$  ratios are estimated to be 16 and 74, and the saturation conversion to  $\text{CH}_3\text{I}$  to be 1.5% and 0.3% of the iodine for the experiments with added air and water, respectively. The value of  $k''$  is estimated to be about 400, and  $k'$  is negligibly small. If this equation is then applied to containment building conditions [ $\text{O}_2/\text{I}_2 = 2 \times 10^4$  and the  $\text{CH}_4$  concentration is  $1.5 \times 10^{-4}$  moles/ $\text{m}^3$ ], the calculated conversion of  $\text{I}_2$  to  $\text{CH}_3\text{I}$  is the order of  $10^{-5}\%$ .

The apparent saturation in  $\text{CH}_3\text{I}$  formation (indicated by both Fig. 11 and Table 4 of BMI-1829) implies that the reverse reaction, radiolytic destruction, is important. A G value of 20 is suggested for the reverse reaction (Zittel), and if this is combined with the G value for formation suggested in Fig. 12 (0.004), the equilibrium yield of  $\text{CH}_3\text{I}$  should be about  $0.004/20 = 2 \times 10^{-4}$ , or 0.02%. It is stated that the G value for formation is an upper limit, so the actual yield should be lower than 0.02%.

These three approaches give methyl iodide yields much lower than that derived in WASH-1233, by 2 orders of magnitude or more. It is suggested here that a realistic estimate might be of the order of 0.01%. This is highly uncertain because of the inappropriateness of the available data, and it is apparent that experimental study is needed to acquire data under realistic conditions. The primary differences in this treatment are to extrapolate from measured values on the basis of the  $(\text{CH}_4/\text{I}_2)$  ratio or the  $(\text{O}_2)/(\text{I}_2)$  ratio, rather than on the  $\text{I}_2$  concentration as done in WASH-1233, and to take account of radiolytic destruction.

It should be pointed out that there is some inconsistency in extrapolating the radiation data to iodine concentrations much lower than 100  $\text{mg}/\text{m}^3$  since a substantially lower iodine concentration also implies a lower radiation level. In the reference case (TID-14844) about 66% of the radiation dose in two hours is from iodine isotopes, and this dose could not be present if the iodine was not present, or the iodine concentration low.

### Discussion

It is suggested in the foregoing that a realistic assessment of organic iodide production, based on existing literature, would include approximately 0.02% from nonradiolytic sources and approximately 0.01% from radiation effects, or 0.03% total. With the present state of knowledge, any such estimate is highly uncertain. There is no apparent reason why meaningful data cannot be acquired so that a more precise estimate can be made.

The figure derived here is surprisingly small, and it is likely that other mechanisms should be considered, also. Some such mechanisms were discussed in WASH-1233, but neglected because the factors discussed above were expected to dominate. With the information available, however, there probably is not much that can be done with respect to extending the treatment. The result appears to be more dependent on the assumptions and mechanisms assumed, in the absence of known mechanisms, than on the actual experimental data available.

It should be pointed out that, following formation of organic iodides by whatever mechanism, the inorganic iodine species will not persist in the containment atmosphere for very long -- certainly not to the extent that organic species will persist. Inorganic iodine will react with water or plate out, ending up in solution and on surfaces. As a result, measurements made some time after the accident will indicate higher airborne organic iodine fractions than were present initially. Thus, for example, data acquired from TMI or PRTR, which give high organic iodine fractions in the atmosphere, cannot be related directly to the treatment given here. In these instances, although the fraction of organic iodine is high, the total amount of airborne iodine is quite low, so the amount of organic iodine shortly after the accident must have been small, also. (At TMI, for example, organic iodine is only a few thousandths of 1% of core inventory but around 70% of airborne iodine.) The high percent organic iodine in such cases results from the removal of the nonorganic species by various mechanisms rather than from a high production of organic species.

APPENDIX D  
TRANSPORT CALCULATIONS FOR THE REACTOR COOLANT SYSTEM

This Appendix contains supplemental information for the results and conclusions presented in Chapter 6. Presented below are the source terms used in the various accident sequences, the flow paths and summary thermal-hydraulic conditions, and the TRAP predictions of fission product iodine distribution as a function of time. Figures D.1 and D.2 refer to the accident sequence involving little or no fuel damage which is discussed in Section 6.3.1. Figure D.3 and Tables D.1 through D.6 pertain to the transient with loss of heat removal in a PWR, discussed in Section 6.3.2.2.1. Figures D.4 and D.5, as well as Tables D.7 through D.10 deal with a large pipe break accident with a failure of the ECC system in a PWR, as discussed in Section 6.3.2.2.2. Supplemental information for the other pipe break accidents discussed in that section of the text is presented in Figure D.6 and Tables D.11 through D.13. The transient with failure to scram in a BWR, as discussed in Section 6.3.2.2.3 is further detailed in Figure D.7 and Table D.14. And, finally, details of the large pipe break with failure of the ECC system in a BWR are given in Figure D.8 and Table D.15.

D.1 Source Terms

Inspection of the estimated source terms presented here and used in the analyses presented in Chapter 6 of this report will indicate that there are some differences from those determined in Chapter 4, although the differences are not great compared with the uncertainties involved in the values. The cause of the discrepancies is that the values used in Chapter 6 are merely estimates of the source term which might be applicable for a range of typical accident sequences, and the values in Chapter 4 result from more detailed analyses of release rates. Substitution of the rates from Chapter 4 into the TRAP analyses would not be expected to significantly affect the predictions of the fractional retention in the primary system, although the absolute masses retained and released would be changed.

D.1.1 Source Term for the Sequence Involving Minor or No Fuel Damage  
(Section 6.3.1)

Experiments on the release of fission products from fuel rods under LOCA conditions (D.1) suggest that the principal fission products released are iodine and cesium and that these transport in vapor form. The best estimate, at this time, of the release fraction of these fission products is 0.0032 of inventory for iodine and 0.0017 of inventory for cesium. The bulk of this release occurs immediately on rupture; the remainder apparently by a diffusional process.

To arrive at an average source rate of either species for the whole core, as is required by TRAP, some estimate of the fuel rod failure rate must be made. Such an estimate was provided by the NRC.(D.2) They suggest that a reasonable assumption is that  $8 \times 10^{-3}$  of the total number of fuel rods in the core fail per second.

## D.2

Using core inventories of iodine and cesium as calculated with ORIGEN (D.3)

$$\begin{aligned}\text{Iodine} &= 1.611 \times 10^4 \text{ g} \\ \text{Cesium} &= 1.665 \times 10^5 \text{ g}\end{aligned}$$

together with the fuel failure rate and the release fractions given above, the average source rates as used in the sensitivity study are calculated to be (D.4)

$$\begin{aligned}0.41 \text{ g/sec Iodine} \\ 2.26 \text{ g/sec Cesium}\end{aligned}$$

### D.1.2 Source Term for Accidents Involving a Melt

For determination of the fractional retention of iodine in the primary system, the source rates of cesium and iodine are not actually as important as that for the particulate matter, although they do, of course, determine the mass input rate for the containment. The source rates used for iodine and cesium for the TMLB' simulations were 11.0 and 108 g/s. For the remaining accident sequences the source rates used were 16.1 and 178 g/s for iodine and cesium. This variance is not meant to imply that this difference is expected among these accidents' actual release rates. The source rate used for particulate matter, having a density of 10 g/cc was 208 g/s for most of the simulations, and 1.4 g/s for the cases referred to as having a weak source rate. The larger value corresponds to release of  $1.5 \times 10^6$  g over the course of two hours.

### D.2 Explanation of TRAP Predictions Tables

The columns in these tables refer to the time since the start of the core melt and the assumed chemical form of the iodine considered. Only the values for iodine at the end of the accident are given since they do not vary significantly during the course of the accident. The "Vapor (%)" column gives the percent of the iodine species released from the core which is in the vapor state, either in the containment or in the primary system. The "Suspended Particles (%)" column gives the percent of the released iodine species which is adsorbed on the surfaces of particles suspended in the containment or in the primary system. The "Deposited Vapor (%)" column gives the percent of the released material which has been deposited from the vapor state onto the primary system surfaces. The "Control Volumes" subcolumn gives the number(s) of the control volume(s) where the deposition occurs. If there are more than one number, they are ordered according to amount of deposition. The "Deposited Particles (%)" refers to the percent of the released material which is adsorbed on suspended particles and subsequently deposited on primary system surfaces. The "Control Volumes" subcolumn again gives the location of deposition.

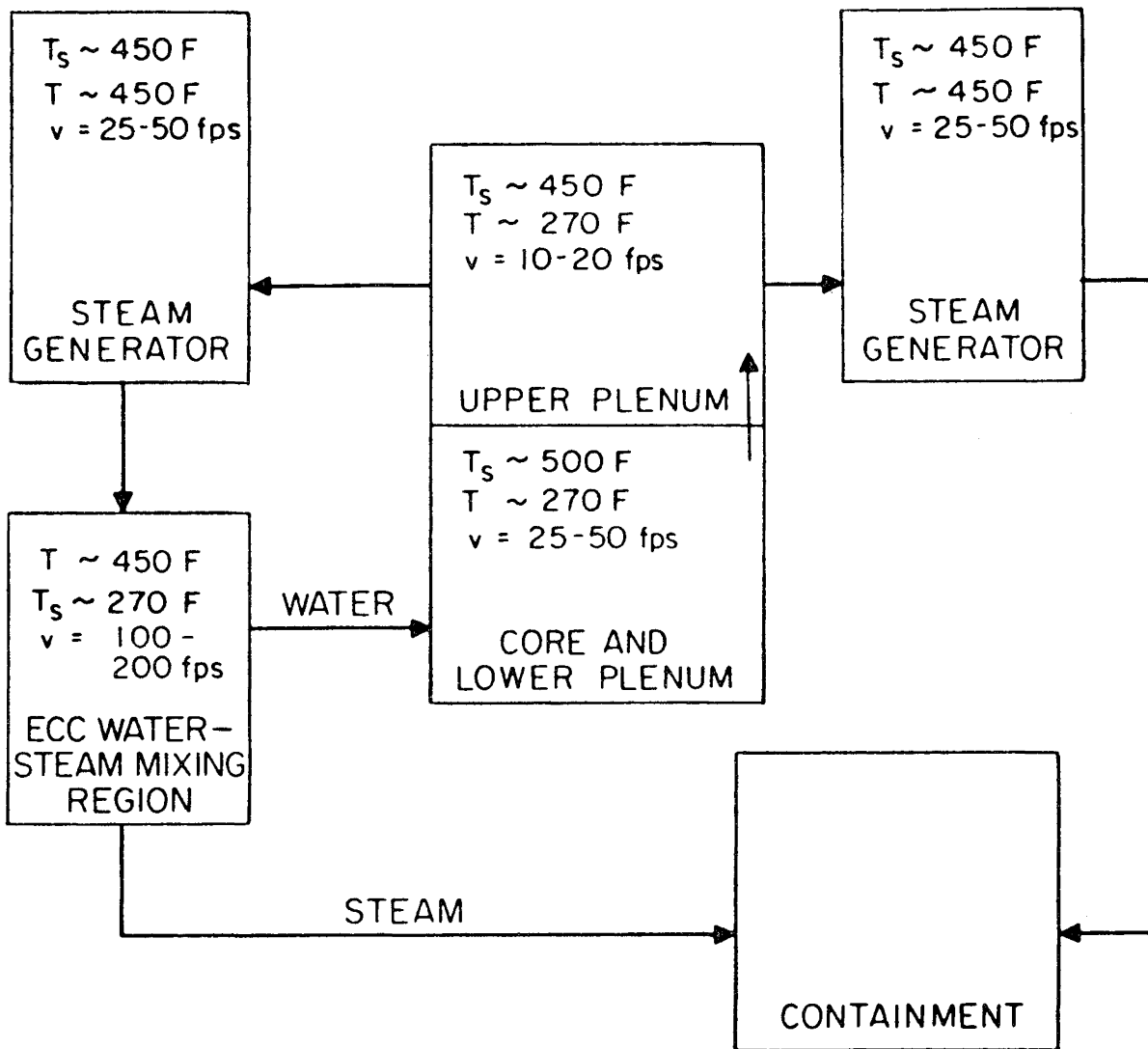


FIGURE D.1. FLOW PATHS, FLUID VELOCITIES, AND SYSTEM TEMPERATURES FOR A SEQUENCE INVOLVING LITTLE OR NO FUEL DAMAGE IN A PWR (SECTION 6.3.1)

( $T_s$  Denotes Surface Temperature,  $T$  Gas Temperature)

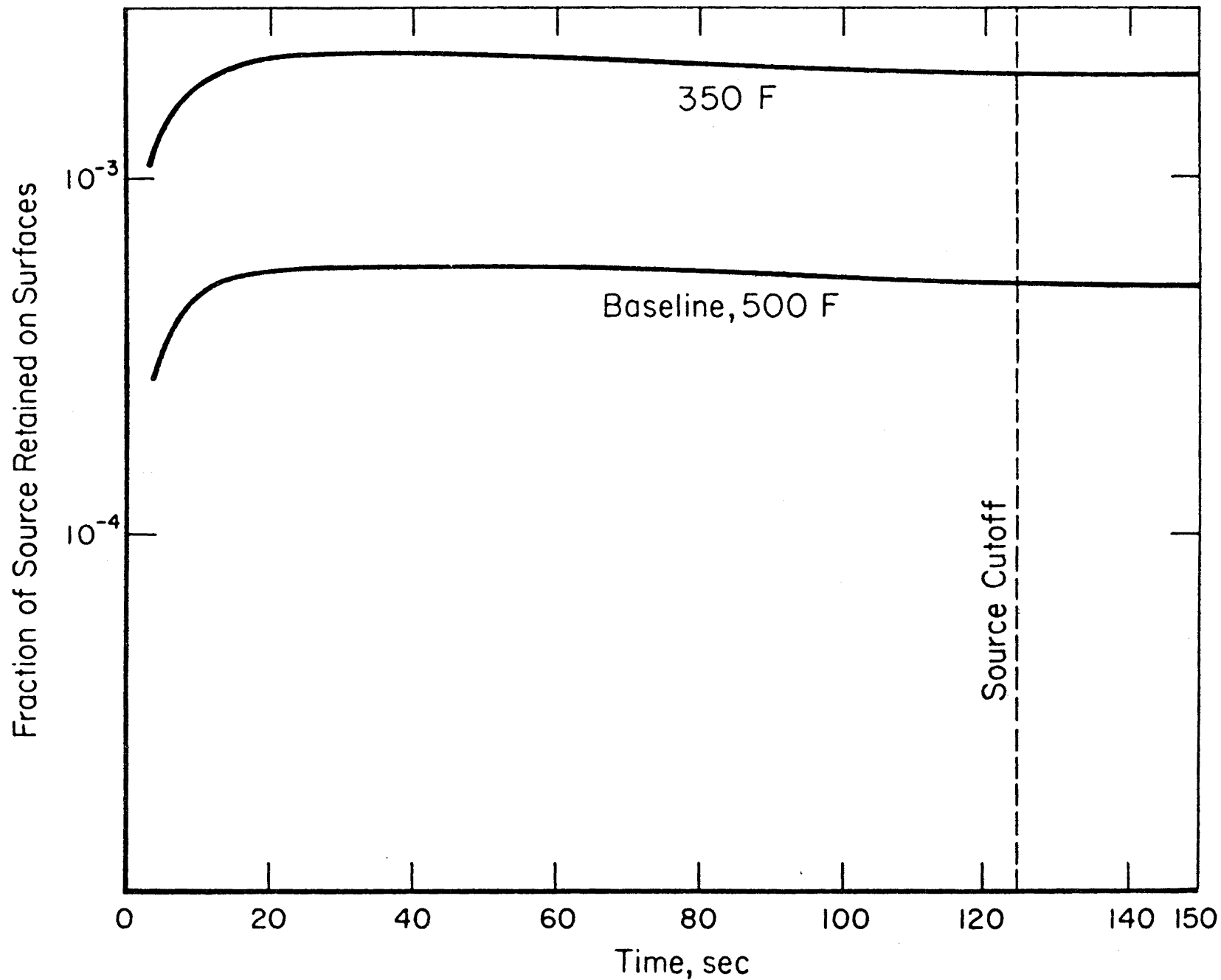
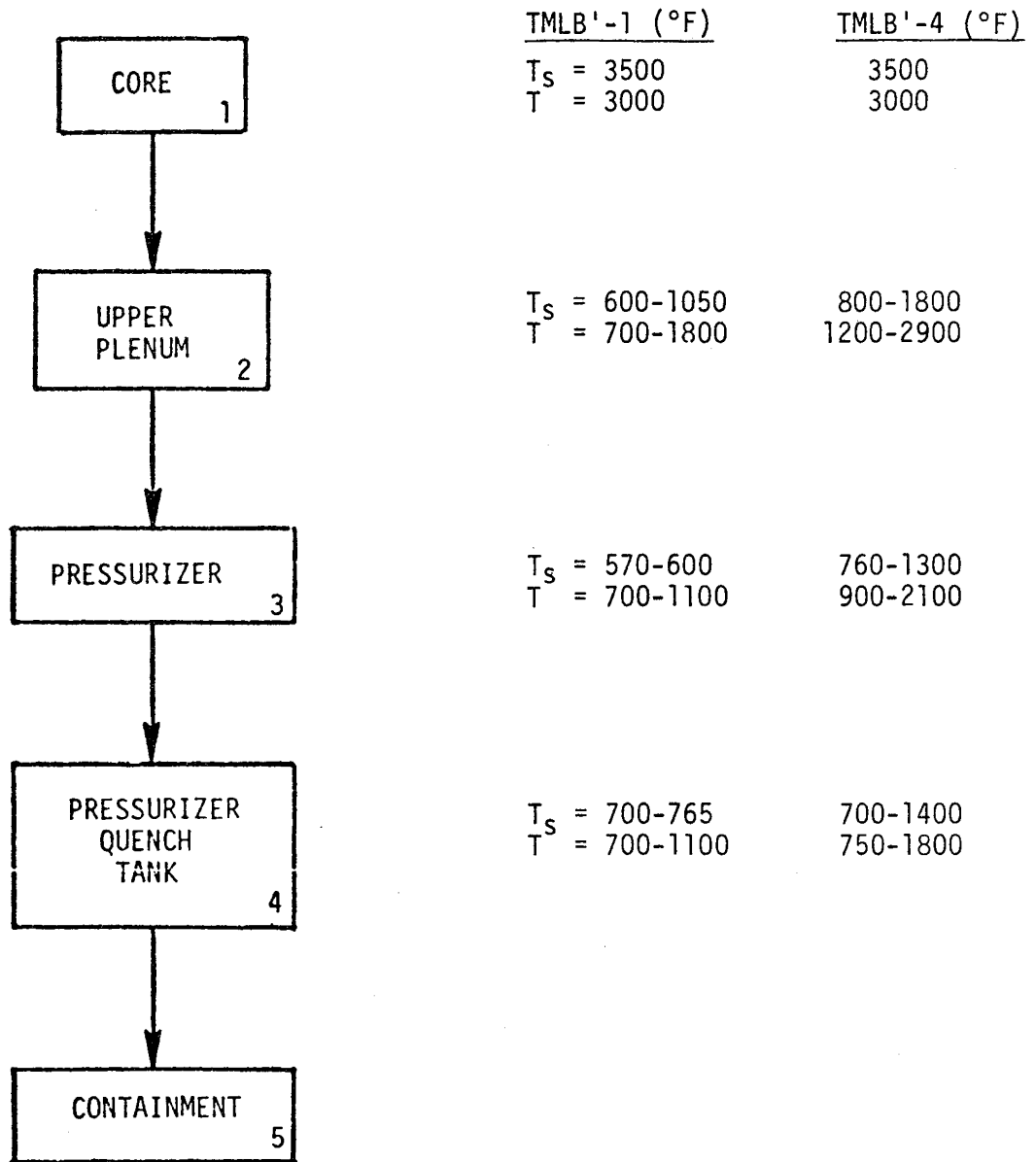


FIGURE D.2. INFLUENCE OF SYSTEM TEMPERATURES ON ELEMENTAL IODINE DEPOSITION ON PRIMARY SYSTEM INTERNALS IN A SEQUENCE INVOLVING MINOR OR NO FUEL DAMAGE

D.5



Control Volume	Length, ft	Equivalent Diameter, ft	Flow Area, ft <sup>2</sup>
Upper Plenum	8	0.5	100
Pressurizer	20	4	12.5
Pressurizer Quench Tank	16	4	12.5

FIGURE D.3. FLOW PATHS, CONTROL VOLUME PARAMETERS, AND SYSTEM TEMPERATURES FOR A TMLB' IN A PWR

TABLE D.1. INPUT THERMAL HYDRAULIC CONDITIONS USED IN TRAP FOR TMLB' BASE CASE CALCULATIONS

Time (s)	Upper Plenum		Pressurizer		Pressurizer Quench Tank		Junction Flow lb/sec
	Fluid Temp. (F)	Surface Temp. (F)	Fluid Temp. (F)	Surface Temp. (F)	Fluid Temp. (F)	Surface Temp. (F)	
0	710	600	710	570	710	700	5.4
60	1090	680	800	570	800	710	5.4
360	1400	780	900	575	900	720	4.3
660	1560	930	1000	580	1000	790	2.9
960	1820	1050	1100	585	1100	765	3.7
1260	700	900	700	600	700	700	197.0
1320	700	900	700	600	700	700	197.0

TABLE D.2. TRAP PREDICTIONS OF THE DISTRIBUTION OF FISSION PRODUCT IODINE AMONG THE VARIOUS STATES DURING ACCIDENT SEQUENCE TMLB'-1 (BASE CASE)

Time (s)	Species	Vapor (%)	Suspended Particles (%)	State		Deposited Particles	
				Deposited Vapor (%)	Control Volumes	(%)	Control Volumes
110	CsI	69.5	30.4	0		0	
220	CsI	52.2	47.7	0		0	
330	CsI	42.1	57.6	0.2	2	0	
440	CsI	36.2	63.1	0.5	2	0	
550	CsI	32.7	66.1	1.0	2	0.2	2
660	CsI	31.0	67.2	1.6	2	0.2	2
770	CsI	29.8	67.4	2.6	2	0.3	2
880	CsI	28.1	66.9	4.6	2	0.3	2
990	CsI	17.7	74.3	7.7	2	0.4	2
1100	CsI	1.0	90.8	7.5	2	0.7	2, 4
1210	CsI	0.5	91.9	6.8	2	0.7	2, 4
1320	CsI	0.4	92.6	6.2	2	0.7	2, 4
1320	I <sub>2</sub>	99.9	0	0.1	2	0	

TABLE D.3. TRAP PREDICTIONS OF THE DISTRIBUTION OF FISSION PRODUCT IODINE AMONG THE VARIOUS STATES DURING ACCIDENT SEQUENCE TMLB'-2 (LARGE SIZE PARTICLE SOURCE)

Time (s)	Species	State					
		Vapor (%)	Suspended Particles (%)	Deposited Vapor		Deposited Particles	
				(%)	Control Volumes	(%)	Control Volumes
110	CsI	69.5	30.4	0		0	
220	CsI	52.2	47.7	0		0	
330	CsI	42.1	57.6	0.2	2	0	
440	CsI	36.2	63.3	0.5	2	0	
550	CsI	32.7	66.2	1.0	2	0	
660	CsI	31.0	67.3	1.6	2	0	
770	CsI	29.7	67.6	2.6	2	0	
880	CsI	28.1	67.2	4.6	2	0.1	2
990	CsI	17.7	74.5	7.7	2	0.1	2
1100	CsI	1.0	90.9	7.5	2	0.4	4, 2
1210	CsI	0.5	92.2	6.8	2	0.5	4, 2
1320	CsI	0.4	92.8	6.3	2	0.5	4, 2
1320	I <sub>2</sub>	99.9	0	0.1	2		

TABLE D.4. TRAP PREDICTIONS OF THE DISTRIBUTION OF FISSION PRODUCT IODINE AMONG THE VARIOUS STATES DURING ACCIDENT SEQUENCE TMLB-3 (WEAK PARTICULATE SOURCE)

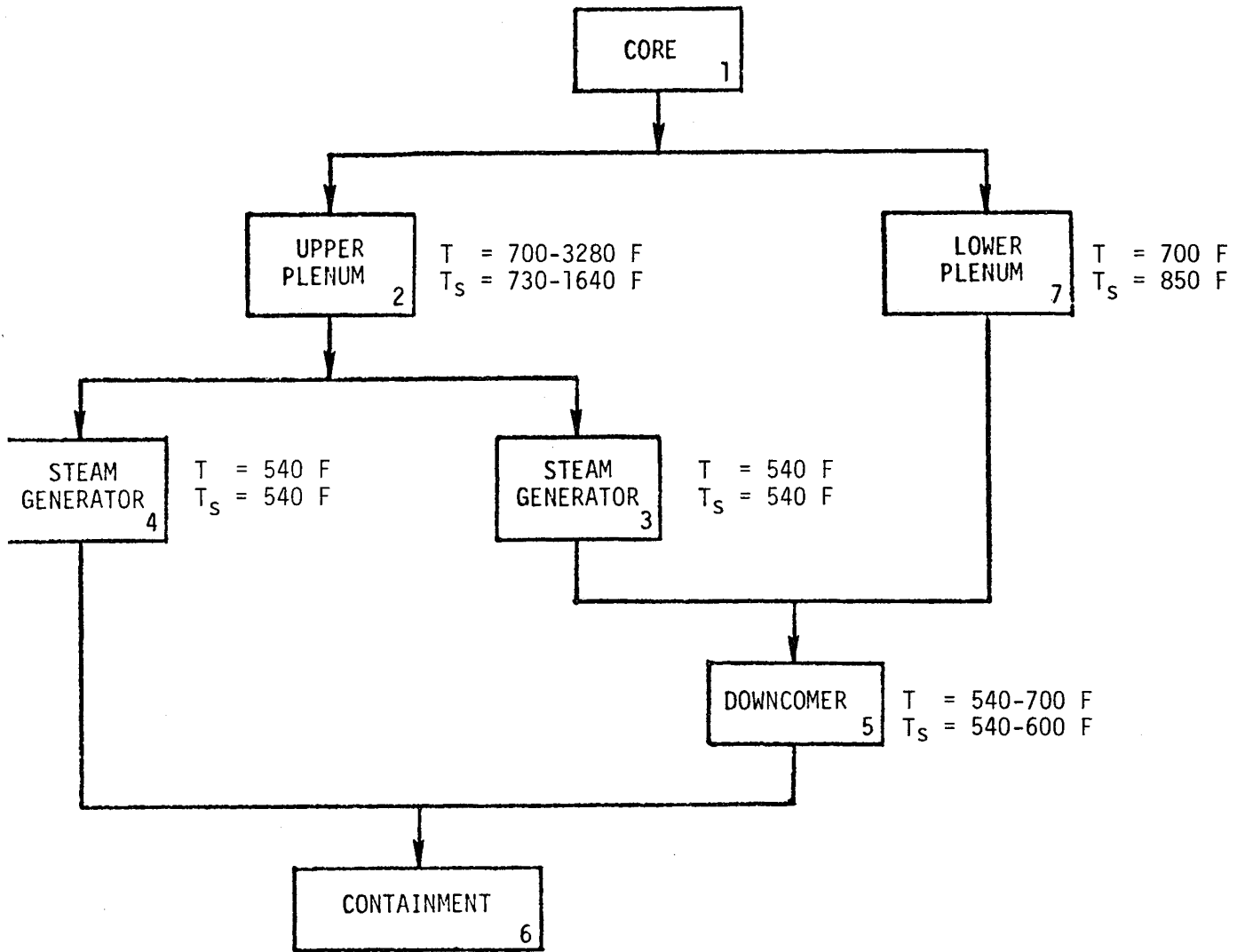
Time (s)	Species	State					
		Vapor (%)	Suspended Particles (%)	Deposited Vapor		Deposited Particles	
				(%)	Control Volumes	(%)	Control Volumes
110	CsI	69.5	30.4	0		0	
220	CsI	52.2	47.7	0		0	
330	CsI	42.2	57.5	0.3	2	0	
440	CsI	36.2	63.1	0.6	2	0	
550	CsI	32.7	66.2	1.0	2	0.1	2
660	CsI	31.0	67.3	1.6	2	0.1	2, 4
770	CsI	29.7	67.6	2.7	2	0.1	2, 4
880	CsI	28.1	67.1	4.7	2	0.1	2, 4
990	CsI	17.6	74.5	7.7	2	0.1	2, 4
1100	CsI	1.1	91.1	7.6	2	0.3	2, 4
1210	CsI	1.6	90.7	7.5	2	0.3	2, 4
1320	CsI	4.3	86.1	9.3	2	0.3	4, 2
1320	I <sub>2</sub>	99.9	0	0.1	2	0	

TABLE D.5. INPUT THERMAL HYDRAULIC CONDITIONS USED IN TRAP FOR TMLB' WITH ALTERED THERMAL-HYDRAULICS

Time (s)	Upper Plenum		Pressurizer		Pressurizer Quench Tank		Junction Flow lb/sec
	Fluid Temp. (F)	Surface Temp. (F)	Fluid Temp. (F)	Surface Temp. (F)	Fluid Temp. (F)	Surface Temp. (F)	
0	1189	772	902	758	750	730	7.3
240	1573	841	1058	798	851	750	7.5
420	2103	945	1307	872	900	800	10.0
540	2364	1040	1449	938	989	840	10.8
660	2518	1155	1504	1017	997	870	12.0
780	2605	1279	1658	1099	1180	910	13.5
900	2516	1391	1653	1166	1223	1030	11.0
1020	2511	1491	1700	1220	1302	1085	12.9
1140	2786	1610	1888	1297	1438	1140	19.2
1260	2890	1845	2114	1532	1784	1370	61.6
1320	672	1613	1055	1318	860	1280	163.7

TABLE D.6. TRAP PREDICTIONS OF THE DISTRIBUTION OF FISSION PRODUCT IODINE AMONG THE VARIOUS STATES DURING ACCIDENT SEQUENCE TMLB'-4 (ALTERED THERMAL HYDRAULIC CONDITIONS)

Time (s)	Species	Vapor (%)	Suspended Particles (%)	State		Deposited Particles (%)	Control Volumes
				Deposited Vapor (%)	Control Volumes		
110	CsI	62.1	37.5	0.4	2	0	
220	CsI	43.1	55.3	1.4	2	0.1	2
330	CsI	44.4	48.5	6.8	2	0.2	2
440	CsI	41.6	33.6	24.5	2	0.2	2
550	CsI	29.3	40.3	34.3	2	0.2	2, 4, 3
660	CsI	21.0	41.9	36.8	2	0.2	2, 4, 3
770	CsI	17.1	43.8	38.9	2	0.2	2, 4, 3
880	CsI	15.4	44.3	40.1	2	0.2	2, 4, 3
990	CsI	15.2	43.5	41.0	2	0.2	2, 4, 3
1100	CsI	16.2	41.6	41.9	2	0.2	2, 4, 3
1210	CsI	20.6	37.3	42.0	2	0.1	2, 4, 3
1320	CsI	22.5	40.2	37.1	2	0.1	2, 4, 3
1320	I <sub>2</sub>	100	0	0		0	



Control Volume	2	3	4	5	7
Length (ft)	8.0	68.0	68.0	14.0	8.0
Equivalent Diameter (ft)	0.500	0.650E-1	0.650E-1	1.0	0.500
Floor Area (ft <sup>2</sup> )	100.0	32.1	10.7	5.0	100

FIGURE D.4. FLOW PATHS, CONTROL VOLUME PARAMETERS, AND SYSTEM TEMPERATURES FOR THE BASE CASE AD (COLD LEG) IN A PWR

TABLE D.7. TRAP PREDICTIONS OF THE DISTRIBUTION OF FISSION PRODUCT IODINE AMONG THE VARIOUS STATES DURING ACCIDENT SEQUENCE AD-1 (BASE CASE)

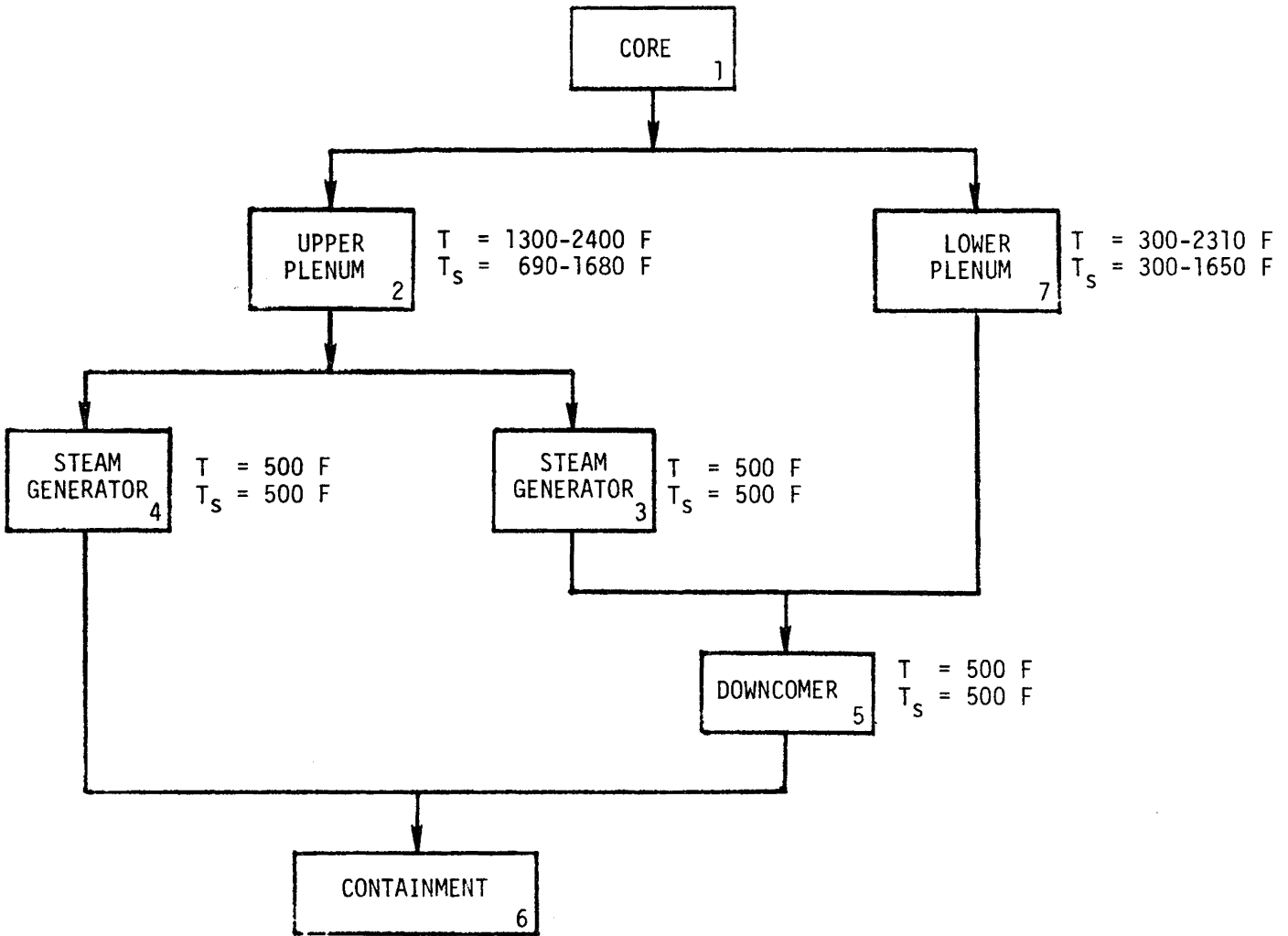
Time (s)	Species	State					
		Vapor (%)	Suspended Particles (%)	Deposited Vapor		Deposited Particles	
				(%)	Control Volumes	(%)	Control Volumes
100	CsI	5.8	76.4	17.1	2	0.5	3, 2, 4
200	CsI	3.2	78.6	17.5	2	0.4	3, 4, 2
300	CsI	2.5	79.3	17.6	2	0.4	3, 4, 2
400	CsI	2.0	79.6	17.8	2	0.4	3, 4, 2
500	CsI	1.7	79.7	18.0	2	0.3	3, 4, 2
600	CsI	1.3	80.2	18.0	2	0.3	3, 4, 2
700	CsI	1.2	83.8	14.3	2	0.3	3, 4, 2
800	CsI	4.8	78.6	14.6	3, 2, 4	1.8	3, 4
900	CsI	10.8	70.7	16.6	3, 2, 4	1.6	3, 4
900	I <sub>2</sub>	99.3	0	0.8	3, 4	0	

TABLE D.8. TRAP PREDICTIONS OF THE DISTRIBUTION OF FISSION PRODUCT IODINE AMONG THE VARIOUS STATES DURING ACCIDENT SEQUENCE AD-2 (LARGE SIZE PARTICLE SOURCE)

Time (s)	Species	Vapor (%)	Suspended Particles (%)	State		State	
				Deposited Vapor (%)	Control Volumes	Deposited Particles (%)	Control Volumes
100	CsI	5.8	75.7	18.1	2	0.2	2
200	CsI	3.2	77.4	19.0	2	0.1	3, 2
300	CsI	2.5	77.4	19.8	2	0.1	3, 2
400	CsI	2.0	76.7	20.9	2	0.1	3, 2, 4
500	CsI	1.7	75.3	22.7	2	0.1	3, 2, 4
600	CsI	1.3	73.6	24.8	2, 3, 4	0.1	3, 2, 4
700	CsI	1.3	67.4	30.3	2, 3	0.1	3, 4, 2
800	CsI	5.5	60.3	33.3	3, 4, 2	0.1	3, 4
900	CsI	11.5	53.7	33.9	3, 4, 2	0.6	3, 4
900	I <sub>2</sub>	99.3	0	0.8	3, 4	0	

TABLE D.9. TRAP PREDICTIONS OF THE DISTRIBUTION OF FISSION PRODUCT IODINE AMONG THE VARIOUS STATES DURING THE ACCIDENT SEQUENCE AD-3 (WEAK PARTICULATE SOURCE)

Time (s)	Species	Vapor (%)	Suspended Particles (%)	State			
				Deposited Vapor		Deposited Particles	
				(%)	Control Volumes	(%)	Control Volumes
100	CsI	5.8	75.6	18.1	2	0.2	2, 3
200	CsI	3.2	75.1	21.3	2, 3	0.2	2, 3
300	CsI	2.6	67.7	29.4	2, 3, 4	0.1	2, 3
400	CsI	2.2	55.9	41.5	3, 2, 4	0	
500	CsI	2.1	45.6	52.0	3, 2, 4	0	
600	CsI	1.9	38.1	59.7	3, 2, 4	0.1	5, 3, 2
700	CsI	2.0	32.7	65.0	3, 2, 4	0.1	5, 3, 2
800	CsI	6.4	29.4	63.8	3, 4, 2	0.1	5, 3, 2
900	CsI	12.4	26.2	61.1	3, 4, 2	0.1	5, 3, 2
900	I <sub>2</sub>	99.3	0	0.8	3, 4	0	

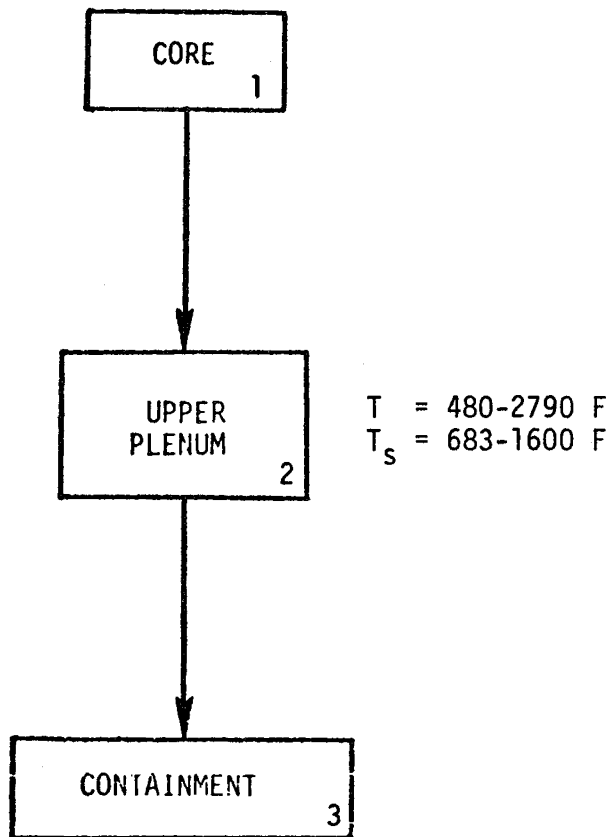


Control Volume	2	3	4	5	7
Length (ft)	8.0	68.0	68.0	14.0	8.0
Equivalent Diameter (ft)	0.500	0.650E-1	0.650E-1	1.0	0.500
Floor Area (ft <sup>2</sup> )	100.0	32.1	10.7	5.0	100.0

FIGURE D.5. FLOW PATHS, CONTROL VOLUME PARAMETERS, AND SYSTEM TEMPERATURES FOR THE AD (COLD LEG) IN A PWR, WITH ALTERED THERMAL HYDRAULIC CONDITIONS

TABLE D.10. TRAP PREDICTIONS OF THE DISTRIBUTION OF FISSION PRODUCT IODINE AMONG THE VARIOUS STATES DURING ACCIDENT SEQUENCE AD-4 (ALTERED THERMAL HYDRAULIC CONDITION)

Time (s)	Species	Vapor (%)	Suspended Particles (%)	State		Deposited	
				Deposited Vapor (%)	Control Volumes	Particles (%)	Control Volumes
67	CsI	13.0	77.4	4.5	2	4.8	2
133	CsI	5.3	74.2	16.8	2	3.5	2
200	CsI	4.9	67.4	22.2	2, 4	5.2	5, 2
267	CsI	13.6	45.8	24.5	4, 3	15.9	5, 2
333	CsI	14.4	37.4	33.1	3, 4	14.9	5, 2
400	CsI	13.3	43.6	29.3	4, 3	13.5	5
467	CsI	14.1	29.3	38.7	7, 4, 3	17.7	5, 7
533	CsI	10.4	25.6	48.3	7, 4, 3	15.5	5, 7
600	CsI	11.3	22.8	51.9	7, 4, 3	13.8	5, 7
600	I <sub>2</sub>	99.5	0	0.6	5, 7	0	



Control Volume	2
Length (ft)	12.0
Equivalent Diameter (ft)	0.358E-1
Floor Area (ft <sup>2</sup> )	49.0

FIGURE D.6. FLOW PATHS, CONTROL VOLUME PARAMETERS, AND SYSTEM TEMPERATURES FOR THE AD (HOT LEG) IN A PWR

TABLE D.11. TRAP PREDICTIONS OF THE DISTRIBUTION OF FISSION PRODUCT IODINE AMONG THE VARIOUS STATES DURING ACCIDENT SEQUENCE AD (HOT LEG)

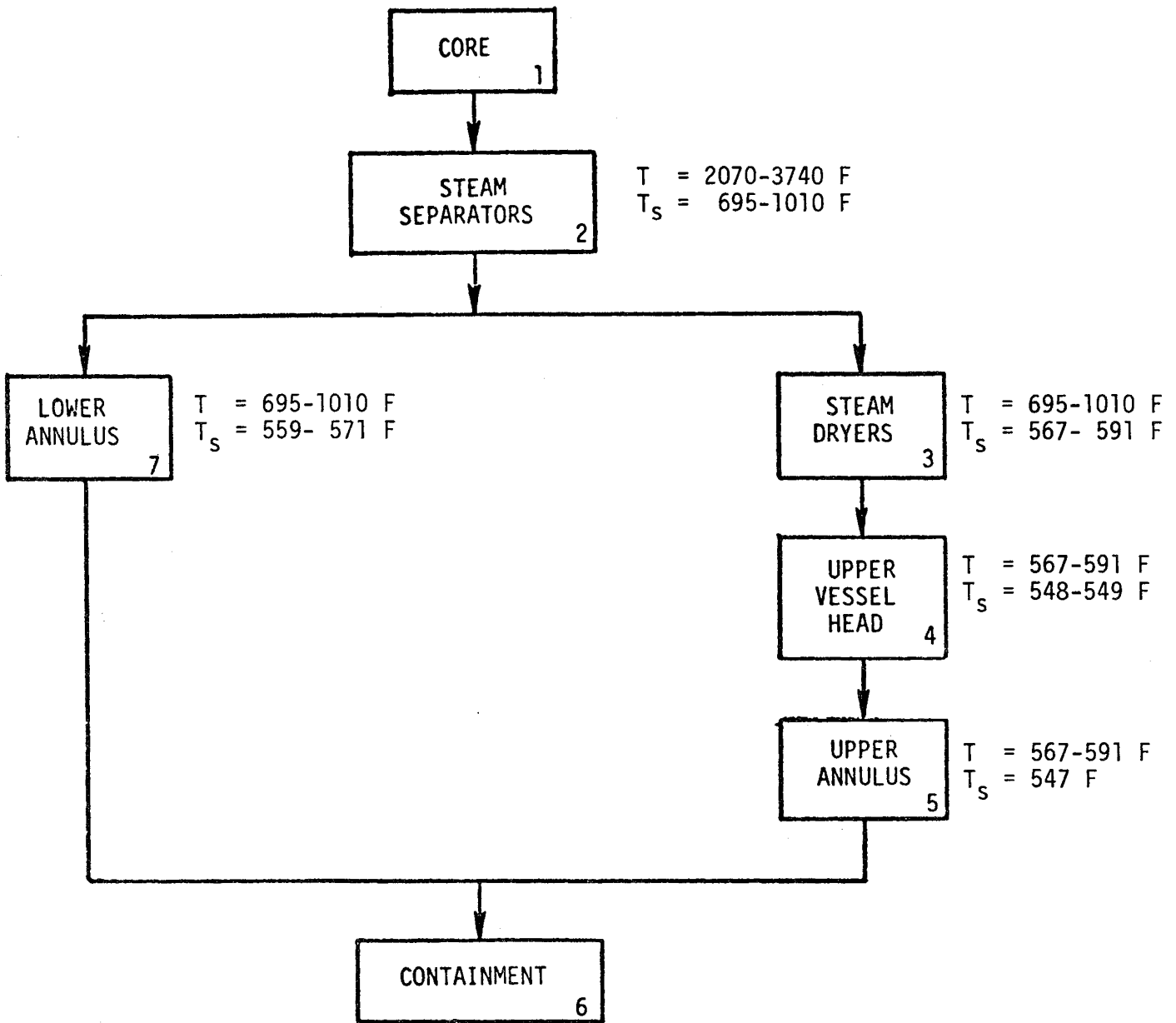
Time (s)	Species	State					
		Vapor (%)	Suspended Particles (%)	Deposited Vapor		Deposited Particles	
				(%)	Control Volumes	(%)	Control Volumes
100	CsI	63.2	24.3	11.4	2	0.8	2
200	CsI	72.9	12.2	14.3	2	0.4	2
300	CsI	76.2	8.1	15.2	2	0.3	2
400	CsI	77.3	6.1	16.2	2	0.3	2
500	CsI	77.3	4.9	17.4	2	0.2	2
600	CsI	79.8	4.1	15.8	2	0.1	2
700	CsI	94.2	5.4	0		0.1	2
800	CsI	86.1	13.6	0		0.1	2
900	CsI	84.9	14.7	0		0.1	2
	I <sub>2</sub>	100.0	-	-		-	

TABLE D.12. TRAP PREDICTIONS OF THE DISTRIBUTION OF FISSION PRODUCT IODINE AMONG THE VARIOUS STATES DURING FIRST 472 s OF ACCIDENT SEQUENCE S2D INITIATED BY A BREAK IN THE SURGE LINE. (AFTER THIS TIME THE FLOWS BECOME TOO HIGH FOR SIGNIFICANT RETENTION TO OCCUR, AND THE RISING TEMPERATURES WILL LEAD TO EVAPORATION OF NEARLY ALL CsI FROM SURFACES.)

Time (s)	Species	Vapor (%)	Suspended Particles (%)	State		State	
				Deposited Vapor (%)	Control Volumes	Deposited Particles (%)	Control Volumes
236	I <sub>2</sub>	100	-	-		-	
236	CsI	73.1	8.2	17.9	2, 3	0.1	2
472	I <sub>2</sub>	100	-	-		-	
472	CsI	77.0	4.3	18.4	2, 3	0.1	2

TABLE D.13. TRAP PREDICTIONS OF THE DISTRIBUTION OF FISSION PRODUCT IODINE AMONG THE VARIOUS STATES DURING ACCIDENT SEQUENCE AB INITIATED BY A BREAK IN THE SURGE LINE. (FOR THE FIRST 600 s OF THIS ACCIDENT FLOW RATES ARE TOO HIGH FOR SIGNIFICANT RETENTION TO OCCUR. THIS IS ALSO THE CASE FOR FINAL 300 s. TIMES SHOWN ABOVE START 600 s AFTER THE MELT BEGINS. ULTIMATELY, ALL THE CsI IS EXPECTED TO BE RELEASED.)

Time (s)	Species	Vapor (%)	Suspended Particles (%)	State		Deposited Particles (%)	Control Volumes
				Deposited Vapor (%)	Control Volumes		
174.7	CsI	87.7	0	12	2, 3	0	
349.3	CsI	86.3	0	13.5	2, 3	0	
524	CsI	83.1	0	16.7	2, 3	0	
524	I <sub>2</sub>	100.0	-	-		-	

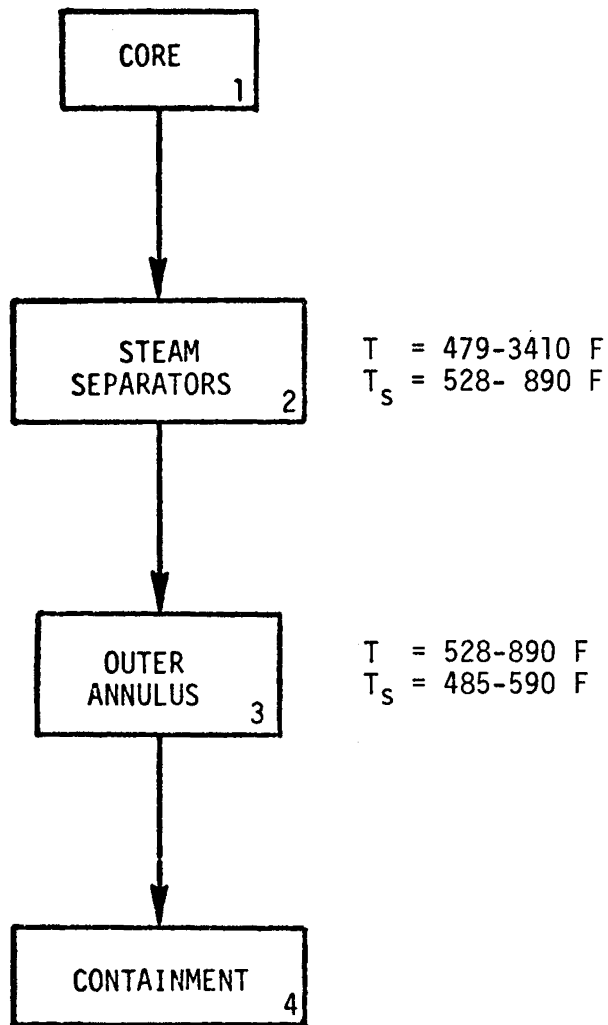


Control Volume	2	3	4	5	7
Length (ft)	10.0	10.0	10.0	15.0	15.0
Equivalent Diameter (ft)	0.670	0.100	21.0	6.0	6.0
Floor Area (ft <sup>2</sup> )	60.0	180.0	180.0	90.0	90.0

FIGURE D.7. FLOW PATHS, CONTROL VOLUME PARAMETERS, AND SYSTEM TEMPERATURES FOR THE TC IN A BWR

TABLE D.14. TRAP PREDICTIONS OF THE DISTRIBUTION OF FISSION PRODUCT IODINE AMONG THE VARIOUS STATES DURING ACCIDENT SEQUENCE TC

Time (s)	Species	State					
		Vapor (%)	Suspended Particles (%)	Deposited Vapor		Deposited Particles	
				(%)	Control Volumes	(%)	Control Volumes
275	CsI	89.5	2.4	8.1	2	0	
550	CsI	68.9	9.1	22.0	2	0	
825	CsI	49.8	16.7	33.2	2	0	
1100	CsI	35.8	23.7	40.3	2	0	
1375	CsI	26.2	29.4	44.0	2	0.1	3
1650	CsI	19.9	34.0	45.8	2	0.2	3
1925	CsI	15.7	37.4	46.4	2	0.2	3
2200	CsI	13.2	39.7	46.5	2	0.3	3
2475	CsI	10.8	42.1	46.4	2	0.4	3
2750	CsI	9.2	43.9	46.1	2	0.5	3
3025	CsI	8.6	44.6	45.9	2	0.7	3
3300	CsI	8.4	44.8	45.7	2	0.8	3
3300	I <sub>2</sub>	94.6	0	5.4	3	0	



Control Volume	2	3
Length (ft)	10.0	15.0
Equivalent Diameter (ft)	0.670	6.0
Floor Area (ft <sup>2</sup> )	60.0	180.0

FIGURE D.8. FLOW PATHS, CONTROL VOLUME PARAMETERS, AND SYSTEM TEMPERATURES FOR THE AE (WET) IN A BWR

TABLE D.15. TRAP PREDICTIONS OF THE DISTRIBUTION OF FISSION PRODUCT IODINE AMONG THE VARIOUS STATES DURING ACCIDENT SEQUENCE AE (WET)

Time (s)	Species	Vapor (%)	Suspended Particles (%)	State			
				Deposited Vapor		Deposited Particles	
				(%)	Control Volumes	(%)	Control Volumes
550	CsI	12.3	79.5	7.5	2	0.5	2
1100	CsI	9.3	80.1	10.1	2	0.3	2, 3
1650	CsI	7.9	81.0	10.7	2	0.2	2, 3
2200	CsI	7.1	81.6	10.9	2	0.2	2, 3
2750	CsI	16.8	72.3	10.5	2	0.2	2, 3
3300	CsI	24.3	62.7	12.5	2	0.3	2, 3
3850	CsI	27.3	58.7	13.5	2	0.3	2, 3
4400	CsI	32.3	53.4	13.9	2	0.3	2, 3
4950	CsI	29.6	56.9	12.9	2	0.4	2, 3
5500	CsI	26.5	61.2	11.6	2	0.4	2, 3
6050	CsI	24.2	64.6	10.6	2	0.3	2, 3
6600	CsI	22.3	67.0	10.2	2	0.3	2, 3
6600	I <sub>2</sub>	100.0	0	0		0	

References

- D.1 Private communication with A. P. Malinauskas, May 17, 1977.
- D.2 Letter from Dr. Raymond DiSalvo, Fuel Behavior Research Branch, U.S. Nuclear Regulatory Commission (November 18, 1976).
- D.3 Bell, M. J., "ORIGEN - The ORNL Isotope Generation and Depletion Code", ORNL-4628 (May 1973).
- D.4 Gieseke, J. A., P. Baybutt, H. Jordan, R. S. Denning, and R. O. Wooton, "Analysis of Fission Product Transport Under Terminated Conditions", BMI-NUREG-1990 (December 30, 1977).

APPENDIX E  
DEPOSITION MODELS FOR CONTAINMENT TRANSPORT ANALYSIS

Vapor Deposition Models

The models described for vapor deposition on walls and vapor removal by sprays are those employed in the CORRAL-2 code. The model for pool scrubbing has been developed at BCL for use in analyzing SGTR accidents.

Mass Transfer to Surfaces in Well-Mixed Volumes

Experimental correlations available in the literature can, conveniently, be used to calculate mass transfer coefficients for vapor species.

$$Sh_1 = 0.59 (Gr Sc)^{1/4} \quad (E-1)$$

for laminar flow ( $Gr < 10^9$ )

$$Sh_2 = 0.13 (Gr Sc)^{1/3} \quad (E-2)$$

for turbulent flow ( $10^9 < Gr < 10^{12}$ )

and

$$Sh = \frac{k\ell}{D_g} = \frac{\ell-10}{\ell} Sh_2 + \frac{10}{\ell} Sh_1 \quad (E-3)$$

where

$Sh_1, Sh_2$

and  $Sh$  = Sherwood numbers

$$Gr = \text{a Grashoff number} = \frac{\ell^3 (T_{\text{wall}} - T_{\text{bulk}}) g}{(\mu/\rho)^2 T_{\text{bulk}}}$$

$Sc$  = a Schmidt number =  $\mu/(D\rho)$

$\ell$  = length of wall in ft

$T$  = temperature

$\mu$  = viscosity of fluid

$\rho$  = density of fluid

## E.2

$g$  = acceleration due to gravity

$D_g$  = diffusivity of iodine in the gas phase

and the subscripts "wall" and "bulk" refer to conditions at the surfaces and in the bulk fluid, respectively.

Equation (E-3) is used to calculate the overall mass transfer coefficient,  $k$ , for vapors in well-mixed compartments. Implicit in the equation is the assumption that in a well-mixed region, turbulence develops at a distance of 10 ft from the leading edge. This assumption is justifiable based on the results of the Containment System Experiments.(E.1)

### Mass Transfer to Surfaces in Forced Convection Regions

The mass transfer coefficient for iodine deposition in a region where the fluid is not well mixed (such as the BWR annulus) can be calculated using correlations for forced convective mass transfer.(E.2) These correlations are:

$$Sh = \frac{k(4R_h)}{D_g} = .026 Re^{0.8} \cdot Sc^{1/3} \quad (E-4)$$

if  $2100 < Re < 20,000$

and

$$Sh = 1.86 \{Re \cdot Sc \cdot (4R_h/\ell)\}^{1/3} \quad (E-5)$$

if  $0 < Re < 2100$

where

$Re$  = a Reynolds' number =  $\rho U(4R_h)/\mu$

$U$  = bulk velocity of fluid in the annulus

and

$R_h$  = hydraulic radius of annulus = wetted perimeter/cross sectional flow area = annular width/2.

In each instance, the calculated mass transfer coefficient can be used to compute a deposition coefficient for natural deposition of vapors ( $\lambda_{\text{vapor, nat.}}$ ) using

$$\lambda_{\text{vapor, nat}} = (A/V) k \quad (E-6)$$

where

$A$  = surface area of deposition

and

$V$  = volume of compartment.

Spray Removal of Iodine

The removal of iodine by the containment sprays is modeled as a mass transfer process. (E.3) The mass transfer coefficients for iodine in the gas phase and within the liquid droplet can be calculated using standard correlations. They would then be used in calculating a spray removal rate coefficient,  $\lambda$ , in terms of the volume of the sprayed volume, the flow rate of the sprayed liquid and the terminal velocity of the spray droplets. The model equation is:

$$\lambda_{\text{vapor,spray}} = \frac{FH}{V} \left[ 1 - \exp \left\{ \frac{-6k_g t_e}{d[H + (k_g/k_\ell)]} \right\} \right] \quad (\text{E-7})$$

where

F = spray flow rate,  $\text{cm}^3/\text{sec} = \text{g}/\text{sec}$  of spray with  $\rho = 1 \text{ g/cc}$  (water)

H = equilibrium Henry's law constant for iodine (ratio of liquid phase concentration to gas phase concentration of iodine at equilibrium)

V = volume of sprayed compartment

d = diameter of sprayed droplets

$t_e$  = height of fall of drop/terminal velocity of droplets,  $V_t$

$D_\ell$  = diffusivity of iodine in the droplet

$k_g$  = gas phase mass transfer coefficient of iodine

$$= \frac{D_g}{d} [2.0 + 0.6 \text{Re}^{1/2} \text{Sc}^{1/3}]$$

and

$k_\ell$  = liquid phase mass transfer coefficient of iodine =  $6.58 D_\ell/d$

The terminal velocity of a falling drop is found by matching the velocity independent dimensionless quantity,

$$f_D \text{Re}^2 = 4\rho (\rho_\ell - \rho) d^3 g / 3\mu^2 \quad (\text{E-8})$$

with the appropriate range of Reynolds' number. For  $10 < \text{Re} < 100$ ,  $f_D \text{Re}^2 = 15.71 \text{Re}^{1.417}$ , and for  $100 < \text{Re} < 700$ ,  $f_D \text{Re}^2 = 6.477 \text{Re}^{1.609}$ .

$\rho_\ell$  is the density of the liquid droplets.

Rate Processes for Particles

Changes in particle size and concentration result from various growth and deposition mechanisms. The several available codes (CORRAL-2, HAARM-3, NAUA, and QUICK) employ various models depending on whether or not the mechanism was chosen because of its expected importance. The CORRAL-2 code is somewhat different than the aerosol behavior codes in that only loss by sedimentation and spray removal are included and in these cases, the models are selected to empirically match results of the CSE experiments. The basic rate expressions described below are used in the aerosol behavior codes. The inclusion or exclusion of these various mechanisms in the codes was summarized in Section 2 of this appendix.

Particle Growth

Particles grow by either condensation or agglomeration. Condensation changes the airborne mass concentration of aerosol but not the number concentration. Agglomeration decreases the airborne number concentration but does not affect the mass concentration.

Agglomeration. The agglomeration of aerosols depends on the particle number concentration in the gas and can occur by several basic mechanisms. The overall rate of change of particle number concentration by agglomeration, removal, and source input is

$$\begin{aligned} \frac{\partial}{\partial t} n(x,t) = K_0 \left[ \frac{1}{2} \int_0^x \phi(\xi, x-\xi) n(\xi, t) n(x-\xi, t) d\xi \right. \\ \left. - n(x,t) \int_0^\infty \phi(x, \xi) n(\xi, t) d\xi \right] \\ - n(x,t) R(x) + S(x,t) \end{aligned} \quad (E-11)$$

where

$\phi(x, \xi)$  = the normalized collision kernel predicting the probability of collision between two particles of volume  $x$  and  $\xi$  resulting from Brownian motion, gravitational settling, and turbulent gas motion

$K_0 = 4kT/3\eta$  = the agglomeration rate constant with

$k$  = Boltzmann constant

$T$  = gas temperature

$\eta$  = gas viscosity

$x = \frac{4}{3} \pi r_1^3$  = volume of particle with radius  $r_1$

$\xi = \frac{4}{3} \pi r_2^3$  = volume of particle with radius  $r_2$

$t$  = time

$n(x,t)$  = the number distribution density function

$R(x)$  = the removal rate of particles produced by gravitational settling to the floor, diffusion to the walls (wall plating), and leakage

$S(x,t)$  = the source rate function of particles input to the vessel.

The first integral in Equation (E-11) represents the formation rate of particles between the sizes  $x$  and  $x + dx$  as a result of collisions between particles of volumes  $\xi$  and  $x - \xi$ . Similarly, the second integral represents the disappearance rate of particles in the size range between  $x$  and  $x + dx$  resulting from collisions with all other particles.

The functional form of the collision kernel  $\phi(x, \xi)$  depends on the coagulation mechanisms present in a given system. In an enclosed containment vessel, possible mechanisms causing relative motion between particles, and thus coagulation, include Brownian motion of the particles, gravitational settling, and turbulent gas motion represented by the kernels  $K_B$ ,  $K_G$ , and  $K_T$ , respectively. In most analyses where more than one of these mechanisms is present, they are assumed to be separable and additive such that

$$K_0 \phi = K_B + K_G + K_T . \quad (E-12)$$

It should be noted that most equations in this appendix include the factors  $\gamma$  and  $\chi$ . The factor  $\gamma$  is a correction to particle-particle collision rates accounting for nonspherical particle shape and the factor  $\chi$  is a correction to mobility for nonspherical shape.

Brownian agglomeration results from the random motion of particles suspended in a gas. The random motion is caused by collisions with gas molecules. This movement gives rise to diffusion of particles in a concentration gradient analogous to gas diffusion. The diffusion coefficient for aerosol particles is a function of the particle size and is given by

$$D = Bkt \quad (E-13)$$

where

$B$  = particle mobility

$k$  = the Boltzmann constant

$T$  = absolute temperature.

The rate constant to be used in Equations (E-11) and (E-12) for agglomeration resulting from Brownian motion is given for particles of two sizes by

$$K_B = \frac{2kT}{3n}(r_1+r_2) \left[ \left( \frac{1}{r_1} + \frac{1}{r_2} \right) + C_m \lambda \left( \frac{1}{r_1^2} + \frac{1}{r_2^2} \right) \right] \frac{\gamma}{\chi} \quad (E-14)$$

where

$C_m$  = the constant defining the Cunningham correction factor that accounts for the low Knudsen number effects present for small particles (slip correction =  $1 + C_m \lambda / r$ )

$\lambda$  = the gas mean free path.

Gravitational agglomeration occurs because the difference in sedimentation rates for particles of different sizes results in situations where one particle overtakes another. The gravitational agglomeration rate is then based on the volume swept out by a particle as it moves through other particles. The swept-out volume must be corrected by the collision efficiency factor, which accounts for hydrodynamic interaction between particles and reduces the swept-out volume to another volume from which all particles are collected or collide. Collision efficiencies are available from both theoretical and experimental results. The gravitational agglomeration rate kernel is

E.6

$$K_G = \epsilon(r_1, r_2) \frac{2\pi g \rho_m}{9\eta} \left[ (r_1 + r_2)^3 |r_1 - r_2| + C_m \lambda (r_1 + r_2)^2 |r_1 - r_2| \right] \frac{\gamma}{X}^2 \quad (E-15)$$

where

$\epsilon(r_1, r_2)$  = the particle-particle collision efficiency

$\rho_m$  = the particle density

$g$  = the gravitational constant.

Turbulent or shear flow agglomeration must be considered because the collision frequency between particles suspended in a gaseous medium may be substantially increased by turbulent motion of the gas. This increase in collisions between particles may be the result of two independent mechanisms acting on the aerosol. The first mechanism produces collisions between particles of all sizes in a given distribution. The collisions occur because of particle motion resulting from the random turbulent motion of the gas. The second mechanism arises from the difference in density between the turbulent fluid and the suspended particles so that particles of various sizes have different response times. Hence, the second mechanism is termed the "inertial collision mechanism"; it produces collisions only between particles of different sizes.

The first mechanism has been analyzed by two methods (E.4, E.5). Although the approaches are quite dissimilar, they lead to strikingly similar results. The second mechanism and term in the following equation result from gas accelerations. Both Levich and Saffman and Turner have analyzed this case but have used the expressions for gas acceleration by Yaglom (E.6) and Batchelor (E.7), respectively. Using Saffman and Turner, (E.5) the sum of these two collision rate kernels is written as

$$K_T = \epsilon(r_1, r_2) \left[ \frac{8\pi \epsilon_T \rho_g}{15 \eta} \right]^{1/2} \gamma (r_1 + r_2)^3 + \epsilon(r_1, r_2) \left[ \frac{4\rho_m \sqrt{2\pi}}{9 \eta} \right] \left[ \frac{1.69 \epsilon_T^3 \rho_g}{15 \eta} \right]^{1/4} | (r_1^2 + C_m \lambda r_1) - (r_2^2 + C_m \lambda r_2) | (r_1 + r_2)^2 \left( \frac{\gamma}{X} \right)^2 \quad (E-16)$$

where

$\epsilon_T$  = the turbulent energy dissipation rate

$\rho_g$  = gas density.

Condensation. The aerosol behavior process of heterogeneous condensation of coolant vapor on already existing surfaces such as aerosol, walls, or spray droplets should be considered. Water vapor condensation on aerosol particles is included in the NAUA code. Condensation is a high-speed molecular interaction but has been modeled for nuclear aerosol analyses in terms of a simple growth equation. Deviations from this ideal are treated with experimentally determined correction factors.

The equation assuming equilibrium between vapor and condensed vapors for condensational growth of a particle of radius  $r$  is

## E.7

$$r \frac{dr}{dt} = A[S - \exp(B/r)] \quad (E-17)$$

where

S = the degree of steam or other vapor saturation

A and B = thermodynamic functions.

This simple equation has been integrated into the NAUA to cover condensation on aerosol particles and, with modified functions A and B, condensation on spray droplets as well. Condensation on cold walls is mainly a transport problem and has been treated separately.

Removal Rates. Aerosols suspended in a containment vessel may deposit by a wide variety of mechanisms, depending on the conditions and specific vessel geometry. Deposition rates for aerosols in containment volumes are used in analytical forms consistent with the term  $R(x)$ . In this case  $R(x)$  is the sum of individual rates, as  $R = P_R + G_R + T_R + L_R$ , where  $P_R$  refers to diffusion (plating),  $G_R$  to gravitational sedimentation,  $T_R$  to thermophoretic, and  $L_R$  to leakage removal rates.

The removal of particles from an enclosed space may result from the diffusion of particles to the internal surfaces of the enclosure. The flux of particles to a surface is given by Fick's law; when written in terms of removal rate from an enclosed volume it becomes

$$P_R = \frac{kTA_w}{6\pi\eta V\Delta\chi} \left[ \frac{1}{r} + C_m \lambda \left( \frac{1}{r^2} \right) \right] \quad (E-18)$$

where

$A_w$  = the wall or deposition surface area

$V$  = the containment volume

$\Delta$  = a parameter representing a distance over which diffusion occurs, perhaps a boundary layer.

Deposition onto available floor or horizontal areas occurs as a result of gravitational settling of particles. The gravitational sedimentation rate,  $G_R$ , is given by

$$G_R = \frac{2g\rho_m A_f}{9\eta V\chi} \left[ r^2 + C_m \lambda r \right] \quad (E-19)$$

where

$A_f$  is the available floor area.

Particles suspended in a gas experience a force directed toward cooler temperatures if the gas exhibits a temperature gradient. This force results from the interactions between gas molecules and the particles; the resulting deposition rate can be written as

## E.8

$$T_R = \frac{3\eta A_w \nabla T k_T}{2\rho_g V T} \quad (\text{E-20})$$

where

$k_T$  = a constant that depends on particle and gas properties

$T$  = absolute temperature

$\nabla T$  = the temperature gradient usually taken as  $(T_{\text{gas}} - T_{\text{wall}})/\Delta T$  with  $\Delta T$  being a boundary layer or deposition distance parameter for thermophoresis.

The factor  $k_T$  is used in various forms. Theories by Brock (E.8), Derjaguin and Yalamov, (E.9) and Stetter (E.10) are usually employed to predict properties, but more detailed verification of these theories is needed to unequivocally determine a proper form. Measurements of thermal forces on sodium oxide particles have provided experimental determinations of constants employed in Brock's theory, which makes the theory directly applicable in LMFBR aerosol behavior models. (E.11)

Particle Removal by Sprays. Because settling velocity depends on size, larger water drops settling more rapidly than smaller particles, overtake and collide with the smaller particles as they fall. The aerosol concentration decay,  $\frac{dn}{dt}$ , is given by

$$\frac{dn}{dt} = \epsilon \pi R^2 N (V_g - v_g) n \quad (E-21)$$

where  $\epsilon$  is the collision efficiency,  $V_g$  and  $v_g$  are settling velocities of the water drop and particle, respectively,  $R$  is the radius of the water drop, and  $N$  is the water drop concentration. The number concentration of water droplets can be expressed in terms of the water mass flow rate, droplet size and residence time and the containment volume,

$$N = \frac{3Fh}{4\pi R^3 \rho_w V_g V} \quad (E-22)$$

where  $F$  is the water mass flow rate,  $h$  is the fall height of the droplets, and  $\rho_w$  is the density of the water droplets. Thus we have

$$\frac{dn}{dt} = \frac{3Fh \epsilon}{4R \rho_w V} \frac{V_g - v_g}{V_g} n \quad (E-23)$$

and if  $V_g \gg v_g$ , as is expected in nearly any case of interest, one can express the loss rate of aerosol due to water spraying as

$$\lambda = \frac{3Fh \epsilon}{4R \rho_w V} \quad (E-24)$$

Because of hydrodynamic interaction between the two particles only a certain fraction of those in the "sweep out area" of a large particle will actually be contacted. If we define the "sweep out area" as the area of a circle with the radius of the larger particle, then  $\epsilon$ , shown in the above equations can be defined further as the fraction of the small particles in the sweep out area which are collected. Furthermore, the smaller particle must stick to the larger one to complete the collision process. Here, the sticking or attachment probability is assumed to be unity since this is likely and very little theoretical or experimental evidence concerning this phenomenon exists.

In general, there are two major pertinent collision mechanisms which enable a particle to overcome the hydrodynamic repulsion and collide with the water drop. The first mechanism is the so called inertial impaction which accounts for the deviation of a particle from a streamline due to its inertia. The other mechanism is called the interception effect which takes into account the increase of collision probability due to the finite extent of small particles. Thus we write

$$\epsilon = \epsilon_1 + \epsilon_2 \quad (E-25)$$

where  $\epsilon_1$  is the collision efficiency due to particle inertia and  $\epsilon_2$  is the collision efficiency due to interception.

For relatively low particle velocities an empirical formula for the efficiency of inertially caused particle collisions is reported by Fuchs and is given by:

## E.10

$$\epsilon_1 = \left[ 1 + \frac{0.75 \ln(2 \text{ Stk})}{\text{Stk} - 1.214} \right]^{-2} \quad (\text{E-26})$$

Here, Stk is the Stokes number defined by

$$\text{Stk} = \frac{2(V_g - v_g)r^2\rho_p}{9\mu R} \quad (\text{E-27})$$

where  $\rho_p$  is the particle density. The efficiency  $\epsilon_1$  is taken as zero when  $\text{Stk} \leq 1.214$ .

For viscous flow about a spherical collector the following equation can be used for the interceptional collision efficiency which is valid for small values of the ratio  $r_i/R$ :

$$\epsilon_2 \approx \frac{3}{2} \frac{(r/R)^2}{(1 + r/R)^{1/3}} \quad (\text{E-28})$$

It is clear from the expressions for  $\epsilon_1$  and  $\epsilon_2$  that separate efficiencies are needed to be calculated for each particle size for each efficiency term.

Calculations of aerosol removal rate for a typical meltdown case show that aerosol concentration is reduced by a factor of 15 by 2 hours of spraying. Thus spraying predominates any other natural aerosol removal mechanism.

Particle Removal by Filters. Contaminated gases in a containment can be recirculated through filters or other particulate collection devices to reduce the airborne radionuclide concentration. For this removal process, the specific rate of concentration reduction is given as

$$\frac{dn}{dt} = -\frac{nQ}{V} \quad (\text{E-29})$$

where  $n$  is the concentration,  $\eta$  is the filter collection efficiency,  $Q$  is the air volumetric flow rate through the filter.

Typically, a flow of roughly 10000 cfm is used through the filter system which consists of high efficiency particulate air filter (HEPA) and charcoal filter. In order to prevent rapid clogging of the high efficiency filter, roughing filters are installed upstream of the filters. Efficiencies of the filters are given based on the removal performance for 0.3  $\mu\text{m}$  particles. Particle collection efficiency is normally over 99 percent. In order to filter out a large volume of the contaminated gas in the containment, several units of such a filter system are simultaneously operated.

To illustrate the role of a filter system in reducing the airborne particulate concentration, results of a computer calculation are given in Figure E.1. The source aerosol was assumed to last for 50 hours at a constant rate and the filter system was initiated 15 hours after initiation of the source aerosol. A flow rate of  $2.7 \times 10^4$  cfm through the filter system and a particulate collection efficiency of 90 percent were used. It is seen from the figure that the particulate concentration decreases to zero immediately after the source of aerosol ceases.

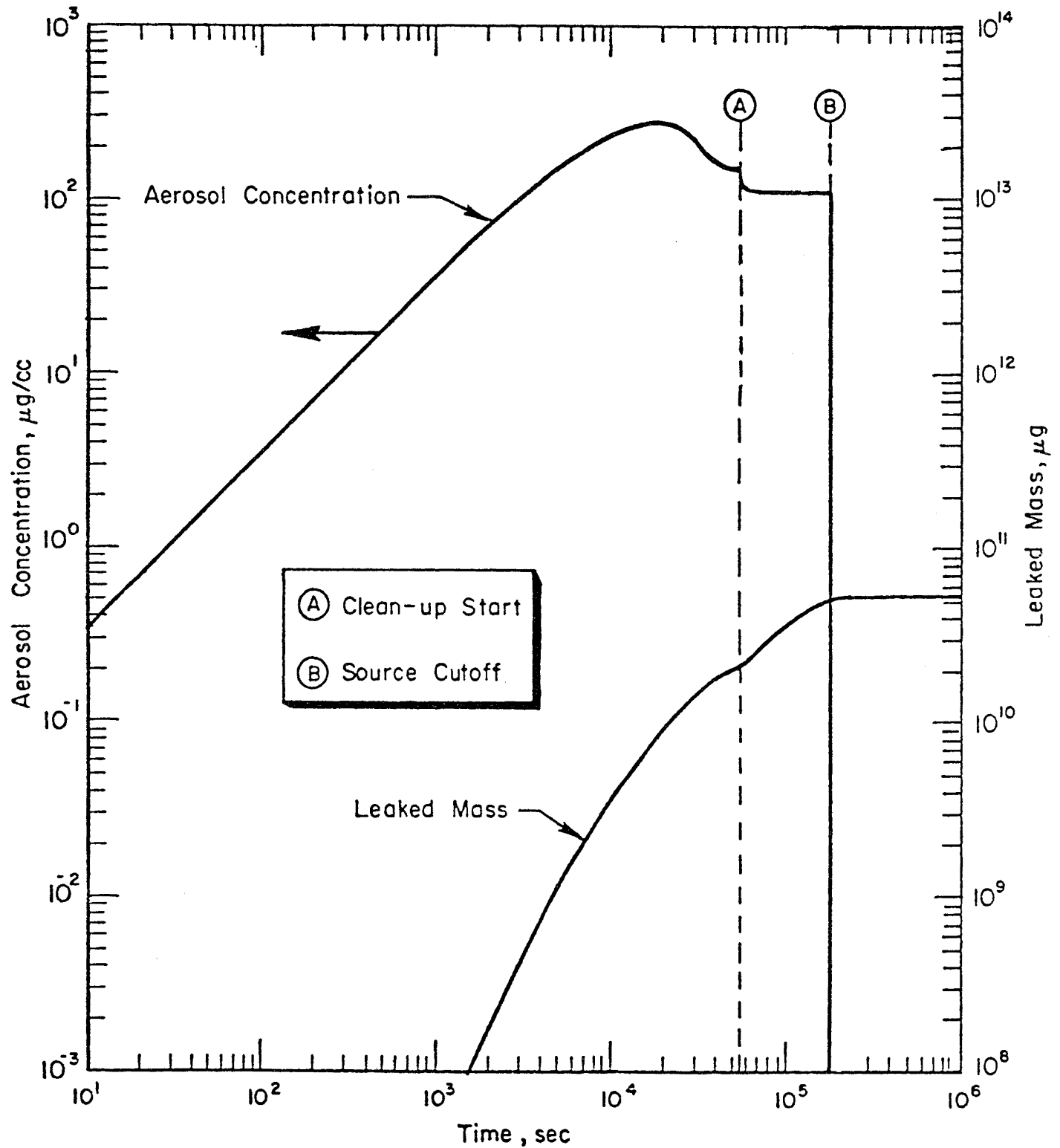


FIGURE E.1. HAARM-3 CALCULATION RESULTS FOR AEROSOL CONCENTRATION AND LEAKED AEROSOL MASS

### Suppression Pool Scrubbing

In the following paragraphs, simple models are presented for vapor scrubbing and particulate removal in suppression pools. The models involve several simplifying assumptions. The physical description of the actual processes could be substantially more complicated. In particular, steam condensation is expected to decrease the bubble size during its rise through the suppression pool. On the other hand, a certain amount of bubble coalescence and rafting should also be expected to occur. These phenomena tend to increase the effective bubble size. The combined effect of all the possible phenomena on decontamination in the suppression pool is a complicated function of several parameters including but not limited to the values of the thermal hydraulic variables in the pool such as temperature and the noncondensable fraction in the steam-gas mixture.

It is, in principle, possible to construct a model to describe the decontamination process while taking into account the various phenomena just described. The required effort to develop such a model and to incorporate it into an existing containment transport code was beyond the scope of this program. For these reasons it was necessary to estimate a possible range of decontamination factors based upon the results of simple models and experiments and to treat decontamination factors parametrically over this range for the analyses in Chapter 7.

References to several experimental studies, (E.12-21) designed to measure DF's in suppression pools, were provided to us by the General Electric Company. There are significantly more data available related to the transport of iodine through pools in a vapor form than for particulates. Additional experiments, in particular with a well-characterized particle source, will be required for the verification of a suppression pool decontamination model.

#### Vapor Scrubbing Model

A model for vapor removal from bubbles rising in water pools may be developed from basic mass transfer considerations. Use of this model results in an expression for the scrubbing factor, SF, which is defined as the fraction of vapor scrubbed from the bubble. This expression is:

$$SF = 1 - \exp\left(\frac{-3k_2\tau}{a}\right) \quad (E-9)$$

where

$k_2$  = overall mass transfer coefficient for vapor transport, cm/sec

$\tau$  = rise time of bubble, seconds

$a$  = radius of bubble, cm.

Although it is possible to use further correlations to calculate  $k_2$  as a function of system temperature, pressure, and rise velocity of the bubble, such a detailed analysis is probably not necessary for application of this model to suppression pools where the range of possible temperature and pressures is fairly narrow. Thus, assuming constant diffusivities of iodine in vapor and liquid ( $0.07$  and  $2 \times 10^{-5}$   $\text{cm}^2/\text{sec}$ , respectively), an iodine partition coefficient of  $100$ , a rise velocity of  $40$   $\text{cm}/\text{sec}$  and a bubble radius of  $1.5$   $\text{cm}$  (the last two assumptions cause the rise of the bubble to be turbulent), a value of  $0.182$   $\text{cm}/\text{sec}$  may be calculated for  $k_2$ . Thus,

$$\text{SF} = 1 - \exp\left(-\frac{0.546 \tau}{a}\right) \quad (\text{E-10})$$

Equation (E-10) may be used to study the effect of rise time and bubble size on the estimated scrubbing factor. These results are tabulated below.

TABLE E.1. SCRUBBING FACTORS AS FUNCTION OF RISE TIME AND BUBBLE SIZE\*

Bubble Diameter cm	Rise Time, seconds			
	1	5	10	20
1.0	0.664	0.996	1.0	1.0
2.0	0.421	0.935	0.996	1.0
3.0	0.305	0.838	0.974	0.999
4.0	0.239	0.745	0.935	0.996
6.0	0.166	0.597	0.838	0.974

\* Note that a constant mass transfer coefficient was assumed in the calculations regardless of the bubble size.

### Particle Scrubbing Model

A simple model similar to the first order mass transfer process for vapors may be developed for the removal of cesium iodide particles from single bubbles. (E.12) This model equation is:

$$\frac{n}{n_0} = \exp\left[-\frac{\tau}{2\mu a}\left(\frac{kT}{\pi r \delta} + \frac{4\rho_p g r^2}{3}\right)\right] \quad (\text{E-30})$$

To good approximation, the Brownian diffusion term may be neglected. Thus, in c.g.s. units:

$$\text{SF} = 1 - \frac{n}{n_0} = 1 - \exp\left[-\frac{653.33 \tau \rho_p r^2}{\mu a}\right] \quad (\text{E-31})$$

where

$T$  = temperature ( $^{\circ}\text{K}$ )

$\tau$  = rise time, seconds = rise height, cm/rise velocity,  $\text{cm}\cdot\text{sec}^{-1}$

$\rho$  = particle density,  $\text{gm}\cdot\text{cm}^{-3}$

$r$  = particle radius, cm

$\mu$  = viscosity of bubble fluid,  $\text{gm}\cdot\text{cm}^{-1}\cdot\text{second}^{-1}$

$a$  = bubble radius, cm

$\frac{n}{n_0}$  = number of particles at end of rise/number of particle initially

SF = a scrubbing factor defined as the fraction of the initial number of particles that are scrubbed.

$\delta$  = boundary layer thickness (cm)

$k$  = Boltzmann's constant ( $\text{erg}/^{\circ}\text{K}$ )

This equation may be used to calculate the scrubbing factor for various particle sizes. The results of these calculations are tabulated in Table E.2.

TABLE E.2. PARTICLE SCRUBBING FACTORS AS FUNCTION OF PARTICLE SIZE

Particle Diameter, $\mu\text{m}$	SF
0.2	$1.8 \times 10^{-3}$
2	0.168
4	0.622
10	0.99
40	1.0

#### Assumptions

1. Bubble size fixed at 3 cm (diameter)
2. Particle density is 1 gm/cc
2. Rise height = 10 ft
4. Rise velocity of bubble - 40 cm/second
5. Viscosity of bubble fluid is constant at  $1.8 \times 10^{-4}$  gm/cm-second. (Air at 20 C has this viscosity).

Bases and Input for Containment  
Transport Calculations

The following three tables, E.3, E.4, and E.5, provide information on which the calculations of radionuclide transport and deposition were based. Table E.3 provides the sequencing of events controlling source rates and flows, Table E.4 gives the geometrical data used for the various containments, and Table 3.5 provides the input used in spraying calculations.

TABLE E-3. ACCIDENT EVENTS AS A FUNCTION OF TIME AS USED FOR CALCULATION

Reactor	Sequence	Event	Time (Hours)
<u>WR</u>			
Large, High Pressure	Large Pipe Break, Delayed ECC	(1) Spray on	0.01
		(2) Melt starts	0.092
		(3) ECC on	0.266
		(4) Melt ends	0.275
Large, High Pressure	S <sub>2</sub> D	(1) Spray on	0.569
		(2) Melt starts	0.822
		(3) Melt ends	1.143
		(4) Head fails - hot drop begins	1.295
		(5) Hot drop ends and vaporization begins	3.130
		(6) Vaporization ends	5.130
Large, High Pressure	TMLB', Basemat Meltthrough	(1) Melt starts	3.767
		(2) Melt ends	4.417
		(3) Head fails and hot drop begins	4.520
		(4) Hot drop ends and vaporization begins	6.817
		(5) Vaporization ends	8.817
Large, High Pressure	TMLB', Overpressure	(1) Melt starts	3.767
		(2) Melt ends	4.417
		(3) Head fails and hot drop begins	4.665
		(4) Containment fails	4.777
		(5) Hot drop ends and vaporization begins	6.150
		(6) Vaporization ends	8.150
Large, High Pressure with Filters	S <sub>2</sub> D	(1) Filters/coolers on	0.083
		(2) Melt starts	1.08
		(3) Melt ends	1.39
		(4) Head fails and hot drop begins	1.50
		(5) Hot drop ends and vaporization begins	3.39
		(6) Vaporization ends	5.39
General	V Sequence	(1) Aux building fails	0.01
		(2) Melt starts	0.636
		(3) Melt ends	0.946
		(4) Head fails and hot drop begins	1.078
		(5) Hot drop ends and vaporization begins	1.685
		(6) Vaporization ends	3.685

TABLE E-3. (Continued)

Reactor	Sequence	Event	Time (Hours)
Ice Condenser	AD	(1) Sprays on	0
		(2) Melt starts	0.091
		(3) Melt ends	0.308
		(4) Head fails with hydrogen explosion	1.07
		(5) Containment fails	1.10
		(6) Hot drop ends and vaporization begins	1.12
		(7) Vaporization ends	3.12
Ice Condenser	TMLB <sup>1</sup>	(1) Melt starts	3.33
		(2) Melt ends	3.78
		(3) Head fails and hot drop begins	3.98
		(4) Containment fails	3.99
		(5) Hot drop ends and vaporization begins	6.39
		(6) Vaporization ends	8.39
Ice Condenser	S <sub>2</sub> HF	(1) Spray on	0.0125
		(2) ECC off	1.5
		(3) Spray off	1.89
		(4) Ice all melted	2.51
		(5) Melt starts	2.52
		(6) Melt ends	2.87
		(7) Head fails and hot drop begins	3.11
		(8) Containment fails	3.15
		(9) Hot drop ends and vaporization begins	5.42
		(10) Vaporization ends	7.42
<u>BWR</u>			
Mark I	AE	(1) Melt starts	0.309
		(2) Containment fails	0.843
		(3) Melt ends	0.843
		(4) Head fails and hot drop begins	1.27
		(5) Hot drop ends and vaporization begins	1.29
		(6) Vaporization ends	3.29
Mark I	TC	(1) Containment fails	0
		(2) Melt starts	1.43
		(3) Melt ends	2.40
		(4) Head fails and hot drop begins	2.59
		(5) Hot drop ends and vaporization begins	2.60
		(6) Vaporization ends	4.60

TABLE E-3. (Continued)

Reactor	Sequence	Event	Time (Hours)
Mark I	TW	(1) Containment fails	Before 75
		(2) Melt starts	75.58
		(3) Melt ends	77.30
		(4) Head fails and hot drop begins	77.7
		(5) Hot drop ends and vaporization begins	81.9
		(6) Vaporization ends	83.9
Mark III	TQUV	(1) Melt starts	1.77
		(2) Melt ends	2.37
		(3) Head fails	2.5
		(4) Vaporization begins	2.90
		(5) Vaporization ends	4.90
		(6) Containment fails	6.68

TABLE E.4. DIMENSIONS OF VARIOUS REACTORS USED FOR CALCULATION

Containment Design	Compartment	Volume (ft <sup>3</sup> )	Wall Area (ft <sup>2</sup> )	Floor Area (ft <sup>2</sup> )
<u>PWR</u>				
Large High Pressure	Main Volume	1.29 E6	1.54 E5	1.35 E4
	Reactor Cavity	5.07 E5	8.20 E4	6.85 E3
Large High Pressure with Filters	Main Volume	2.61 E6	1.89 E5	1.43 E4
	Reactor Cavity	1.25 E5	1.47 E4	3.67 E3
General, for V Sequence	Containment	1.29 E6	1.45 E5	9.00 E3
	Aux Building	1.01 E6	3.42 E4	1.78 E4
Ice Condenser	Lower Volume	3.88 E5	1.04 E5	9.00 E3
	Upper Volume	8.98 E5	3.27 E5	5.40 E3
<u>BWR</u>				
Mark I	Drywell	1.59 E5	6.74 E4	1.41 E3
	Wetwell	1.19 E5	1.71 E4	7.93 E3
	Annulus	2.78 E1	(a)	(a)
Mark III	Drywell	2.70 E5	1.95 E4	4.00 E3
	Wetwell	1.40 E6	5.03 E5	1.20 E4

(a) Has cross sectional flow area 23.7 ft<sup>2</sup> with hydraulic diameter 0.33 ft.

TABLE E.5. INPUT INFORMATION ON SPRAYING

Reactor Type	Water Flow Flow Rate (ft <sup>3</sup> /hr)	Height (ft)	Drop Diameter (μm)
Large High Pressure	$2.53 \times 10^4$	90	1000
Ice Condensor	$3.81 \times 10^4$	100	1000

## References

- E.1 Knudsen, J. G., and R. K. Hilliard, "Fission Product Transport by Natural Processes in Containment Vessels", BNWL-943, Battelle-Northwest (1969).
- E.2 Bird, R. B., W. E. Stewart, and E. N. Lightfoot, Transport Phenomena John Wiley and Sons, New York (1960).
- E.3 Postma A.K. and W. F. Pasedag, "A Review of Mathematical Models for Predicting Spray Removal of Fission Products in Reactor Containment Vessels" WASH-1329, U.S. Atomic Energy Commission (1974)
- E.4 Levich, B. G., Physicochemical Hydrodynamics, Englewood Cliffs, New Jersey: Prentice-Hall, Inc. (1962).
- E.5 Saffman, P. G., and J. S. Turner, J. Fluid Mech., 1:16 (1956).
- E.6 Yaglom, A. M., Doklady AN SSSR, Vol. 67, No. 5 (1949).
- E.7 Batchelor, G. K., Proc. Camb. Phil. Soc., 47:359 (1951).
- E.8 Brock, J. R., J. Colloid Sci., 17:568 (1962).
- E.9 Derjaguin, B. V., and Y. I. Yalamov, "The Theory of Thermophoresis and Diffusiophoresis of Aerosol Particles and Their Experimental Testing", International Reviews in Aerosol Physics and Chemistry, Vol. 3, Pt. 2, G. M. Hidy and J. R. Brock, Eds. (1972).
- E.10 Stetter, G., Staub, 20:244 (1960).
- E.11 Gieseke, J. A. et al., "Characteristics of Agglomerates of Sodium Oxide Aerosol Particles" (1977).
- E.12 "Fission Product Entrainment Evaluation Tests for the Pressure Suppression System," GEAP-3206 (1959), General Electric Company.
- E.13 McGoff, M. J., Rodgers, S. J., "Simulation of Container Venting Under Seawater", Technical Report 59, Contract NOBS-65426, Mine Safety Appliances Co., Gallery, PA (December, 1957).
- E.14 Siegwarth, D. P., Siegler, M., "Scale Model Fission-Product Removal in Suppression Pools", GEAP-13172, April 1971, General Electric Co.
- E.15 Hillary, J. J., et al., "Iodine Removal by a Scale Model of the S.G.H.W. Reactor Vented Steam Suppression System", TRG Report 1256, (1966).
- E.16 Diffey, H. R., et. al., "Iodine Cleanup in a Steam Suppression System", CONF-650407 2 (1965) 776.
- E.17 Malinowski, D. D., et al., "Radiological Consequences of a Fuel Handling Accident", WCAP-7828, December 1971, Westinghouse Electric Corporation.

- E.18 "Energy Suppression and Fission Product Transport in Pressure Suppression Pools", Stanford, L. E., Webster, C. C., ORNL-TM-3448, April, 1972.
- E.19 Geisse, G., "Diffusion of Iodine in Water", CEA-R-3199, AEC Lib. Trans. 623 (April, 1967).
- E.20 Devell, L., et al., "Trapping of Iodine in Water Pools at 100°C, Containment and Siting of Nuclear Power Plants Proc. of Symposium IAEA 1967 (Vienna) CONF-670402.
- E.21 Raghuram, S., et al., "Iodine Behavior in SGTR Accidents", NUREG report to be published.

## APPENDIX F - RESPONSE TO COMMENTS ON DRAFT REPORT

F.1 SUMMARY OF REVIEWS ON DRAFT NUREG-0772

The first draft of NUREG-0772 was completed on March 6, 1981. Shortly thereafter, on March 10 and 11, the draft report was reviewed by the Subcommittee on Reactor Radiological Effects of the Advisory Committee on Reactor Safeguards (ACRS) and by the full Committee on March 12. The ACRS comments on the contents of draft NUREG-0772 were contained in a letter (Attachment 1) from ACRS Chairman J. Carson Mark to NRC Chairman Joseph Hendrie, dated March 17, 1980. A second review by a Special Peer Review Group of the draft report was held on March 17 and 18. This review group consisted of scientists and engineers from various national laboratories, private industry, government agencies, foreign countries, universities, and public interest groups. A list of individuals who participated in this review is reproduced in Attachment 2.

At the Peer Review Meeting, the authors of NUREG-0772 requested that the reviewers submit detailed written comments on the draft report. Twenty-seven individuals and organizations responded. These commenters are listed in Attachment 3.

As a result of the large number of comments received (over 160 pages), it is not possible to reproduce each comment and the way the authors resolved each comment, in this appendix. However, it was possible to identify a number of major comments, which are addressed in the next section. A listing of the major comments is shown on Figure F.1. In Section F.2 of this appendix, these comments are summarized and the authors' response to these comments are presented.

Detailed responses to each comment have been developed and can be inspected in the NRC Public Document Room (PDR) at 1717 H Street, Washington, D.C. Also available for inspection in the PDR are copies of the written comments on the report, a copy of the original draft report, and unedited transcripts from the ACRS and Special Peer Review Meetings on the draft report.

F.2 RESPONSES TO MAJOR COMMENTS

## CHAPTER 1

1.1 Lack of Systematic Analysis of Fission Product Transport Through the Plant

The analyses in Chapters 4, 5, 6, and 7 were performed separately without accounting for interactions that could be important between the release conditions in the fuel region, transport through the primary system, and transport through the containment. These analyses should be performed in a systematic manner which accounts for these interactions.

Authors' Response

We agree. The development of the interfaces between these parts of the analysis are being undertaken within ongoing NRC research programs. It was beyond the

FIGURE F.1 MAJOR COMMENTS

Chapter 1

- 1.1 Lack of Systematic Analysis of Fission Product Transport Through the Plant
- 1.2 Conservative WASH-1400 Assumptions and Models Used
- 1.3 Uncertainties Associated with Estimates of Fission Product Release
- 1.4 Uncertainties in Thermal-Hydraulic Conditions
- 1.5 Assumptions in the Analyses
- 1.6 Verification of Computer Codes Used in the Analyses
- 1.7 Past Reactor Accident Experience
- 1.8 Research Data Needs Identified in Report
- 1.9 Report Should/Should Not be Published

Chapter 3

- 3.1 Accident Sequences Selected for Analysis
- 3.2 Containment Failure Modes, Failure Location, Event Times, and Leak Pathways

Chapter 4

- 4.1 Validity of Chemical Thermodynamic Calculations
- 4.2 Experimental Bases for Fission Product Release-from-Fuel Estimates
- 4.3 Experimental Observations of Iodine Chemical Form in Fuel
- 4.4 Model for Fission Product Release-from-Fuel
- 4.5 Description of Fission Product Release Mechanisms Incomplete

Chapter 5

- 5.1 Radiation Effects on Fission Product Chemistry
- 5.2 Tellurium Chemical Form in Vapor Phase
- 5.3 Data Base for High Temperature Chemical Thermodynamic Calculations
- 5.4 Volatility and Existence of HOI
- 5.5 Kinetics of Iodine Hydrolysis Reactions
- 5.6 Effects of Other Chemicals on Aqueous Iodine Chemistry
- 5.7 Chemical Form of Iodine in the Vapor Phase
- 5.8 Organic Iodide Formation Rates

Chapter 6

- 6.1 Fission Product Chemical Form Changes During Transport Not Considered
- 6.2 Aerosol Agglomeration in the Primary Coolant System
- 6.3 Nucleation of Aerosols and Timing of Releases from the Core
- 6.4 Interaction Between Molecular Iodine and Particulates

Chapter 7

- 7.1 Effects of Steam and Water on Fission Product Behavior
- 7.2 Aerosol Deposition in Containment Leakage Pathways
- 7.3 Fission Product Trapping in BWR Pressure Suppression Pools
- 7.4 Effect of Iodine Chemical Form on Iodine Attenuation within the Plant

scope of the Technical Bases Report to perform the types of consistent analyses that are most desirable. The results of these analyses for each separate area are examined, however, to determine the potential impact on other areas. For example, Chapter 7 discussions have been expanded to include the potential impact on containment transport caused by agglomeration in the primary system.

### 1.2 Conservative WASH-1400 Assumptions and Models Used

The methods of analysis used in WASH-1400 were overly conservative. The methods of analysis in the Technical Bases Report are the same as used in WASH-1400 without modification or qualification and the Technical Bases Report is therefore also overly conservative.

#### Authors' Response

CORRAL was the only code used in this study that was also used in WASH-1400. In order to examine the validity of the CORRAL analyses, a number of comparison calculations were made between the aerosol transport models in CORRAL and the mechanistic aerosol codes HAARM-3, QUICK, and NAUA. Fission product deposition in the primary system, which could not be evaluated in WASH-1400 because of a lack of applicable models, was examined using the TRAP and QUICK codes. Fission product release and aerosol production were examined using release rate data developed subsequent to WASH-1400. The thermal-hydraulic analyses that supported these investigations were performed with the MARCH computer code, which was also written following WASH-1400. Thus, much of the analyses in the Technical Bases Report represents significant extensions beyond WASH-1400 methodology. Further, these analyses were supported by a number of sensitivity studies.

In the examination of potential areas of conservatism in the WASH-1400 methods, the only area where strong evidence of conservatism was identified involves the retention of fission products in the primary system. Considering the state of the art, it is possible that, in the future, other aspects of the WASH-1400 methods may be found conservative (or nonconservative). Before these presumed areas of conservatism can be removed from the analysis of accident consequences, significant model development and verification will be required.

### 1.3 Uncertainties Associated with Estimates of Fission Product Release

Many commenters indicated that the range of uncertainties in the projections of fission product release from the plant should be provided. In addition, the range of uncertainty of each important assumption and code model should be described along with the impact of these uncertainties on the overall release from containment estimates. The conclusions in the Abstract of the draft report, which refer to the magnitude of potential release of radioactive material from the containment in severe accidents, do not adequately reflect the uncertainties associated with retention mechanisms.

### Authors' Response

We agree that quantification of the uncertainties in the predicted release from containments and the sources of these uncertainties are important information that is needed both for an assessment of the validity of the predictions and for defining future research directions. Results of uncertainty analyses for primary system transport and for containment transport are presented in Chapters 6 and 7. However, as discussed in Chapter 1 of the report, because of time constraints, it was not possible to undertake a systematic analysis of fission product transport from the fuel to the environment. In order to determine the relative importance of uncertainties in individual parameters, an evaluation of the potential range of uncertainties and a systematic propagation of these uncertainties through the analysis is required. As part of a follow-on study to this report, the NRC plans to conduct systematic uncertainty and sensitivity analysis of fission product release and transport behavior for a range of accident conditions and to develop a revised set of accident source terms with associated uncertainty estimates for these accidents. The limited uncertainty analyses and sensitivity studies that were done indicate that the uncertainties in the prediction of the radioactive material release to the environment are quite large. The conclusions in the Abstract are being modified to account for the magnitude of these uncertainties.

#### 1.4 Uncertainties in Thermal-Hydraulic Conditions

Uncertainties in the prediction of thermal-hydraulic conditions can have a major impact on fission product release estimates. This relationship should be better described in the report.

### Authors' Response

The MARCH computer code was used to predict the gross thermal-hydraulic behavior in the primary system and in the containment building during core meltdown. In order to obtain the degree of detail necessary for the calculation of fission product and aerosol release from the fuel and for the analysis of transport and deposition in the primary system, the results of the MARCH analyses were extended with hand calculations. The uncertainties in the prediction of time-dependent thermal-hydraulic conditions obtained with these methods are quite large. The effect of these uncertainties on fission product transport mechanisms can be significant, as demonstrated by analyses in Chapter 6. Thermal-hydraulic results can affect the release estimates to the environment not only by their direct influence on retention mechanisms but also indirectly by affecting the prediction of the timing or mode of containment failure.

It is apparent that the development of improved methods of thermal-hydraulic analysis should have high priority. Chapters 3, 4, 6, and 7 have been modified to emphasize the importance of thermal-hydraulic uncertainties.

#### 1.5 Assumptions In the Analyses

A large number of commenters indicated that a listing of the assumptions that are incorporated into the analyses is necessary in order for readers to

independently evaluate the adequacy and appropriateness of the calculations. In particular, a listing of the assumptions associated with input and models used in the computer code analysis performed in Chapters 5, 6, and 7 were judged to be necessary by many commenters.

#### Authors' Response

The chapter authors have developed and incorporated into their respective chapters (and appendices) detailed listings of those assumptions, code inputs, and models that they believe most influence the results of their analysis.

#### 1.6 Verification of the Computer Codes Used in the Analyses

Several commenters indicated that since computer code calculations constituted the majority of the analyses in Chapters 6 and 7 (and were important elsewhere), that the extent of validation of these codes and the experimental bases for the models in these codes be described.

#### Authors' Response

The only methods of analyses used in the report that have been subject to appreciable testing and verification are the aerosol transport codes HAARM-3 and QUICK. The fundamental processes in the NAUA-4 code can also be considered to be well established except for the steam condensation effect, which although verified at small-scale, should be compared with the results of larger scale experiments under more prototypic conditions. The CORRAL-2 code is based upon the results of the Containment System Experiments program but has not been compared with the results of experiments at different scale or geometry. Since more advanced codes are currently being developed and tested for calculating fission product transport in LWR containments, it is expected that the more advanced code rather than CORRAL-2 will be put through the verification process.

Plans for the verification of the TRAP code have been under development for a number of years. To date, only bench-scale and small-scale experiments have been performed. These experiments are more directed at model development than verification.

The MARCH code is also unverified. A series of cross-comparison calculations have been initiated with the German KESS code. Adequate data do not currently exist for the verification of many of the MARCH models.

#### 1.7 Past Reactor Accident Experience

Eight comments were received recommending that past-accident (and destructive test) fission product release experience be evaluated and compared with the conclusions in this report. The commenters generally indicated that the Technical Bases Report underestimates the value of information from past experience. Several commenters recommend that we evaluate the current fission product release and transport codes (e.g., TRAP-MELT, CORRAL, HAARM-3, etc.) against these accidents to judge whether the code predictions are in reasonable agreement with the observed consequences of these accidents and tests.

### Authors' Response

Because of the difficulty anticipated in the reconstruction and evaluation of accident data, it was felt that a review of past reactor accident experience would be beyond the scope of the Technical Bases Report. Instead, a research project is being initiated for this purpose.

Accident results can offer a unique opportunity to observe accidents under realistic conditions and possibly to identify mechanisms that had not been recognized in the development of models. The limitations of accident experience as it relates to the testing of severe accident analysis models must be recognized, however. The severe core damage accidents that are predicted to dominate risk are believed to be very rare events. With the exception of the Three Mile Island 2 accident, there have been no accidents in commercial light-water reactors that have even approached the conditions of a core meltdown accident. As a result, there are very little data from accident experience with direct relevance to the testing of core meltdown models. The inability to use accident data to test these models, however, does not imply that the emphasis on the development of models for low probability/high consequence core meltdown accidents has been misdirected.

Accidents in other types of reactors or of a different nature, such as reactivity accidents, may also be of very limited value in evaluating codes developed for LWR core meltdown accidents. The physical processes controlling under non-prototypic conditions could differ substantially. The other major drawback of accident experience is the integral nature and inaccuracy of the measured data. The verification of core meltdown models can definitely not rely on accident experience alone. Separate effects tests and highly instrumented integral experiments will be necessary to assure that the models have the required accuracy.

### 1.8 Future Research Needs Identified in Report

In general most of the comments received supported the research needs identified in the report.

#### List of Comments on Specific Research Needs

Specific research areas that were mentioned by commenters are listed below in decreasing order of the number of comments received.

<u>Information Needed</u>	<u>Number of Commenters</u>
Better thermal/hydraulic information	III
More information on high temperature fission product vapor phase chemistry (both thermodynamic and kinetic information)	III
Aerosol formation (self nucleation, vapor deposition, and agglomeration)	III
Effects of radiation on fission product chemistry	II

<u>Information Needed</u>	<u>Number of Commenters</u>
Effect of hydrogen deflagration on fission product chemical form	II
Better understanding of the chemistry of other fission products (besides Cs and I)	II
Large-scale integral experiments with prototypic fuel (in this area several commenters pointed out that large-scale experiments should always be supplemented with small-scale experiments to understand the underlying physical mechanisms)	II
More definitive information on transport pathways, containment failure modes, and timing of containment failure	II
Fission product decay chain effects	I
Effect of the chemical environment on expected fission product chemical form	I
Fission product interactions with prototypic surfaces	I
Deposition of fission products in the leak path through the failed containment	I
Leaching of fission products from the fuel	I
Aqueous iodine chemistry	I

#### Authors' Response

We have reviewed our summary list of research needs in Chapter 1 and have integrated the above recommendations into our list.

#### Specific Comment

The ACRS recommended that a list of research needs and a prioritization of these needs be prepared.

#### Authors' Response

This report presents a list of research data needs that were identified during preparation of this report. The authors also believe that prioritization of these data requirements is needed. However, the authors believe that prioritization of the data needs identified in this study should await completion of the detailed systematic uncertainty and sensitivity analyses that are planned for the near future as a continuation of the work initiated in this report.

#### 1.9 Report Should/Should Not Be Published

The vast majority of the commenters indicated that they thought that development of this report was a necessary and worthwhile effort and that the report was a good up-to-date summary of knowledge of fission product behavior under LWR accidents conditions. However, several commenters indicated they are not convinced that this report represents an accurate and realistic assessment of

accident consequences. A number of reviewers expressed concerns regarding various limitations in the report and suggested that the report either should not be issued at the current time (to allow for further review and input from outside groups), or if the report is issued, the preliminary nature of the report be pointed out. Several other commenters suggested we incorporate the comments we have received and issue the report now and specify a time when a revised document will be issued.

A number of commenters recommended that regulatory changes not be made at the current time based on this report.

### Authors' Response

The authors believe that in general, the assumptions, models, codes, and other analyses presented in this report represent the best information currently available for evaluating the behavior of fission products under LWR accident conditions.

The commenters identified a number of limitations and shortcomings in the analyses. In general, the authors believe that these limitations either are a result of limitations in our current understanding of the basic mechanisms of severe accident phenomena and fission product behavior or are a result of necessary limitations in the scope of the study. A number of the identified limitations will be addressed in near-term follow-on studies to this report (e.g., systematic analysis, analysis of past reactor experience). However, other identified limitations will require a longer term effort to resolve (e.g., containment failure timing, location, and mode; fission product attenuation in BWR suppression pools, etc.).

The authors believe that this report will help to focus attention on the important elements of, and the current limitations associated with, realistically (mechanistically) estimating fission product behavior during LWR accidents. Consequently, the author's believe the report should be issued as soon as possible in order to solicit review from a wide and diverse audience.

The NRC requests that persons having comments on the report or suggestions for improved methods of analysis in any of the areas addressed in this report should send their comments to the Director, Office of Nuclear Regulatory Research, USNRC. The NRC will review these comments and factor them into the follow-on studies as appropriate.

The question as to whether changes in any NRC regulatory procedures should be changed as a result of the findings in this report is outside the scope of this report. These issues are addressed in the "Regulatory Impact Report" that will be issued for public comment concurrently with the "Technical Bases Report."

## CHAPTER 3

### 3.1 Accident Sequences Selected for Analysis

A number of comments were received concerning the types and range of accidents considered in this report. Several commenters stated that the accident sequences that were selected for analysis are only important to the risk of some specific plant designs. In addition, there is disagreement about the course of accident sequences including success criteria for safety systems, event times, physical conditions, and failure modes. A number of commenters felt that insufficient attention was addressed at the less severe accidents and that the impression was given in the report that the low probability-high consequence accidents (which were subjected to detailed analysis in the report) would be typical of LWR accidents.

#### Authors' Response

Risk importance was only one of the criteria used in the selection of accident sequences. Sequences were chosen to cover a broad range of core damage, reactor coolant system conditions, containment building conditions, plant design features, and engineered safety feature performance.

Since one of the objectives of the report was to examine the realism of accident consequence predictions in previous risk studies, a number of the most important accident sequences in WASH-1400 were selected for analysis. These sequences would not necessarily be expected to be important risk contributors for all plant designs because both the likelihood and consequences of an accident sequence are design dependent. In general, however, a common characteristic of accident sequences that have been found to be major contributors to risk in these studies is that they involve not only complete fuel melting but impaired performance of the containment safety features as well. Some of the reviewers questioned the emphasis that has been placed on these very low probability accident sequences in this report. Not only are these sequences found to dominate the results of risk studies because of their predicted large consequences, they are also the focus of public concern in reactor accidents. Accidents in which the containment does not fail, in which containment failures are substantially delayed, or in which safety systems (e.g., sprays, pools, or filters) are effective in retaining the fission products and do not pose an immediate threat to the lives of members of the public.

The reader should recognize that the probabilities of accidents with potentially high consequences and low probabilities are difficult to predict using methods of reliability analysis. Because of the combinations of failures involved, the analyses frequently are dominated by very "soft" data such as assumptions about human behavior, common mode dependencies, or the interaction between the mode of containment failure and the subsequent performance of safety features. The assumptions made about these sequences are frequently easy to debate but difficult to resolve.

### 3.2 Containment Failure Modes, Failure Location, Event Times, and Leak Pathways

The report has not provided adequate consideration of containment failure modes, failure location, event times, leak pathways, and the uncertainties in these parameters as they affect fission product release to the environment.

#### Authors' Response

Uncertainties in the prediction of fission product release from the containment arise not only in the treatment of fission product retention mechanisms, but also from other aspects of accident analysis. The importance of uncertainties in thermal-hydraulic analyses was discussed in a previous comment. Another very important contributor to uncertainties is the prediction of containment failure modes and pathways of release to the environment. The time of containment failure in relationship to the time of fission product release from the fuel can have a particularly large effect on accident consequences. Reactor containment buildings are designed to include significant safety margins. The conditions of pressure and temperature, beyond design, at which the various containment designs would be expected to fail have not been well established. Even less information is available to predict the mode of containment failure. Because of these uncertainties, assumptions are frequently made about containment failure modes in risk analyses which may be conservative (for example, that the hole size in containment is large and in an unfavorable location). Additional analysis and experimentation should help to reduce uncertainties in the prediction of containment failure modes and release pathways. However, some uncertainties, particularly those related to quality of workmanship, design weakness, and construction flaws, will be very difficult to reduce to a level that would enable the mode of failure to be predicted with confidence. A discussion of uncertainties in the prediction of containment failure modes and release pathways has been added to Chapter 3.

## CHAPTER 4

### 4.1 Validity of Chemical Thermodynamic Calculations (Fission Product Form in Fuel)

A number of reviewers commented on the appropriateness of using chemical thermodynamics for determining the chemical form of iodine in fuel and released from overheated fuel. There were several comments on both sides; i.e., both pro and con.

#### Authors' Response

In examining this set of comments, we find that those who advocate the appropriateness of chemical thermodynamics for this purpose, and who consequently place large weight in its predictions, have not satisfactorily addressed the question of the inherent uncertainties of this approach. The principal uncertainty in our view is specification of the phases present in fuel in the 1400 to 2000°C temperature range where a major portion of iodine evolution occurs. Other inherent uncertainties of this approach are cited in the report and in some of the review comments. We therefore feel that the manner in

which this evidence was handled in the report was proper. Briefly, this was as follows: (1) results of a thermodynamic analysis reported in the literature were cited, (2) the inherent limitations were cited, and (3) we concluded that these calculated results could not be afforded great significance without further supporting work.

#### 4.2 Experimental Bases for Fission Product Release from Fuel Estimates

A number of review comments stated that our selection of (only) three fission product release experiments to form the basis of the developed release rate estimates was not proper for several reasons. The principal objection apparently was that these three selected experiments were small scale and so do not properly reflect releases from a larger mass of fuel element material. Another comment reflected doubt in the validity of the result in view of the large range in estimated release rate coefficients.

##### Authors' Response

The original draft of Chapter 4 contained a summary of approximately a dozen major fission release-from-fuel experiments. Excluded in this survey were those experiments dealing solely with noble gas release and those that relate to in-reactor leakage, such as iodine spiking experiments. This survey illustrated to us that all the major release rate experiments have one or more significant limitations. In addition, we found no duplication, therefore, direct comparisons between the various experiments could (and should) not be made. Contributing to the variety were different fuel samples (real discharged fuel, pure  $UO_2$  with added fission product simulants, trace-irradiated chunks, clad and unclad, powdered), different atmospheres (steam, helium, air, carbon dioxide, argon, liquid water), different temperature ranges, plus other experimental differences, e.g., different materials of construction and analytical methods.

In this circumstance, some judgment had to be used to meet the objective of obtaining an interim release rate estimate. In this regard, the following aspects were taken into consideration: (1) We selected Lorenz's experimental series because it employed real, discharged LWR fuel rod segments under generally well set up test conditions. However, it was limited in temperature ( $T < 1600^\circ C$ ) and scope of monitored fission products. (2) To expand the number of fission product types, we employed the SASCHA (air and steam) tests and two early Parker experiments, although both admittedly possessed some drawbacks. (3) We did not choose to include the large scale, PBF tests because their complexity required a degree of effort with respect to data evaluation, which was beyond the scope of this report.

The large variations observed in release rate coefficients from the various experiments are believed due mainly to the different experimental conditions. In one case (Lorenz), a large variation was observed in one test series. In this case, the large range in reported release rate coefficients for cesium and iodine are due mainly to our application of a simple release model to a case where factors are important (i.e., grain boundary release) that do not lend themselves readily to description via the first order release rate model.

### 4.3 Experimental Observations of Iodine Chemical Form in Fuel

A number of reviewers commented on the degree to which the cited experimental evidence proves or disproves the contention that the chemical forms of iodine released from the fuel is cesium iodide. Some presumed the evidence was conclusive while others expressed doubt.

#### Authors' Response

On this important point it is perhaps best to list these comments verbatim. "The question of whether cesium iodide is released from heating various fuels at high temperatures (over 1000°C) is a dicey issue. As discussed in Chapter 4, some experiments would suggest that this is the case; all others do not bear out his conclusion. Of course, at the heart of the issue is the fact that the form of the released iodine will be a sensitive function of concentration and temperature, as well as perhaps kinetics. However, I think the kinetic issue is a less serious one because the reactions should be rather fast at the high temperatures. Nevertheless, if the cesium and iodine are bound in other forms, even if cesium iodide is the more stable product, the interconversion to this species could perhaps under some conditions be rate limited. At high temperatures the dissociation pressure of cesium iodide is rather appreciable and, therefore, the concentration dependence becomes an important consideration.... In the abstract... I think I would tend to rephrase it that there is some evidence that cesium iodide will be a predominant form of iodine."

(A. W. Castleman, Jr.)

"...the abstract is not an adequate summary of what is contained in the report. For example, the conclusion on p. (i) that cesium iodide is the expected predominant iodine form is stronger than the conclusions in Paragraph 4.5, which states that the results of several experiments are inconclusive or even contradictory while, in the experiments of Lorenz, et al., which provide the best available evidence for the presence of CsI, in tests using steam, the percent of iodine identified as cesium iodide ranged from 4 to 90% with the balance as the molecular specie and on particulates. Several reasons for low cesium iodide release fractions in some of the steam runs are speculated but not proven."

(Saul Levine)

"Although cesium iodide may be an important specie during accidents, other iodides and elemental iodine may also be present. The evidences for cesium iodide dominance over other iodides are not clearly demonstrated."

(L. Devell)

"As was pointed out at the meeting by, for example, Malinauskas, a stronger recommendation on the release of iodine as cesium iodide seem justified. The weight of the evidence now points strongly to cesium iodide as the major chemical form of iodine."

(J. B. Ainscough)

"Equal weights are being placed on experiments involving very low levels and higher levels of iodine in flowing gas.... Of the 17 experiments on iodine release presented in Table 4.3 as part of the data base, 8 involved less than 20 micrograms of iodine each.

Some of these experiments involved flowing gas atmospheres for as long as 20 hours. If one assumes the following as a typical experiment

2.54 cm diameter reaction tube  
 1 atmosphere pressure for steam  
 100 cm/min flow rate  
 1 hour duration for experiment  
 10 micrograms of iodine  
 900°C

it can be calculated that the  $O_2$  in the steam must be less than 0.1 ppm by weight to avoid converting all of the CsI to iodine (CsI very likely will have been vaporized from the fuel sample and condensed on the apparatus wall). The use of sufficiently pure gas is unlikely. Therefore, at least half of the data should be discarded. Indeed if one considers that data of Table 4.3 involving more than 100 micrograms of iodine the percent released as  $I_2$  is always less than 1%. For iodine levels less than 100 micrograms the iodine releases as  $I_2$  are always greater than 1% rising to as high as 88%."

(R. C. Vogel)

"Additional evidence on the state of fission products in the fuel rod gap space may be ascertained from fission product spiking data. Westinghouse has published WCAP-9588, "Fission Product Spiking," which shows that iodines and cesiums in the gap space are in a water soluble form while other nongaseous fission products appear to be in a nonwater soluble form. The results of Lorenz, et al., indicate that the oxygen potential in experiments must be known in order to allow interpretation of out-of-reactor experiments."

(T. M. Anderson)

"The large number of variables in Lorenz's experiments make it difficult to reach definite conclusions about the reaction effects between the quartz furnace tube liner and fuel-rod holder on the release of free iodine. In HBU-1 and HBU-4, it is clear that most of the free iodine came from the fuel rod since the Cs/I ratio is low.

From data in NUREG/CR-0722, it is clear that the cesium reacted with the quartz liner, but the fraction reacting decreases with increasing temperature and decreasing time. This is probably a combination of increased kinetics and decreased stability of  $Cs_2SiO_3$  with temperature. In spite of the impression that large amounts of free iodine are released (column 7), it is seen that these large percentages only occur for small total release. The total free iodine for all experiments is ~0.6% of the total iodine released. Some of the free iodine could come from the reaction of CsI with quartz and some may have come from the reaction of steam with CsI to form HI. The total flow of gas

through the quartz furnace tube is too large for any of the cesium gases (Cs, CsI, CsOH) to condense. Thus, any cesium found in the quartz tube and holder must have reacted with the quartz.

Page 4.30. The conclusions put too much weight on the free iodine release of very small releases (most of these between  $10^{-7}$  and  $2 \times 10^{-5}$  g I). The total free iodine release from the steam experiments is 1.2% of the total iodine release. Some of this release is caused by the quartz reaction with CsI."

(P. E. Blackburn)

"Returning to the question already touched upon in the general comments of the chemical form and release of iodine and cesium, the basic arguments for support of the existence of cesium iodide are made from thermodynamic considerations. The application of these results to the conditions likely to prevail during an accident would presume a quasi-steady-state in the fuel chemistry, since thermodynamics is involved with chemical equilibria and not reaction kinetics. The actual state of the system cannot be established without consideration of the reaction kinetics. In this context, the effect of the radiation environment needs some consideration, since the photochemical reactions may favor the dissociation reactions.

As has already been mentioned in the foregoing, it is felt that the experimental evidence given in Table 4.3 for the existence of CsI as the dominant form of the iodine species is inconclusive. Interestingly enough, however, there appears to be a strong correlation between the fractional release 'presumably as CsI' and the test duration, when steam was used. The attached table presents a resumé of tests to illustrate this point. There seems to be a tendency for the fraction released 'presumably as CsI' to increase with increasing test temperature. These general effects remain to be adequately explained, as well as their implications with respect to the ultimate fate of radioiodine during an accident sequence."

(Saul Levine)

#### Authors' Response

As indicated by the reviewer comments as well as the Chapter 4 text, an appreciable degree of uncertainty exists regarding the chemical form of iodine released from the fuel. We disagree with those reviewers who seem solidly assured that the released form is clearly shown to be cesium iodide. The major pieces of evidences are the following:

1. Chemical thermodynamic calculations predict the main chemical form on the fuel to be cesium iodide. However, the proper degree of force to place on these results is open to question.
2. Lorenz's "Gap Purge" tests clearly show the released form to be CsI, but these tests were conducted below  $1200^{\circ}\text{C}$  and so released only the gap and open porosity inventory. This amounts to  $\sim 0.5\%$  and  $\sim 8\%$  of the tested PWR and BWR fuel rod segment inventories of iodine, respectively.

3. Lorenz's steam tests show a range of exit iodine compositions, from 4 to 90% as presumably CsI, from 0.1 to 88% as mainly I<sub>2</sub>, and from 6 to 58% on particulates. As several reviewers noted, there are trends in this experimental series with the mass of the total release and the test duration, and also the possibilities of reaction with vessel materials, sweep gas impurities or the sweep gas itself (steam). Therefore, firm conclusions regarding chemical forms based on this experimental series seems inappropriate.
4. This approximate equality of cesium and iodine release rates with that of xenon casts some doubt that the released species is CsI. Particularly we note that cesium, iodine, and xenon release rates were observed to be approximately equal above 1400°C in Lorenz's tests. If the major released form of iodine was CsI, with a normal boiling point of 1280°C, we feel it should have shown up as a noticeable lower (than xenon) release at this point.

Therefore, it is felt that the conclusions presented in Chapter 4 regarding this question, show the appropriate degree of uncertainty. In addition, we feel the summary section in Chapter 1 and the abstract now properly reflects this uncertainty regarding the chemical form of iodine as released from the fuel.

#### 4.4 Model for Fission Product Release from Fuel

The model proposed for fission product release from fuel is quite primitive, therefore of doubtful validity or value.

##### Authors' Response

Available models for fission product release from fuel are either limited to noble gas release or restricted to low temperatures (<1400°C) and therefore not suitable for the purpose intended in Chapter 4. What was needed here was a means for comparing diverse release experiments on a common basis for a range of fission products up to fuel melt temperatures.

#### 4.5 Description of Fission Product Release Mechanisms Incomplete

The fission product release-from-fuel mechanisms cited in Chapter 4 inadequately describe the complex processes that contribute to release.

##### Authors' Response

We agree with this assertion. No attempt was made to provide a comprehensive discourse in release mechanisms. Indeed, except for noble gases, such a discussion would be highly speculative. Required was some recognition that various processes do contribute to transport in the fuel, and that one or more mechanisms may predominate depending on the temperature, temperature ramp rate, atmosphere, etc. Such recognition was necessary when attempting to compare the various experiments in a logical way. One reviewer pointed out that one cited mechanism termed "grain boundary release" is actually composed

of a number of contributory phenomena including grain boundary growth, bubble growth and coalescence, and grain cracking. For our purpose, it sufficed to group these under the cited overall category.

## CHAPTER 5

### 5.1 Effects of Radiation on Iodine Aqueous Chemistry

An iodide,  $I^-$ , source dissolved into LWR water will remain as the nonvolatile iodide species unless the oxidation potential is such that oxidation occurs. An iodine,  $I_2$ , source in LWR accident quantities will react with water, and at equilibrium essentially all of that source will have been converted to nonvolatile iodide and iodate species. What will be the effects of LWR accident radiation on those aqueous systems? Will the oxidation potential be changed by radiation such that volatile iodine species will be formed?

#### Author's Response

Chapter 5.3 and Appendix C.8 clearly state that the immediate effect of radiation on an LWR accident aqueous system will be the well-known effects of radiation on water. The question then becomes, what will be the effects of water radiolysis products on the iodide and iodate species? The water radiolysis products and the relative amounts are given in Equation C.8.1. Water in an LWR accident will have many impurities that will significantly scavenge the water radiolysis products before they can interact with the iodine species. However, the extent of scavenging could be only approximated and the iodine species interacting with the water radiolysis products deserve consideration. The oxidizing radical,  $\cdot OH$ , would react rapidly with appreciable concentrations of iodide to form I atoms and hence molecular  $I_2$ . However, the water radiolysis products include an equivalent or greater number of reducing agents ( $e^-$ ,  $H\cdot$ ,  $H_2O_2$ ,  $H$ ) that could reduce iodine species to iodide,  $I^-$ . At the same time any atomic or molecular iodine would also tend to react with water as discussed in Chapter 5.3.5. From these considerations the  $I_2$  molecule is the least stable iodine species in an LWR aqueous system in a radiation field.

### 5.2 Tellurium Chemical Form in Vapor Phase

Reservations were expressed by some reviewers concerning the statement that  $TeO_2$  would be the predominant form of Te in high temperature steam environments.

#### Authors' Response

Their concern was also shared by the authors. Correcting an error in the input data to the chemical thermodynamics code changed this conclusion for species in reducing atmospheres and the Te-H-O section was rewritten.

### 5.3 Data Base for High Temperature Chemical Thermodynamic Calculations

A number of comments were made on the data used to perform the high temperature equilibrium thermodynamic calculation on vapor phase fission product chemistry.

### Authors' Response

Differing thermodynamic data bases will have their greatest impact whenever several species are of comparable stability. In that case, even a relatively small difference may result in a large concentration swing. On the other hand, if there is only one very stable species, then even large differences in the data base can have a minimal affect on the calculations.

For the Cs-I-H-O system calculations, the data used for CsI was that of Baren, et al. (5.2) Other, later data was subsequently obtained (5.6); these data are considered to be a better set. These sets of data differ most at lower temperatures but approach one another at high temperatures. Calculations using the later data were made for a limited set of conditions but not for the full range of system parameters. Comparisons of the two calculational sets indicate minimal change in composition at low temperatures. The effect at high temperatures is a persistence of CsI stability to temperature 50°-150°C higher than first calculated. The onset of CsI dissociation may be experimentally difficult to detect to a better degree of precision.

### 5.4 Volatility and Existence of HOI

The existence of HOI and how it affects iodine partition coefficients is not well established. What are the probable answers to these questions?

### Authors' Response

There is little doubt that HOI can exist in aqueous solutions when conditions favor HOI. Aqueous systems at equilibrium in an LWR accident will have insignificant quantities of HOI. However, there may be preequilibrium conditions such that the HOI concentration could be as much as 50% of the total iodine concentration. The primary concern then is with regard to the HOI partition coefficient. The partition coefficient, PC (the concentration in the aqueous phase divided by the concentration in the gas phase), certainly favors the liquid phase. In Chapter 5.3 the magnitude of the partition coefficient (166) was conservatively set at two times that for the molecular I<sub>2</sub> species. However, the HOI coefficient probably is much greater and could easily be as great as 10<sup>3</sup>. A partition coefficient of 10<sup>3</sup> would imply that the concentration of HOI in a gas phase above an aqueous solution in an LWR accident is insignificant even at times before the aqueous solution equilibrates. Even though this has not been absolutely proven, some recent excellent work using very sensitive analytical procedures could not detect HOI above aqueous solutions at conditions favoring HOI [R. J. Lemire, D. J. Paquette, D. F. Torgerson, D. J. Wren, and J. W. Fletcher, Whiteshell Nuclear Research Establishment, AECL-6812 (1981), also private communication with D. F. Torgerson].

### 5.5 Kinetics of Iodine Hydrolysis Reactions

How does the difference in the kinetics of reactions 5.1 and 5.4 affect the total iodine partition coefficient?



### Authors' Response

Reaction 5.1 approaches equilibrium at a faster rate than that for 5.4. Therefore, the amount of HOI at short times may be considerably greater than the equilibrium concentration of HOI, and at those times the concentration of HOI in the gas phase would be proportionately higher. The extreme case for this situation would be when reaction 5.1 essentially reaches equilibrium before reaction 5.4 begins. This extreme situation is discussed in the text and the corresponding total iodine partition coefficients are given in figure 5.5 with an assumption that the HOI partition coefficient is two times that of  $\text{I}_2$  (see 5.4 above). If the HOI partition coefficient is ten times that of  $\text{I}_2$ , as suggested above, the total iodine partition coefficients as given in figure 5.5 should level out at about 1660 rather than near 330. On the other hand, the coefficients for solutions at equilibrium, figure 5.4, would hardly change because the equilibrium solutions contain insignificant amounts of HOI.

### 5.6 Effects of Other Chemicals on Aqueous Iodine Chemistry

The distribution of a given amount of iodine into the various iodine species in an aqueous solution will depend on the redox potential of the solution. What will be the effects of the redox potential being controlled by chemicals other than iodine?

### Authors' Response

Probably the greatest uncertainty is the effect of hydrogen and oxygen on the aqueous iodine chemistry. The real effects can be addressed as introduced in Appendix C.5. There the oxidation of iodide,  $\text{I}^-$ , to molecular iodine,  $\text{I}_2$ , and on to iodate,  $\text{IO}_3^-$ , was shown. Similar information can be generated for the effects of hydrogen or other chemicals by proper utilization of redox potentials given in reference 5.16. However, the kinetics of such reactions are not well known and a time frame could not be estimated.

### 5.7 Chemical Form of Iodine in the Vapor Phase

Comments from reviewers on the subject of the chemical form of iodine ranged from (a) strong evidence was presented, to (b) weak evidence was presented for the existence of  $\text{CsI}$ . In comments on high temperature chemistry, several reviewers observed that effects such as chemical kinetics, radiation, the presence of other fission products, deflagration, and surface reactions could influence the form of iodine (as well as the form of other fission product species) during transport through the reactor.

### Authors' Response

Most reviewers agreed with the authors that very little data exists to describe the influence of these effects on the possible forms of iodine, especially in

high temperature steam environments. An additional point can be made on the stability of CsI in reactor environments. Available evidence indicates CsI is more stable than other iodides that could be formed from the reaction of iodine with reactor materials such as iron, uranium, zirconium, nickel, and chromium. Also as mentioned in the text, the presence of other fission products could influence the form of iodine, but experimental data in steam are lacking and no thermodynamic data was found for compounds of two fission products - with the exception of CsI. Therefore, according to the results of the equilibrium chemical thermodynamic calculations in the vapor state, CsI will be stable if released as CsI from the fuel into a reducing steam atmosphere. In addition, it is probable that CsI vapor would be produced if cesium and iodine were simultaneously, but separately, released from the fuel. However, additional effects, including those mentioned above, may well determine the ultimate form of iodine during transport through the system.

### 5.8 Organic Iodide Formation Rates

Organic iodide will form by the reaction of molecular iodine with organics such as methane and lubricants. What is a reasonable rate of organic iodide buildup after an LWR accident?

Answer: At this time there is no decision on the amount of organic iodide that could be expected in an LWR accident, and an estimate of a rate of formation is therefore unrealistic. However, Chapter 5.3, Section 5.3.9, and Appendix C.9 suggest that 0.03% of the iodine that exists as atomic or molecular iodine,  $I_2$ , would be converted to organic iodide. We have no basis for estimating the time required for the small amount of molecular  $I_2$  to be converted to organic iodide under LWR accident conditions. Good and applicable experiments are needed.

## CHAPTER 6

### 6.1 Fission Product Chemical Form Changes During Transport Not Considered

Changes in fission product chemical form, due to chemical reactions during release and transport through the plant and as a result of radioactive decay are not modeled.

#### Authors' Response

Such changes are not directly modeled in the TRAP code, and this does represent a potential shortcoming in the analyses since some fission products may transport through the primary system as different species at various points along their path. Thus, different removal mechanisms can be operative at different points in the RCS. This deficiency of the code does not significantly influence the results presented in Chapter 6 since (1) the attainment of chemical equilibrium in the Cs-I-H-O system is believed to be rapid with respect to the removal processes operative, (2) the principal removal mechanism, condensation, is effective only for CsI, and (3) condensation of CsI does not become important until lower temperatures are encountered in the system - temperatures low enough so that nearly all of the iodine is predicted to be CsI.

If there were a removal mechanism at high temperatures that affected one form of a fission product, and another mechanism for removal at low temperatures that affected a form of the fission product present only at the low temperatures, the situation would not be so clear. In such a case, the TRAP code would require modification by inclusion of artificial sink and source terms for the species involved, for each volume in the system. In this way, one can account for changes from one chemical form to another.

## 6.2 Aerosol Agglomeration in the Primary Coolant System

Aerosol agglomeration in the primary system is not considered.

### Authors' Response

Agglomeration is not considered in the TRAP analyses presented in Chapter 6, and this would represent a serious shortcoming of the study if only these TRAP analyses were used to examine fission product behavior in the primary system. As is now pointed out in Section 6.3.2.2.1 and in Appendix D, coagulation has been examined separately to assess its importance and influence on the aerosol. (The present structure of the TRAP code renders it unsuitable for handling the high aerosol concentrations predicted for certain accident sequences.) As indicated in Chapter 6, it is clear that for certain accident sequences (those with very low flow rates) agglomeration should be a major contributor to particle retention in the primary system. For these accidents, only a very small percentage of the aerosol mass is expected to escape the core region during the time from melt initiation to vessel failure.

The analyses of agglomeration performed also makes it clear that for accident sequences characterized by higher flow rates, this mechanism has little if any effect because of the short residence time and lower aerosol concentration involved. The inclusion of agglomeration in the TRAP code is desirable, and efforts are currently underway to accomplish this goal. But the results from such a model should not differ significantly from those arrived at using the TRAP code supplemented by QUICK code analyses as presented in this report.

## 6.3 Nucleation of Aerosals and Timing of Releases from the Core

The timing of release from the core may be improperly accounted for, and nucleation of particles in the primary system is not considered in the model.

### Authors' Response

These items are interrelated and both are potentially important in determining the nature of fission product transport in the primary system. The draft version of Chapter 6 has been improved by including further discussion of these items in Section 6.2. The discussion in that section will not be repeated here, but the author does wish to emphasize that the approach to these two items used in the TRAP analyses contains no assumptions that are inconsistent with our current limited understanding of aerosol (and gaseous fission product) behavior in the vicinity of the molten core.

#### 6.4 Interactions Between Molecular Iodine and Particulates

The interaction of molecular iodine with the aerosol particles is not considered in the primary system analyses.

##### Authors' Response

This is true, but the author does not believe that omission of this potential mechanism for iodine removal from the gas stream has any significant impact on the results presented in Chapter 6. The analyses presented in Chapter 5 indicate  $I_2$  to be a much less prevalent species than CsI for all conditions of interest in the primary system. Also, the experimental evidence cited by reviewers indicates adsorption on particles of only a few percent of the  $I_2$  in experiments. For these reasons, the adsorption of molecular iodine on particles is expected to have little, if any, influence on iodine retention in the primary system.

It should be pointed out that chemical adsorption of  $I_2$  on the surface of the primary system is included in the TRAP analyses, based on empirical data. Mechanistic adsorption data are not available for surfaces such as those of the aerosol particles originating from the molten core. If such data become available, the process can be included in TRAP, but it is not anticipated that a significant change in the code predictions will result from inclusion of this process.

### CHAPTER 7

#### 7.1 Effects of Steam and Water on Fission Product Behavior

The containment cannot be considered dry because of the large amounts of steam and water expected to be present following blowdown of the primary system. The effects of such water were ignored, were analyzed insufficiently, or because of inadequate thermal-hydraulic predictions, were not treated properly.

##### Authors' Response

As noted in the text, it is well recognized that the containment building will contain considerable amounts of steam and water. The extent of condensation in the containment atmosphere will be dependent on the specific accident sequence being considered. The dry aerosol codes (HAARM-3, QUICK) were used for several cases where condensation in the containment is not predicted to be a major factor and also to serve as a baseline for evaluating the effects of condensation in these cases through comparisons with other codes that do account for condensation. The CORRAL-2 code is based empirically on CSE experiments in which condensation was occurring and therefore inherently treats condensing conditions. The NAUA code mechanistically considers condensation onto aerosol particles as one particle growth mechanism and was run using MARCH code calculations for the TMLB sequence. The MARCH code is generally believed to provide the best available predictions of condensation in the containment. Sequences other than those considered in the report may indicate greater effects of water and condensation but the results presented preclude one from generalizing that the effects are always significant for all sequences.

## 7.2 Aerosol Deposition in Containment Leakage Pathways

Insufficient allowance was made for aerosol attenuation along leak paths through containment building walls or for plugging of these pathways by depositing aerosols. Uncertainties in analyzing such processes and needs for further work should be identified.

### Authors' Response

It is recognized that aerosols will be attenuated and will plug leak paths of considerable diameter depending on the nature of the aerosol particles. At issue in this case is not so much whether attenuation or plugging could be calculated given specified leak path characteristics, but rather, whether leak path characteristics could be specified sufficiently to make such attenuation or plugging calculations meaningful. For sequences assuming no containment failure, design leak rates could have been used although the Markiven full-scale containment experiments indicated that leakage was increased after blowdown. Because of gross uncertainties associated with failure modes, it was decided that to account for attenuation along leak paths would be an excessively speculative process.

## 7.3 Fission Product Trapping in BWR Pressure Suppression Pools

The effectiveness of suppression pools in the retention of fission products has not been recognized adequately in the analyses presented.

### Authors' Response

It was not possible to include a mechanistic analysis of suppression pool decontamination in the analyses in Chapter 7 because of limitations in the containment transport codes. In the CORRAL-2 code, decontamination in the pool is treated with an input decontamination factor. Models for vapor and aerosol deposition in bubbles rising in a suppression pool are presented in Appendix F. The amount of retention expected is quite sensitive to the fraction of noncondensable gases entering the pool as well as to other parameters that vary during the progress of an accident. Thus, significant modeling changes would be required to predict suppression pool behavior mechanistically. In the analyses in Chapter 7, decontamination factors were therefore treated parametrically.

There are some data available for the validation of a suppression pool model (a number of references were provided to this study by the General Electric Company that are identified in Appendix E). Much less data are available on aerosol behavior than for the transport behavior of elemental iodine. The parametric treatment of decontamination factors in Chapter 7 did not differentiate between aerosol behavior and elemental iodine behavior in the pool. However, the reader should not infer from the similarity of results of the analyses performed for the two chemical forms that the physicochemical form of iodine would not significantly affect the release to the environment.

A few comments should also be made regarding the cases analyzed for which the suppression pool was saturated at the time of release from the fuel. A range of decontamination factors from 1 to 10 was used in these analyses. Potentially larger decontamination factors would be possible in a saturated pool for iodine either in the form of vapor or aerosol. For the specific cases analyzed (all involving the Mark I design), however, the containment was predicted to fail in the region of the suppression pool. There was, as a result, significant uncertainty about whether there would be adequate water in the suppression pool to provide for effective decontamination.

In response to comments by the reviewers, the range of decontamination factors covered in the analyses in Chapter 7 was increased. Discussion of decontamination factors was also expanded in Appendix E and Chapter 7.

#### 7.4 Effect of Iodine Chemical Form on Iodine Attenuation Within the Plant

Why is the release from the containment for CsI predicted to be as high or higher than that predicted for  $I_2$  when the volatility of CsI is so much lower and its solubility in water so much higher than  $I_2$ ?

##### Authors' Response

Because of its lower volatility, CsI is expected to condense onto particles or ions or at other nucleation sites in the gas phase either in the primary system or in the containment. Some desposition on surfaces and dissolving in water is expected to occur, but saturation will be achieved within the RCS or as the primary emissions enter the containment giving rise to condensation of CsI into a particulate form. The deposition rates are therefore diminished dramatically since particle diffusivities are several orders of magnitude lower than vapor diffusivities. Particulate material can grow by condensation or by agglomeration to achieve sizes that will settle more rapidly. It is evident that the relative deposition rates for CsI are dependent on aerosol processes such as agglomeration and sedimentation whereas  $I_2$  deposition is dependent on  $I_2$  vapor diffusion and solubility. Volatility is only of significance then in determining physical form, and solubility is only of significance in vapor deposition processes.





UNITED STATES  
NUCLEAR REGULATORY COMMISSION  
ADVISORY COMMITTEE ON REACTOR SAFEGUARDS  
WASHINGTON, D. C. 20555

March 17, 1981

Honorable Joseph M. Hendrie  
Chairman  
U. S. Nuclear Regulatory Commission  
Washington, DC 20555

SUBJECT: COMMENTS ON FISSION PRODUCT BEHAVIOR DURING LWR ACCIDENTS

Dear Dr. Hendrie:

During its 251st meeting, March 12-14, 1981, the Advisory Committee on Reactor Safeguards met with members of the NRC Staff and its contractors to continue our review of the draft report, NUREG-0772 on the "Technical Bases for Estimating Fission Product Behavior During LWR Accidents," dated March 6, 1981. This was also the subject of a meeting of the ACRS Subcommittee on Reactor Radiological Effects on March 10 and 11, 1981. Earlier Committee comments on this effort were provided to Chairman Ahearne on February 11, 1981.

On the basis of these latest meetings, which included a review of the initial draft report being prepared under guidance of the NRC Staff, we offer the following comments:

1. The NRC Staff and its contractors have prepared a comprehensive document in a short period of time. The report provides a good up-to-date summary of knowledge on potential fission product releases under a range of postulated accidents.
2. We believe the report does not contain data or information that would justify changing current regulatory criteria at this time. Although regulatory changes may ultimately prove to be warranted, they should be made only after the report has been completed and has been carefully evaluated.
3. While pointing out what is known, the report also identifies what is not known. As such, it represents a useful resource for planning future research on this subject. Such planning should include preparation of a list of research needs and a designation of the priority with which each should be addressed.
4. Specific research areas brought out by the report as requiring attention include the development of a better understanding of:

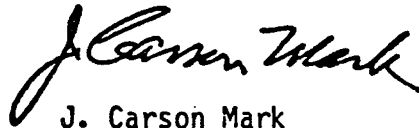
- a. The impact on the behavior of the fission products of various thermal-hydraulic and material transport processes accompanying severe accident sequences.
  - b. The impact of intense radiation on the physical and chemical behavior of fission products within a post-accident environment as well as the effects of radioactive decay on the transport of radioactive fission products.
  - c. The effect on fission product behavior of the presence of hydrogen gas, boric acid and other chemicals. Also to be considered is the potential effect of a hydrogen deflagration on fission product behavior.
  - d. Other key factors governing the behavior of the significant fission products so that their movements and releases can be adequately predicted. This effort should not be confined to iodine and cesium.
5. Inasmuch as the use of computer code models (TRAP-MELT, CORRAL, MARCH, etc.) plays a major role in assessing the risks associated with various accidents, it is important that work be continued on improving such codes. This should include developing a better understanding of the soundness of the basic assumptions used in their preparation and in the identification of the range of uncertainties in the projections they produce. Independent review and evaluation of these computer models would also be warranted.
  6. Considerable attention has been directed to possible changes in our concepts of the chemistry of the source term fission products. Comparable attention, however, does not appear to have been directed to the influence of the chemical properties of the fission products on the performance of systems for their removal, on their behavior within the environment, or on their associated health impacts.
  7. The draft report contains a number of assumptions on the behavior of various fission products. In some cases, for example, steady states were assumed when dynamic situations will more probably exist. In many cases, extrapolations were made from the behavior of chemicals in macroconcentrations to that at trace levels; in other cases, data from bench scale experiments have been extrapolated to estimates of conditions in full scale plants. The Committee recommends that the final report include a summary of such assumptions and the associated uncertainties they introduce.

March 17, 1981

8. In reviewing plans for the development of the report, the Committee understood that the effort was to include a review and evaluation of past accident experience. We have noted, however, that the draft report does not include this information. Because of the benefits it might provide, we recommend that consideration be given to conducting such a review.

The Committee reiterates its view that development of the technical report has been a worthwhile effort. We believe, however, that issuance of the draft report, NUREG-0771 on the "Regulatory Impact of Nuclear Reactor Accident Source Term Assumptions," dated March 1981 should be delayed until the data developed in the technical report can be thoroughly reviewed and evaluated.

Sincerely,

A handwritten signature in black ink, reading "J. Carson Mark". The signature is written in a cursive style with a large, sweeping initial "J".

J. Carson Mark  
Chairman



## APPENDIX F

## ATTACHMENT 2

March 17-18, 1981 Attendance  
Special Peer Review Meeting on "Technical Bases" Report

Name	Affiliation	Name	Affiliation
C. N. Kelber	NRC-RES (17th only)	J. T. Bell	ORNL (17th only)
M. Silberberg	NRC-RES	T. S. Kress	ORNL
R. Sherry	NRC-RES	W. F. Pasedag	NRC
R. C. Vogel	EPRI	A. K. Postma	NRC
B. Washburn	DOE	B. D. Liaw	NRC/OCM
D. Schweitzer	BNL	D. W. Pyatt	NRC/SD
A. P. Malinauskas	ORNL (17th only)	R. M. Elrock	Sandia
D. O. Campbell	ORNL (17th only)	R. A. Sallach	Sandia
W. R. Stratton	LANL	R. P. Wichner	ORNL
L. Devell	STUDSVIK SWE	J. A. Gieseke	BCL
C. Devillers	CEA-France	M. R. Kuhlman	Battelle
J. B. Ainscough	UKAEA-UK	K. W. Lee	Battelle
D. F. Torgerson	AECL-Canada	R. R. Hobbins	EG&G Idaho
C. E. Johnson	ANL	A. Spano	NRC-RES (17th only)
R. K. Hilliard	HEDL	Jacques Read	NRC-NRR (17th only)
R. M. Wallace	SRL	John Long	NRC-NRR
David Garvin	NBS	M. A. Cunningham	NRC-RES
Lloyd R. Zumwalt	NCSU	Joanne Dann	McGraw-Hill (17th only)
D. Walker	W-OPS	T. J. Walker	NRC-RES
Paul Blackburn	ANL	J. G. Stampelos	NSOC
John Matuszek	N. Y. State Health	Raphael Kasper	NSOC
Gordon Thompson	U.C.S.	Garry G. Young	ACRS
James Smith	General Elec. Co.	Wm. Bock	ACRS
N. R. Horton	General Elec. Co.	M. Ichikawa	JAERI-Japan (18th only)
Donald A. Nitti	Babcock & Wilcox	T. R. Young	C. E. Inc.
Alan D. Miller	EPRI/NSAC		
Harry A. Morewitz	Rockwell Int'l.		
Robert L. Ritzman	SAI		
G. Kaiser	NUS		



APPENDIX F  
ATTACHMENT 3

List of Commenters on Draft NUREG-0772

---

Individual	Organization
R. C. Vogel	Electric Power Research Institute
J. B. Ainscough	United Kingdom Atomic Energy Authority, Springfields Laboratory
C. E. Johnson	Argonne National Laboratory
P. E. Blackburn	Argonne National Laboratory
A. W. Castleman, Jr.	U. of Colorado
S. Levine	NUS Corporation
L. Devell	Studsvik Energie Teknik AB
R. L. Ritzman	Science Applications, Inc.
A. E. Scherer	Combustion Engineering, Inc.
L. Brewer	U. of California, Berkeley
R. K. Hilliard	Hanford Engineering Development Laboratory
D. F. Torgerson	Atomic Energy of Canada Limited
G. Thompson	Union of Concerned Scientists
S. M. Gehl	Argonne National Laboratory
W. R. Stratton	Los Alamos Scientific Laboratory
L. S. Tong	U.S. Nuclear Regulatory Commission
R. M. Wallace	Savannah River Laboratory
A. K. Postma	Benton City Technology (NRC Consultant)
A. P. Malinauskas	Oak Ridge National Laboratory
D. Garvin	U.S. National Bureau of Standards
D. O. Campbell	Oak Ridge National Laboratory
L. R. Zumwalt	North Carolina State University
R. H. Buchholz	General Electric Company
C. Devillers	Commissariat A. L'Energie Atomique (France)
M. Levenson	Bechtel Power Corporation
T. M. Anderson	Westinghouse Electric Corporation
D. Schweitzer	Brookhaven National Laboratory

---



<b>NRC FORM 335</b> (7-77)		<b>U.S. NUCLEAR REGULATORY COMMISSION</b> <b>BIBLIOGRAPHIC DATA SHEET</b>		<b>1. REPORT NUMBER (Assigned by DDC)</b> NUREG-0772	
<b>4. TITLE AND SUBTITLE (Add Volume No., if appropriate)</b> Technical Bases for Estimating Fission Product Behavior During LWR Accidents				<b>2. (Leave blank)</b>	
<b>7. AUTHOR(S)</b>				<b>3. RECIPIENT'S ACCESSION NO.</b>	
<b>9. PERFORMING ORGANIZATION NAME AND MAILING ADDRESS (Include Zip Code)</b> 1. USNRC (RES/NRR)-Wash., D.C. 20555; 2. Battelle Columbus Labs-505 King Ave., Columbus, OH 43201; 3. Sandia National Labs-P.O. Box 5800, Albuquerque, NM 87115; 4. Oak Ridge National Lab-P.O. Box Y, Oak Ridge, TN 37830				<b>5. DATE REPORT COMPLETED</b> MONTH   YEAR March   1981	
<b>12. SPONSORING ORGANIZATION NAME AND MAILING ADDRESS (Include Zip Code)</b> U. S. Nuclear Regulatory Commission Office of Nuclear Regulatory Research and Office of Nuclear Reactor Regulation Washington, D.C. 20555				<b>6. (Leave blank)</b>	
<b>13. TYPE OF REPORT</b> Technical Report				<b>7. (Leave blank)</b>	
<b>15. SUPPLEMENTARY NOTES</b>				<b>10. PROJECT/TASK/WORK UNIT NO.</b>	
<b>16. ABSTRACT (200 words or less)</b> <p>The objective of this report is to provide the Nuclear Regulatory Commission and the public with a description of the best technical information currently available for estimating the release of radioactive material during postulated reactor accidents, and to identify where gaps exist in our knowledge. This report focuses on those low probability-high consequence accidents involving severe damage to the reactor core and core meltdown that dominate the risk to the public. Furthermore, in this report particular emphasis is placed on the accident behavior of radioactive iodine since:</p> <p>(1) radioiodine is predicted to be a major contributor to public exposure,          (2) current regulatory accident analysis procedures focus on iodine, and          (3) several technical issues have been raised recently about the magnitude of iodine release. The generation, transport, and attenuation of aerosols were also investigated in some detail to assess their effect on fission product release estimates and to determine the performance of engineered safety features under accident conditions exceeding their design bases.</p>				<b>11. CONTRACT NO.</b>	
<b>17. KEY WORDS AND DOCUMENT ANALYSIS</b> Fission Products Accident Analysis Fission Product Release Light Water Reactors Source Terms				<b>17a. DESCRIPTORS</b>	
<b>17b. IDENTIFIERS/OPEN-ENDED TERMS</b>					
<b>18. AVAILABILITY STATEMENT</b> Unlimited				<b>19. SECURITY CLASS (This report)</b> Unclassified	
<b>20. SECURITY CLASS (This page)</b> Unclassified				<b>21. NO. OF PAGES</b>	
<b>22. PRICE</b> S					





UNITED STATES  
NUCLEAR REGULATORY COMMISSION  
WASHINGTON, D. C. 20555

OFFICIAL BUSINESS  
PENALTY FOR PRIVATE USE, \$300

POSTAGE AND FEES PAID  
U.S. NUCLEAR REGULATORY  
COMMISSION

